UNIVERSITY OF CALIFORNIA

Santa Barbara

Synthesis and Characterization of Coordination Complexes of Actinide Chalcogenides

A dissertation submitted in partial satisfaction of the

requirements for the degree Doctor of Philosophy

in Chemistry

by

Danil E. Smiles

Committee in charge:

Professor Trevor W. Hayton Chair

Professor Alison Butler

Professor Peter C. Ford

Professor R. Daniel Little

September 2016

The dissertation of Danil E. Smiles is approved.

_____
Professor Alison Butler

_____
Professor Peter C. Ford

_____
Professor R. Daniel Little

_____
Professor Trevor W. Hayton, Committee Chair

August 2016

Synthesis and Characterization of Coordination Complexes of Actinide Chalcogenides

Acknowledgements

Going chronologically, I'd like to thank my high school chemistry teachers Ms. Najwa Dajani and Mr. Frank Sticha who introduced me to chemistry and made it fun. I'd like to thank my undergraduate research advisor, Prof. Ken Raymond, who took a lowly sophomore into his group and kept finding me new mentors when the old ones graduated. I'd like to thank Dr. Géza Szigethy, my first mentor, who introduced me to the f-elements, and taught me, among many other important things, that sleeping in the lab could be very useful. I'd like to thank Dr. Ankona Datta for taking me in and introducing me to the MRI project when Géza graduated. And I'd like to thank Dr. Piper Klemm for not only being the only mentor to not leave me behind, but also for making me the inaugural member of the Klemm subgroup.

I wouldn't be here at UCSB if it wasn't for my boss, Prof. Trevor Hayton. I'd like to thank him for letting me do the chemistry I was interested in, and for pushing me to do the chemistry that I was less interested in, it all worked out for the best in the end. I'm grateful for him putting up with all the questions I had and for making most of the ones he asked relatively simple (i.e., What was the yield?). 'Was it *brown* brown or brown *brown*?' remains my favorite, as well as the most puzzling, question that I was fielded. Overall, it has been an enjoyable experience. I'm thankful for my thesis committee, Prof. Alison Butler, Prof. Peter Ford and Prof. Dan Little, who helped along the way in addition to making sure I wasn't going to be stuck here forever.

To the labmates who preceded me, I have to thank Dr. Richard Lewis and Dr. Jessie Brown for training me how to use a glovebox, and how to fix everything. I am eternally grateful for Richard taking my calls about fixing things even after he graduated. I'd like to thank my

incoming cohort, the scientist formerly known as Ellie Pedrick, now known as Dr. Ellie Owens. We joined the group at similar times, and despite her leaving me behind when she graduated a short time ago, I am very grateful to have been able to have her as a friend. To the people who came after, I'd like to thank Ed Paul. We shared a glovebox and an office for four years and it's been nice to have someone to talk to about something other than chemistry. To the wonder twins, Peter 'pet the cat' Damon, and Bi 'good god what are you eating' Nguyen, I thank you for many sad, yet still entertaining, moments. Peter's ability to communicate entirely in tv references, and Bi's utter lack of awareness about anything going on around her afforded many good times.

I'd also like thank my mentor during my time at Los Alamos National Lab, Dr. Andrew Gaunt. He put his family's livelihood in my hands by letting me do transuranic chemistry, and I now can proudly say I've worked with weapons grade plutonium as a result. I'd also like to thank Dr. Jessie Brown, who also happened to be at Los Alamos when I was there, and got to train/help me all over again.

Lastly, and probably most importantly, I have to thank my family, without whom I would not be here both figuratively and literally. It's been nice to have parents who don't mind the fact that I still don't have a 'real' job, and put up with me explaining what I do as 'stuff'.

Vita of Danil E. Smiles

August 2016

EDUCATION

Doctor of Philosophy in Chemistry (expected) August 2016
University of California, Santa Barbara
Advisor: Professor Trevor W. Hayton
Dissertation: "Synthesis and Characterization of Coordination Complexes of Actinide Chalcogenides"

Bachelor of Science, Chemistry May 2011
University of California, Berkeley
Advisor: Professor Kenneth N. Raymond

PROFESSIONAL EMPLOYMENT

07/11-Present	Graduate Student Researcher, Dept. of Chemistry, UCSB
07/15-09/15, 06/14-08/14	Graduate Student Researcher, Los Alamos National Laboratory
09/11-06/13	Teaching Assistant, Dept. of Chemistry, UCSB
01/09-05/11	Undergraduate Researcher, Dept. of Chemistry, UC Berkeley
08/08-05/11	Stockroom Chemist, Instructional Support Facility, UC Berkeley
08/08-05/09	Undergraduate Student Instructor, Dept. of Chemistry, UC Berkeley

PUBLICATIONS

Smiles, D. E.; Wu, G.; Hrobárik, P.; Hayton, T. W. Use of ^{77}Se and ^{125}Te NMR Spectroscopy to Probe Covalency of the Actinide-Chalcogen Bonding in $[Th(E_n)(N(SiMe_3)_2)_3]^-$ (E = Se, Te; *n* =1,2) and Their Oxo-Uranium(VI) Congeners. *J. Am. Chem. Soc.* **2016**, *138*, 814. Link

Smiles, D. E.; Wu, G.; Hayton, T. W. Reactivity of $[U(CH_2SiMe_2NSiMe_3)(NR_2)_2]$ (R = $SiMe_3$) with elemental chalcogens: Towards a better understanding of chalcogen atom transfer in the actinides. *New. J. Chem.* **2015**, *39*, 7563. Link.

Smiles, D. E.; Wu, G.; Kaltsoyannis, N.; Hayton, T. W. Thorium-ligand multiple bonds *via* reductive deprotection of a trityl group. *Chem. Sci.* **2015**, *6*, 3891. Link.

Hayton, T. W.; Smiles, D. E., Coordination Chemistry of the Actinide Elements. In *McGraw-Hill Yearbook of Science and Technology*, New York: McGraw-Hill Education, 2015. Link.

Smiles, D. E.; Wu, G.; Hayton, T. W. Reversible Chalcogen-Atom Transfer to a Terminal Uranium Sulfide. *Inorg. Chem.* **2014**, *53*, 12683. Link.

Smiles, D. E.; Wu, G.; Hayton, T. W. Synthesis of Terminal Monochalcogenide and Dichalcogenide Complexes of Uranium Using Polychalcogenides, $[E_n]^{2-}$ (E = Te, n = 2; E = Se, n = 4), as Chalcogen Atom Transfer Reagents. *Inorg. Chem.* **2014**, *53*, 10240. Link.

Smiles, D. E.; Wu, G.; Hayton, T. W. Synthesis of Uranium-Ligand Multiple Bonds by Cleavage of a Trityl Protecting Group. *J. Am. Chem. Soc.* **2014**, *136*, 96. Link.

Lewis, R. A.; Smiles, D. E.; Darmon, J. M.; Stieber, C. E.; Wu, G.; Hayton, T. W. Reactivity and Mössbauer Spectroscopic Characterization of an Fe(IV) Ketimide Complex and Reinvestigation of an Fe(IV) Norbornyl Complex. *Inorg. Chem.* **2013**, *52*, 8218. Link.

Klemm, P. J.; Floyd III, W. C.; Smiles, D. E.; Fréchet, J. M. J.; Raymond, K. N. Improving T1 and T2 Magnetic Resonance Imaging Contrast Agents through the Conjugation of an Esteramide Dendrimer to High-Water-Coordination Gd(III) Hydroxypyridinone Complexes. *Contrast Media Mol. Imaging* **2012**, *7*, 95. Link.

Floyd III, W. C.; Klemm, P. J.; Smiles, D. E.; Kohlgruber, A.; Pierre, V. C.; Mynar, J. L.; Fréchet, J. M. J.; Raymond, K. N. Conjugation Effects of Various Linkers on Gd(III) MRI Contrast Agents and Dendrimers: Optimizing the Hydroxypyridinonate (HOPO) Ligands with Nontoxic, Degradable Esteramide (EA) Dendrimers For High Relaxivity. *J. Am. Chem. Soc.* **2011**, *133*, 2390. Link.

AWARDS

- Graduate Division Dissertation Award, University of California, Santa Barbara 2015
- G. T. Seaborg Institute Research Fellowship, Los Alamos National Laboratory 2014, 2015
- Innovations in Fuel Cycle Research Award, U.S. Department of Energy 2014

- Robert H. DeWolfe Graduate Teaching Fellowship. University of California, Santa Barbara 2013
- Melvin J. Heger-Horst Scholarship. University of California, Berkeley 2009, 2010
- Summer Research Scholarship, University of California, Berkeley 2010
- Robert C. Byrd Honors Scholarship, U.S. Department of Education 2007-2011

Major Field: Inorganic Chemistry

Studies in Organometallic Actinide Chemistry

Abstract

Synthesis and Characterization of Coordination Complexes of Actinide Chalcogenides

by

Danil E. Smiles

Treatment of the U(III) trisamide, $[U(NR_2)_3]$ (R = $SiMe_3$) with 1 equiv of $KSCPh_3$ in the presence of 1 equiv of 18-crown-6 affords the U(IV) terminal sulfide complex, $[K(18\text{-crown-}6)][U(S)(NR_2)_3]$ in moderate yield. The reaction of $[U(NR_2)_3]$ with 1 equiv of $KOCPh_3$ generates a complex mixture of products from which, the U(IV) terminal oxo complex, $[K(18\text{-crown-}6)][U(O)(NR_2)_3]$, the U(IV) alkoxide complex, $[U(OCPh_3)(NR_2)_3]$, and the triphenylmethyl anion salt, $[K(18\text{-crown-}6)(THF)_2][CPh_3]$ can be isolated. Addition of 2 equiv of KC_8 and 18-crown-6 to $[U(OCPh_3)(NR_2)_3]$ affords both $[K(18\text{-crown-}6)][U(O)(NR_2)_3]$ and $[K(18\text{-crown-}6)(THF)_2][CPh_3]$ via reductive deprotection of the triphenylmethyl group.

Treatment of $[Th(I)(NR_2)_3]$ with 1 equiv of $KOCPh_3$ or $KSCPh_3$ affords $[Th(OCPh_3)(NR_2)_3]$ and $[Th(SCPh_3)(NR_2)_3]$ in moderate yields. Reductive deprotection of these with 2 equiv KC_8 and 18-crown-6 generates the Th(IV) terminal chalcogenide complexes, $[K(18\text{-crown-}6)][Th(O)(NR_2)_3]$ and $[K(18\text{-crown-}6)][Th(S)(NR_2)_3]$, respectively. Both feature short Th=E distances indicative of multiple bond character.

Treatment of $[U(NR_2)_3]$ or $[U(I)(NR_2)_3]$ with 0.5 or 1 equiv, respectively, of $[K(L)][Te_2]$ (L =18-crown-6, 2,2,2-cryptand) affords the U(IV) terminal tellurides, $[K(L)][U(Te)(NR_2)_3]$, $[K(L)][U(\eta^2\text{-}Te_2)(NR_2)_3]$ in moderate yields. Addition of 0.5 equiv of $[K(18\text{-crown-6})][Se_4]$ to $[U(NR_2)_3]$ generates $[K(18\text{-crown-6})][U(\eta^2\text{-}Se_2)(NR_2)_3]$, which can be converted to $[K(18\text{-crown-6})][U(Se)(NR_2)_3]$ via addition of 1 equiv of Ph_3P.

Treatment of $[Th(I)(NR_2)_3]$ with 1 equiv of $[K(18\text{-crown-6})][Se_4]$ or $[K(18\text{-crown-6})][Te_2]$ affords the dichalcogenide complexes, $[K(18\text{-crown-6})][Th(\eta^2\text{-}Se_2)(NR_2)_3]$ and $[K(18\text{-crown-6})][Th(\eta^2\text{-}Te_2)(NR_2)_3]$, respectively. These can be converted to the monochalcogenides, $[K(18\text{-crown-6})][Th(Se)(NR_2)_3]$ and $[K(18\text{-crown-6})][Th(Te)(NR_2)_3]$, via addition of Et_3P or Et_3P and Hg, respectively.

Addition of 0.125 equiv of S_8 or 1 equiv of Se to $[K(18\text{-crown-6})][U(S)(NR_2)_3]$ generates the dichalcogenide complexes, $[K(18\text{-crown-6})][U(\eta^2\text{-}S_2)(NR_2)_3]$ and $[K(18\text{-crown-6})][U(\eta^2\text{-}SSe)(NR_2)_3]$, respectively. These reactions are reversible and addition of 1 equiv of R_3P (R = Et, or Ph) regenerates $[K(18\text{-crown-6})][U(S)(NR_2)_3]$ and the corresponding phosphine-chalcogenide, $R_3P{=}E$ (E = S, Se). $[K(18\text{-crown-6})][U(\eta^2\text{-}S_2)(NR_2)_3]$ is reversibly converted to the U(IV) trisulfide, $[K(18\text{-crown-6})][U(\eta^3\text{-}S_3)(NR_2)_3]$ via addition or removal of S, with 0.125 equiv of S_8 or R_3P, respectively.

Table of Contents

List of Figures

List of Schemes

List of Tables

List of Abbreviations

°	degree
°C	degree Celsius
ε	extinction coefficient *or* bond critical point ellipticity
Δ	heat *or* difference
δ	chemical shift, ppm
η^n	hapticity of order n
κ^n	denticity of order n
μ	micro or denotes bridging atom
ν	stretching frequency, cm^{-1}
ρ	bond critical point electron density
Å	angstrom, 10^{-10} m
Ad	adamantyl
An	actinide
Ar	aryl
av.	average
BCP	bond critical point
BDE	bond dissociation energy
br	broad
Bu	butyl
calcd.	calculated
$^{13}C\{^1H\}$	carbon-13 proton decoupled
ca.	circa
CCD	charge coupled device
Cp^*	η^5-C_5Me_5
Cp	η^5-C_5H_5
cm^{-1}	wavenumber
CV	cyclic voltammetry
d	doublet *or* day(s)
d_n	deuterated in *n* positions
deg	degree
DFT	density functional theory
DI	delocalization index
DME	1,2-dimethoxyethane
$E_{1/2}$	average wave potential, $(E_{p,a} + E_{p,c})/2$
$E_{p,a}$	anodic half-wave potential
$E_{p,c}$	cathodic half-wave potential
e^-	electron

equiv	equivalent
Et_2O	diethyl ether
Et	ethyl
$^{19}F\{^1H\}$	fluorine-19 proton decoupled
Fc	ferrocene
FTIR	Fourier transform infrared
FWHM	full width at half maximum
g	gram(s)
GOF	goodness of fit
H	enthalpy *or* bond critical point energy density
^1H	hydrogen-1
$^1H\{^{31}P\}$	hydrogen-1 phosphorus decoupled
h	hour(s)
Hz	Hertz
$i_{p,a}$	anodic half-wave current
$i_{p,c}$	cathodic half-wave current
^{i}Pr	isopropyl
IR	infrared
J	NMR coupling constant
K	Kelvin
k	kilo
L	liter *or* ligand
$^7Li\{^1H\}$	lithium-7 proton decoupled
M	Molar
m	meter *or* multiplet *or* medium
m	meta
Me	methyl
min	minute(s)
mL	milliliter(s)
mmol	millimole(s)
mol	mole(s)
NBO	natural bond order
^{n}Bu	n-butyl
NIR	near infrared
NMR	nuclear magnetic resonance
NR_2	$N(SiMe_3)_2$
o	ortho
ORTEP	Oak Ridge Thermal Ellipsoid Program
OTf	triflate, $[CF_3SO_3]^-$
p	para

$^{31}P\{^{1}H\}$	phosphorus-31 proton decoupled
Ph	phenyl
ppm	parts per million
py	pyridine
q	quartet
QTAIM	Quantum Theory of Atoms-in-Molecules
R	alkyl
redox	reduction-oxidation
RT	room temperature
s	singlet *or* strong *or* second(s)
$^{77}Se\{^{1}H\}$	selenium-77 proton decoupled
sh	shoulder
t	triplet
$^{125}Te\{^{1}H\}$	tellurium-125 proton decoupled
^{t}Bu	*tert*-butyl
THF	tetrahydrofuran
UV	ultraviolet
V	Volt
vis	visible
VT	variable temperature
w	weak
xs	excess

Do they give a Nobel Prize in attempted chemistry?

-Dr. Robert Terwilliger (Sideshow Bob)

Chapter 1 Introduction

Table of Contents

1.1 Nuclear Power and the Challenges Associated with Nuclear Waste

The growing demand for energy in addition to the effects that carbon based fuels have on the climate has turned focus towards alternative energy sources.[1] Nuclear power remains a popular alternative as across the world: there are currently 447 reactors in operation and another 62 currently under construction.[2] The amount of power generated varies considerably by country, for example, in the United States nuclear power accounts for approximately 20% of all the electricity generated, whereas in France this is closer to 75%.[2] Despite the benefits of nuclear power, there remains considerable resistance to its use due, in part, to safety concerns about operating the power plants, as well as dealing with the waste that is generated.

One of the biggest challenges in the nuclear energy community is the processing and storage of nuclear waste.[3] Much of this waste is in the form of spent nuclear fuel, and the majority of the material in this fuel can be recovered and reused.[4] This is useful not only because it makes the overall process more efficient, but also because it reduces the hazards associated with these wastes. Towards these goals, considerable work has been done to recover both uranium and plutonium.[3-5] However, removal of the minor actinides, like Np, Am, and Cm, which account for less than 1% of the waste has proven more complicated.[6,7] Despite the small percentage of the waste these elements represent, they account for the majority of the long term radiotoxicity of the waste.[8] In addition, the presence of the lanthanides in these wastes poses a problem as well.[4,9] As a result, removal of these elements is essential for reducing the hazards associated with spent fuel, in addition to recovery and reuse of other components within the fuel.

A great amount of work has been done designing complexation agents that can preferably bind the actinides over the lanthanides as a way to afford these separations.[6,9-12] Interestingly,

it has been found that the presence of softer donor atoms in a complexation agent can lead to a dramatic increase in the preference for the actinide over the corresponding lanthanide.[6,12-16] For example, Zhu and co-workers reported that the separation factor for Am^{3+} versus Eu^{3+} for bis(2,2,4-trimethylpentyl)dithiophosphinic acid was four orders of magnitude greater than the identical oxygen derivative, bis(2,2,4-trimethylpentyl)phosphinic acid.[16] The presence of the softer donor atoms in the former, sulfur versus oxygen, is believed to be responsible for this remarkable difference. A variety of other dithiophosphinic acids have been studied, including bis(*o*-trifluoromethylphenyl)dithiophosphinic acid, which was found to have a separation factor for Am^{3+} versus Eu^{3+} of ~100,000, the highest reported (Figure 1.1).[12,17-19] While the reasons for this are still under debate, it has been posited that the ability of the actinides to form more covalent bonds with ligands, versus their lanthanide counterparts, may be responsible.

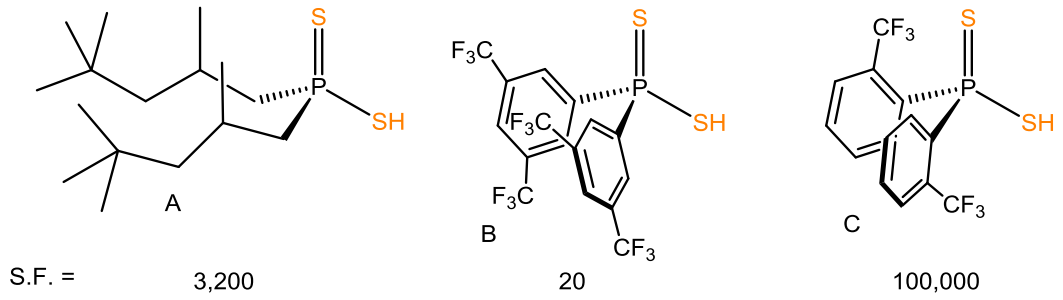

Figure 1.1. Dithiophosphinic acid extractants and separation factors for Am^{3+}/Eu^{3+}. A, Ref. 12; B & C, Ref. 17.

1.2 Roles of the f-orbitals and Covalency in Actinide Ligand Bonding

The actinides are typically considered hard metal ions whose chemistry is dictated by their charge and ionic radii.[20,21] Due in part to the similarities between the ionic radii of the actinides and lanthanides and the preference for the +3 oxidation state, the chemistry of these elements can be extremely similar.[22] Recent studies have demonstrated that in certain situations these

elements can behave differently, and this has been attributed to covalency in the actinides and the ability of the 5f orbitals of the actinides to participate in bonding, more so than the 4f orbitals of their lanthanide counterparts.[23-28] Typically the 4f orbitals are considered core-like orbitals, whereas the 5f orbitals have been shown to extend farther radially, and are now thought to play a role in bonding alongside the other valence orbital sets.[20,29]

As interest has grown in this field more and more evidence for the participation of the 5f orbitals in bonding has emerged.[30-34] Over the years various methods have been developed to probe these aspects of actinide ligand bonding.[35-39] X-ray absorption spectroscopy (XAS) has been demonstrated to very useful for measuring the covalency of metal-ligand bonds,[40-43] and has since been applied to various actinide systems.[30,33,34,44] For example, Kozimor and co-workers investigated the bonding of various of metal chloride complexes, including $[UCl_6]^{2-}$, using Cl K-edge XAS and found that there is both the 6d and 5f orbitals both play a role in bonding.[33,34] These results demonstrated that covalency is important, however, as might be expected for metal-halide bonds, the degree of covalency was rather small. Similar work by Shuh and co-workers demonstrated that both the 5f and 6d orbitals play roles in the bonding of $[(C_8H_8)_2An]$ (An = Th, U), using C K-edge XAS, further illustrating the utility of this technique.[30]

Many of these experiments also employ computational methods, such as Density Functional Theory (DFT), to complement the experimental analyses. These have also been used extensively as a standalone method to probe actinide-ligand bonding as well.[45-48] For example, Hayton and co-workers reported the synthesis and characterization of a series of chalcogenido substituted uranyl analogues, $[Cp^*_2Co][U(O)(E)(NR_2)_3]$ (E = O, S, Se; R = $SiMe_3$).[49] The electronic structures of these complexes were investigated using DFT and it

was found that the U-E bonding not only exhibited a considerable amount of covalency, but also that the 5f orbitals contributed significantly to this bonding. Similarly, Liddle and co-workers reported the synthesis and characterization of the U(VI) nitride complex, [U(N)($Tren^{TIPS}$)] ($Tren^{TIPS}$ = $N(CH_2CH_2NSi^iPr_3)_3$), and analyzed the U-N bond using DFT.[50] This analysis determined that there was a substantial amount of uranium character to both the σ (41%) and π (30%) bonds, indicative of a significant amount of covalency. Furthermore, the vast majority of the uranium contributions were found to be from the 5f orbitals (σ, 89%; π, 81%). These results illustrate the benefits of using theoretical techniques to study actinide-ligand bonding, as it relates to covalency and the role of the f orbitals, as well as the value of studying complexes with actinide-ligand multiple bonds.

1.3 Metal-Ligand Multiple Bonds

Metal-ligand multiple bonded ligands, including oxos, imidos, nitridos, and carbenes, play extremely important roles throughout inorganic chemistry.[51] Transition metal oxos are extremely important for both enzymatic and synthetic processes.[52-55] In particular, an Fe(IV) oxo species has been shown to be an intermediate in the catalytic activity of cytochrome P450.[56] These enzymes have been shown to be responsible a number of catalytic reactions including the decomposition of hydrogen peroxide and oxidation of a variety of organic substrates.[57,58] This latter ability has been exploited using synthetic metal oxo complexes, as well.[59-61]

The importance of metal nitrogen multiple bonded ligands, in the form of imidos and nitridos, is derived from the role they place in the process of nitrogen fixation. Industrially this is done via the Haber-Bosch process, which accounts for 1-2% of all energy consumption in the world and whose importance cannot be understated.[62] In nature nitrogen fixation is

carried out by nitrogenase, an iron and molybdenum containing enzyme,[63,64] whose mechanism is believed to involve the formation of both imido and nitrido moieties.[65,66] Synthetic complexes that can catalytically reduce dinitrogen have also studied extensively to gain insight into this mechanism.[58,67-69] For example, Schrock and co-workers studied the reaction of [(HIPTN$_3$N)Mo] (HIPT = 3,5-(2,4,6-^{i}Pr$_3$C$_6$H$_2$)$_2$-C$_6$H$_3$) with N_2 to generate NH_3, and were able to isolate and characterize many of the intermediates formed, including imido and nitrido complexes, along the way.[70-73]

The first examples of metal carbene complexes were reported by Fischer and co-workers in the 1960s and featured a heteroatom stabilized carbene moiety.[74-76] Since then there have been numerous examples reported, including N-heterocyclic carbenes,[77-79] again possessing heteroatom stabilization, and alkylidenes, which do not.[80-82] These complexes have been used in a wide variety of transformations.[83-86] Most notably is their use in olefin metathesis,[87-90] for which a Nobel Prize was awarded.[91-93]

While complexes containing actinide-ligand multiple bonds have not been studied as nearly as extensively as their transition metal counterparts, there has been a surge of interest in these complexes over the past several decades.[94-96] This has led to significant advances including the synthesis of oxo,[97-101] imido,[102-111] and nitrido complexes,[50,112-115] among others.[116-127] This includes the synthesis of the first uranium mono oxo complex, [Cp$^*_2$U(O)(E-2,6-^{i}Pr$_2$-C$_6$H$_3$)] (E = O, N), reported by Burns and co-workers in 1993,[128] and the first thorium mono oxo complex, [(1,2,4-(^{t}Bu)$_3$C$_5$H$_2$)Th(O)], reported by Zi and co-workers in 2011.[101] The first carbene complex, [Cp$_3$U(CHP(CH$_3$)$_2$Ph)], was reported by Gilje and co-workers in 1981.[118] Additionally, Liddle and co-workers reported the synthesis of the first uranium terminal nitride complex, [Na(12-crown-4)$_2$][U(N)(Tren^{TIPS})], in 2012.[112] Also

of note are the synthesis of several uranium bis-imido complexes reported by Boncella and co-workers,[109-111] in addition to the synthesis of the first transuranic bis-imido complex, [Np(NDipp)$_2$(^{t}Bu$_2$bipy)$_2$(Cl)] (DIPP = 2,6-^{i}Pr$_2$C$_6$H$_3$), reported by Gaunt and co-workers.[107] However, despite the progress in this field, chalcogenide complexes remain relatively rare.[125,126,129-134]

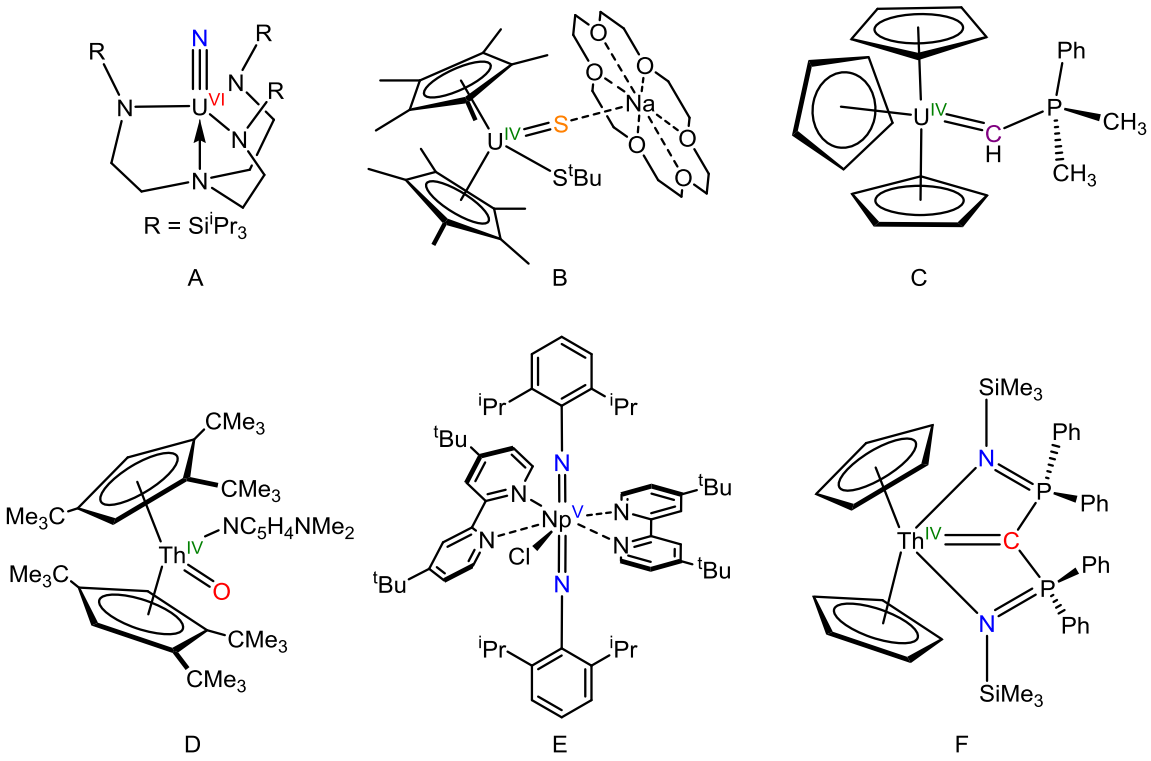

Figure 1.2. Examples of complexes with actinide-ligand multiple bonds. A, Ref. 50; B, Ref. 125; C, Ref. 118; D, Ref. 101; E, Ref. 107; F, Ref. 123.

1.4 General Remarks

The goal of this research is to improve the understanding of actinide ligand bonding through the synthesis of complexes containing actinide ligand multiple bonds, with a particular focus upon actinide chalcogenides.

Chapter 2 describes two methods of synthesizing complexes with uranium ligand multiple bonds using a triphenylmethyl protecting group, including reductive deprotection of this moiety via addition of an external reducing agent. These complexes are characterized both by NMR spectroscopy and X-ray crystallography. The differing reactivity observed, and how this relates to the BDEs of the bonds being cleaved, is also discussed.

Chapter 3 details the synthesis of complexes with thorium ligand multiple bonds utilizing the reductive deprotection protocol developed in chapter 2. X-ray crystallography and NMR spectroscopy are used to characterize these complexes. Additionally, DFT analysis is performed to study the electronic structure of these complexes and their uranium analogues from chapter 2.

Chapter 4 describes a new method for the synthesis of polychalcogenide salts, and the use of this method to synthesize new ditelluride and tetraselenide salts. These polychalcogenides are used to synthesize new uranium terminal selenides and tellurides. X-ray crystallography and NMR spectroscopy are used to study these complexes.

Chapter 5 describes the synthesis of the first terminal selenides and tellurides of thorium using the polychalcogenides salts described in chapter 4. NMR spectroscopies, X-ray crystallography, and DFT are all used to probe the electronic structure of these complexes, and a discussion of how NMR spectroscopy coupled with DFT can be used to probe actinide ligand bonding is also included.

Chapter 6 describes the reactivity of a uranium terminal monosulfide complex, synthesized in chapter 2, with elemental chalcogens, as well as characterization of the di- and trichalcogenide complexes that are formed as a result. The reversible nature of these reactions is discussed in the context of chalcogen atom transfer catalysis, and preliminary results are

discussed. Additionally, the synthesis of a tetrasulfide salt, similar to the polychalcogenides of chapter 4, and its use in an alternate route to the synthesis of uranium terminal sulfides is detailed.

Chapter 7 details chalcogen atom transfer to and from a uranium metallacycle complex. These experiments are discussed in relation to the formation of a previously reported uranium disulfide complex. In addition, the reactivity of several new chalcogen atom transfer reagents with uranium are explored and the results are detailed.

Chapter 8 describes the synthesis of a thorium trisulfide complex analogous to the uranium species of chapter 6. The electrochemistry of these complexes are studied in concert using cyclic voltammetry in addition to chemical oxidation experiments. The results of these experiments and how they relate to the chemistry of the $[S_3]^{\bullet -}$ radical anion are described.

Chapter 9 details the synthesis and characterization of a new thorium carbene complex. X-ray crystallography and NMR spectroscopies were used to characterize this complex. Additionally, variable temperature NMR spectroscopy was used to probe the thermodynamics of this species. The results are discussed and compared to those for the identical uranium complex.

1.5 References

(1) IEA *World Energy Outlook 2015*; OECD Publishing.
(2) IAEA: 2016.
(3) OECD *Actinide and Fission Product Partitioning and Transmutation*; OECD Publishing.
(4) Choppin, G.; Liljenzin, J.-O.; Rydberg, J.; Ekberg, C. In *Radiochemistry and Nuclear Chemistry (Fourth Edition)*; Academic Press: Oxford, 2013, p 685.
(5) Vijay, K. M.; Pathak, P. N.; Mohapatra, P. K. In *Ion Exchange and Solvent Extraction*; CRC Press: 2009, p 65.
(6) Nash, K. L. *Solvent Extr. Ion Exch.* **1993**, *11*, 729.
(7) Wenzel, U.; Branquinho, C. L.; Herz, D.; Ritter, G. In *Actinide Separations*; Navratil, J. D., Schulz, W. W., Eds.; ACS: Washington D.C., 1980; Vol. 117.
(8) Madic, C.; Lecomte, M.; Baron, P.; Boullis, B. *C. R. Phys.* **2002**, *3*, 797.
(9) Hill, C. In *Ion Exchange and Solvent Extraction*; CRC Press: 2009, p 119.
(10) Kolarik, Z. *Chem. Rev.* **2008**, *108*, 4208.
(11) Dam, H. H.; Reinhoudt, D. N.; Verboom, W. *Chem. Soc. Rev.* **2007**, *36*, 367.
(12) Ionova, G.; Ionov, S.; Rabbe, C.; Hill, C.; Madic, C.; Guillaumont, R.; Krupa, J. C. *Solvent Extr. Ion. Exch.* **2001**, *19*, 391
(13) Bhattacharyya, A.; Mohapatra, P. K.; Manchanda, V. K. *Solvent Extr. Ion Exch.* **2007**, *25*, 27.
(14) Watanabe, M.; Mirvaliev, R.; Tachimori, S.; Takeshita, K.; Nakano, Y.; Morikawa, K.; Chikazawa, T.; Mori, R. *Solvent Extr. Ion Exch.* **2004**, *22*, 377.
(15) Modolo, G.; Odoj, R. *J. Alloys Compounds* **1998**, *271–273*, 248.
(16) Zhu, Y.; Chen, J.; Choppin, G. R. *Solvent Extr. Ion Exch.* **1996**, *14*, 543.
(17) Klaehn, J. R.; Peterman, D. R.; Harrup, M. K.; Tillotson, R. D.; Luther, T. A.; Law, J. D.; Daniels, L. M. *Inorg. Chim. Acta* **2008**, *361*, 2522.
(18) Peterman, D. R.; Greenhalgh, M. R.; Tillotson, R. D.; Klaehn, J. R.; Harrup, M. K.; Luther, T. A.; Law, J. D. *Sep. Sci. Technol.* **2010**, *45*, 1711.
(19) Hill, C.; Madic, C.; Baron, P.; Ozawa, M.; Tanaka, Y. *J. Alloys Compd.* **1998**, *271–273*, 159.
(20) Kaltsoyannis, N.; Scott, P. *The f elements*; Oxford University Press: New York, 1999.
(21) Katz, J. J.; Morss, L. R.; Seaborg, G. T. *The Chemistry of the Actinide Elements, 2nd ed.*, 1986.
(22) Choppin, G. R. *J. Less-Common Met.* **1983**, *93*, 323.
(23) Ingram, K. I. M.; Kaltsoyannis, N.; Gaunt, A. J.; Neu, M. P. *J. Alloys Compd.* **2007**, *444–445*, 369.
(24) Jones, M. B.; Gaunt, A. J.; Gordon, J. C.; Kaltsoyannis, N.; Neu, M. P.; Scott, B. L. *Chem. Sci.* **2013**, *4*, 1189.
(25) Ingram, K. I. M.; Tassell, M. J.; Gaunt, A. J.; Kaltsoyannis, N. *Inorg. Chem.* **2008**, *47*, 7824.
(26) Gaunt, A. J.; Reilly, S. D.; Enriquez, A. E.; Scott, B. L.; Ibers, J. A.; Sekar, P.; Ingram, K. I. M.; Kaltsoyannis, N.; Neu, M. P. *Inorg. Chem.* **2008**, *47*, 29.
(27) Neidig, M. L.; Clark, D. L.; Martin, R. L. *Coord. Chem. Rev.* **2013**, *257*, 394.
(28) Choppin, G. R. *J. Alloys Compd.* **2002**, *344*, 55.

(29) Schreckenbach, G.; Hay, P. J.; Martin, R. L. *J. Comput. Chem.* **1999**, *20*, 70.
(30) Minasian, S. G.; Keith, J. M.; Batista, E. R.; Boland, K. S.; Clark, D. L.; Kozimor, S. A.; Martin, R. L.; Shuh, D. K.; Tyliszczak, T. *Chem. Sci.* **2014**, *5*, 351.
(31) Seaman, L. A.; Wu, G.; Edelstein, N. M.; Lukens, W. W.; Magnani, N.; Hayton, T. W. *J. Am. Chem. Soc.* **2012**, *134*, 4931.
(32) Lukens, W. W.; Edelstein, N. M.; Magnani, N.; Hayton, T. W.; Fortier, S.; Seaman, L. A. *J. Am. Chem. Soc.* **2013**, *135*, 10742.
(33) Kozimor, S. A.; Yang, P.; Batista, E. R.; Boland, K. S.; Burns, C. J.; Clark, D. L.; Conradson, S. D.; Martin, R. L.; Wilkerson, M. P.; Wolfsberg, L. E. *J. Am. Chem. Soc.* **2009**, *131*, 12125.
(34) Minasian, S. G.; Keith, J. M.; Batista, E. R.; Boland, K. S.; Clark, D. L.; Conradson, S. D.; Kozimor, S. A.; Martin, R. L.; Schwarz, D. E.; Shuh, D. K.; Wagner, G. L.; Wilkerson, M. P.; Wolfsberg, L. E.; Yang, P. *J. Am. Chem. Soc.* **2012**, *134*, 5586.
(35) Clark, J. P.; Green, J. C. *J. Chem. Soc. Dalton Trans.* **1977**, 505.
(36) Brennan, J. G.; Green, J. C.; Redfern, C. M. *J. Am. Chem. Soc.* **1989**, *111*, 2373.
(37) Green, J. C.; de Simone, M.; Coreno, M.; Jones, A.; Pritchard, H. M. I.; McGrady, G. S. *Inorg. Chem.* **2005**, *44*, 7781.
(38) Pepper, M.; Bursten, B. E. *Chem. Rev.* **1991**, *91*, 719.
(39) Kaltsoyannis, N. *Chem. Soc. Rev.* **2003**, *32*, 9.
(40) Löble, M. W.; Keith, J. M.; Altman, A. B.; Stieber, S. C. E.; Batista, E. R.; Boland, K. S.; Conradson, S. D.; Clark, D. L.; Lezama Pacheco, J.; Kozimor, S. A.; Martin, R. L.; Minasian, S. G.; Olson, A. C.; Scott, B. L.; Shuh, D. K.; Tyliszczak, T.; Wilkerson, M. P.; Zehnder, R. A. *J. Am. Chem. Soc.* **2015**, *137*, 2506.
(41) Solomon, E. I.; Hedman, B.; Hodgson, K. O.; Dey, A.; Szilagyi, R. K. *Coord. Chem. Rev.* **2005**, *249*, 97.
(42) Altman, A. B.; Pacold, J. I.; Wang, J.; Lukens, W. W.; Minasian, S. G. *Dalton Trans.* **2016**, *45*, 9948.
(43) Daly, S. R.; Keith, J. M.; Batista, E. R.; Boland, K. S.; Clark, D. L.; Kozimor, S. A.; Martin, R. L. *J. Am. Chem. Soc.* **2012**, *134*, 14408.
(44) Kozimor, S. A.; Yang, P.; Batista, E. R.; Boland, K. S.; Burns, C. J.; Christensen, C. N.; Clark, D. L.; Conradson, S. D.; Hay, P. J.; Lezama, J. S.; Martin, R. L.; Schwarz, D. E.; Wilkerson, M. P.; Wolfsberg, L. E. *Inorg. Chem.* **2008**, *47*, 5365.
(45) Kirker, I.; Kaltsoyannis, N. *Dalton Trans.* **2011**, *40*, 124.
(46) Tassell, M. J.; Kaltsoyannis, N. *Dalton Trans.* **2010**, *39*, 6719.
(47) Kaltsoyannis, N. *Inorg. Chem.* **2013**, *52*, 3407.
(48) Huang, Q.-R.; Kingham, J. R.; Kaltsoyannis, N. *Dalton Trans.* **2015**, *44*, 2554.
(49) Brown, J. L.; Fortier, S.; Wu, G.; Kaltsoyannis, N.; Hayton, T. W. *J. Am. Chem. Soc.* **2013**, *135*, 5352.
(50) King, D. M.; Tuna, F.; McInnes, E. J. L.; McMaster, J.; Lewis, W.; Blake, A. J.; Liddle, S. T. *Nat. Chem.* **2013**, *5*, 482.
(51) Nugent, W. A.; Mayer, J. M. *Metal-Ligand Multiple Bonds*; John Wiley & Sons: New York, NY, 1988.
(52) Meyer, T. J. In *Oxygen Complexes and Oxygen Activation by Transition Metals*; Martell, A. E., Sawyer, D. T., Eds.; Springer US: Boston, MA, 1988, p 33.
(53) Costas, M.; Mehn, M. P.; Jensen, M. P.; Que, L. *Chem. Rev.* **2004**, *104*, 939.

(54) Krebs, C.; Galonić Fujimori, D.; Walsh, C. T.; Bollinger, J. M. *Acc. Chem. Res.* **2007**, *40*, 484.
(55) Baik, M.-H.; Newcomb, M.; Friesner, R. A.; Lippard, S. J. *Chem. Rev.* **2003**, *103*, 2385.
(56) Meunier, B.; de Visser, S. P.; Shaik, S. *Chem. Rev.* **2004**, *104*, 3947.
(57) Groves, J. T. *J. Inorg. Biochem.* **2006**, *100*, 434.
(58) Hohenberger, J.; Ray, K.; Meyer, K. *Nat. Commun.* **2012**, *3*, 720.
(59) Chantarojsiri, T.; Sun, Y.; Long, J. R.; Chang, C. J. *Inorg. Chem.* **2015**, *54*, 5879.
(60) Park, J.; Morimoto, Y.; Lee, Y.-M.; Nam, W.; Fukuzumi, S. *Inorg. Chem.* **2014**, *53*, 3618.
(61) Fujii, H. *Coord. Chem. Rev.* **2002**, *226*, 51.
(62) Smil, V. *Enriching the Earth: Fritz Haber, Carl Bosch, and the Transformation of World Food Production*; MIT Press: Cambridge, MA, 2004.
(63) Einsle, O.; Tezcan, F. A.; Andrade, S. L. A.; Schmid, B.; Yoshida, M.; Howard, J. B.; Rees, D. C. *Science* **2002**, *297*, 1696.
(64) Lancaster, K. M.; Roemelt, M.; Ettenhuber, P.; Hu, Y.; Ribbe, M. W.; Neese, F.; Bergmann, U.; DeBeer, S. *Science* **2011**, *334*, 974.
(65) Seefeldt, L. C.; Hoffman, B. M.; Dean, D. R. *Annu. Rev. Biochem.* **2009**, *78*, 701.
(66) Hoffman, B. M.; Lukoyanov, D.; Yang, Z.-Y.; Dean, D. R.; Seefeldt, L. C. *Chem. Rev.* **2014**, *114*, 4041.
(67) Schrock, R. R. *Acc. Chem. Res.* **2005**, *38*, 955.
(68) Rittle, J.; Peters, J. C. *J. Am. Chem. Soc.* **2016**, *138*, 4243.
(69) McWilliams, S. F.; Holland, P. L. *Acc. Chem. Res.* **2015**, *48*, 2059.
(70) Yandulov, D. V.; Schrock, R. R. *J. Am. Chem. Soc.* **2002**, *124*, 6252.
(71) Yandulov, D. V.; Schrock, R. R.; Rheingold, A. L.; Ceccarelli, C.; Davis, W. M. *Inorg. Chem.* **2003**, *42*, 796.
(72) Yandulov, D. V.; Schrock, R. R. *Inorg. Chem.* **2005**, *44*, 1103.
(73) Yandulov, D. V.; Schrock, R. R. *Science* **2003**, *301*, 76.
(74) Fischer, E. O. In *Pure Appl. Chem.* 1970; Vol. 24, p 407.
(75) Mills, O. S.; Redhouse, A. D. *Angew. Chem. Int. Ed.* **1965**, *4*, 1082.
(76) Fischer, E. O.; Maasböl, A. *Angew. Chem. Int. Ed.* **1964**, *3*, 580.
(77) Wanzlick, H. W.; Schönherr, H. J. *Angew. Chem. Int. Ed.* **1968**, *7*, 141.
(78) Öfele, K. *J. Organomet. Chem.* **1968**, *12*, P42.
(79) Diez-Gonzalez, S.; Nolan, S. P. *Annu. Rep. Prog. Chem., Sect. B: Org. Chem.* **2005**, *101*, 171.
(80) Schrock, R. R. *J. Am. Chem. Soc.* **1974**, *96*, 6796.
(81) Nguyen, S. T.; Johnson, L. K.; Grubbs, R. H.; Ziller, J. W. *J. Am. Chem. Soc.* **1992**, *114*, 3974.
(82) Nguyen, S. T.; Grubbs, R. H.; Ziller, J. W. *J. Am. Chem. Soc.* **1993**, *115*, 9858.
(83) Dötz, K. H.; Stendel, J. *Chem. Rev.* **2009**, *109*, 3227.
(84) Kaufhold, S.; Petermann, L.; Staehle, R.; Rau, S. *Coord. Chem. Rev.* **2015**, *304–305*, 73.
(85) Velazquez, H. D.; Verpoort, F. *Chem. Soc. Rev.* **2012**, *41*, 7032.
(86) Doyle, M. P. *Chem. Rev.* **1986**, *86*, 919.
(87) Cardin, D. J.; Cetinkaya, B.; Lappert, M. F. *Chem. Rev.* **1972**, *72*, 545.
(88) Vougioukalakis, G. C.; Grubbs, R. H. *Chem. Rev.* **2010**, *110*, 1746.

(89) Dötz, K. H. *Metal Carbenes in Organic Synthesis*; Springer Berlin Heidelberg: Berlin, Heidelberg, 2004.
(90) Tebbe, F. N.; Parshall, G. W.; Reddy, G. S. *J. Am. Chem. Soc.* **1978**, *100*, 3611.
(91) Grubbs, R. H. *Angew. Chem. Int. Ed.* **2006**, *45*, 3760.
(92) Schrock, R. R. *Angew. Chem. Int. Ed.* **2006**, *45*, 3748.
(93) Chauvin, Y. *Angew. Chem. Int. Ed.* **2006**, *45*, 3740.
(94) Hayton, T. W. *Chem. Commun.* **2013**, *49*, 2956.
(95) Hayton, T. W. *Dalton Trans.* **2010**, *39*, 1145.
(96) Zi, G. *Sci. China Chem.* **2014**, *57*, 1064.
(97) Fortier, S.; Brown, J. L.; Kaltsoyannis, N.; Wu, G.; Hayton, T. W. *Inorg. Chem.* **2012**, *51*, 1625.
(98) Fortier, S.; Kaltsoyannis, N.; Wu, G.; Hayton, T. W. *J. Am. Chem. Soc.* **2011**, *133*, 14224.
(99) Zi, G.; Jia, L.; Werkema, E. L.; Walter, M. D.; Gottfriedsen, J. P.; Andersen, R. A. *Organometallics* **2005**, *24*, 4251.
(100) Bart, S. C.; Anthon, C.; Heinemann, F. W.; Bill, E.; Edelstein, N. M.; Meyer, K. *J. Am. Chem. Soc.* **2008**, *130*, 12536.
(101) Ren, W.; Zi, G.; Fang, D.-C.; Walter, M. D. *J. Am. Chem. Soc.* **2011**, *133*, 13183.
(102) Anderson, N. H.; Odoh, S. O.; Yao, Y.; Williams, U. J.; Schaefer, B. A.; Kiernicki, J. J.; Lewis, A. J.; Goshert, M. D.; Fanwick, P. E.; Schelter, E. J.; Walensky, J. R.; Gagliardi, L.; Bart, S. C. *Nat. Chem.* **2014**, *6*, 919.
(103) King, D. M.; McMaster, J.; Tuna, F.; McInnes, E. J. L.; Lewis, W.; Blake, A. J.; Liddle, S. T. *J. Am. Chem. Soc.* **2014**, *136*, 5619.
(104) Haskel, A.; Straub, T.; Eisen, M. S. *Organometallics* **1996**, *15*, 3773.
(105) Ren, W.; Zi, G.; Walter, M. D. *Organometallics* **2012**, *31*, 672.
(106) Jilek, R. E.; Spencer, L. P.; Lewis, R. A.; Scott, B. L.; Hayton, T. W.; Boncella, J. M. *J. Am. Chem. Soc.* **2012**, *134*, 9876.
(107) Brown, J. L.; Batista, E. R.; Boncella, J. M.; Gaunt, A. J.; Reilly, S. D.; Scott, B. L.; Tomson, N. C. *J. Am. Chem. Soc.* **2015**, *137*, 9583.
(108) Bell, N. L.; Maron, L.; Arnold, P. L. *J. Am. Chem. Soc.* **2015**, *137*, 10492.
(109) Hayton, T. W.; Boncella, J. M.; Scott, B. L.; Palmer, P. D.; Batista, E. R.; Hay, P. J. *Science* **2005**, *310*, 1941.
(110) Hayton, T. W.; Boncella, J. M.; Scott, B. L.; Batista, E. R. *J. Am. Chem. Soc.* **2006**, *128*, 12622.
(111) Hayton, T. W.; Boncella, J. M.; Scott, B. L.; Batista, E. R.; Hay, P. J. *J. Am. Chem. Soc.* **2006**, *128*, 10549.
(112) King, D. M.; Tuna, F.; McInnes, E. J. L.; McMaster, J.; Lewis, W.; Blake, A. J.; Liddle, S. T. *Science* **2012**, *337*, 717.
(113) King, D. M.; Liddle, S. T. *Coord. Chem. Rev.* **2014**, *266–267*, 2.
(114) Fortier, S.; Wu, G.; Hayton, T. W. *J. Am. Chem. Soc.* **2010**, *132*, 6888.
(115) Fox, A. R.; Creutz, S. E.; Cummins, C. C. *Dalton Trans.* **2010**, *39*, 6632.
(116) Fortier, S.; Walensky, J. R.; Wu, G.; Hayton, T. W. *J. Am. Chem. Soc.* **2011**, *133*, 6894.
(117) Cramer, R. E.; Bruck, M. A.; Edelmann, F.; Afzal, D.; Gilje, J. W.; Schmidbaur, H. *Chem. Ber.* **1988**, *121*, 417.

(118) Cramer, R. E.; Maynard, R. B.; Paw, J. C.; Gilje, J. W. *J. Am. Chem. Soc.* **1981**, *103*, 3589.
(119) Cramer, R. E.; Maynard, R. B.; Paw, J. C.; Gilje, J. W. *Organometallics* **1983**, *2*, 1336.
(120) Cantat, T.; Arliguie, T.; Noel, A.; Thuery, P.; Ephritikhine, M.; Le Floch, P.; Mezailles, N. *J. Am. Chem. Soc.* **2009**, *131*, 963.
(121) Tourneux, J.-C.; Berthet, J.-C.; Cantat, T.; Thuery, P.; Mezailles, N.; Ephritikhine, M. *J. Am. Chem. Soc.* **2011**, *133*, 6162.
(122) Tourneux, J.-C.; Berthet, J.-C.; Cantat, T.; Thuery, P.; Mezailles, N.; Le Floch, P.; Ephritikhine, M. *Organometallics* **2011**, *30*, 2957.
(123) Ma, G.; Ferguson, M. J.; McDonald, R.; Cavell, R. G. *Inorg. Chem.* **2011**, *50*, 6500.
(124) Ren, W.; Deng, X.; Zi, G.; Fang, D.-C. *Dalton Trans.* **2011**, *40*, 9662.
(125) Ventelon, L.; Lescop, C.; Arliguie, T.; Leverd, P. C.; Lance, M.; Nierlich, M.; Ephritikhine, M. *Chem. Commun.* **1999**, 659.
(126) Brown, J. L.; Fortier, S.; Lewis, R. A.; Wu, G.; Hayton, T. W. *J. Am. Chem. Soc.* **2012**, *134*, 15468.
(127) Gardner, B. M.; Balázs, G.; Scheer, M.; Tuna, F.; McInnes, E. J. L.; McMaster, J.; Lewis, W.; Blake, A. J.; Liddle, S. T. *Angew. Chem. Int. Ed.* **2014**, *53*, 4484.
(128) Arney, D. S. J.; Burns, C. J. *J. Am. Chem. Soc.* **1993**, *115*, 9840.
(129) Smiles, D. E.; Wu, G.; Hayton, T. W. *J. Am. Chem. Soc.* **2014**, *136*, 96.
(130) Smiles, D. E.; Wu, G.; Hayton, T. W. *Inorg. Chem.* **2014**, *53*, 10240.
(131) Smiles, D. E.; Wu, G.; Kaltsoyannis, N.; Hayton, T. W. *Chem. Sci.* **2015**, *6*, 3891.
(132) Smiles, D. E.; Wu, G.; Hrobárik, P.; Hayton, T. W. *J. Am. Chem. Soc.* **2016**, *138*, 814.
(133) Andrez, J.; Pecaut, J.; Scopelliti, R.; Kefalidis, C. E.; Maron, L.; Rosenzweig, M. W.; Meyer, K.; Mazzanti, M. *Chem. Sci.* **2016**.
(134) Rosenzweig, M. W.; Scheurer, A.; Lamsfus, C. A.; Heinemann, F. W.; Maron, L.; Andrez, J.; Mazzanti, M.; Meyer, K. *Chem. Sci.* **2016**.

Chapter 2 Reductive Deprotection of a Triphenylmethyl Protecting Group for the Synthesis of Uranium-Ligand Multiple Bonds

Portions of this work were published in:

Danil E. Smiles, Guang Wu, Trevor W. Hayton

J. Am. Chem. Soc., **2014**, *136*, 96-99.

Table of Contents

2.1 Introduction

The growing interest in uranium-ligand multiple bonds is driven by both the unique reactivity and the insight these species can provide into fundamental concepts of actinide-ligand bonding. Great strides have been made towards the synthesis and characterization of complexes with these moieties,[1-3] and while some areas have seen considerable progress, examples containing group 16 elements, specifically the heavier chalcogens (S, Se, Te) remain relatively rare.[4,5] The first reported example of a terminal actinide chalcogenide was the uranium(IV) sulfide, [Na(18-crown-6)][U(Cp^*)$_2$(S^tBu)(S)], reported by Ephritikhine and co-workers in 1999.[4] This complex was synthesized via the reaction of the bisthiolate, [U(Cp^*)$_2$(S^tBu)$_2$], with Na(Hg) amalgam. The identification of isobutane and isobutylene in the reaction mixture suggest the formation of the *tert*-butyl radical, formed via homolytic C-S bond cleavage of the S^tBu ligand. Changing the alkyl group of the thiolates from *tert*-butyl to isopropyl results in reduction to U(III), rather than C-S bond cleavage. This change is likely a due to the difference in stabilities between the *tert*-butyl and isopropyl radicals,[6] and demonstrates the difficulty associated with developing a rational route to these complexes. In 2012, Hayton and co-workers reported the synthesis of a series of uranium chalcogenides, [Ph_3PCH_3][U(E)(NR_2)$_3$] (E = S, Se, Te; R = $SiMe_3$),[5] isolated from the reaction of the U(III) ylide adduct, [U(H_2CPPh_3)(NR_2)$_3$],[7] with the corresponding elemental chalcogen. Mechanistic studies suggest that an additional equivalent of the starting U(III) species is consumed to form the final product, thus limiting the maximum yield to only 50%. In 2016, Meyer and co-workers and Mazzanti and co-workers reported the syntheses of new U(IV) terminal sulfides via either deprotonation of a U(IV) thiol, or reaction of a U(III) species with

$Ph_3P{=}S$, respectively.[8,9] These works are important examples of the synthesis of uranium-chalcogen multiple bonds, and demonstrate that advances are still ongoing.

One of the biggest challenges to overcome in the synthesis of uranium-chalcogen multiple bonds is the tendency of these reactions to yield bimetallic bridging species. For example, reaction of the U(III) tris-amide, $[U(NR_2)_3]$, with elemental chalcogen (S, Se, Te) affords the bimetallic bridged monochalcogenides, $[U(NR_2)_3]_2(\mu\text{-}E)$.[10] Similar outcomes have been observed a wide variety of different supporting ligand frameworks.[9,11-14] Because of these complications new methods for installing these moieties must be developed. Organic chemists have seen wide success in a variety of synthetic fields due to their ability to install reactive functional groups in a controlled and selective manner, specifically through the use of a protecting group. There is a wide range of protecting groups that have been utilized for the installation of an even wider array of functional groups.[15] One of particular interest is the triphenylmethyl (CPh_3) or trityl protecting group, that has been used in organic synthesis for the protection of alcohols,[16] thiols,[17] and amines.[18] Furthermore, the removal of this protecting group can be accomplished under a variety of different conditions.[15]

While the use of a trityl protecting group in inorganic synthesis considerably less common, there are a few examples. Kitajima and co-workers reported in 1994 that the Cu(I) thiolate,

Scheme 2.1 Synthesis of metal sulfides using a trityl protecting group.

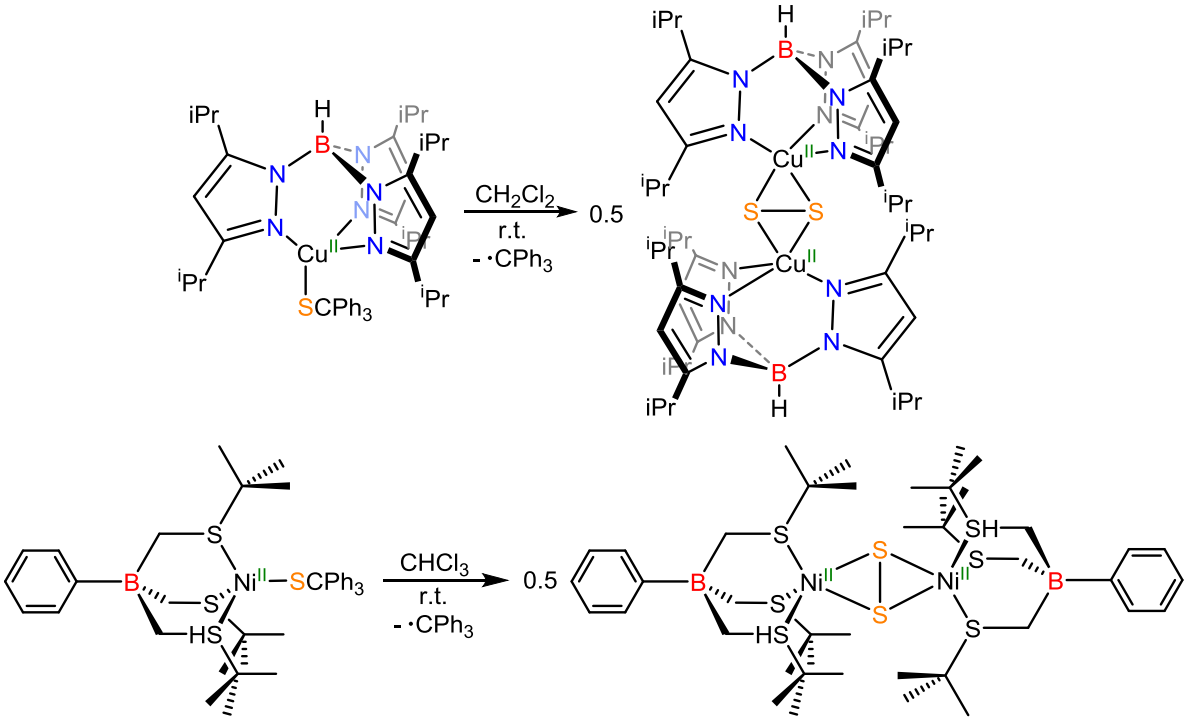

[Tp′Cu(SCPh$_3$)], undergoes homolytic C-S bond cleavage via thermolysis to form the dimeric Cu(II) disulfide, [Tp′Cu]$_2$(μ-η^2:η^2-S$_2$) (Tp′ = HB(3,5-^{i}Pr$_2$pz) (Scheme 2.1).[19] The triphenylmethyl radical, which couples to form Gomberg's dimer,[20,21] is also observed in this reaction. A similar reaction was reported by Riordan and co-workers in 2008 describing the formation of a Ni(II) disulfide complex, [(PhTt^{tBu})Ni]$_2$(μ-η^2:η^2-S$_2$) (PhTt^{tBu} = phenyl(tris((*tert*-butylmethyl)thio)methyl)borate) (Scheme 2.1). In addition, in 1997, Tatsumi and co-workers reported the synthesis of the tantalum(V) terminal sulfide, [(Cp*)Ta(S)(SCPh$_3$)(Cl)], via reaction of [(Cp*)TaCl$_4$] with 2 equivalents of Ph$_3$CSH; evidence of the formation of the trityl radical, supporting homolytic C-S bond cleavage, was also observed.[22] Furthermore, Arnold and co-workers demonstrated that reaction of [U(NR$_2$)$_3$] with ClCPh$_3$ affords the U(IV) chloride complex, [U(Cl)(NR$_2$)$_3$] in addition to Gomberg's dimer.[23] The examples described all employ homolytic cleavage of the C-E bond

for removal of the protecting group. However, there are reports of carrying out this cleavage heterolytically, including the use of Li/naphthalene,[24,25] or Na in liquid NH_3.[26,27]

These examples demonstrate that a trityl protecting group can be used to install functional groups not only in organic systems, but in inorganic systems as well, including those containing uranium. This chapter describes the use of a triphenylmethyl protecting group to install terminal chalcogenide moieties and access complexes with uranium ligand multiple bonds. Removal of this protecting group is accomplished via both homolytic and heterolytic C-E bond cleavage, the latter of which utilizes an external reducing agent. The development of this reductive deprotection protocol is detailed, and the scope of the methodology is explored. The differences observed during the installation of various moieties, and how this relates to C-E bond strengths, is discussed. The purpose of this work is to demonstrate the utility of a trityl protecting group for these syntheses, as well as the applicability of these methods for other complicated actinide and transition metal systems.

2.2 Results and Discussion

2.2.1 Synthesis and Characterization of [K(18-crown-6)][U(S)(NR_2)$_3$] (2.1) and [K(2,2,2-cryptand)][U(S)(NR_2)$_3$] (2.2)

The addition of 1 equiv of $KSCPh_3$ to a solution of [U(NR_2)$_3$] in THF-d_8 results in a color change from purple to orange. The ^{1}H NMR spectrum of this mixture features a new broad resonance at -2.48 ppm assignable to a new U(IV) sulfide species, as well as resonances indicative of the formation of Gomberg's dimer (Figure A2.1). This reaction proceeds via spontaneous homolytic bond C-S bond cleavage, as evidenced by the formation of Gomberg's dimer. Addition of 1 equiv of $KSCPh_3$, to a solution of [U(NR_2)$_3$] in THF, followed by

Scheme 2.2 Synthesis of [K(L)][U(S)(NR_2)$_3$] (**2.1**, L = 18-crown-6; **2.2**, L = 2,2,2-cryptand).

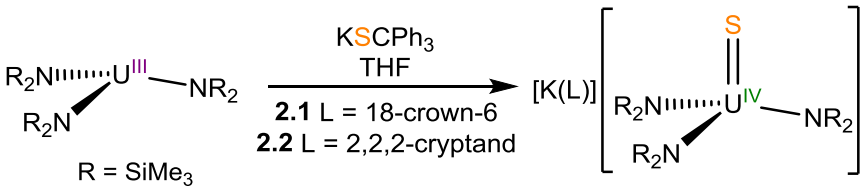

1 equiv of 18-crown-6 affords [K(18-crown-6)][U(S)(NR_2)$_3$] (**2.1**), which can be isolated as yellow-orange blocks in 48% yield upon crystallization from diethyl ether (Scheme 2.2). Similarly, addition of 1 equiv of $KSCPh_3$, to a solution of [U(NR_2)$_3$] in THF, followed by 1 equiv of 2,2,2-cryptand affords [K(2,2,2-cryptand)][U(S)(NR_2)$_3$] (**2.2**), as yellow-orange needles in 45% yield after crystallization from diethyl ether (Scheme 2.1). The ^{1}H NMR spectrum of **2.1** in benzene-d_6 exhibits two broad resonances at -2.02 and -1.11 ppm, in a 54:24 ratio, which correspond to the methyl groups of the silylamide ligands and the methylene groups of the 18-crown-6 moiety, respectively. The ^{1}H NMR spectrum of **2.2**, in benzene-d_6, features four resonances at -2.26, 0.32, 1.16 and 1.22 ppm, in a 54:12:12:12 ratio. These resonances are assignable to the methyl groups of the silylamide ligands as well as the three distinct proton environments of the 2,2,2-cryptand moiety, respectively. UV-Vis / NIR spectra of **2.1**, and **2.2** are consistent with the presence of a U(IV) metal center (Figure A2.4).[5,10,28]

2.2.2 Solid-State and Solution-State Molecular Structures of 2.1 and 2.2

Complex **2.1** crystallizes in the triclinic spacegroup $P\bar{1}$, and it features two independent molecules in its asymmetric unit. Complex **2.2** crystallizes in the monoclinic spacegroup $P2_1/c$, as a THF solvate, **2.2**·0.5THF. Their solid-state molecular structures are shown in Figure 2.1, and selected bond distances and angles can be found in Table 2.1. Both complexes **2.1** and **2.2** feature a pseudotetrahedral geometry about uranium, similar to what has been seen previously for the [U(S)(NR_2)$_3$]$^-$ anion in [Ph_3PCH_3][U(S)(NR_2)$_3$].[5] The U-S bond distances

in **2.1** (U1-S1 = 2.4463(6), U2-S2 = 2.4513(6) Å) and **2.2** (U1-S1 = 2.442(2) Å) are significantly shorter than the average U-S single bond length ~2.7 Å,[29] and shorter than those of other previously reported U(IV) terminal sulfides, $[Ph_3PCH_3][U(S)(NR_2)_3]$ (U-S = 2.4805(5) Å),[5] [Na(18-crown-6)][$U(Cp^*)_2(S^tBu)(S)$] (U-S = 2.462(2) and 2.477(2) Å),[4] [K(dibenzo-18-crown-6)][$((^{Ad,Me}ArO)_3tacn)U(S)$] (U-S = 2.507(1) Å),[8] and $[K_2(U(S)(OSi(O^tBu)_3)_4)]_2(\mu$-(18-crown-6)) (U-S = 2.534(2) Å).[9] The S-K bond distances in **2.1** (S1-K1 = 3.0684(8) and S2-K2 = 3.1551(8) Å) are similar to the S-Na distances of [Na(18-crown-6)][$U(Cp^*)_2(S^tBu)(S)$] (S-Na = 3.135(4) Å),[4] as well as the S-K bond distance of [K(dibenzo-18-crown-6)][$((^{Ad,Me}ArO)_3tacn)U(S)$] (S-K = 3.136(1) Å),[8] indicative of a weak dative interaction.

Table 2.1. Selected Bond Distances (**Å**) and Angles (deg) of Uranium Sulfides

Complex	**2.1**	**2.2**	$[Ph_3PCH_3][U(S)(NR_2)_3]^a$
U-S	(av.) 2.4488	2.442(2)	2.4805(5)
S-cation$^+$	(av.) 3.112	3.727	3.641(2)
U-N (av.)	2.304	2.311	2.302
N-U-N (av.)	116.8	116.5	115.2

[a] Taken from Ref 5

Whereas, **2.1** exists as a contact ion pair in the solid state, **2.2** exists as a separated cation/anion pair. The long distance between the S^{2-} ligand of complex **2.2** and the nearest C atom of the $[K(2,2,2\text{-cryptand})]^+$ moiety (S1-C21B = 3.727 Å) is comparable to the interaction between the S^{2-} and the C of the methyl group of the $[Ph_3PCH_3]^+$ moiety in $[Ph_3PCH_3][U(S)(NR_2)_3]$ (S1-C1 = 3.641(2) Å).[5]

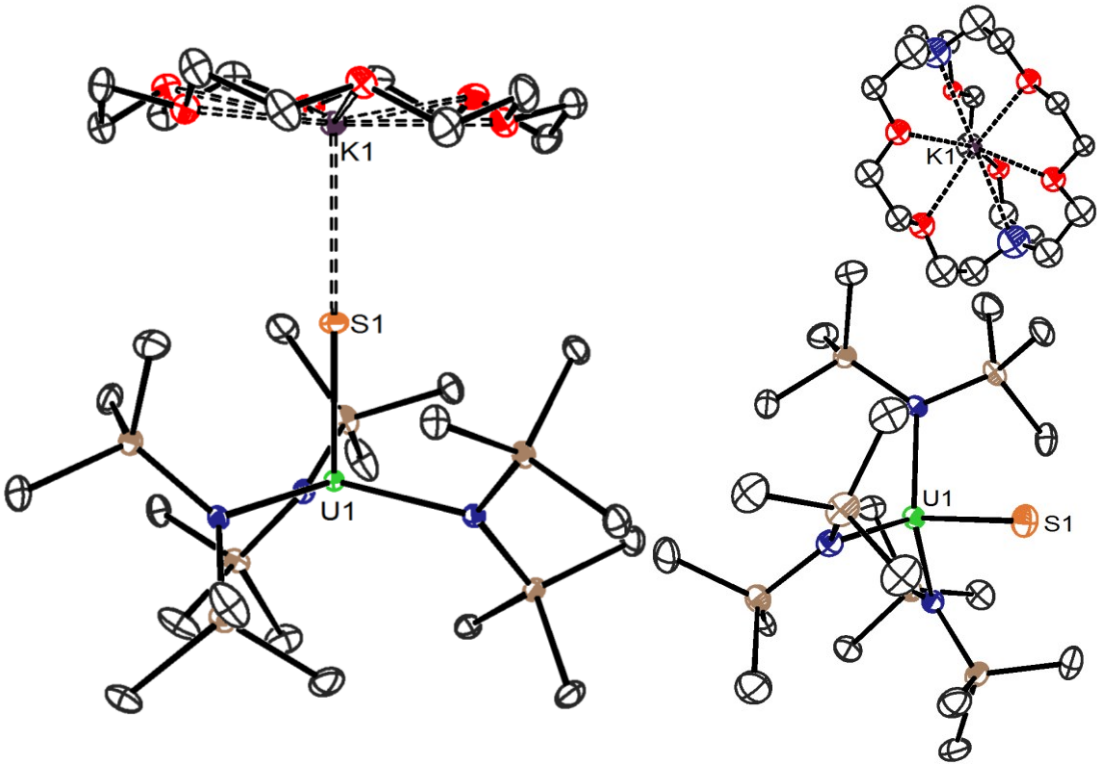

Figure 2.1. ORTEP diagram of [K(18-crown-6)][U(S)$(NR_2)_3$] (**2.1**) and [K(2,2,2-cryptand)][U(S)$(NR_2)_3$] (**2.2**·0.5THF) with 50% probability ellipsoids. One molecule of **2.1**, the THF solvate and hydrogen atoms are omitted for clarity. Selected bond lengths (Å): **2.1**, U1-S1 = 2.4463(6), U2-S2 = 2.4513(6), S1-K1 = 3.0684(8), S2-K2 = 3.1551(8); **2.2**, U1-S1 = 2.442(2).

While complexes **2.1** and **2.2** exhibit different structures in the solid state, in solution they display similar behavior depending upon the nature of the solvent. In a non-polar and non-coordinating solvent both **2.1** and **2.2** exist as contact ion pairs, with the $[K(L)]^+$ moiety directly interacting with the uranium metal center. This is evidenced by the large paramagnetic shifts of the resonances attributable to either the 18-crown-6 (-1.11 pm) or 2,2,2-cryptand (0.32, 1.16 and 1.22 ppm) observed in benzene-d_6. When dissolved in a more polar, more coordinating solvent, such as pyridine-d_5, this interaction is broken and complexes **2.1** and **2.2** exist as solvent separated cation/anion pairs (Figure 2.2). This is verified by the downfield shift of the resonances assignable to the 18-crown-6 (3.30 ppm) and 2,2,2-cryptand

(2.25, 3.25, and 3.29), closer to that of free 18-crown-6 (3.57 ppm) and 2,2,2-cryptand (2.67, 3.64, and 3.73 ppm).

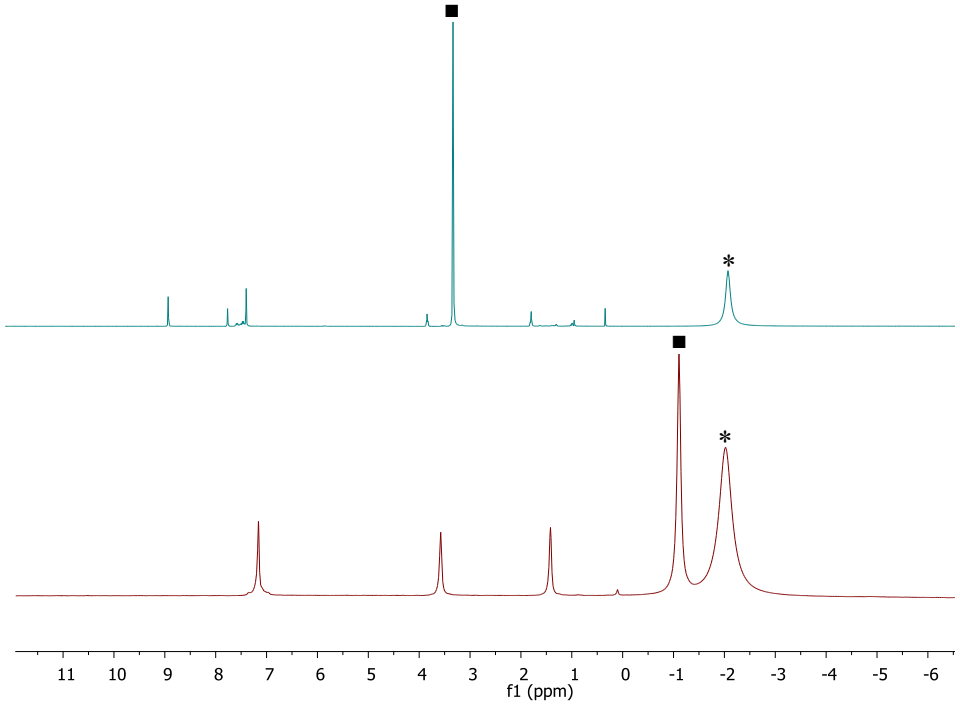

Figure 2.2. ^{1}H NMR spectra of [K(18-crown-6)][U(S)(NR$_2$)$_3$]. Above in pyridine-d_5 and below in benzene-d_6. (*) indicates the resonance assignable to (N(Si(CH_3)$_3$)$_2$)$_2$ and (■) indicates the resonance assignable to the 18-crown-6 moiety.

2.2.3 Reaction of [U(NR$_2$)$_3$] with KOCPh$_3$ and 18-crown-6

The elimination of a triphenylmethyl group was also investigated as a route to synthesize an analogous oxo species. Addition of 1 equiv of KOCPh$_3$ to a frozen, purple solution of [U(NR$_2$)$_3$], in benzene-d_6, in the presence of 1 equiv of 18-crown-6, and warming to room temperature, results in the immediate color change to deep red, as well as the deposition of a red solid. After 24 h the ^{1}H NMR spectrum obtained reveals the formation of several new

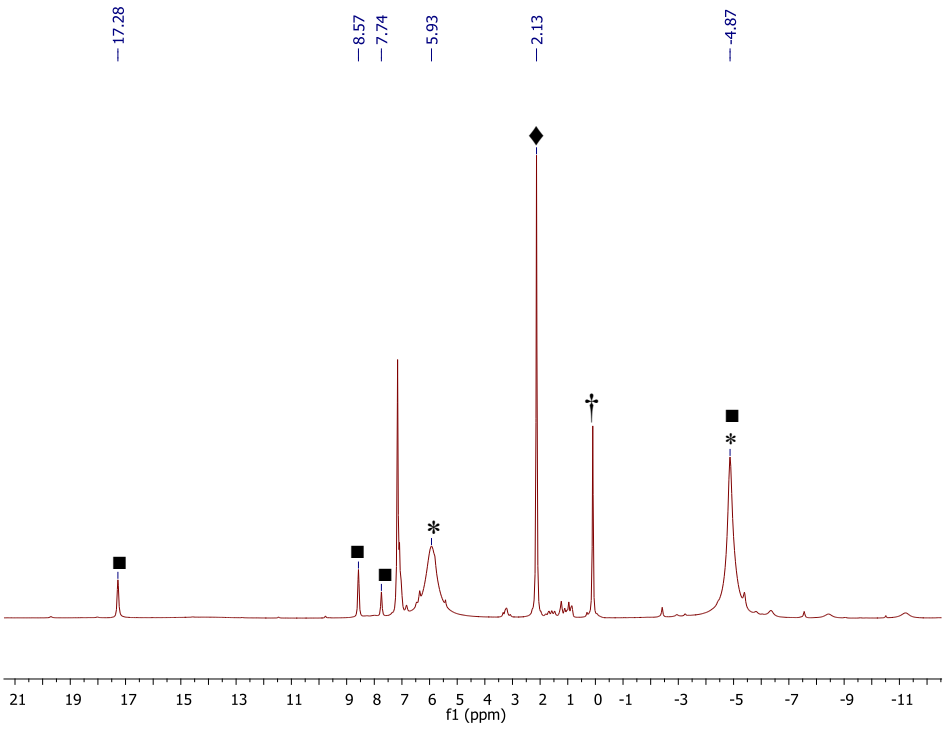

Figure 2.3. In-situ ^{1}H NMR spectrum of the reaction of $[U(NR_2)_3]$ with $KOCPh_3$ and 18-crown-6, in benzene-d_6. (*) indicates the presence of **2.3**, (■) indicates the presence of **2.4**, (†) indicates the presence of $HN(SiMe_3)_2$, and (♦) indicates the presence of hexamethylbenzene. Note that the $N(SiMe_3)_2$ signals for **2.3** and **2.4** overlap.

products, however, evidence for the formation of Gomberg's dimer is not seen (Figure 2.3). However, the formation of a new U(IV) oxo complex, $[K(18\text{-crown-6})][U(O)(NR_2)_3]$ (**2.3**), is evidenced by the broad resonance at -4.87 ppm, assignable to the methyl groups of the silylamide ligands. In addition to complex **2.3**, the formation of a U(IV) alkoxide complex, $[U(OCPh_3)(NR_2)_3]$, (**2.4**) is also observed, evidenced by three new broad resonances at 7.44, 8.57 and 17.28 ppm, assignable to the three different aryl proton environments. The red solid was identified as $[K(18\text{-crown-6})(THF)_2][CPh_3]$ (**2.5**) by both spectroscopic and X-ray crystallographic analyses (Scheme 2.3).

Scheme 2.3 Reaction of $[U(NR_2)_3]$ with $KOCPh_3$ and 18-crown-6

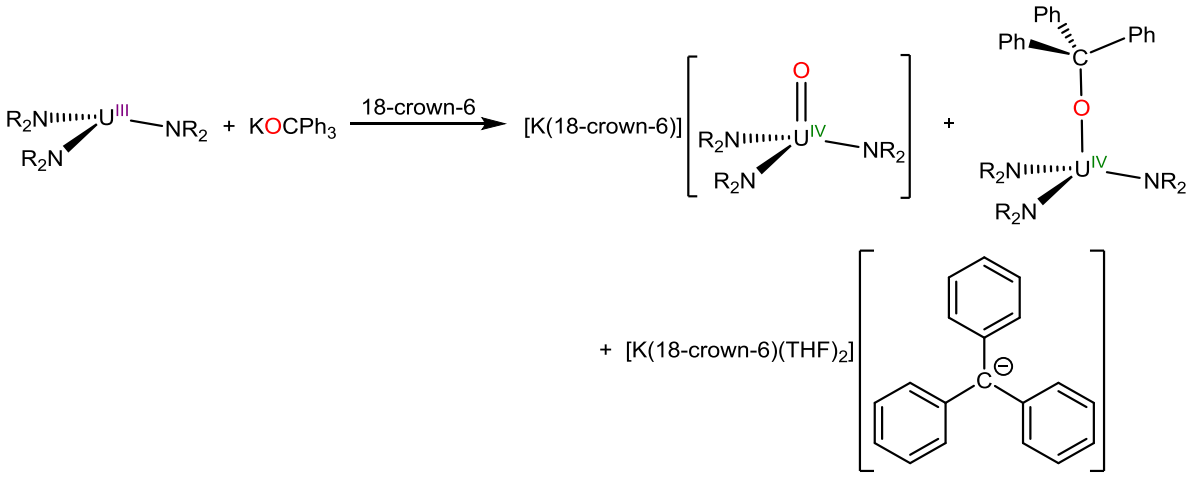

2.2.4 Synthesis and Characterization of [K(18-crown-6)][U(O)(NR₂)₃] (2.3)

Complex **2.3** can be independently prepared by reduction of the previously reported U(V) oxo complex, $[U(O)(NR_2)_3]$.[28] Thus, addition of 1.5 equiv of KC_8 to a deep red solution of $[U(O)(NR_2)_3]$ and 18-crown-6, in THF results in a lightening of the color after 10 minutes. [K(18-crown-6)][U(O)(NR₂)₃] (**2.3**) can be isolated in a 50% yield, as pale purple blocks, after crystallization from diethyl ether (Scheme 2.4).

Scheme 2.4 Synthesis of [K(18-crown-6)][U(O)(NR₂)₃] (**2.3**)

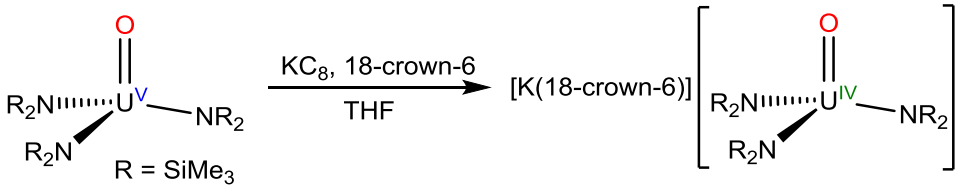

Complex **2.3** crystallizes in the triclinic spacegroup $P\bar{1}$, and its solid-state molecular structure is shown in Figure 2.4. Complex **2.3** is structurally identical to its sulfido analogue, complex **2.1**, featuring a pseudotetrahedral arrangement about uranium and a dative interaction between the terminal chalcogenide and the $[K(18\text{-crown-6})]^+$ moiety. The U-O bond distance in **2.3** (U1-O1 = 1.890(5) Å) is equivalent to that of the previously reported,

U(IV) oxo complex, $[Cp^*_2Co][U(O)(NR_2)_3]$ (U1-O1 = 1.878(5) Å),[5] which features an identical $[U(O)(NR_2)_3]^-$ anion. Additionally, the O-K distance in **2.3** (O1-K1 = 2.640(5) Å) is shorter than the S-K in **2.1**, consistent with the shorter ionic radius of O^{2-} vs. S^{2-}. The ^1H NMR spectrum of **2.3**, in benzene-d_6, consists of two broad resonances at -4.91 and 16.15 ppm, which are in a 54:24 ratio and assignable to the methyl groups of the silylamide ligands and methylene groups of the 18-crown-6 moiety, respectively. Lastly, the UV-Vis / NIR spectrum of complex **2.3** is consistent with the presence of a U(IV) metal center (Figure A2.4).[5,10,28]

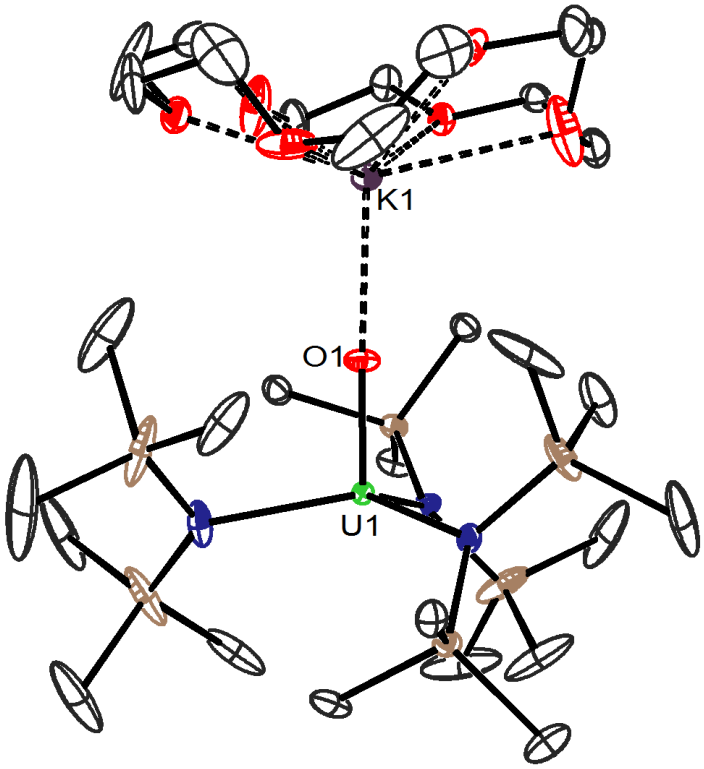

Figure 2.4. ORTEP diagram of $[K(18\text{-crown-6})][U(O)(NR_2)_3]$ (**2.3**) with 50% probability ellipsoids. Hydrogen atoms are omitted for clarity. Selected bond lengths (Å): U1-O1 = 1.890(5), O1-K1 = 2.640(5).

2.2.5 Synthesis and Characterization of [U(OCPh$_3$)(NR$_2$)$_3$] (2.4)

Complex **2.4** can also be independently prepared via a simple salt metathesis between the previously reported U(IV) iodide species, [U(I)(NR$_2$)$_3$], and KOCPh$_3$ (Scheme 2.5). Accordingly, addition of 1 equiv of KOCPh$_3$ to a THF suspension of [U(I)(NR$_2$)$_3$] results in the formation of a light brown solution concomitant with the deposition of a white precipitate. Filtration and crystallization from diethyl ether affords [U(OCPh$_3$)(NR$_2$)$_3$] (**2.4**) as pale purple plates in 38% yield.

Scheme 2.5 Synthesis of [U(OCPh$_3$)(NR$_2$)$_3$] (**2.4**)

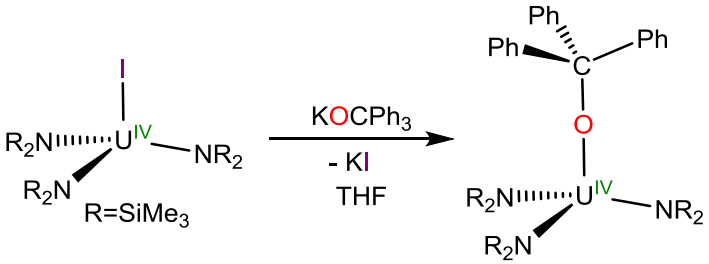

Complex **2.4** crystallizes in the triclinic spacegroup $P\bar{1}$, as a diethyl ether solvate, **2.4**·Et$_2$O, and its solid-state molecular structure is shown in Figure 2.5. Complex **2.4** features a tetrahedral geometry about uranium, (av. N-U-N = 108.0°, av. N-U-O = 110.9°). Furthermore, the U-O and U-N bond distances in **2.4** (U1-O1 = 2.098(3) and av. U-N = 2.28 Å) are consistent with U-O and U-N single bonds, respectively. The ^{1}H NMR spectrum of **2.4**, in benzene-d_6, exhibits four resonances at -4.85, 7.74, 8.56, and 17.22, in a 54:3:6:6 ratio, respectively, attributable to the methyl groups of the silylamide ligands and the *p*-, *m*-, and *o*-aryl protons of the triphenylmethyl-alkoxide ligand. These resonances correspond well with those seen in the reaction between [U(NR$_2$)$_3$] and KOCPh$_3$ (Figure 2.3), and confirm that complex **2.4** is forming in this reaction.

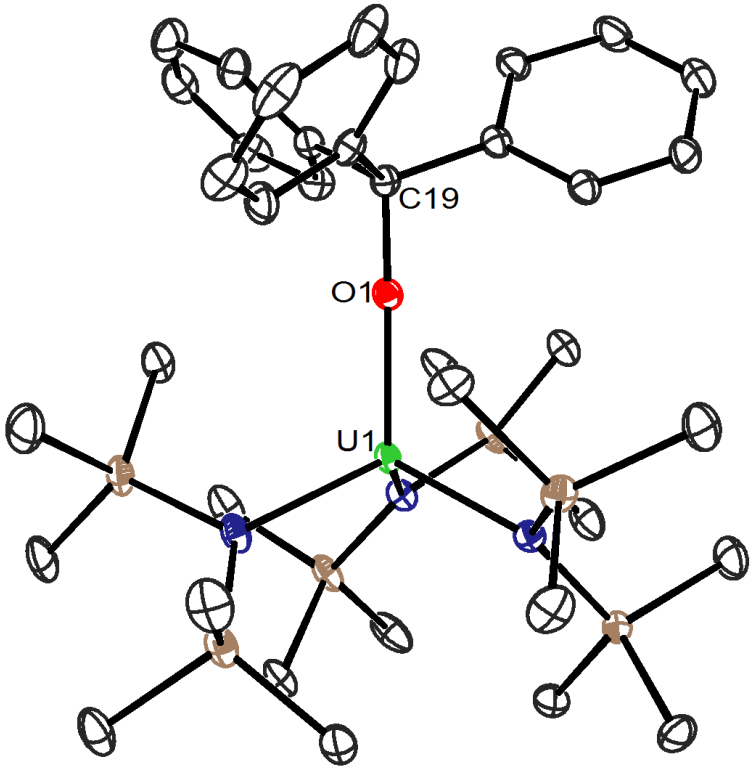

Figure 2.5. ORTEP diagram of $[U(OCPh_3)(NR_2)_3]$ (**2.4**·Et_2O) with 50% probability ellipsoids. Hydrogen atoms and a diethyl ether solvate are omitted for clarity. Selected bond lengths (Å) and angles (deg): U1-O1 = 2.098(3), O1-C19 = 1.445(6), U1-O1-C19 = 177.8(3).

2.2.6 Synthesis and Characterization of $[K(18\text{-crown-6})(THF)_2][CPh_3]$ (2.5)

The last product identified from the reaction of $[U(NR_2)_3]$ with $KOCPh_3$, $[K(18\text{-crown-6})(THF)_2][CPh_3]$ (**2.5**), can be independently synthesized to further confirm the assignment and its formation in this reaction. Addition of 1 equiv of KC_8 to a colorless solution of triphenylmethane and 18-crown-6 in THF results in the immediate formation of a deep red solution concomitant with the deposition of a vibrant red solid. After filtration to remove the

Scheme 2.6 Synthesis of $[K(18\text{-crown-6})(THF)_2][CPh_3]$ (**2.5**)

$$Ph_3CH + KC_8 \xrightarrow[THF]{\text{18-crown-6}} [K(18\text{-crown-6})(THF)_2][CPh_3]$$
$$- H_2 \; - C_8$$

C_8 formed, the solid was dissolved in additional THF and combined with the deep red filtrate. Storage of this solution at -25 °C for 24 h affords [K(18-crown-6)$(THF)_2$][CPh_3] (**2.5**) as red needles in 44% yield (Scheme 2.6). Complex **2.5** crystallizes in the triclinic spacegroup $P\bar{1}$, and its solid-state molecular structure is shown in Figure 2.6. **2.5** exists as cation / anion pair in the solid state, and the angles around the central carbon (C6-C15-C22 = 121.7(3)°, C6-C15-C19 = 117.8(2)°. C19-C15-C22 = 120.5(2)°) are indicative of an sp^2 hybridized carbon, consistent with the presence of a negative charge residing on this carbon. Furthermore, the metrical parameters of the triphenylmethyl anion are comparable to those of other structurally characterized molecules containing the triphenylmethyl anion, as well as the perchloro derivative [K(18-crown-6)][$C(C_6Cl_5)_3$].[29,30] Complex **2.5** is soluble in THF and pyridine, and insoluble in diethyl ether and non-polar solvents. The ^1H and $^{13}C\{^1H\}$ spectral data of the triphenylmethyl anion in **2.5** match with those previously recorded for this material.[31] The ^1H NMR spectrum of **2.5**, in pyridine-d_5, consists of four resonances, a singlet at 3.44 ppm, and two triplets and a doublet at 6.49, 7.08 and 8.17 ppm, assignable to the 18-crown-6 moiety and the *p*-, *m*-, and *o*-aryl protons of the triphenylmethyl anion, respectively. The $^{13}C\{^1H\}$ NMR spectrum exhibits five resonances, the central carbon appears at 91.14 ppm, while the expected sixth resonance, attributable to the *ipso* carbon of the aryl rings, is not seen due to overlap with a pyridine-d_5 resonance.

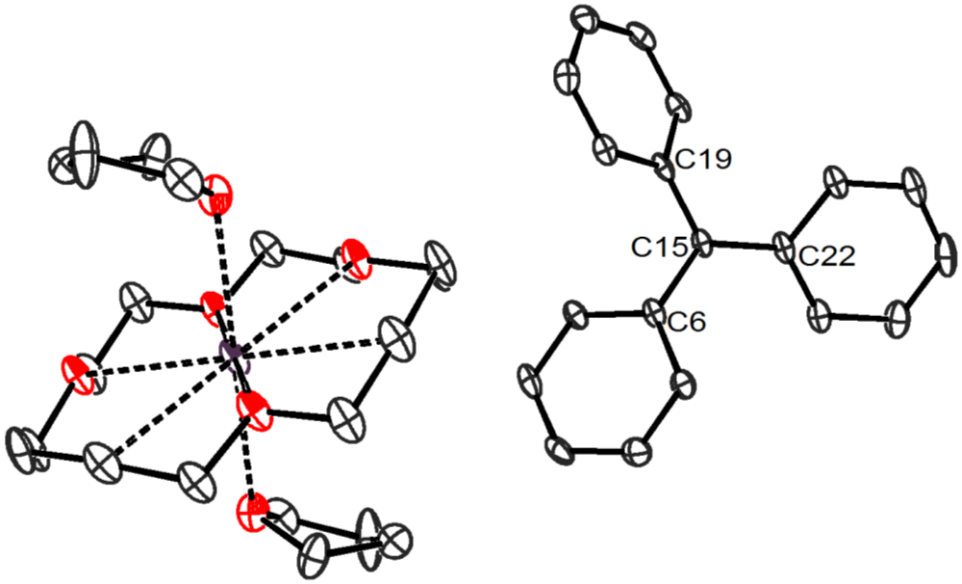

Figure 2.6. ORTEP diagram of [K(18-crown-6)(THF)$_2$][CPh$_3$] (**2.5**) with 50% probability ellipsoids. Hydrogen atoms are omitted for clarity. Selected bond lengths (Å) and angles (deg): C6-C15 = 1.466(4), C15-C22 = 1.437(4), C15-C19 = 1.458(4), C6-C15-C22 = 121.7(3), C6-C15-C19 = 117.8(2). C19-C15-C22 = 120.5(2).

2.2.7 Investigation of the Reaction of [U(NR$_2$)$_3$] with KOCPh$_3$ and 18-crown-6

In order to better understand the formation of complexes **2.3**, **2.4**, and **2.5**, the reaction of [U(NR$_2$)$_3$] with KOCPh$_3$ and 18-crown-6 was monitored by ^{1}H NMR spectroscopy. Addition of 1 equiv of KOCPh$_3$ to a cold (-25 °C) solution of [U(NR$_2$)$_3$] and 1 equiv of 18-crown-6 results in the formation of a deep purple/red solution.

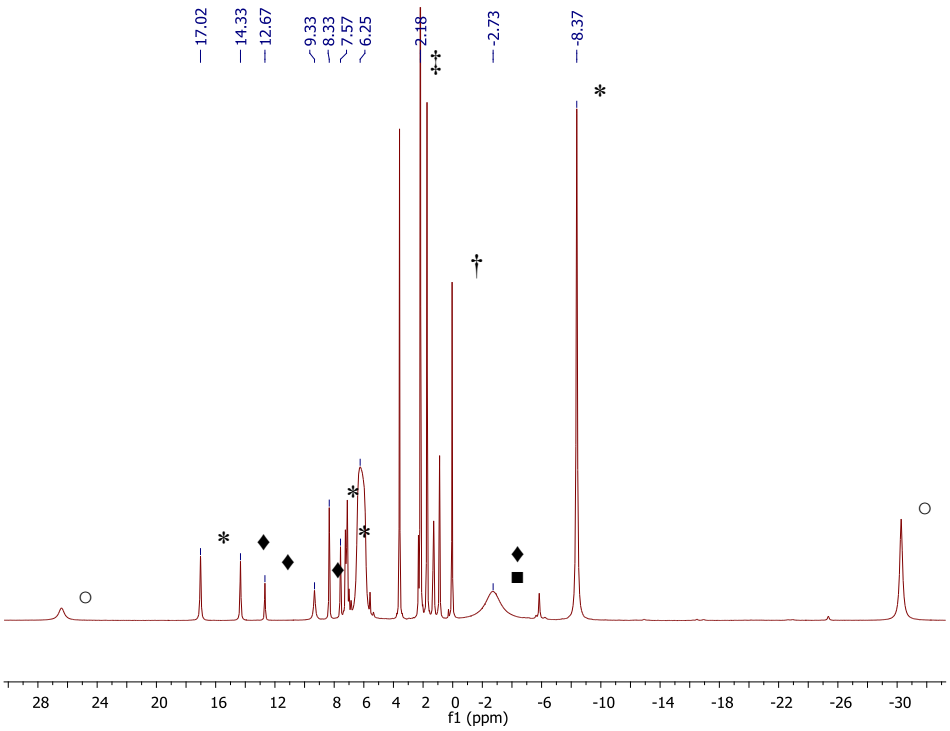

Figure 2.7. In-situ ^{1}H NMR spectrum of the reaction of $[U(NR_2)_3]$ with $KOCPh_3$ and 18-crown-6, in THF-d_8, after standing at -25 °C. (*) indicates the presence $[K(18\text{-crown-}6)][U(OCPh_3)(NR_2)_3]$, (■) indicates the presence of **2.3**, (♦) indicates the presence of **2.4**, (†) indicates the presence of $HN(SiMe_3)_2$, (‡) indicates the presence of hexamethylbenzene, and (○) indicates the presence of as-yet-unidentified products. Note that the $N(SiMe_3)_2$ signals for **2.3** and **2.4** overlap.

A ^{1}H NMR spectrum was obtained after standing for 30 min at -25 °C. This spectrum reveals the formation of a new species, that is tentatively assigned to a U(III) alkoxide complex, $[K(18\text{-crown-}6)][U(OCPh_3)(NR_2)_3]$. This assignment is based upon the presence of four new resonances at -8.37, 7.57, 8.33, and 17.02 ppm, in a 54:6:3:6 ratio. These resonances are attributable to the methyl groups of the silylamide ligands, and the *m*-, *p*-, and *o*- aryl protons of the triphenylmethyl alkoxide ligand, respectively (Figure 2.7). In addition, resonances attributable to complexes **2.3** and **2.4** are also observed. After warming to 25 °C

the resonances associated with [K(18-crown-6)][U(OCPh$_3$)(NR$_2$)$_3$] disappear, and those associated with complexes **2.3** and **2.4** grow in intensity. These observations can be explained

Scheme 2.7 Proposed Mechanism for the Formation of Complexes **2.3**, **2.4** and **2.5**

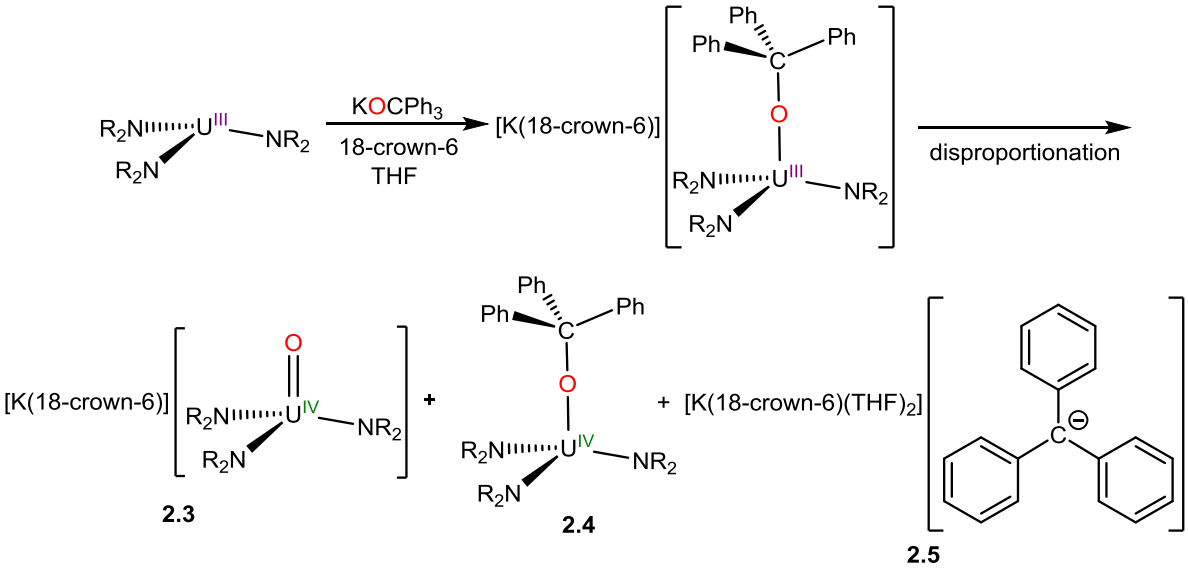

via two different mechanisms. In the first the U(III) alkoxide, [K(18-crown-6)][U(OCPh$_3$)(NR$_2$)$_3$], undergoes a disproportionation, in which one molecule of this U(III) species, reduces the triphenylmethyl fragment of a second molecule. The first molecule is thereby oxidized to form complex **2.4**, and reduction of the second molecule initiates heterolytic cleavage of the C-O bond, and gives rise to the formation of complexes **2.3** and **2.5** (Scheme 2.7). The second mechanism invokes the formation of a U(V) intermediate. In this case, the U(III) alkoxide, undergoes heterolytic cleavage to form the U(V) oxo, [U(O)(NR$_2$)$_3$] and complex **2.5**. This is followed by the reaction of another molecule of the U(III) alkoxide with this U(V) oxo that results in formation of both complexes **2.3** and **2.4** (Scheme 2.8).

Scheme 2.8 Alternative Mechanism for the Formation of Complexes **2.3**, **2.4** and **2.5**

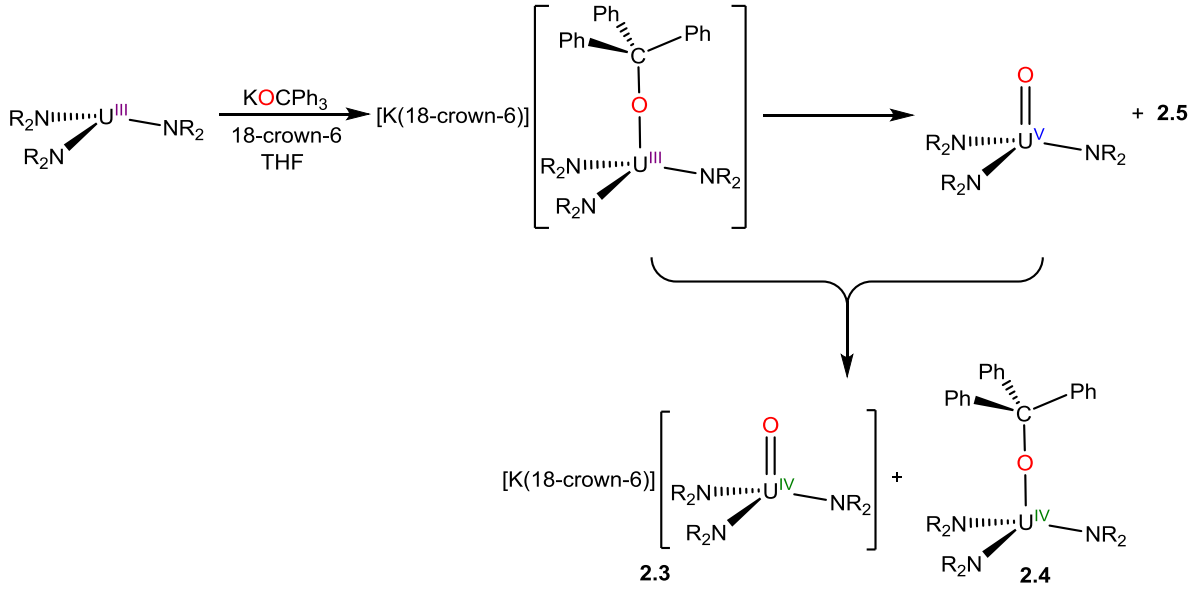

2.2.8 Reaction of $[U(OCPh_3)(NR_2)_3]$ (2.4) with KC_8 and 18-crown-6

The first mechanism (Scheme 2.7) suggests that removal of the triphenylmethyl group, in this system, can be achieved via reduction with an external reducing agent, similar to what has been seen in organic systems.[24-27] To test this hypothesis the reaction of complex **2.4** with an external

Scheme 2.9 Reductive Deprotection of $[U(OCPh_3)(NR_2)_3]$ (**2.4**)

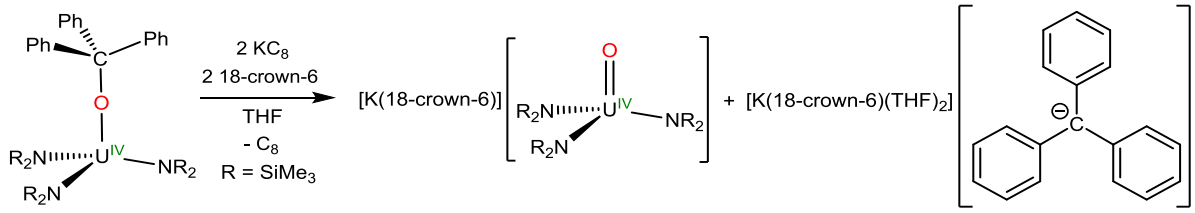

reducing agent was investigated. Addition of 1 equiv of KC_8 to a THF solution of **2.4** in the presence of 18-crown-6, results in the formation of complexes **2.3** and **2.5**, which can be isolated in 36% and 52% yields, respectively (Scheme 2.9). This reaction supports the first

mechanism, and is the first example of reductive deprotection of a triphenylmethyl group to form a terminal oxo ligand, which supports the idea that traditional organic synthetic protocols can be applied to inorganic systems.

2.2.9 Reaction of $[U(O)(NR_2)_3]$ with $[K(18\text{-crown-6})][CPh_3]$ (2.5)

In the second mechanism (Scheme 2.8), the first step affords both complex **2.5** and $[U(O)(NR_2)_3]$ via heterolytic cleavage of the U(III) alkoxide, $[K(18\text{-crown-6})][U(OCPh_3)(NR_2)_3]$. In order to probe the viability of this mechanism, the reaction of $[U(O)(NR_2)_3]$ with $[K(18\text{-crown-6})][CPh_3]$ (**2.5**), the microscopic reverse of the first step, was explored (Scheme 2.10).

Scheme 2.10 Reaction of $[U(O)(NR_2)_3]$ with $[K(18\text{-crown-6})][CPh_3]$ (**2.5**)

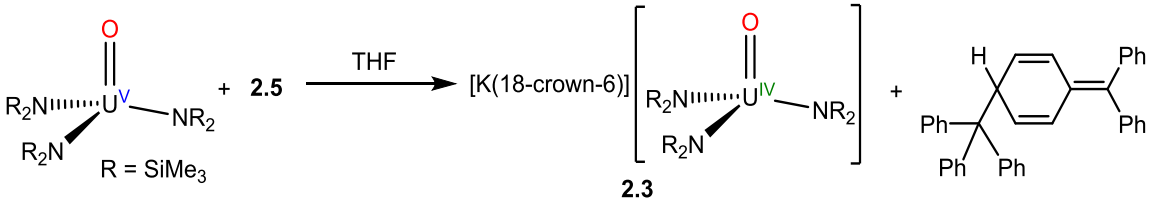

Monitoring the reaction of 1 equiv of **2.5** with $[U(O)(NR_2)_3]$, in THF-d_8, over the course of 90 min reveals the formation of complex **2.3** and Gomberg's dimer (Figure 2.8). Since no evidence for the formation of either $[U(O)(NR_2)_3]$ or Gomberg's dimer is observed in the reaction of $[U(NR_2)_3]$ with $KOCPh_3$ and 18-crown-6 (Figure 2.3), it again suggests that the first mechanism, involving disproportionation, is the operative one (Scheme 2.7).

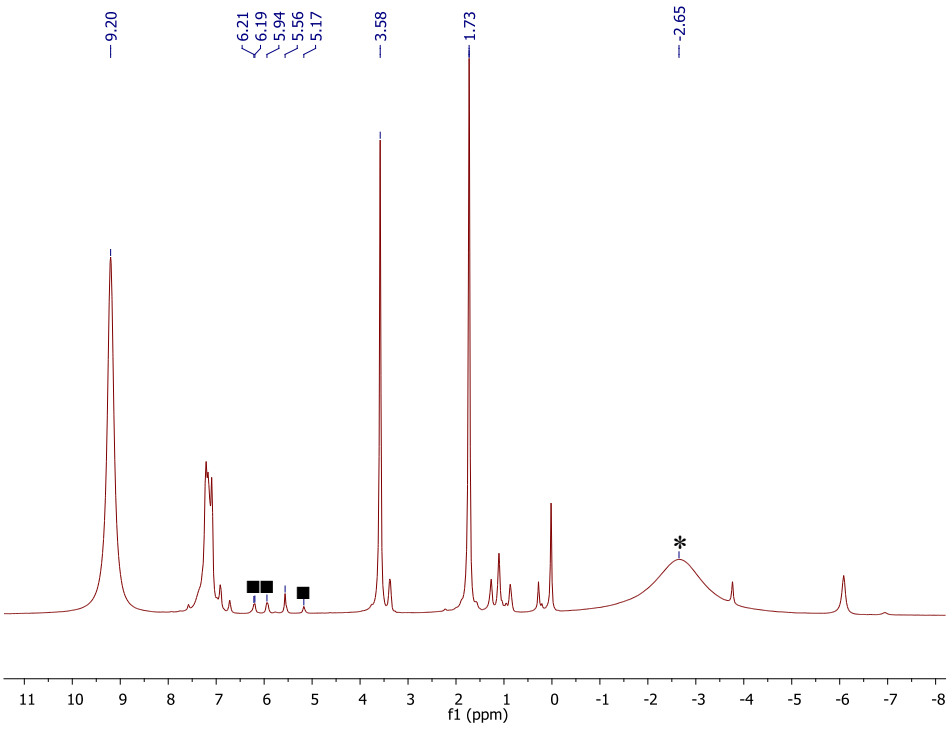

Figure 2.8. In situ ^{1}H NMR spectrum of the reaction of [U(O)(NR_2)$_3$] with **2.5** after 90 min in tetrahydrofuran-d_8. (*) indicates the presence of **2.3** and (■) indicates the presence of Gomberg's dimer.

2.2.10 Synthesis and Characterization of [Li(NHCPh$_3$)(THF)] (2.6)

With the desire to extend the deprotection protocol to the synthesis of an imido complex, the triphenylmethyl-amide salt was synthesized. This procedure is a modification of a literature procedure that did not isolate nor characterize the product.[32] Thus, addition of 1 equiv of *n*-BuLi to a 1:1 THF / diethyl ether solution of Ph_3CNH_2 results in the formation of a salmon colored solution. A salmon colored precipitate forms after 5 min, after which the solvent was removed in vacuo. Crystallization of this material from THF layered with hexanes affords [Li(NHCPh$_3$)(THF)] (**2.6**) as a salmon colored crystalline solid in 80% yield. The ^{1}H NMR spectrum of complex **2.6**, in THF-d_8, consists of six resonances. There are two multiplets at 1.77 and 3.62 ppm are assignable to the coordinated molecule of THF. The four

remaining resonances, a singlet, two triplets, and a doublet, at -0.26, 6.99, 7.08, and 7.27 ppm, are in a 1:3:6:6 ratio, and correspond to the N-H and *p*-, *m*-, and *o*-aryl proton environments, respectively. The $^{13}C\{^{1}H\}$ NMR spectrum of **2.6** exhibits five resonances at 73.11, 124.79, 127.11, 129.37, 157.87 ppm, attributable to the quaternary, *p*-, *m*-, and *o*- aryl, and ipso carbon environments, respectively. Lastly, the $^{7}Li\{^{1}H\}$ NMR spectrum exhibits a single broad resonance at 1.84 ppm as expected.

2.2.11 Synthesis and Characterization of $[Li(12\text{-crown-}4)_2][U(NHCPh_3)(NR_2)_3]$ (2.7)

With complex **2.6** in hand its reactivity with $[U(NR_2)_3]$ was explored. Addition of 1 equiv of $[Li(NHCPh_3)(THF)]$ (**2.6**) to a THF-d_8 solution of $[U(NR_2)_3]$ was followed by the addition of 2 equiv of 12-crown-4 after 30 min. No evidence is observed for either the formation of Gomberg's dimer or the triphenylmethyl anion. However, a set of new broad resonances, assignable to a new U(III) amide complex, are observed. This experiment was then repeated

Scheme 2.11 Synthesis of $[Li(12\text{-crown-}4)_2][U(NHCPh_3)(NR_2)_3]$ (**2.7**)

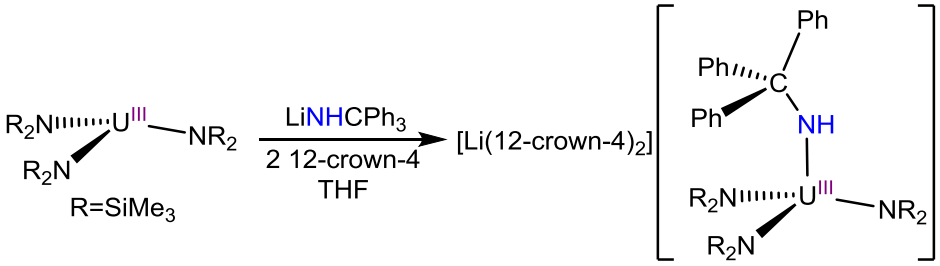

on a preparative scale; addition of 1 equiv of $[Li(NHCPh_3)(THF)]$ (**2.6**) to a THF solution of $[U(NR_2)_3]$ followed shortly by the subsequent addition of 2 equiv of 12-crown-4 results in the formation of a dark red-brown solution after 90 min. Crystallization from diethyl ether affords $[Li(12\text{-crown-}4)_2][U(NHCPh_3)(NR_2)_3]$ (**2.7**), as a dark red-brown microcrystalline solid in 42% yield (Scheme 2.11). The ^{1}H NMR spectrum of **2.7** features five broad resonances at -

7.41, 3.64, 6.22, 7.36, and 12.23 ppm, in a 54:24:3:6:6 ratio. These five resonances are assignable to the methyl groups of the silylamide ligands, the methylene groups of the 12-crown-4 moieties, and the *p*-, *m*-, and *o*-aryl protons of the triphenylmethyl group, respectively. The expected sixth resonance, attributable to the N-H proton of the $[NHCPh_3]^-$ is not observed. Despite its absence, the UV-Vis/NIR spectrum of complex **2.7** is consistent with a U(III) metal center (Figure A2.4).

Complex **2.7** crystallizes in the orthorhombic spacegroup $Pna2_1$, and its solid-state molecular structure is shown in Figure 2.9. Complex **2.7** features a tetrahedral geometry about uranium (av. N-U-N = 109.2°). The $U\text{-}N_{trityl}$ bond distance (U1-N4 = 2.342(4) Å) and the U-N-C angle (U1-N4-C19 = 151.2(3)°) are similar to those observed in the previously reported U(III) amide, $[K(THF)_2]_2[U(NH\text{-}2,6\text{-}^iPr_2C_6H_3)_5]$ (av. U-N = 2.34 Å; av. U-N-C = 149°),[33] further supporting the presence of a U(III) center. Additionally, the $U\text{-}N_{trityl}$ bond distance is markedly longer than the $U(IV)\text{-}N_{imido}$ bond lengths of the structurally similar, $[K][U(NCPh_3)(NR_2)_3]$ (U-N = 1.993(1) Å) or $[K][U(NSiMe_3)(NR_2)_3]$ (U-N = 2.010(3) Å).[34]

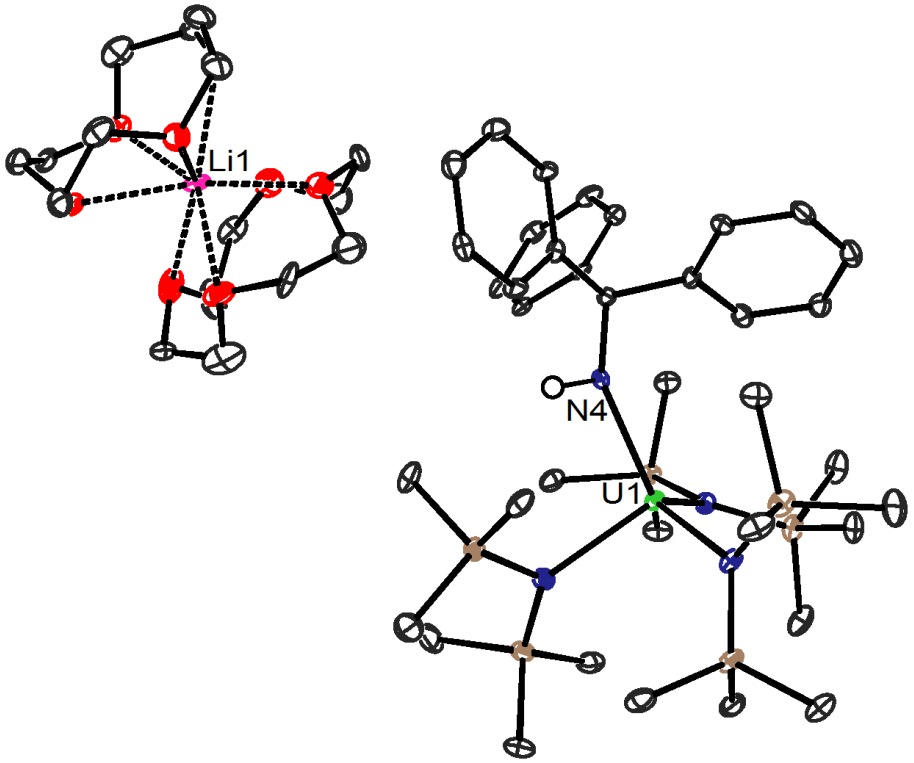

Figure 2.9. ORTEP diagram of $[Li(12\text{-crown-4})_2][U(NHCPh_3)(NR_2)_3]$ (**2.7**) with 50% probability ellipsoids. Hydrogen atoms, except the N-H proton, are omitted for clarity. Selected bond lengths (Å) and angles (deg): U1-N4 = 2.342(4), U1-N_{NR_2} (av.) = 2.402; U1-N4-C19 = 151.2(3), N-U-N (av.) = 109.2.

2.2.12 Synthesis and Characterization of $[U(NHCPh_3)(NR_2)_3]$ (2.8)

Scheme 2.12 Synthesis of $[U(NHCPh_3)(NR_2)_3]$ (**2.8**)

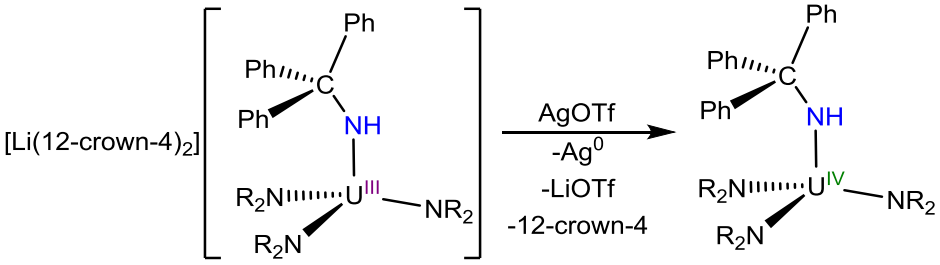

Attempts to remove the triphenylmethyl group of complex **2.7** were unsuccessful via reduction, however, during these experiments it was determined that **2.7** can be readily oxidized. Consequently, addition of 1 equiv of AgOTf to a THF solution of **2.7** results in a

color change from yellow-orange to yellow concomitant with the deposition of a black precipitate. Crystallization from diethyl ether affords the new U(IV) amide complex, [U(NHCPh$_3$)(NR$_2$)$_3$] (**2.8**), which can be isolated in 56% yield (Scheme 2.12). The ^{1}H NMR spectrum of **2.7** in THF-d_8 exhibits 3 broad resonances at -2.92, 1.62 and 4.51 ppm, in a 54:6:9 ratio, assignable to the methyl groups of the silylamide ligands, the *m*-, and overlapping *p*- and *o*-aryl protons of the triphenylmethyl ligand, respectively. In benzene-d_6, these peaks no longer overlap, and two distinct resonances can be observed in a 3:6 ratio (Figure A2.3). Similar to complex **2.7**, the resonance assignable to the N-H proton was not able to be definitively assigned. It should be noted that all attempts to cleave the C-N bond of complex **2.8** via reduction simply regenerated the U(III) amide (**2.7**).

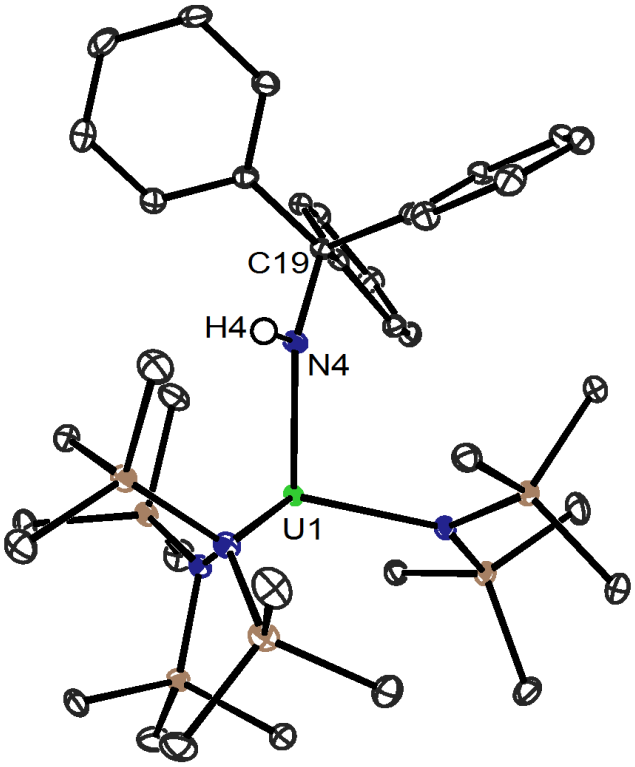

Figure 2.10. ORTEP diagram of [U(NHCPh$_3$)(NR$_2$)$_3$] (**2.8**) with 50% probability ellipsoids. Hydrogen atoms, except the N-H proton, are omitted for clarity. Selected bond lengths (Å)

and angles (deg): U1-N4 = 2.237(2), U1-N_{NR_2} (av.) = 2.275; U1-N4-C19 = 151.0(2), N-U-N (av.) = 109.4.

Complex **2.8** crystallizes in the triclinic spacegroup $P\bar{1}$, and its solid-state molecular structure is shown in Figure 2.10. Complex **2.8** is structurally identical to the $[U(NHCPh_3)(NR_2)_3]^-$ anion of complex **2.7**, featuring a tetrahedral geometry about uranium (av. N-U-N = 109.4°) as well as a bent U-N-C angle of 151.0(2)°. One notable difference is the U-N_{trityl} bond distance in **2.8** (U1-N4 = 2.237(2) Å), which is slightly shorter than the corresponding bond distance in complex **2.7**, consistent with the decrease in ionic radius going U(III) to U(IV).[35] Furthermore, the UV-Vis / NIR spectrum of complex **2.8** is consistent with a U(IV) metal center,[5,10,28] and similar to other structurally similar U(IV) complexes (Figure A2.4).

2.2.13 Bond Dissociation Energy and Cleavage of the Triphenylmethyl Group.

The differing reactivity observed between $[U(NR_2)_3]$ and the varying $[ECPh_3]^-$ ligands is due to several competing properties. The triphenylmethyl cleavage and formation of complexes **2.1**, **2.2**, and **2.3** can be explained in part as being driven by the favorable U(III/IV) redox potential. However, this alone cannot explain the differences between $KSCPh_3$ and $KOCPh_3$ that are observed. In addition to any favorable redox component, there is also an enthalpic component dependent upon both the bond dissociation energy (BDE) of the C-E bond being broken as well as the BDE of the new U-E bond being formed. Data for triphenylmethyl-heteroatom BDEs is not known, however, the C-E BDEs of a series of benzyl derivatives, $PhCH_2EH$, (E = S, 60.4 kcal/mol; O, 81 kcal/mol; NH, 74.0 kcal/mol) is known.[6,36] Taking into account this data, the spontaneous C-S bond cleavage and release of the triphenylmethyl radical in the reaction with $KSCPh_3$ can be explained by the relatively weak

C-S bond. This does not occur with the oxygen or nitrogen derivatives because of the stronger C-E bond in both these cases. However, disproportionation is an operative pathway in the case of the oxygen analogue, due to the oxophilic nature of uranium, which favors the formation of U-O multiple bonds,[37] and is likely not seen in the case of the nitrogen analogue because the energy required to break the C-N bond of $[HNCPh_3]^-$ is not outweighed by that of the new U-N multiple bond.

2.3 Summary

In summary, this chapter details the synthesis of new uranium-ligand multiple bonds utilizing a triphenylmethyl protecting group as the means of installation. Reaction of $[U(NR_2)_3]$ with $KSCPh_3$, in the presence of 18-crown-6, affords the U(IV) sulfide, [K(18-crown-6)][U(S)$(NR_2)_3$] (**2.1**) via homolytic C-S bond cleavage. This contrasts with the reaction of $[U(NR_2)_3]$ with $KOCPh_3$, in the presence of 18-crown-6, which yields the analogous oxo species, [K(18-crown-6)][U(O)$(NR_2)_3$] (**2.3**), as well as the U(IV) alkoxide, [U$(OCPh_3)(NR_2)_3$] (**2.4**), and the carbanion, [K(18-crown-6)$(THF)_2$][CPh_3] (**2.5**). Importantly, [K(18-crown-6)][U(O)$(NR_2)_3$] (**2.3**) can be synthesized rationally; addition of KC_8 to alkoxide complex **2.4** generates both complexes **2.3** and **2.5** via reductive cleavage of the triphenylmethyl fragment. In addition, reaction of $[U(NR_2)_3]$ with [Li$(NHCPh_3)$(THF)], in the presence of 12-crown-4, generates the U(III) amide, [Li(12-crown-4)$_2$][U$(NHCPh_3)(NR_2)_3$] (**2.7**). The divergent reactivities observed are believed to be a result of the differing bond dissociation energies of the C-E bond of the triphenylmethyl moiety as well as the new U-E bonds being formed. These results demonstrate the utility of protecting groups in inorganic syntheses. Furthermore, careful consideration of the installation as well

as the removal of the protecting group is necessary to successfully install these moieties in a controlled manner.

2.4 Experimental

2.4.1 General Methods

All reactions and subsequent manipulations were performed under anaerobic and anhydrous conditions under an atmosphere of nitrogen. Hexanes, diethyl ether (Et_2O), and toluene were dried using a Vacuum Atmospheres DRI-SOLV Solvent Purification system and stored over 3Å sieves for 24 h prior to use. Tetrahydrofuran (THF) was distilled twice, first from calcium hydride and then from sodium benzophenone ketyl, and stored over 3Å molecular sieves for 24 h prior to use. Dimethoxyethane (DME) was distilled from sodium benzophenone ketyl and stored over 3Å molecular sieves for 24 h prior to use. Pyridine, benzene-d_6, pyridine-d_5, and tetrahydrofuran-d_8 were dried over 3Å molecular sieves for 24 h prior to use. $[U(NR_2)_3]$,[38] $[U(O)(NR_2)_3]$,[28] $[U(I)(NR_2)_3]$,[28] $KSCPh_3$,[39] $KOCPh_3$,[40] $LiNHCPh_3$,[32] and Gomberg's dimer,[41] were synthesized according to the previously reported procedures. All other reagents were purchased from commercial suppliers and used as received.

NMR spectra were recorded on a Varian UNITY INOVA 400, a Varian UNITY INOVA 500 spectrometer, or a Varian UNITY INOVA 600 MHz spectrometer. ^1H and $^{13}C\{^1H\}$ NMR spectra were referenced to external $SiMe_4$ using the residual protio solvent peaks as internal standards. $^7Li\{^1H\}$ NMR spectra were referenced to external LiCl in D_2O. IR spectra were recorded on a Nicolet 6700 FT-IR spectrometer with a NXR FT Raman Module. UV-Vis / NIR experiments were performed on a UV-3600 Shimadzu spectrophotometer. Elemental analyses were performed by the Micro-Mass Facility at the University of California, Berkeley.

2.4.2 Synthesis of [K(18-crown-6)][U(S)(NR$_2$)$_3$] (2.1)

To a deep purple, cold (-25 °C), stirring solution of [U(N(SiMe$_3$)$_2$)$_3$] (98.8 mg, 0.14 mmol) in THF (3 mL) was added dropwise a cold (-25 °C), yellow solution of KSCPh$_3$ (46.9 mg, 0.15 mmol) in THF (2 mL). The solution became dark red-orange immediately upon addition, but lightened to vibrant orange after stirring for 20 min. The solvent was removed in vacuo and the orange solid was dissolved in hexanes (5 mL). This mixture was filtered through a Celite column supported on glass wool (0.5 cm × 2 cm) to provide a bright orange filtrate. To this filtrate was added 18-crown-6 (36.3 mg, 0.14 mmol), which resulted in the deposition of a yellow-orange solid. The solvent was removed in vacuo, and the resulting yellow-orange solid was extracted with diethyl ether (6 mL) and filtered through a Celite column supported on glass wool (0.5 cm × 2 cm). The yellow-orange filtrate was concentrated to 2 mL in vacuo. This solution was then transferred to a 4 mL scintillation vial which was placed inside a 20 mL scintillation vial filled with toluene (5 mL). Further concentration of the solution occurred as the diethyl ether slowly transferred, via the vapor phase, into the toluene–containing vial. Storage of the two-vial system at -25 °C for 24 h resulted in the deposition of yellow-orange blocks, which were isolated by decanting off the supernatant (70.1 mg, 48%). Anal. Calcd for $C_{30}H_{78}KN_3O_6SSi_6U$: C, 34.16; H, 7.45; N, 3.98. Found: C, 34.20; H, 7.36; N, 3.83. ^{1}H NMR (400 MHz, 25 °C, benzene-*d*$_6$): δ -2.02 (br s, 54H, NSiC*H*$_3$), -1.11 (br s, 24H, 18-crown-6). ^{1}H NMR (400 MHz, 25 °C, tetrahydrofuran-*d*$_8$): δ -2.67 (br s, 54H, NSiC*H*$_3$), 1.46 (br s, 24H, 18-crown-6). IR (KBr Mull, cm^{-1}): 608 (w), 665 (w), 687 (w), 756 (w), 773 (w), 841 (s), 937 (m), 964 (m), 1109 (s), 1182 (w), 1252 (m), 1354 (m), 1475 (w), 2895 (m), 2955 (m). UV-Vis/NIR (C_4H_8O, 3.90 mM, 25 °C, L·mol^{-1}·cm^{-1}): 612 (ε = 10.9), 704 (ε = 33.0), 720 (ε = 28.9), 946 (ε = 6.1), 1120 (ε = 21.1), 1216 (ε = 29.3).

2.4.3 Synthesis of [K(2,2,2,-cryptand)][U(S)(NR$_2$)$_3$] (2.2)

To a deep purple, cold (-25 °C), stirring solution of [U(N(SiMe$_3$)$_2$)$_3$] (214.2 mg, 0.30 mmol) in THF (3 mL) was added dropwise a cold (-25 °C), yellow solution of KSCPh$_3$ (96.8 mg, 0.31 mmol) in THF (2 mL). This resulted in an immediate color change to dark orange. After stirring for 3 min, a cold (-25 °C), colorless solution of 2,2,2-cryptand (113.8 mg, 0.30 mmol) in THF (3 mL) was added dropwise to the orange solution. This solution was allowed to stir for 1 h, whereupon the orange amber mixture was filtered through a Celite column supported on glass wool (0.5 cm × 3 cm). The volume of the amber filtrate was reduced to 5 mL in vacuo, and subsequently layered with a mixture of hexanes (6 mL) and DME (0.2 mL). Storage of this solution at -25 °C for 24 h resulted in the deposition of yellow-orange needles, which were isolated by decanting off the supernatant (236.1 mg). Recrystallization of this material from a solution of THF (3 mL) layered with a hexanes (4 mL) and DME (0.1 mL) yielded analytically pure yellow-orange needles (162.4 mg, 45%). Anal. Calcd for $C_{36}H_{90}KN_5O_6SSi_6U\cdot0.5C_4H_8O$: C, 37.94; H, 7.88; N, 5.82. Found: C, 37.82; H, 7.68; N, 5.79. ^{1}H NMR (400 MHz, 25 °C, benzene-d_6): δ -2.26 (br s, 54H, NSiCH_3), 0.32 (br s, 12H, NCH_2), 1.16 (br s, 12H, OCH_2CH$_2$N), 1.22 (br s, 12H, OCH_2CH_2O). ^{1}H NMR (400 MHz, 25 °C, pyridine-d_5): δ -2.23 (br s, 54H, NSiCH_3), 2.25 (t, 12H, J_{HH} = 4.6 Hz, NCH_2), 3.25 (t, 12H, J_{HH} = 4.6 Hz, OCH_2CH$_2$N), 3.29 (s, 12H, OCH_2CH_2O). IR (KBr Mull, cm^{-1}): 608 (w), 663 (w), 688 (w), 754 (w), 771 (w), 841 (s), 883 (m), 933 (s), 951 (s), 1107 (s), 1134 (m), 1182 (w), 1252 (m), 1298 (w), 1356 (m), 1446 (w), 1479 (w), 2816 (w), 2889 (m), 2956 (m). UV-Vis/NIR (C_4H_8O, 5.24 mM, 25 °C, L·mol^{-1}·cm^{-1}): 704 (ε = 38.8), 720 (ε = 33.2), 942 (ε = 10.7), 1122 (ε = 22.7), 1222 (ε = 30.4), 1512 (ε = 9.2).

2.4.4 Synthesis of [K(18-crown-6)][U(O)(NR$_2$)$_3$] (2.3)

To a deep red, cold (-25 °C), stirring solution of [U(O)(N(SiMe$_3$)$_2$)$_3$] (107.6 mg, 0.15 mmol) in THF (3 mL) was added KC_8 (34.4 mg, 0.25 mmol). After stirring for 2 min, a cold (-25 °C) solution of 18-crown-6 (38.5 mg, 0.15 mmol) in THF (2 mL) was added to this solution. This mixture was allowed to stir for 10 min, whereupon the color became pale red. Filtration of this mixture through a Celite column supported on glass wool (0.5 cm × 2 cm) gave a pale purple-red solution. The solvent was removed in vacuo and the solid was extracted with diethyl ether (6 mL) to provide a pale purple-red mixture. This mixture was filtered through a Celite column supported on glass wool (0.5 cm × 2 cm), whereupon the volume of the solution was reduced in vacuo to 2 mL. Storage of this solution at -25 °C for 24 h resulted in the deposition of pale purple blocks, which were isolated by decanting off the supernatant (75.7 mg, 50%). Anal. Calcd for $C_{30}H_{78}KN_3O_7Si_6U$: C, 34.69; H, 7.57; N, 4.05. Found: C, 34.89; H, 7.66; N, 4.00. ^{1}H NMR (400 MHz, 25 °C, benzene-*d*$_6$): δ -4.91 (br s, 54H, NSiC*H*$_3$), 16.15 (br s, 24H, 18-crown-6). IR (KBr Mull, cm^{-1}): 602 (w), 663 (w), 687 (w), 754 (w), 841 (s), 876 (sh), 937 (m), 964 (m), 1107 (s), 1182 (w), 1252 (m), 1286 (w), 1354 (m), 1456 (w), 1475 (w), 2895 (m), 2955 (m). UV-Vis/NIR (C_4H_8O, 5.60 mM, 25 °C, L·mol^{-1}·cm^{-1}): 610 (ε = 7.6), 704, (ε =23.1), 720 (ε = 20.3), 948 (ε = 4.3), 1120 (ε =14.8), 1216 (20.5).

2.4.5 Synthesis of [U(OCPh$_3$)(NR$_2$)$_3$] (2.4)

To a light brown, cold (-25 °C), stirring suspension of [U(I)(N(SiMe$_3$)$_2$)$_3$] (160.1 mg, 0.19 mmol) in THF (4 ml) was added dropwise a cold (-25 °C) solution of $KOCPh_3$ (86.8 mg, 0.29 mmol) in THF (2 mL). This resulted in the formation of a light brown solution. After stirring for 2 h, a fine white precipitate formed (KI). Filtration of this mixture through a Celite column supported on glass wool (0.5 cm × 2 cm) produced a faint purple filtrate. The solvent was

removed in vacuo, and the faint purple solid was extracted into diethyl ether (4 mL) and filtered through a Celite column supported on glass wool (0.5 cm × 2 cm). This yielded a faint purple filtrate. The volume of this solution was reduced in vacuo to 1 mL. Storage of this solution at -25 °C for 24 h resulted in the deposition of faint purple plates, which were isolated by decanting off the supernatant (70.1 mg, 38%). Anal. Calcd for $C_{37}H_{69}N_3OSi_6U$: C, 45.42; H, 7.11; N, 4.29. Found: C, 45.46; H, 7.26; N, 4.20. ^{1}H NMR (400 MHz, 25 °C, benzene-d_6): δ -4.85 (br s, 54H, NSiCH_3), 7.74 (br s, 3H, *p*-C*H*), 8.56 (br s, 6H, *m*-C*H*), 17.22 (br s, 6H, *o*-C*H*). IR (KBr Mull, cm^{-1}): 474 (w), 611 (m), 638 (w), 660 (m), 700 (m), 760 (m), 775 (m), 849 (s), 891 (s), 997 (m), 1036 (m), 1184 (w), 1252 (s), 1404 (w), 1446 (m), 1491 (w), 2899 (w), 2954 (m), 3024 (w), 3061 (w). UV-Vis/NIR (C_4H_8O, 6.00 mM, 25 °C, L·mol^{-1}·cm^{-1}): 462 (ε = 10.6), 520 (ε = 15.9), 578 (ε = 11.2), 684 (ε = 55.0), 840 (ε = 6.4), 908 (ε = 4.8), 1084 (ε = 12.7), 1182 (ε = 18.3), 1398 (ε = 7.2), 1572 (ε = 11.1).

2.4.6 Synthesis of [K(18-crown-6)(THF)$_2$][CPh$_3$] (2.5)

To a colorless, cold (-25 °C), stirring solution of triphenylmethane (270.9 mg, 1.11 mmol) and 18-crown-6 (293.2 mg, 1.11 mmol) in THF (5 mL) was added KC_8 (150.9 mg, 1.12 mmol). This mixture turned deep red immediately upon addition, and was allowed to stir for 15 min, whereupon a vibrant red solid was deposited. This mixture was then filtered through a Celite column supported on glass wool (0.5 cm × 3 cm). The red solid was dissolved in THF (20 mL) and filtered through this same column. The volume of this filtrate was reduced to 15 mL in vacuo. Storage of this solution at -25 °C for 24 h resulted in the deposition of vibrant red needles, which were isolated by decanting off the supernatant (339 mg, 44% yield). Anal. Calcd for $C_{31}H_{39}KO_6$: C, 68.10; H, 7.19. Found: C, 67.99; H, 7.42. ^{1}H NMR (600 MHz, 25 °C, pyridine-d_5): δ 3.44 (s, 24H, 18-crown-6), 6.49 (t, 3H, J_{HH} = 6.6 Hz, *p*-C*H*), 7.08

(t, 6H, J_{HH} = 7.5 Hz, *m*-C*H*), 8.17 (d, 6H, J_{HH} = 7.8 Hz, *o*-C*H*). $^{13}C\{^1H\}$ NMR (150 MHz, 25 °C, pyridine-d_5): δ 70.86 (18-crown-6), 91.44 ($C(C_6H_5)_3$), 114.17 (*p*-*C*), 125.09 (*o*-*C*), 129.14 (*m*-*C*). Resonance assignable to the ipso carbon was not observed due to overlap with a pyridine-d_5 resonance. The ^1H and ^{13}C spectral parameters of the trityl anion in **2.5** match with those previously recorded for this material.[31]

2.4.7 Synthesis of [Li(NHCPh$_3$)(THF)] (2.6)

To a colorless, cold (-25 °C), stirring solution of Ph_3CNH_2 (651.3 mg, 2.51 mmol), dissolved in a 1:1 mixture of THF/diethyl ether (3 mL), was added a cold (-25 °C) solution of *n*-butyllithium (0.36 mL, 0.90 mmol, 2.5M, and 1.00 mL, 1.60 mmol, 1.6M), dissolved in a mixture of THF (1.5 mL) and hexanes (1.5 mL). The resulting salmon colored mixture was stirred for 5 min, whereupon a salmon colored precipitate formed. The solvent was removed in vacuo and the solids were dissolved in THF (5 mL). The volume of this solution was reduced to 3 mL, and the solution was layered with hexanes (7 mL). Storage of this solution at -25 °C for 24 h resulted in the deposition of salmon colored crystalline solid, which was isolated by decanting off the supernatant (673.6 mg, 80% yield). ^1H NMR (400 MHz, 25 °C, tetrahydrofuran-d_8): δ -0.26 (s, 1H, N*H*), 1.77 (m, 2H, OCH_2CH_2), 3.62 (m, 2H, OCH_2H_2), 6.99 (t, 3H, J_{HH} = 7 Hz, *p*-C*H*), 7.08 (t, 6H, J_{HH} = 7.4 Hz, *m*-C*H*), 7.27 (d, 6H, J_{HH} = 7.2 Hz, *o*-C*H*). $^7Li\{^1H\}$ NMR (59 MHz, 25 °C, tetrahydrofuran-d_8): δ 1.84 (br, s). $^{13}C\{^1H\}$ NMR (100 MHz, 25 °C, tetrahydrofuran-d_8): δ 73.11 (C_q), 124.79 (C_p), 127.11 (C_m), 129.37 (C_o), 157.87 (C_{ipso}). The number of coordinated THF ligands was assumed to be one per Li; however the amount of THF, as determined by relative integrations in the ^1H NMR spectrum, was always found to be less than one, presumably due to partial removal of THF upon application of vacuum.

2.4.8 Synthesis of [Li(12-crown-4)$_2$][U(NHCPh$_3$)(NR$_2$)$_3$] (2.7)

To a deep purple, cold (-25 °C), stirring solution of [U(NR$_2$)$_3$] (253.9 mg, 0.35 mmol) was added a cold (-25 °C) solution of **2.6** (118.3 mg, 0.35 mmol) dissolved in THF (2 mL). After stirring for 2 min, a cold (-25 °C) solution of 12-crown-4 (130.8 mg, 0.74 mmol) in THF (2 mL) was added to the mixture. This mixture was allowed to stir for 90 min during which time the color of the solution became a dark red-brown. The solvent was removed in vacuo and triturated with diethyl ether (3 mL) and hexanes (3 mL). Extraction of the solids with diethyl ether (15 mL) and subsequent filtration through a Celite column supported on glass wool (0.5 cm × 3 cm) provided a dark red-brown solution. The volume of this solution was reduced in vacuo to 7 mL. Storage of this solution at -25 °C for 24 h resulted in the deposition of a dark red-brown microcrystalline solid, which was isolated by decanting off the supernatant (200.4 mg, 42%). Anal. Calcd for $C_{53}H_{102}LiN_4O_8Si_6U$: C, 47.62; H, 7.69; N, 4.19. Found: C, 47.71; H, 7.87; N, 4.15. ^{1}H NMR (400 MHz, 25 °C, tetrahydrofuran-d_8): δ -7.41 (br s, 54H, N(SiCH_3)$_2$), 3.64 (br s, 32H, 12-crown-4), 6.22 (br s, 3H, *p*-C*H*), 7.36 (br s, 6H, *m*-C*H*), 12.23 (br s, 6H, *o*-C*H*). ^{7}Li{^{1}H} NMR (59 MHz, 25 °C, tetrahydrofuran-d_8): δ -0.41 (br, s). IR (KBr Mull, cm^{-1}): 702 (m), 766 (w), 847 (m), 887 (w), 914 (m), 930 (m), 1026 (w), 1070 (m), 1095 (s), 1134 (s), 1182 (w), 1252 (m), 1290 (w), 1304 (w), 1363 (w), 1446 (w), 1489 (w), 1597 (w), 1630 (w), 2866 (m), 2918 (m), 2955 (m). UV-Vis/NIR (C_4H_8O, 4.18 mM 25 °C, L·mol^{-1}·cm^{-1}): 932 (ε = 82.7), 1024 (ε = 56.0), 1216 (ε = 20.8), 1482 (ε = 6.4), 2144 (ε = 16.8).

2.4.9 Synthesis of [U(NHCPh$_3$)(NR$_2$)$_3$] (2.8)

To a deep red-brown, cold (-25 °C), stirring solution of [Li(12-crown-4)$_2$][U(NHCPh$_3$)(NR$_2$)$_3$] (**2.7**) (215.3 mg, 0.16 mmol) in THF (4 mL) was added AgOTf (42.3 mg, 0.16 mmol). This mixture was allowed to stir for 10 min during which a black precipitate

forms. This mixture was then filtered through a Celite column supported on glass wool (0.5 cm × 3 cm) to give yellow-orange filtrate. The solvent was then removed in vacuo to give a yellow-orange solid. This was then extracted with diethyl ether (4 mL) and filtered through a Celite column supported on glass wool (0.5 cm × 3 cm) to give a cloudy yellow-orange solution. This solution was then filtered again through a Celite column supported on glass wool (0.5 cm × 3 cm) to give a yellow-orange filtrate. The volume of this filtrate was reduced in vacuo to 3 mL. Storage of this solution at -25 °C for 24 h resulted in the deposition of yellow-orange crystals, which were isolated by decanting off the supernatant (56.0 mg, 36%). The supernatant was then concentrated in vacuo to 1.5 mL and storage of this solution at -25 °C for 24 h resulted in the deposition of additional yellow-orange crystals. Total yield: 88.6 mg, 56%. Anal. Calcd for $C_{37}H_{70}N_4Si_6U$: C, 45.46; H, 7.22; N, 5.73. Found: C, 45.34; H, 7.41; N, 5.81. ^{1}H NMR (400 MHz, 25 °C, tetrahydrofuran-d_8): δ -2.92 (br s, 54H, N(SiCH_3)$_2$), 1.62 (br s, 6H, *m*-C*H*), 4.51 (br s, 9H, overlapping *p*-C*H* and *o*-C*H*). ^{1}H NMR (400 MHz, 25 °C, benzene-d_6): δ -2.82 (br s, 54H, N(SiCH_3)$_2$), 1.97 (br s, 6H, *m*-C*H*), 4.40-4.48 (m, 3H, *p*-C*H*), 4.53 (br s, 6H, *o*-C*H*). IR (KBr Mull, cm^{-1}):

2.4.10 Reaction of [U(NR$_2$)$_3$] with KSCPh$_3$

To a purple solution of [U(N(SiMe$_3$)$_2$)$_3$] (19.9 mg, 0.028 mmol) in tetrahydrofuran-d_8 (0.75 mL), in an NMR tube fitted with a J-Young valve, was added a faint yellow solution of KSCPh$_3$ (9.7 mg, 0.031 mmol) in tetrahydrofuran-d_8 (0.5 mL) A color change to orange was observed immediately upon addition. After 5 min a ^{1}H NMR spectrum was obtained that revealed the formation of **2.1** and Gomberg's dimer. ^{1}H NMR (400 MHz, 25 °C, tetrahydrofuran-d_8): δ -2.48 (br s, 54H, NSiCH_3, **2.1**), 5.21 (m, 1H, allylic), 5.98 (m, 2H, vinylic), 6.23 (m, 2H vinylic), 6.90-7.56 (m, 25H, aryl C*H*).

2.4.11 Reaction of $[U(NR_2)_3]$ with $KOCPh_3$ and 18-crown-6

Room Temperature

To a purple, frozen (-25 °C) solution of $[U(N(SiMe_3)_2)_3]$ (27.6 mg, 0.038 mmol), 18-crown-6 (10.0 mg, 0.038 mmol), and hexamethylbenzene (HMB) (4.4 mg, 0.027 mmol) in benzene-d_6 (1.5 mL), in an NMR tube fitted with a J-Young valve, was added a colorless solution of $KOCPh_3$ (10.7 mg, 0.036 mmol) in benzene-d_6 (0.5 mL). A color change to red was observed upon warming, concomitant with the deposition of a red solid. This reaction was monitored by ^{1}H NMR spectroscopy over the course of 24 h. ^{1}H NMR (400 MHz, 25 °C, benzene-d_6): δ -4.87 (br s, 54H, overlapping NSiCH_3 resonances from **2.3** and **2.4**), 5.93 (br s, 24H, 18-crown-6), 7.74 (br s, 3H, **2.4** *p*-C*H*), 8.57 (br s, 6H, **2.4** *m*-C*H*), 17.28 (br s, 6H, **2.4** *o*-C*H*). The resonances associated with complex **2.5** were not observed, due to overlap from the solvent and also its insolubility in this solvent. Comparison of the area of the CH_3 resonance of the HMB internal standard to the *meta*-C*H* resonance of **2.4** revealed a 61% yield of this product. Likewise, a comparison of the CH_3 resonance of HMB with the Si(CH_3)$_3$ resonance of **2.3**, after taking into account the amount of complex **2.4** that contributed to this signal, revealed a ratio of 1.1:1 for **2.3**: **2.4**, consistent with the proposed reaction stoichiometry.

Low Temperature

To a purple, cold (-25 °C) solution of $[U(N(SiMe_3)_2)_3]$ (19.3 mg, 0.027 mmol), 18-crown-6 (7.4 mg, 0.028 mmol), and HMB (3.3 mg, 0.020 mmol) in tetrahydrofuran-d_8 (0.75 mL), in an NMR tube fitted with a J-Young valve, was added a colorless solution of $KOCPh_3$ (8.3 mg, 0.028 mmol) in tetrahydrofuran-d_8 (0.25 mL). This dark red-purple solution was stored at -25 °C for 30 min, whereupon a ^{1}H NMR spectrum was obtained. ^{1}H NMR (400 MHz, 25 °C,

tetrahydrofuran-d_8): δ -8.37 (br s, 54H, [K(18-crown-6)][U(OCPh$_3$)(NR$_2$)$_3$] NSiCH_3), -2.73 (br s, 54H, overlapping NSiCH_3 resonances from **2.3** and **2.4**), 6.25 (br s, 24H, overlapping 18-crown-6 resonances from **2.3**, **2.4**, and **2.5**), 7.11-7.24 (m, 15H, **2.8** aryl C*H*), 7.57 (br s, 3H, **6** *p*-C*H*), 8.33 (br s, 6H, [K(18-crown-6)][U(OCPh$_3$)(NR$_2$)$_3$] *m*-C*H*), 9.33 (br s, 6H, **2.4** *m*-C*H*), 12.67 (br s, 3H, **2.4** *p*-C*H*), 14.33 (br s, 6H, **2.4** *o*-C*H*), 17.02 (br s, 6H, [K(18-crown-6)][U(OCPh$_3$)(NR$_2$)$_3$] *o*-C*H*). The solution was then allowed to stand at 25 °C for 10 min, whereupon the solution became vibrant red in color and another ^{1}H NMR spectrum was recorded. ^{1}H NMR (400 MHz, 25 °C, tetrahydrofuran-d_8): δ -2.69 (br s, 54H, overlapping NSiCH_3 resonances from **2.3** and **2.4**), 7.12-7.25 (m, 15H, **2.5** aryl C*H*), 7.66 (br s, 24H, overlapping 18-crown-6 resonances from **2.3**, and **2.4**), 9.31 (br s, 6H, **2.4** *m*-C*H*), 12.66 (br s, 3H, **2.4** *p*-C*H*), 14.31 (br s, 6H, **2.4** *o*-C*H*). Comparison of the area of the CH_3 resonance of HMB to the *ortho*-C*H* of **2.4** revealed a 99% yield of **2.4**. The yield for **2.3** was not able to be determined due to the broadness of the resonance attributed to N(SiCH$_3$)$_2$. The yield of **2.5** was not able to be determined due to overlap of the resonances attributed to the 18-crown-6 moiety of **2.3**.

Isolation of 2.5 from the Reaction Mixture

To a purple, cold (-25 °C). stirring solution of [U(NR$_2$)$_3$] (45.1 mg, 0.063 mmol) in toluene (2 mL) was added a cold solution of KOCPh$_3$ (20.3 mg, 0.068 mmol) in toluene (2 mL). The color of the solution became deep red upon addition. After 5 min 18-crown-6 was added (16.0 mg, 0.061 mmol). The solution was then allowed to stir for another 15 min. After stirring the solution was dried in vacuo, extracted with diethyl ether (6 mL), and filtered through a Celite column supported on glass wool (0.5 cm × 2 cm). This gave a red-purple filtrate, while a plug of bright red solid was trapped on the Celite column. This red solid was dissolved in

tetrahydrofuran (4 mL), which gave a vibrant red solution. The volume of this solution was reduced in vacuo to 1 mL. Storage of this solution at -25 °C for 24 h resulted in the deposition of vibrant red needles, which were isolated by decanting off the supernatant (2.6 mg, 12%). The identity of the red needles was determined to be [K(18-crown-6)(THF)$_2$][Ph$_3$C] (**2.5**) by X-ray crystallography.

2.4.12 Reaction of [U(NR$_2$)$_3$] with [(LiNHCPh$_3$)(THF)] and 12-crown-4

To a deep purple solution of [U(NR$_2$)$_3$] (28.9 mg, 0.040 mmol) in tetrahydrofuran-d_8 (0.75 mL), was added a solution of **2.5** (13.7 mg, 0.041 mmol) in tetrahydrofuran-d_8 (0.25 mL). After standing for 30 min, 12-crown-4 was added (7 μL, 0.043 mmol). This reaction was monitored by ^{1}H NMR spectroscopy over the course of 15 min.

2.4.13 Reaction of [U(OCPh$_3$)(NR$_2$)$_3$] (2.4) with KC$_8$ and 18-crown-6

To a purple, cold (-25 °C), stirring solution of **2.4** (94.9 mg, 0.097 mmol) in THF (2 mL) was added KC$_8$ (26.9 mg, 0.20 mmol), which immediately yielded a dark red mixture. After 2 min, a cold (-25 °C), colorless solution of 18-crown-6 (51.7 mg, 0.20 mmol) in THF (3 mL) was added to this solution. This mixture was allowed to stir for 2 min, and then stored without stirring at -25 °C for 24 h. The solvent was then removed in vacuo, the solids were extracted with diethyl ether (6 mL), and subsequent filtration through a Celite column supported on glass wool (0.5 cm × 3 cm) provided an orange filtrate, while a plug of bright red solid was trapped on the Celite column. The volume of the filtrate was reduced in vacuo to 1 mL and storage of this solution at -25 °C for 24 h resulted in the deposition of faint purple crystalline solid. This solid was isolated by decanting off the supernatant (36.1 mg, 36%). Dissolution of the red solid in THF (10 mL) and filtration through the same Celite column gave a bright

red solution. Drying this solution in vacuo yielded a bright red powder (27.6 mg, 52%). The purple solid was identified as **2.3** by comparison of its ^{1}H NMR spectrum to that of an independently synthesized sample. The red solid was identified as **2.5** by comparison of its ^{1}H NMR spectrum to that of an independently synthesized sample. **2.3**: ^{1}H NMR (400 MHz, 25 °C, benzene-d_6): δ -4.90 (br s, 54H, N(SiCH_3)$_2$)), 17.00 (br s, 24H, 18-crown-6). **2.5**: ^{1}H NMR (500 MHz, 25 °C, pyridine-d_5): δ 3.46 (m, 24H, 18-crown-6), 6.50 (m, 3H, *p*-C*H*), 7.08 (m, 6H, *m*-C*H*), 8.19 (m, 6H, *o*-C*H*).

2.4.14 Reaction of [U(O)(NR$_2$)$_3$] with [K(18-crown-6)(THF)$_2$][Ph$_3$C] (2.5)

To a red solution of [U(O)(NR$_2$)$_3$] (12.1 mg, 0.016 mmol) in tetrahydrofuran-d_8 (1 mL), in an NMR tube fitted with a J-Young valve, was added a vibrant red solution of **2.5** (12.8 mg, 0.019 mmol) in tetrahydrofuran-d_8 (0.75 mL). The reaction was monitored by ^{1}H NMR spectroscopy over the course of 90 min, revealing the formation of **2.3** and Gomberg's dimer. ^{1}H NMR (400 MHz, 25 °C, tetrahydrofuran-d_8): δ -2.65 (br s, 54H, N(SiCH_3)$_2$)), 5.17 (m, 1H, allylic), 5.94 (m, 2H, vinylic), 6.21 (m, 2H, vinylic), 6.98-7.28 (m, 25H, aryl C*H*), 9.20 (br s, 24H, 18-crown-6).

2.4.15 Reaction of [K(18-crown-6)][U(O)(NR$_2$)$_3$] (2.3) with Gomberg's dimer

To a faint purple solution of **2.3** (12.7 mg, 0.012 mmol) in benzene-d_6 (1 mL), in an NMR tube fitted with a J-Young valve, was added a yellow solution of Gomberg's dimer (3.3 mg, 0.068 mmol) in benzene-d_6 (0.5 mL). The reaction was monitored by ^{1}H NMR spectroscopy over the course of 24 h. No reaction was observed during this time frame.

2.4.16 Reaction of $[U(O)(NR_2)_3]$ with Gomberg's dimer

To a bright red solution of $[U(O)(NR_2)_3]$ (19.7 mg, 0.027 mmol), in benzene-d_6 (1 mL), in an NMR tube fitted with a J-Young valve, was added a yellow solution of Gomberg's dimer (6.3 mg, 0.013 mmol), in benzene-d_6 (0.5 mL). This reaction was monitored by ^{1}H NMR spectroscopy over the course of 24 h. No formation of complexes **2.3** or **2.4** was observed; however, the formation of the U(IV) metallacycle, $[U(CH_2SiMe_2NSiMe_3)(NR_2)_2]$, was observed in the spectrum. This is a known product of the thermal decomposition of $[U(O)(NR_2)_3]$.[28]

2.4.17 Reaction of $[K(18\text{-crown-}6)][U(O)(NR_2)_3]$ (2.3) with $[K(18\text{-crown-}6)(THF)_2][CPh_3]$ (2.5)

To a faint purple solution of **2.3** (13.6 mg, 0.013 mmol) in tetrahydrofuran-d_8 (0.75 mL), in an NMR tube fitted with a J-Young valve, was added a red solution of **2.5** (12.8 mg, 0.019 mmol) in tetrahydrofuran-d_8 (0.75 mL). This reaction was monitored by ^{1}H NMR spectroscopy over the course of 72 h. No reaction was observed during this time frame.

2.4.18 Reaction of $[K(18\text{-crown-}6)][U(O)(NR_2)_3]$ (2.3) with KC_8

To a faint purple solution of **2.3** (10.2 mg, 0.01 mmol), in benzene-d_6 (0.75 mL) in an NMR tube fitted with a J-Young valve, was added KC_8 powder (4.0 mg, 0.03 mmol). The reaction was monitored by ^{1}H NMR spectroscopy over the course of 24 h. No reaction was observed during this time frame.

2.4.19 X-ray Crystallography

Data for **2.1**, **2.2**, **2.3**, **2.4**, **2.5**, **2.7**, and **2.8** were collected on a Bruker KAPPA APEX II diffractometer equipped with an APEX II CCD detector using a TRIUMPH monochromator

with a Mo Kα X-ray source (α = 0.71073 Å). The crystals were mounted on a cryoloop under Paratone-N oil, and all data were collected at 100(2) K using an Oxford nitrogen gas cryostream. Data were collected using ω scans with 0.5° frame widths. Frame exposures of 10 s were used for **2.3**, **2.7**, and, **2.5**. Frame exposures of 2 s (low angle), 5 s (medium angle), and 10 s (high angle) were used for **2.1**. Frame exposures of 10 s (low angle) and 15 s (high angle) were used for **2.2**. Frame exposures of 5 s (low angle) and 10 s (high angle) were use for **2.4** Data collection and cell parameter determination were conducted using the SMART program.[42] Integration of the data frames and final cell parameter refinement were performed using SAINT software.[43] Absorption correction of the data was carried out using the multi-scan method SADABS.[44] Subsequent calculations were carried out using SHELXTL.[45] Structure determination was done using direct or Patterson methods and difference Fourier techniques. All hydrogen atom positions were idealized, and rode on the atom of attachment. Structure solution, refinement, graphics, and creation of publication materials were performed using SHELXTL.[45]

The 2,2,2-cryptand of **2.2** exhibited positional disorder and was modeled over two positions in a 66:34 ratio. In addition, the C-N, C-O, and C-C bond distances were constrained to 1.45, 1.45, 1.53 Å, respectively, using the DFIX command. Furthermore, a disordered THF solvate in this structure was refined with 50% occupancy. For **2.3**, the 18-crown-6 moiety also exhibited positional disorder. It was modeled over two positions in a 56:44 ratio, while the C-O and C-C bond distances of the 18-crown-6 molecule were constrained to 1.45 and 1.50 Å, respectively, using the DFIX command. Finally, the two THF molecules in **2.5** exhibited positional disorder. A single carbon of one was modeled over two positions in a 62:38 ratio, while the other THF molecule was modeled over two positions in a 66:34 ratio.

Additionally, the C-O and C-C bond distances of this THF molecule were constrained to 1.45 and 1.50 Å, respectively, using the DFIX command. Hydrogen atoms were not assigned to disordered carbon atoms.

Table 2.2. X-ray Crystallographic Data for Complexes **2.1**, **2.2**, and **2.3**

	2.1	**2.2**·0.5C_4H_8O	**2.3**
empirical formula	$C_{30}H_{78}KN_3O_6SSi_6U$	$C_{38}H_{95}KN_5O_{6.5}SSi_6U$	$C_{30}H_{78}KN_3O_7Si_6U$
crystal habit, color	block, yellow-orange	needle, yellow-orange	plate, purple
crystal size (mm)	0.3 × 0.3 × 0.2	0.2 × 0.1 × 0.1	0.2 × 0.2 × 0.1
space group	$P\bar{1}$	$P2_1/c$	$P\bar{1}$
volume (Å^3)	5007.7(2)	5946.0(3)	2480.7(3)
a (Å)	12.7175(3)	11.2243(3)	11.0235(7)
b (Å)	18.8400(5)	16.4779(4)	12.7783(8)
c (Å)	21.7489(6)	32.1639(8)	18.3992(12)
α (deg)	91.460(2)	90.00	91.254(4)
β (deg)	105.661(2)	91.774(2)	93.268(4)
γ (deg)	92.752(2)	90.00	106.365(4)
Z	4	4	2
formula weight (g/mol)	1054.68	1203.92	1038.62
density (calculated) (Mg/m^3)	1.399	1.345	1.390
absorption coefficient (mm^{-1})	3.546	2.997	3.538
F_{000}	2152	2484	1060
total no. reflections	58315	34949	26297
unique reflections	30057	12361	12156
R_{int}	0.0508	0.0368	0.0273
final R indices (I >2σ(I)]	R_1 = 0.0250 wR_2 = 0.0539	R_1 = 0.0512 wR_2 = 0.1473	R_1 = 0.0535 wR_2 = 0.1277
largest diff. peak and hole (e$^-$ A^{-3})	2.076 and -2.180	3.502 and -1.191	2.749 and -3.170
GOF	0.901	1.148	1.100

Table 2.3. X-ray Crystallographic Data for Complexes **2.4**, **2.5**, **2.7**, and **2.8**

	2.4·$C_4H_{10}O$	**2.5**	**2.7**	**2.8**
empirical formula	$C_{41}H_{79}N_3O_2Si_6U$	$C_{39}H_{55}KO_8$	$C_{53}H_{102}LiN_4O_8Si_6U$	$C_{37}H_{70}N_4Si_6U$
crystal habit, color	plate, purple	block, red	block, red-brown	plate, yellow

crystal size (mm)	0.2 × 0.2 × 0.05	0.4 × 0.4 × 0.2	0.2 × 0.2 × 0.2	0.1 × 0.1 × 0.1
space group	$P\bar{1}$	$P\bar{1}$	$Pna2_1$	$P\bar{1}$
volume (Å^3)	2584.26(16)	1854.94(10)	6494.0(12)	2281.16(11)
a (Å)	11.7031(4)	12.4741(4)	15.8489(17)	10.6213(3)
b (Å)	12.7108(4)	12.5528(4)	34.478(4)	11.4947(3)
c (Å)	17.4991(7)	12.8731(4)	11.8844(13)	18.9241(6)
α (deg)	90.802(2)	87.589(2)	90.00	84.613(2)
β (deg)	92.647(2)	67.196(2)	90.00	89.674(2)
γ (deg)	96.274(2)	86.878(2)	90.00	82.630(2)
Z	2	2	4	2
formula weight (g/mol)	1052.64	1381.86	1336.90	977.54
density (calculated) (Mg/m^3)	1.353	1.237	1.367	1.423
absorption coefficient (mm^{-1})	3.313	0.193	2.659	3.744
F_{000}	1076	744	2764	992
total no. reflections	24786	30836	47274	26343
unique reflections	12489	10533	13733	14077
R_{int}	0.0230	0.0428	0.0524	0.0386
final R indices (I >2σ(I)]	R_1 = 0.0345 wR_2 = 0.1257	R_1 = 0.0794 wR_2 = 0.1664	R_1 = 0.0406 wR_2 = 0.0644	R_1 = 0.0307 wR_2 = 0.0597
largest diff. peak and hole (e$^-$ A^{-3})	2.788 and -1.403	1.497 and -0.605	0.981 and -1.136	1.138 and -1.304
GOF	1.057	3.496	1.027	0.963

2.5 Appendix

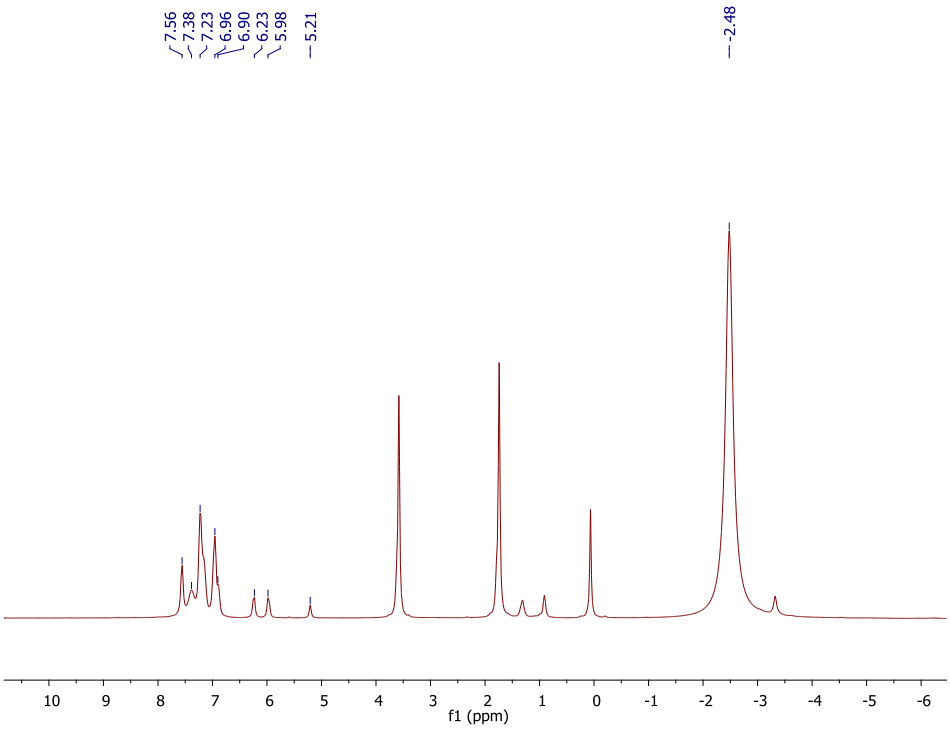

Figure A2.1. In-situ ^{1}H NMR spectrum of the reaction of $[U(NR_2)_3]$ with 1 equiv of $KSCPh_3$ in THF-d_8.

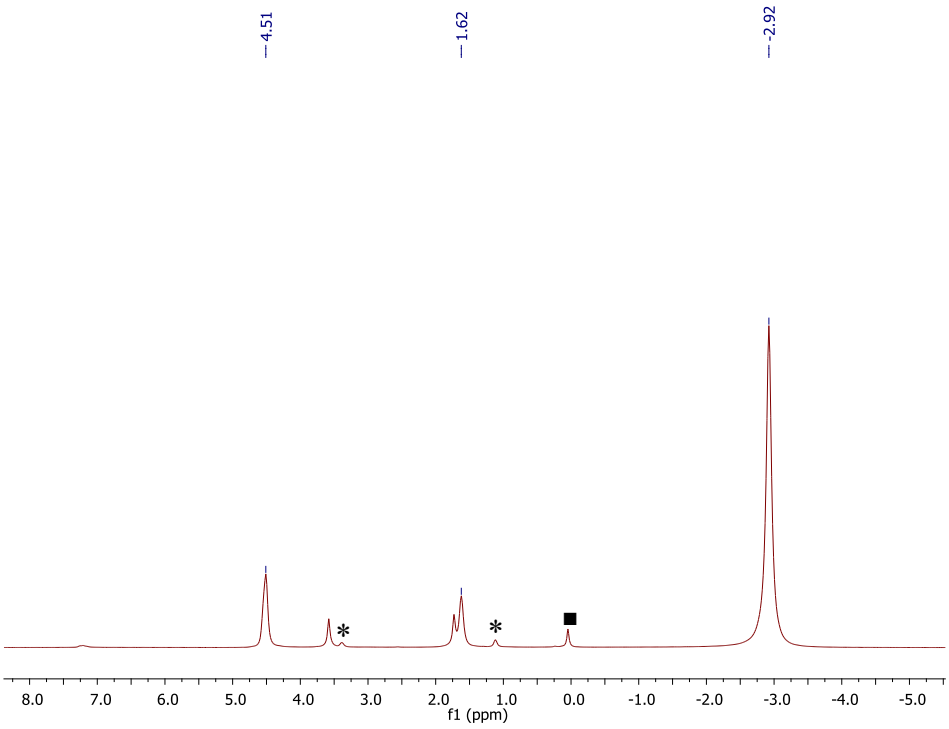

Figure A2.2. ^{1}H NMR spectrum of [U(NHCPh$_3$)(NR$_2$)$_3$] (**2.8**) in THF-d_8. (*) indicates the presence diethyl ether and (■) indicates the presence of HN(SiMe$_3$)$_2$.

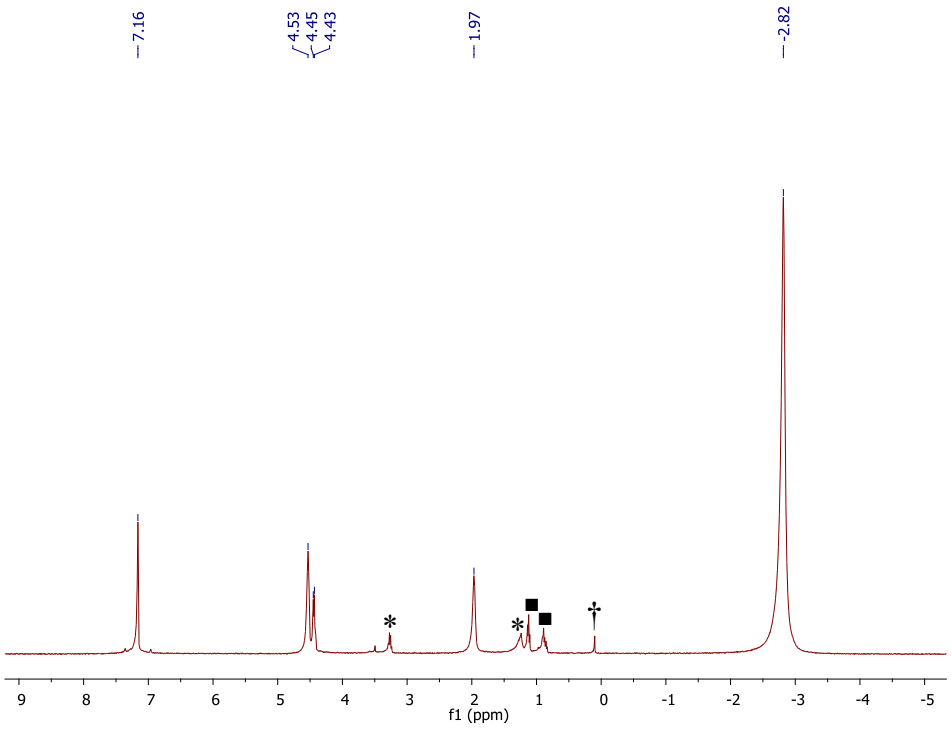

Figure A2.3. ^{1}H NMR spectrum of [U(NHCPh$_3$)(NR$_2$)$_3$] (**2.8**) in benzene-d_6. (*) indicates the presence diethyl ether, (■) indicates the presence of hexanes, and (†) indicates the presence of HN(SiMe$_3$)$_2$.

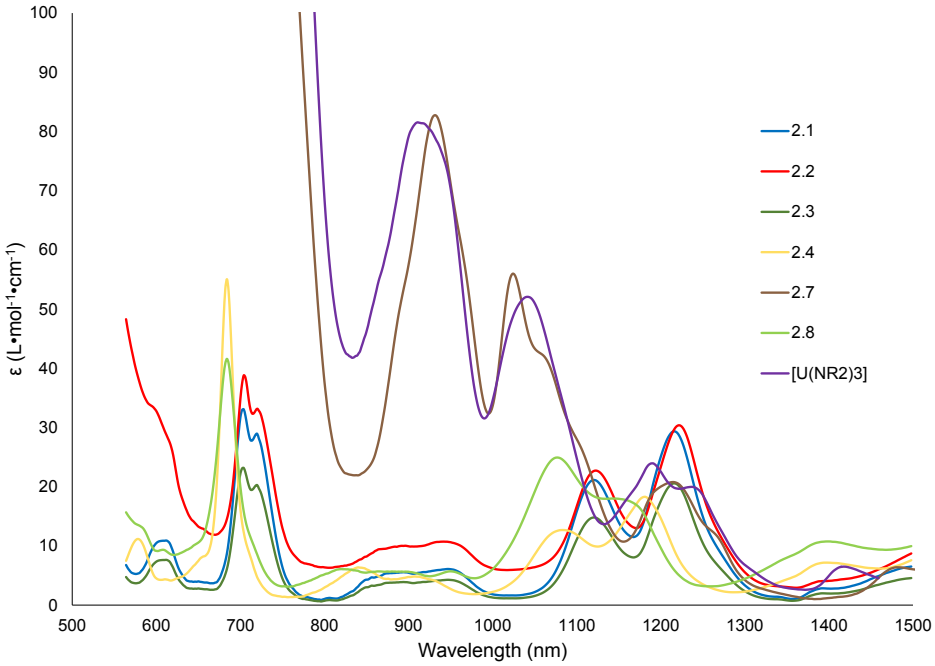

Figure A2.4. UV-VIS / NIR Spectra of Complexes **2.1**, **2.2**, **2.3**, **2.4**, **2.7**, **2.8**, and $[U(NR_2)_3]$. Concentration (mM) in C_4H_8O: **2.1**, 3.90; **2.2**, 5.24; **2.3**, 5.60; **2.4**, 6.00; **2.7**, 4.18; **2.8**, 6.02; $[U(NR_2)_3]$, 4.90. Data for $[U(NR_2)_3]$ taken from reference [7].

2.5.1 Synthesis and Characterization of [K(18-crown-6)][U(NTs)(NR_2)$_3$] (2.9)

Schelter and co-workers recently reported the synthesis of the U(IV) triphenylmethylimido complex, [K][U($NCPh_3$)(NR_2)$_3$], via the reduction of the analogous U(V) imido complex with excess KC_8.[34] Cleavage of the trityl group and formation of a nitride was not reported, and is likely due in part to the strength of the C-N bond of the imido ligand, similar to what was seen for the related U(IV) triphenylmethylamide complex, **2.8**. Based upon these results it was hypothesized that use of a different protecting group could afford access to the desired nitrido complex via the reductive deprotection protocol. A *p*-toluenesulfonyl (Ts, $MeC_6H_4SO_2$) or tosyl protecting group was chosen, as a S-N bond should be weaker than the corresponding C-N bond.[6] Also of note, Arnold and co-workers recently reported the synthesis of several thorium imido complexes via protonation of the Th(IV) metallacycle, [Th(*C*$H_2$$SiMe_2$*N*$SiMe_3$)($NR_2$)$_2$].[46] Thus, reaction of 1 equiv of KNHTs (Ts = $MeC_6H_4SO_2$)[47] with the U(IV) metallacycle, [U(*C*$H_2$$SiMe_2$*N*$SiMe_3$)($NR_2$)$_2$], in the presence of 18-crown-6, in THF affords the U(IV) imido complex, [K(18-crown-6)][U(NTs)(NR_2)$_3$] (**2.9**), as a tan powder in 78% yield (Scheme 2.13).

Scheme 2.13 Synthesis of [K(18-crown-6)][U(NTs)(NR$_2$)$_3$] (**2.9**)

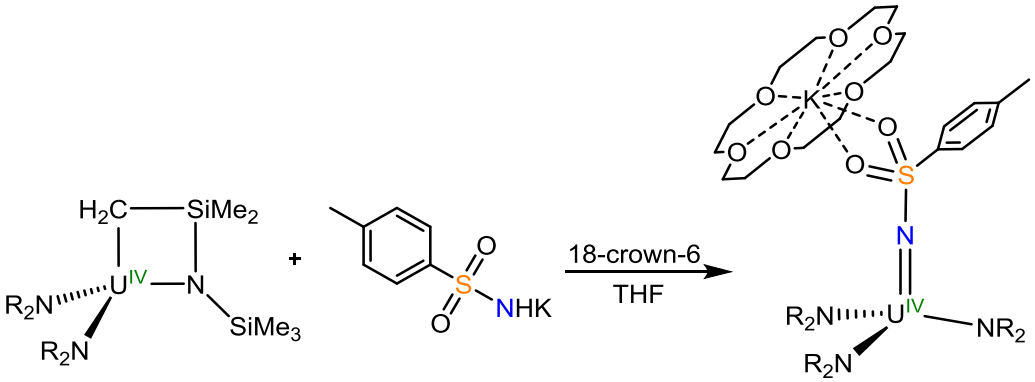

Crystals suitable for X-ray diffraction were grown from a concentrated pentane solution stored at -25 °C for 24 h. Complex **2.9** crystallizes in the triclinic spacegroup $P\bar{1}$, and its solid state molecular structure is shown in Figure A2.5. **2.9** features a pseudotetrahedral geometry about uranium (av. N-U-N = 109.1°). The U-N_{imido} bond distance (U1-N4 = 2.084(3) Å) of complex **2.9** is similar to those of other U(IV) imido complexes, including that of [K][U(NSiMe$_3$)(NR$_2$)$_3$] (U-N_{imido} = 2.010(3) Å).[34]

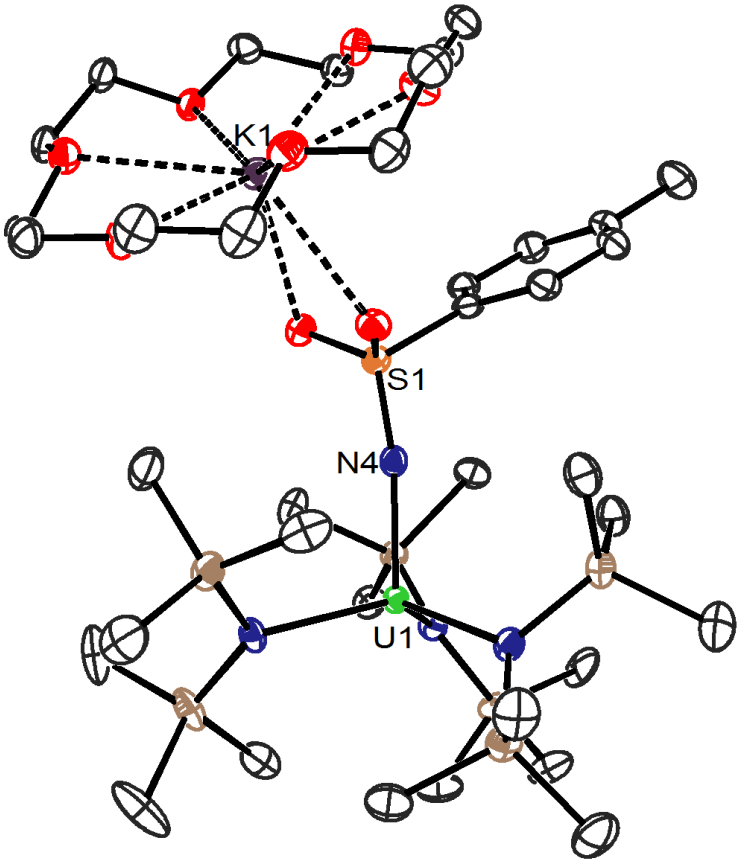

Figure A2.5. ORTEP diagram of [K(18-crown-6)][U(NTs)(NR_2)$_3$] (**2.9**) with 50% probability ellipsoids. Hydrogen atoms are omitted for clarity. Selected bond lengths (Å) and angles (deg): U1-N4 = 2.084(3), U1-N_{NR_2} (av.) = 2.299, N4-S1 = 1.551(3), N-U-N (av.) = 109.1, U1-N4-S1 = 169.7(2).

The ^{1}H NMR spectrum of complex **2.9**, in benzene-d_6, features two resonances at -2.79 and 2.98 ppm, assignable to the methyl groups of the silylamide ligands and the methylene groups of the 18-crown-6 moiety. Three additional resonances are observed at 0.69, 4.04 and 4.89 ppm, in a 3:2:2 ratio, attributable to the methyl group and two distinct aryl environments of the tosyl moiety (Figure A2.6).

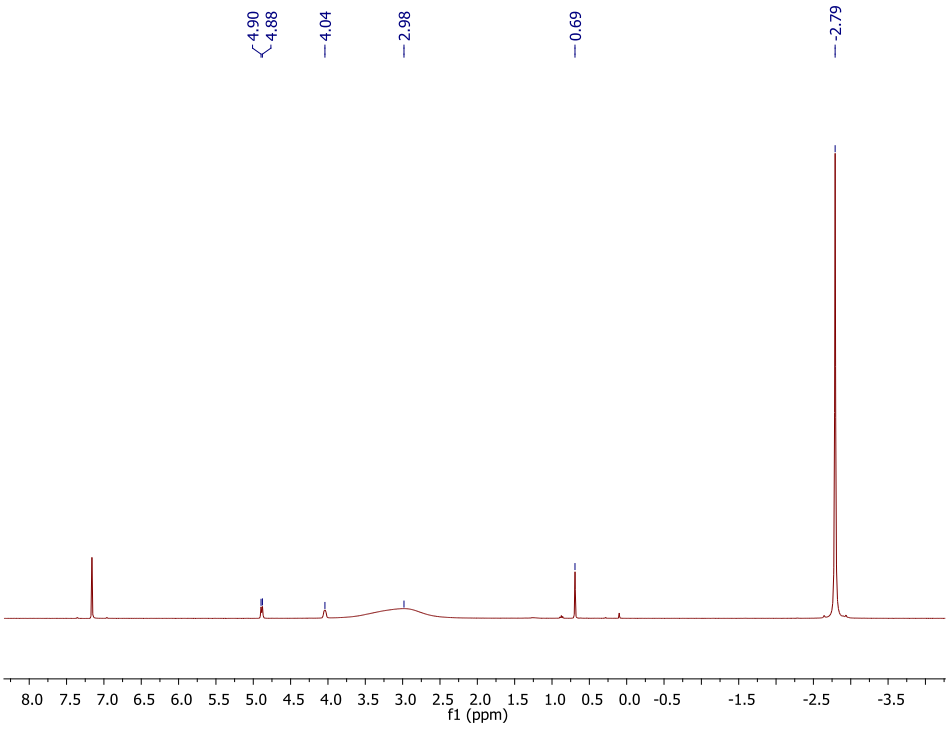

Figure A2.6. ^{1}H NMR spectrum of [K(18-crown-6)][U(NTs)(NR$_2$)$_3$] (**2.9**) in benzene-d_6.

2.6 References

(1) Hayton, T. W. *Chem. Commun.* **2013**, *49*, 2956.
(2) Hayton, T. W. *Dalton Trans.* **2010**, *39*, 1145.
(3) King, D. M.; Tuna, F.; McInnes, E. J. L.; McMaster, J.; Lewis, W.; Blake, A. J.; Liddle, S. T. *Science* **2012**, *337*, 717.
(4) Ventelon, L.; Lescop, C.; Arliguie, T.; Leverd, P. C.; Lance, M.; Nierlich, M.; Ephritikhine, M. *Chem. Commun.* **1999**, 659.
(5) Brown, J. L.; Fortier, S.; Lewis, R. A.; Wu, G.; Hayton, T. W. *J. Am. Chem. Soc.* **2012**, *134*, 15468.
(6) Luo, Y.-R. *Handbook of Bond Dissociation Energies in Organic Compounds*; CRC Press: Boca Raton, Florida, 2003.
(7) Fortier, S.; Walensky, J. R.; Wu, G.; Hayton, T. W. *J. Am. Chem. Soc.* **2011**, *133*, 6894.
(8) Rosenzweig, M. W.; Scheurer, A.; Lamsfus, C. A.; Heinemann, F. W.; Maron, L.; Andrez, J.; Mazzanti, M.; Meyer, K. *Chem. Sci.* **2016**.
(9) Andrez, J.; Pecaut, J.; Scopelliti, R.; Kefalidis, C. E.; Maron, L.; Rosenzweig, M. W.; Meyer, K.; Mazzanti, M. *Chem. Sci.* **2016**.
(10) Brown, J. L.; Wu, G.; Hayton, T. W. *Organometallics* **2013**, *32*, 1193.
(11) Lam, O. P.; Heinemann, F. W.; Meyer, K. *Chem. Sci.* **2011**, *2*, 1538.
(12) Franke, S. M.; Heinemann, F. W.; Meyer, K. *Chem. Sci.* **2014**, *5*, 942.
(13) Brennan, J. G.; Andersen, R. A.; Zalkin, A. *Inorg. Chem.* **1986**, *25*, 1761.
(14) Camp, C.; Antunes, M. A.; Garcia, G.; Ciofini, I.; Santos, I. C.; Pecaut, J.; Almeida, M.; Marcalo, J.; Mazzanti, M. *Chem. Sci.* **2014**, *5*, 841.
(15) Wuts, P. G. M.; Greene, T. W. *Greene's Protective Groups in Organic Synthesis*; John Wiley & Sons, Inc., 2006.
(16) Wuts, P. G. M.; Greene, T. W. In *Greene's Protective Groups in Organic Synthesis*; John Wiley & Sons, Inc.: 2006, p 16.
(17) Wuts, P. G. M.; Greene, T. W. In *Greene's Protective Groups in Organic Synthesis*; John Wiley & Sons, Inc.: 2006, p 647.
(18) Wuts, P. G. M.; Greene, T. W. In *Greene's Protective Groups in Organic Synthesis*; John Wiley & Sons, Inc.: 2006, p 696.
(19) Fujisawa, K.; Moro-Oka, Y.; Kitajima, N. *Chem. Commun.* **1994**, 623.
(20) Gomberg, M. *J. Am. Chem. Soc.* **1900**, *22*, 757.
(21) Lankamp, H.; Nauta, W. T.; MacLean, C. *Tetrahedron Lett.* **1968**, *9*, 249.
(22) Kawaguchi, H.; Tatsumi, K. *Organometallics* **1997**, *16*, 307.
(23) Arnold, P. L.; Turner, Z. R.; Kaltsoyannis, N.; Pelekanaki, P.; Bellabarba, R. M.; Tooze, R. P. *Chem. Eur. J.* **2010**, *16*, 9623.
(24) Yus, M.; Behloul, C.; Guijarro, D. *Synthesis* **2003**, *2003*, 2179.
(25) Behloul, C.; Guijarro, D.; Yus, M. *Synthesis* **2004**, *2004*, 1274.
(26) Kováč, P.; Bauer, Š. *Tetrahedron Lett.* **1972**, *13*, 2349.
(27) Hanessian, S.; Cooke, N. G.; DeHoff, B.; Sakito, Y. *J. Am. Chem. Soc.* **1990**, *112*, 5276.
(28) Fortier, S.; Brown, J. L.; Kaltsoyannis, N.; Wu, G.; Hayton, T. W. *Inorg. Chem.* **2012**, *51*, 1625.
(29) *Cambridge Structural Database*, version 1.18. 2015

(30) Miravilles, C.; Molins, E.; Solans, X.; Germain, G.; Declercq, J. P. *J. Inclusion Phenom.* **1985**, *3*, 27.
(31) Fernández, I.; Martínez-Viviente, E.; Breher, F.; Pregosin, P. S. *Chem. Eur. J.* **2005**, *11*, 1495.
(32) Theodorou, V.; Ragoussis, V.; Strongilos, A.; Zelepos, E.; Eleftheriou, A.; Dimitriou, M. *Tetrahedron Lett.* **2005**, *46*, 1357.
(33) Nelson, J. E.; Clark, D. L.; Burns, C. J.; Sattelberger, A. P. *Inorg. Chem.* **1992**, *31*, 1973.
(34) Mullane, K. C.; Lewis, A. J.; Yin, H.; Carroll, P. J.; Schelter, E. J. *Inorg. Chem.* **2014**, *53*, 9129.
(35) Shannon, R. D. *Acta Crystallogr. Sect. A* **1976**, *A32*, 751.
(36) Johnson, E. R.; Clarkin, O. J.; DiLabio, G. A. *J. Chem. Phys. A* **2003**, *107*, 9953.
(37) Barros, N.; Maynau, D.; Maron, L.; Eisenstein, O.; Zi, G. F.; Andersen, R. A. *Organometallics* **2007**, *26*, 5059.
(38) Andersen, R. A. *Inorg. Chem.* **1979**, *18*, 1507.
(39) Chadwick, S.; Englich, U.; Ruhlandt-Senge, K. *Organometallics* **1997**, *16*, 5792.
(40) Poulton, J. T.; Sigalas, M. P.; Folting, K.; Streib, W. E.; Eisenstein, O.; Caulton, K. G. *Inorg. Chem.* **1994**, *33*, 1476.
(41) Neumann, W. P.; Uzick, W.; Zarkadis, A. K. *J. Am. Chem. Soc.* **1986**, *108*, 3762.
(42) *SMART Apex II*, Version 2.1. 2005
(43) *SAINT Software User's Guide*, Version 7.34a. 2005
(44) *SADABS*, 2005
(45) *SHELXTL PC*, Version 6.12. 2005
(46) Bell, N. L.; Maron, L.; Arnold, P. L. *J. Am. Chem. Soc.* **2015**, *137*, 10492.
(47) Breugst, M.; Tokuyasu, T.; Mayr, H. *J. Org. Chem.* **2010**, *75*, 5250.

Chapter 3 Reductive Deprotection of a Triphenylmethyl Protecting Group for the Synthesis of Thorium-Ligand Multiple Bonds

Portions of this work were published in:

Danil E. Smiles, Guang Wu, Nikolas Kaltsoyannis, Trevor W. Hayton

Chem. Sci., **2015**, *6*, 3891-3899.

Table of Contents

3.1 Introduction

The importance of actinide-ligand multiple bonds to the study of covalency and f-orbital participation in bonding has spurred intense growth in the development of these species.[1-8] The last decade has seen reports of a wide variety of compounds with actinide-ligand multiple bonds, including oxos,[9-12] imidos,[13-15] and nitridos,[16-19] to highlight a few. Notably, almost all of these reported complexes are of uranium, and despite the success had with uranium, examples with other actinides, such as thorium, remain relatively rare.[20]

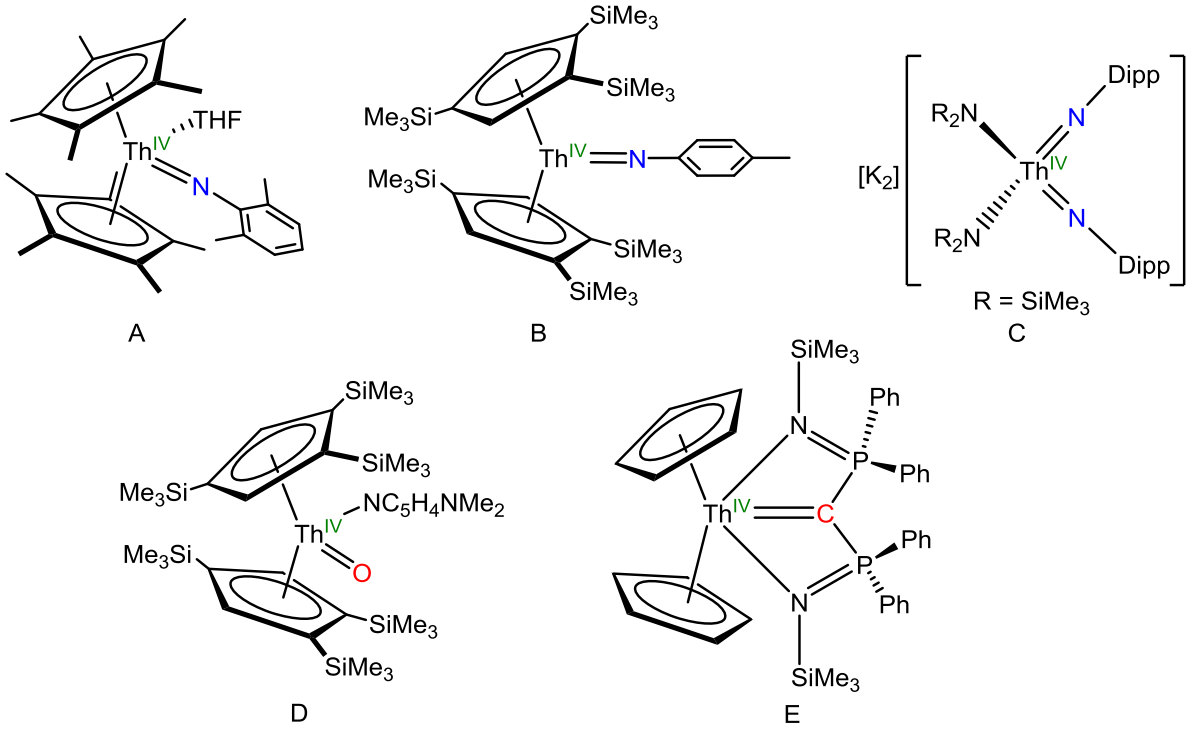

Figure 3.1. Previously reported complexes containing thorium-ligand multiple bonds. A, Ref. 21; B, Ref. 22; C, Ref. 23; D, Ref. 24; E, Ref. 25.

There are a few examples that have been reported, some of which are shown in Figure 3.1. The first thorium imido species, $[Cp^*_2Th(NAr)(THF)]$ (Ar = 2,6-dimethylphenyl), was reported by Eisen and co-workers in 1996, and was synthesized via the reaction of $[Cp^*_2Th(Me)_2]$ with 2,6-dimethylaniline.[21] In 2012, Zi and co-workers reported the synthesis

of a series of terminal imido complexes, [(η^5-1,2,4-^{t}Bu$_3$C$_5$H$_2$)$_2$Th(NR)] (R = *p*-tolyl, Ph$_3$C, Me$_3$Si).[22] More recently in 2015, Arnold and co-workers reported the synthesis of mono-, [K][Th(NDipp)(NR$_2$)$_3$], and bis-imido, [K$_2$][Th(NDipp)$_2$(NR$_2$)$_2$] (R = SiMe$_3$, Dipp = 2,6-^{i}Pr$_2$C$_6$H$_3$) complexes of thorium via protonation of the thorium metallacycles [Th(*C*H$_2$SiMe$_2$*N*SiMe$_3$)(NR$_2$)$_2$][26] and [K][Th(*C*H$_2$SiMe$_2$*N*SiMe$_3$)$_2$(NR$_2$)$_2$], respectively, with KNHDipp.[23] The only thorium terminal oxo known, [(η^5-1,2,4-^{t}Bu$_3$C$_5$H$_2$)$_2$Th(O)(dmap)] (dmap = dimethylaminopyridine) was reported by Zi and co-workers in 2011.[24] This complex was isolated from the reaction of [(η^5-1,2,4-^{t}Bu$_3$C$_5$H$_2$)$_2$Th(NR)] (R = *p*-tolyl) with Ph$_2$CO. Several thorium carbene complexes have also been reported.[25,27,28] This includes the first examples reported by Cavell and co-workers in 2011 that all utilized a bis(iminophosphorano) methanediide ligand [C(Ph$_2$P=NSiMe$_3$)$_2$]$^{2-}$.[25] Also in 2011, Zi and co-workers reported the synthesis of bis and tris carbene complexes of thorium, utilizing the structurally similar bis(thiophosphorano) methanediide ligand [C(Ph$_2$P=S)$_2$)]$^{2-}$.[27] Lastly, Liddle and co-workers reported the synthesis of several thorium carbenes again utilizing chelating pincer ligands with an NCN binding motif.[28]

The scarcity of complexes of thorium-ligand multiple bonds can be ascribed to both the difficulty installing these types of moieties in thorium based systems and the energetics of the thorium valence orbitals, especially compared to uranium. Specifically, it is believed that the higher energy of the 5f orbitals of thorium, weaken any metal-ligand π-bonding that may arise, making it harder to form a multiple bond.[29] Another challenge is the absence of nearly any metal based redox chemistry associated with thorium.[30-34] Numerous pathways developed for the synthesis of uranium-ligand multiple bond utilize oxidative atom transfer that cannot occur in an analogous thorium system due to this lack of redox chemistry. For example, Burns and

co-workers synthesized the uranium terminal oxo complex, $[Cp^*_2U(OAr)(O)]$ via reaction of $[Cp^*_2U(OAr)(THF)]$ with pyridine-*N*-oxide.[35] Similarly, Liddle and co-workers reported that reaction of $[U(Tren^{TIPS})]$ with NaN_3 and 12-crown-4 affords the first uranium terminal nitride, $[Na(12\text{-crown-}4)_2][U(N)(Tren^{TIPS})]$.[16] Both reactions proceeds via a $2e^-$ oxidation of U(III) to U(V). These reactions demonstrate the diversity of products that are inaccessible due to the inability of thorium to undergo redox chemistry. Notably, Zi and co-workers reacted $[(\eta^5\text{-}1,2,4\text{-}^tBu_3C_5H_2)_2Th(bipy)]$, which contains a dianionic bipy ligand, with azides RN_3 (R = *p*-tolyl, Ph_3C, Me_3Si) to afford the corresponding thorium imido complexes, $[(\eta^5\text{-}1,2,4\text{-}^tBu_3C_5H_2)_2Th(NR)]$.[36]

While limited progress has been made, new methods are still needed for installing thorium-ligand multiple bonds. In this regard the reductive deprotection protocol, which requires no oxidation state change, and discussed in Chapter 2, should be ideal for thorium based multiply bonded systems. This chapter describes the use of this reductive deprotection methodology for the synthesis of new thorium-ligand multiple bonds. These complexes are investigated both spectroscopically and structurally. In addition, in collaboration with Dr. Nikolas Kaltsoyannis, at the University of Manchester, DFT, in the form of Natural Bond Order (NBO) and Quantum Theory of Atoms-in-Molecules (QTAIM) analyses, is used to probe the electronic structure of the thorium terminal chalcogenides as well as their uranium analogues.

3.2 Results and Discussion

3.2.1 Synthesis and Characterization of $[Th(Cl)(NR_2)_3]$ (3.1) and $[Na(THF)_{4.5}][Th(Cl)_2(NR_2)_3]$ (3.2)

In order to test the efficacy of the reductive deprotection protocol in the analogous thorium system, equivalent starting materials needed to be synthesized, and while the synthesis of complex **3.1** has been previously reported by Bradley[37] and Andersen,[38] full characterization, including its solid state molecular structure, was not reported. Reaction of $ThCl_4(DME)_2$ with 3 equiv of $NaNR_2$ affords $[Th(Cl)(NR_2)_3]$ (**3.1**), as colorless crystals in 56% yield, after crystallization from diethyl ether / hexanes. Interestingly, crystallization instead from THF / hexanes affords the 'ate' complex, $[Na(THF)_{4.5}][Th(Cl)_2(NR_2)_3]$ (**3.2**), as determined by X-ray crystallographic analysis, in 63% yield.

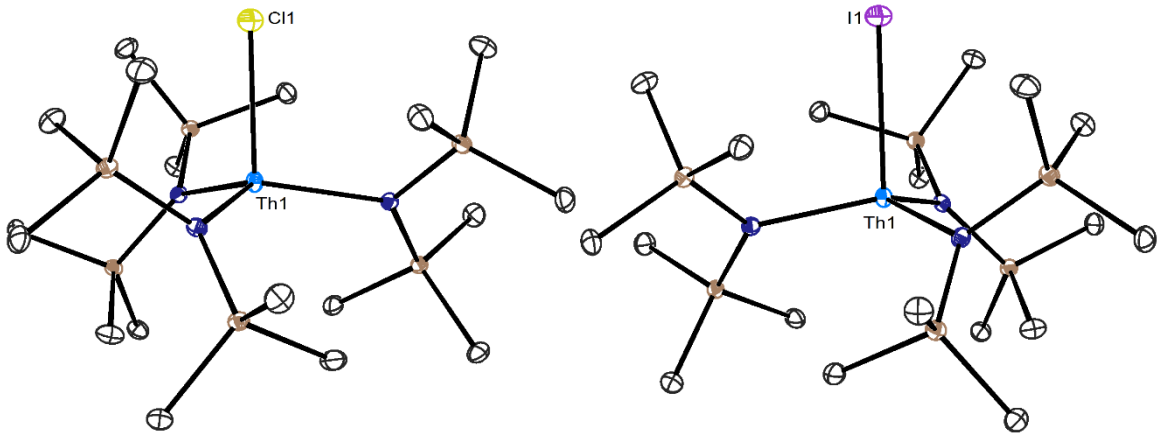

Figure 3.2. ORTEP diagram of $[Th(Cl)(NR_2)_3]$ (**3.1**) and $[Th(I)(NR_2)_3]$ (**3.3**) with 50% probability ellipsoids. Hydrogen atoms are omitted for clarity. Selected bond lengths (Å) and angles (deg): **3.1**, Th1-Cl1 = 2.647(1), Th1-N = 2.293(2), N-Th1-N = 116.74(3); **3.3**, Th1-I1 = 3.052(1), Th1-N = 2.299(4), N-Th1-N = 116.83(6).

The solid state molecular structures of complexes **3.1** and **3.2** are shown in Figure 3.2 and Figure 3.3, respectively. Complex **3.1** crystallizes in the hexagonal setting of the

rhombohedral spacegroup *R*3*c* and features a pseudotetrahedral geometry about thorium (N-Th1-N = 116.74(3)° and N-Th1-Cl1 = 100.53(4)°). Complex **3.2** crystallizes in the rhombohedral spacegroup $R\bar{3}$ and exhibits a trigonal bipyramidal geometry (N-Th1-N = 119.93(1)° and Cl1-Th1-Cl2 = 180.0°). Additionally, both complexes feature similar Th-Cl (**3.1**, Th1-Cl1 = 2.647(1) Å; **3.2**, Th1-Cl1 = 2.725(3) Å, Th1-Cl2 = 2.743(3) Å) and Th-N (**3.1**, Th1-N = 2.293(2) Å; **3.2**, Th1-N = 2.332(4) Å) bond distances, consistent with Th-Cl and Th-N single bonds.

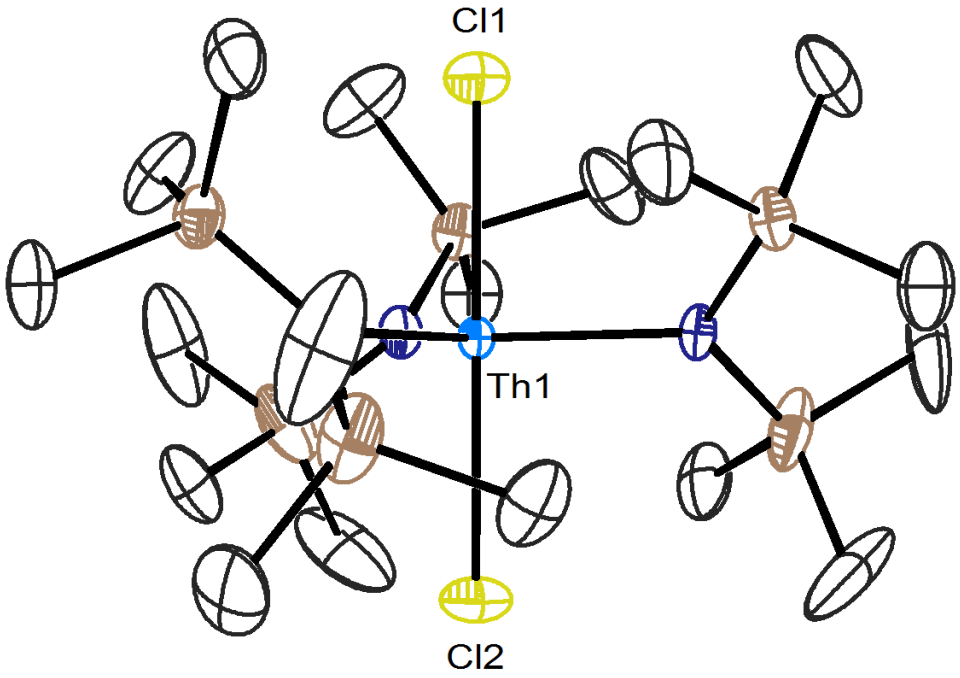

Figure 3.3. ORTEP diagram of $[Na(THF)_{4.5}][Th(Cl)_2(NR_2)_3]$ (**3.2**) with 50% probability ellipsoids. Na^+ cation, coordinated molecules of THF and hydrogen atoms are omitted for clarity. Selected bond lengths (Å) and angles (deg): Th1-Cl1 = 2.725(3), Th1-Cl2 = 2.743(3), Th1-N = 2.332(4), N-Th1-N = 119.93(1), Cl1-Th1-Cl2 = 180.0.

Complexes **3.1** and **3.2** exhibit nearly identical ^1H and $^{13}C\{^1H\}$ NMR spectra each with a single resonance at 0.41 and 4.26 ppm, corresponding to the proton and carbon environments of the silylamide ligands, respectively, the only difference being two additional resonances in

the spectra of complex **3.2**, corresponding to the molecules of coordinated THF. The melting point of complex **3.1** is 208-210 °C, consistent with that previously reported for this material,[38] while that of complex **3.2** is 196-199 °C. It should be noted that complex **3.2** can be readily converted into **3.1** upon extraction with and recrystallization from diethyl ether.

3.2.2 Synthesis and Characterization of [Th(I)(NR$_2$)$_3$] (3.3)

Conversion of complex **3.1** into the iodide analogue can be achieved via reaction with excess trimethylsilyliodide (TMSI), a procedure previously demonstrated to synthesize the related cerium iodide complex, [Ce(I)(NR$_2$)$_3$].[39] Accordingly, addition of excess TMSI to **3.1** in diethyl ether affords [Th(I)(NR$_2$)$_3$] (**3.3**) as a white powder in 95% yield (Scheme 3.1). The ^{1}H and ^{13}C{^{1}H} spectra of **3.3** are very similar to that of complex **3.1**. Each spectrum displays a single resonance, at 0.45 ppm and 5.13 ppm, respectively, assignable to the methyl groups of the silylamide ligands.

Scheme 3.1 Synthesis of [Th(I)(NR$_2$)$_3$] (**3.3**)

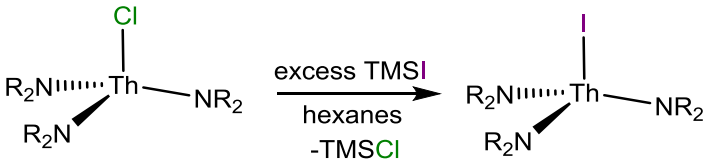

Crystals suitable for X-ray diffraction were grown from a concentrated diethyl ether solution stored at -25 °C for 24 h. Complex **3.3** crystallizes in the hexagonal setting of the rhombohedral space group *R*3c, and its solid state molecular structure is shown in Figure 3.2. Complex **3.3** is isostructural to its chloride analogue **3.1** again featuring a pseudotetrahedral geometry about thorium (N-Th1-N = 116.83(6)°). The Th-N bond distance in **3.3** (2.299(4) Å) is identical to that of **3.1**, and the Th-I bond length (3.052(1) Å) is longer than the Th-Cl

bond length of **3.1** consistent with the larger single bond covalent radius of I^- (1.33 Å) vs. Cl^- (0.99 Å).[40]

3.2.3 Synthesis and Characterization of $[Th(OCPh_3)(NR_2)_3]$ (3.4) and $[Th(OCPh_3)_2(NR_2)_2]$ (3.5)

Based upon the successful synthesis of the U(IV) alkoxide complex, $[U(OCPh_3)(NR_2)_3]$ (**2.4**), via reaction of $[U(I)(NR_2)_3]$ with $KOCPh_3$, and with complex **3.3** in hand, we endeavored to synthesize the analogous thorium alkoxide complex. Thus, the addition of 1 equiv of $KOCPh_3$ to a suspension of **3.3** in toluene affords a colorless solution, concomitant with the deposition of a white powder. Careful workup of this mixture affords a colorless oil, see experimental details, from which $[Th(OCPh_3)(NR_2)_3]$ (**3.4**) can be isolated as a colorless crystalline solid in 33% yield (Scheme 3.2). The formation of a bis-alkoxide complex,

Scheme 3.2 Synthesis of $[Th(OCPh_3)(NR_2)_3]$ (**3.4**) and $[Th(OCPh_3)_2(NR_2)_2]$ (**3.5**)

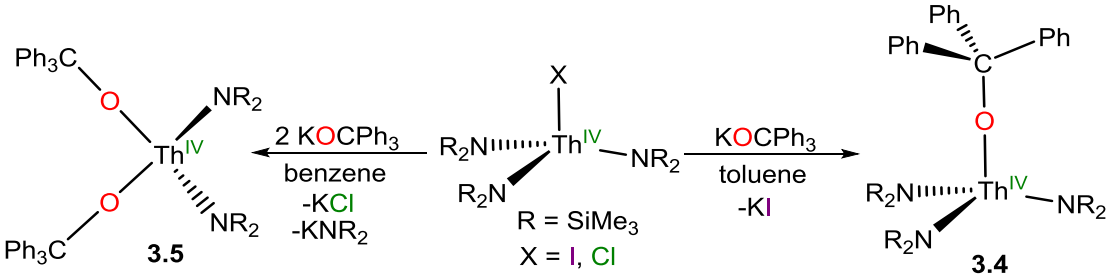

$[Th(OCPh_3)_2(NR_2)_3]$ (**3.5**) is also observed in this reaction. Complex **3.5** can be synthesized via the addition of 2 equiv of $KOCPh_3$ to a benzene solution of complex **3.1**, and can be isolated as colorless crystals in 34% yield, after crystallization from hexanes (Scheme 3.2). It should be noted that formation of both complexes **3.4** and **3.5** is observed for all reactions, and that reaction conditions as well as the starting halide complex appear to play a role as to which product is preferentially formed. Furthermore, while one can envision complex **3.5**

forming from the reaction of **3.4** and $KOCPh_3$, all attempts to transform complex **3.4** into **3.5**, via addition of excess $KOCPh_3$ were unsuccessful.

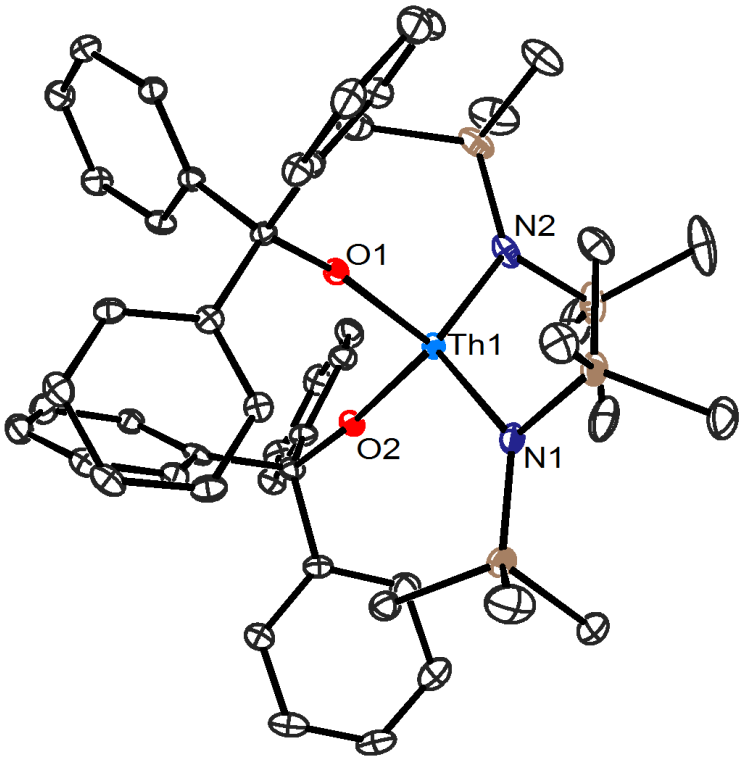

Figure 3.4. ORTEP diagram of $[Th(OCPh_3)_2(NR_2)_2]$ (**3.5**·$0.5C_6H_{14}$) with 50% probability ellipsoids. Hydrogen atoms and a hexanes solvate are omitted for clarity. Selected bond lengths (Å) and angles (deg): Th1-O1 = 2.123(2), Th1-O2 = 2.131(2), Th1-N1 = 2.358(3), Th1-N2 = 2.367(3); O2-Th1-O1 = 105.05(9), O2-Th1-N1 = 113.70(9), O1-Th1-N1 = 98.95(9), O2-Th1-N2 = 100.35(9), O1-Th1-N2 = 112.7(1), N1-Th1-N2 = 125.1(1).

Crystals of complex **3.4** suitable for X-ray diffraction analysis were not able to be obtained. This was not the case for complex **3.5**, which crystallizes in the triclinic spacegroup $P\bar{1}$, as a hexanes solvate, **3.5**·$0.5C_6H_{14}$, and its solid state molecular structure is shown in Figure 3.4. Complex **3.5** features a tetrahedral geometry about thorium with an average L-Th-L angle of 109.3° and a τ_4 value of 0.96.[41] The Th-O bond lengths in **3.5** (2.131(2) and 2.123(2) Å) are comparable to those reported for other complexes with Th-O single bonds (av.

2.20 Å),[42-47] and slightly longer than the U-O bond length of the uranium alkoxide, [U(OCPh$_3$)(NR$_2$)$_3$] (**2.4**) (2.098(3) Å), consistent with the longer ionic radius of Th^{4+} vs. U^{4+}.[48]

The ^{1}H NMR spectrum of **3.4** exhibits four resonances in benzene-d_6, in a 54:3:6:6 ratio. These resonances consists of a singlet at 0.39 ppm, assignable to the methyl groups of the silylamide ligands, as well as, two triplets and a doublet at 7.09, 7.18 and 7.39 ppm, assignable to the *p*-, *m*-, and *o*-aryl protons of the triphenylmethyl-alkoxide ligand. The $^{13}C\{^1H\}$ NMR spectrum of **3.4** exhibits six resonances at 5.53, 96.13, 127.56, 127.88, 129.90, and 148.16 ppm, assignable to the methyl groups of the silylamide ligands, and the five difference carbon environments of the triphenylmethyl-alkoxide ligand, respectively. The ^{1}H NMR spectrum of complex **3.5**, in benzene-d_6, exhibits a singlet at 0.26 ppm, and two multiplets at 7.06 and 7.38 ppm in a 54:18:12 ratio, respectively, assignable to the methyl groups of the silylamide ligands, the overlapping, *o*- and *p*-aryl protons and the *m*-aryl protons of the triphenylmethyl-alkoxide ligand. The $^{13}C\{^1H\}$ spectrum of **3.5** exhibits five resonances, at 4.18, 94.87, 127.25, 129.26 and 149.12, assignable to the methyl groups of the silylamide ligands, and four of the carbon environments of the triphenylmethyl-alkoxide ligands. The expected sixth resonance, assignable to the *o*-C, was not observed due to overlap with the benzene-d_6 resonance.

3.2.4 Synthesis and Characterization of [K(18-crown-6)][Th(O)(NR$_2$)$_3$] (3.6)

Spurred by our success at cleaving the C-O bond in complex **2.4**, [U(OCPh$_3$)(NR$_2$)$_3$], to afford the uranium oxo, [K(18-crown-6)][U(O)(NR$_2$)$_3$], **2.3**, we explored the reductive cleavage of the C-O bond in complex **3.4**. Gratifyingly, reduction of **3.4** with 2 equiv of

Scheme 3.3 Synthesis of [K(18-crown-6)][Th(O)(NR$_2$)$_3$] (**3.6**)

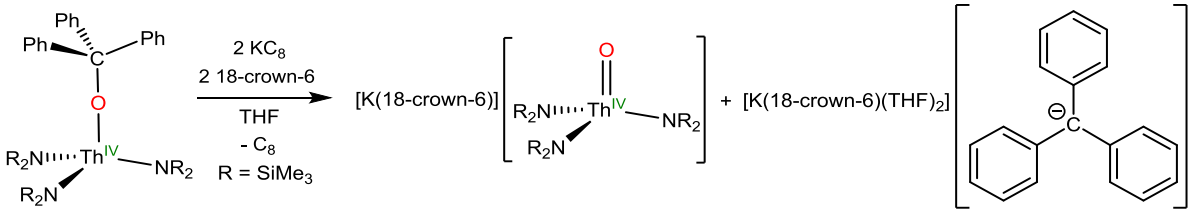

KC_8, in the presence of 18-crown-6, in THF results in the formation of a vibrant red mixture. This color is indicative of the presence of the $[CPh_3]^-$ anion. Extraction of this mixture with diethyl ether allows for removal of the [K(18-crown-6)(THF)$_2$][CPh$_3$] (**2.5**) a byproduct of the reaction. Crystallization from diethyl ether affords the thorium oxo complex, [K(18-crown-6)][Th(O)(NR$_2$)$_3$] (**3.6**), as colorless blocks in 23% yield (Scheme 3.3). The ^{1}H NMR spectrum of **3.6**, in benzene-d_6, exhibits two resonances at 0.64 and 3.09 ppm in a 54:24 ratio, assignable to the methyl groups of the silylamide ligands and the methylene groups of the 18-crown-6 moiety, respectively. The $^{13}C\{^1H\}$ also exhibits two resonances, at 5.47 and 70.30 ppm, assignable to the methyl groups of the silylamide ligands and the 18-crown-6 moiety, respectively.

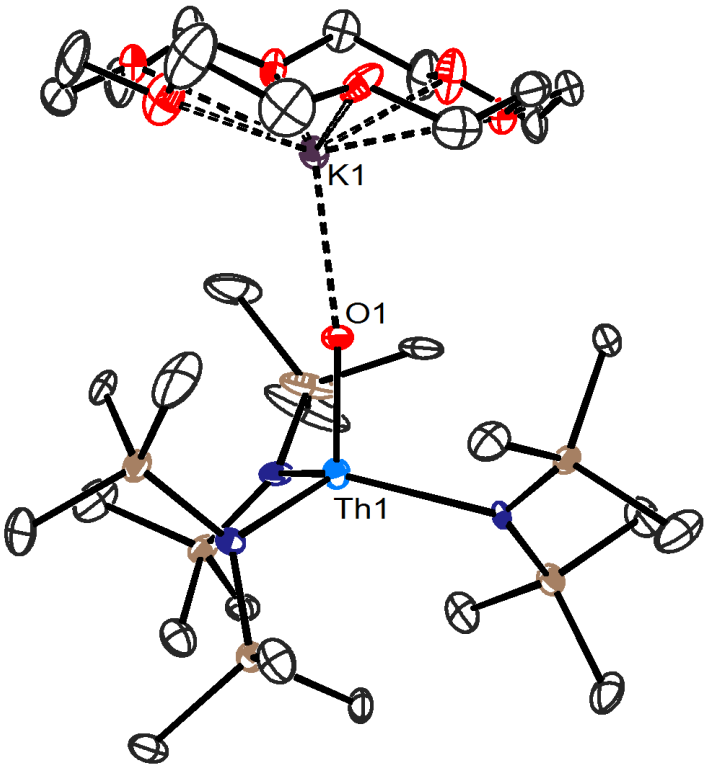

Figure 3.5. ORTEP diagram of [K(18-crown-6)][Th(O)$(NR_2)_3$] (**3.6**·0.5Et_2O) with 50% probability ellipsoids. Hydrogen atoms and a diethyl ether solvate are omitted for clarity. Selected bond lengths (Å) and angles (deg): Th1-O1 = 1.983(7), O1-K1 = 2.645(7), Th-N (av.) = 2.42, N-U-N (av.) = 115.6.

Complex **3.6** crystallizes in the orthorhombic spacegroup *Pbca*, as a diethyl ether solvate, **3.6**·0.5Et_2O, and its solid state molecular structure is shown in Figure 3.5. Complex **3.6** is structurally identical to its uranium analogue, [K(18-crown-6)][U(O)$(NR_2)_3$] (**2.3**), featuring a pseudotetrahedral geometry about thorium, and a dative interaction between the oxo ligand and the $[K(18\text{-crown-6})]^+$ moiety. The Th-O bond length (1.983(7) Å) is slightly longer than that of [(η^5-1,2,4-(^{t}Bu)$_3C_5H_2)_2$Th(O)], (Th-O = 1.929(4) Å),[24] but significantly shorter than typical Th-O single bonds (*ca.* 2.20 Å)[42-44,46,47,49], suggestive of some multiple bond character in this interaction. Furthermore, the Th-O bond distance in **3.6** is 0.09 Å longer than the analogous distance in [K(18-crown-6)][U(O)$(NR_2)_3$] (**2.3**), which is greater than the

difference in the ionic radii of Th^{4+} vs. U^{4+} (0.05 Å).[48]**Synthesis and Characterization [Th(SCPh$_3$)(NR$_2$)$_3$] (3.7)**

Similar to the synthesis of alkoxide complex **3.4**, a new thorium thiolate can also be synthesized from the thorium iodide, **3.3**. Thus, addition of 1 equiv of $KSCPh_3$ to a solution

Scheme 3.4 Synthesis of [Th(SCPh$_3$)(NR$_2$)$_3$] (**3.7**)

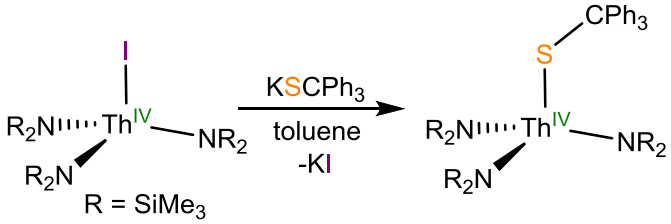

of **3.3,** in toluene, affords [Th(SCPh$_3$)(NR$_2$)$_3$] (**3.7**), which can be isolated as colorless crystals, in 57% yield, after crystallization from hexanes (Scheme 3.4). The ^{1}H NMR spectrum of complex **3.7**, in benzene-d_6, is extremely similar to that of **3.4**. The spectrum again features a total of four resonances, consisting of a sharp singlet at 0.42 ppm, assignable to the methyl groups of the silylamide ligands, in addition to two triplets and a doublet at 7.02, 7.16, and 7.66 ppm, assignable to the *p*-, *m*-, and *o*-aryl proton environments of the triphenylmethyl-thiolate ligand, in a 54:3:6:6 ratio, respectively. The ^{13}C{^{1}H} NMR spectrum of **3.7** features five resonances, at 5.21, 80.70, 126.78, 130.97 and 149.57, assignable to the methyl groups of the silylamide ligands, and four of the carbon environments of the triphenylmethyl-thiolate ligand. The expected fifth resonance of the triphenylmethyl-thiolate ligand, assignable to the *o*-C, was again not observed due to overlap with the benzene-d_6 resonance.

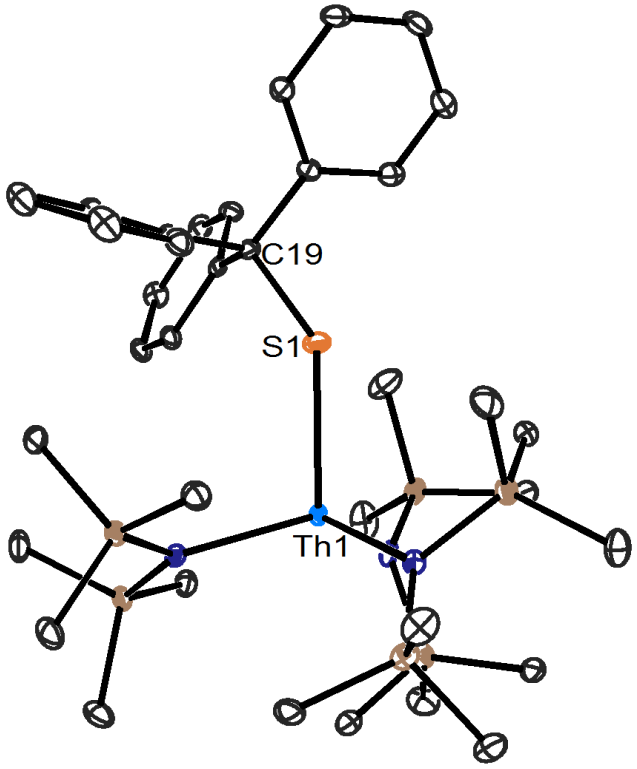

Figure 3.6. ORTEP diagram of [Th(SCPh$_3$)(NR$_2$)$_3$] (**3.7**) with 50% probability ellipsoids. Hydrogen atoms are omitted for clarity. Selected bond lengths (Å) and angles (deg): Th1-S1 = 2.704(1), S1-C19 = 1.866(4), Th-N (av.) = 2.31, N-Th-N (av.) = 112.2, Th1-S1-C19 = 13.72(1).

Complex **3.7** crystallizes in the triclinic spacegroup $P\bar{1}$, and its solid state molecular structure is shown in Figure 3.6. Complex **3.7** features a pseudotetrahedral geometry about thorium (av. N-Th-N = 112.2°, av. N-Th-S = 106.6°). The Th1-S1 bond distance in **3.7** (2.704(1) Å) is similar to those of other structurally characterized thorium thiolate complexes.[50,51] The Th-S-C bond angle in **3.7** (136.72(1)°) is similar to those of other thorium thiolate complexes,[50,51] and its acuteness likely indicates that there is very little 3p π-donation from S to Th.

3.2.6 Synthesis and Characterization of [K(18-crown-6)][Th(S)(NR$_2$)$_3$] (3.8)

In an identical manner to the synthesis of complex **3.6**, reduction of **3.7** with 2 equiv of KC_8 in the presence of 18-crown-6 in THF affords a bright red mixture. Extraction with

Scheme 3.5 Synthesis of [K(18-crown-6)][Th(S)(NR$_2$)$_3$] (**3.8**)

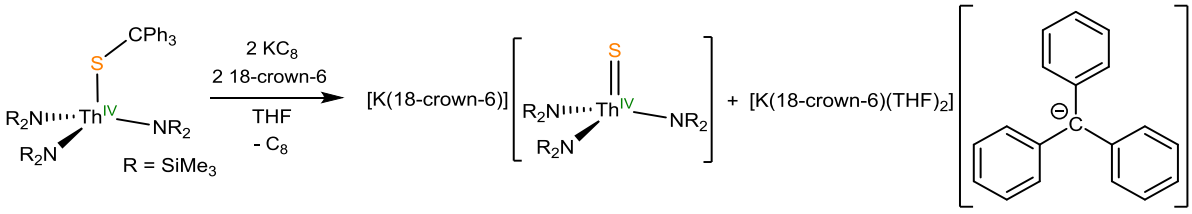

diethyl ether, to remove the anion byproduct, [K(18-crown-6)(THF)$_2$][CPh$_3$] (**2.5**), followed by crystallization from diethyl ether provides the thorium sulfido, [K(18-crown-6)][Th(S)(NR$_2$)$_3$] (**3.8**), as colorless crystals in 62% yield (Scheme 3.5). The ^{1}H NMR spectrum of **3.8**, in benzene-d_6, is very similar to that of complex **3.6**, exhibiting two resonances at 0.74 and 3.17 ppm in a 54:24 ratio, assignable to the methyl groups of the silylamide ligands and the methylene groups of the 18-crown-6 moiety, respectively. This is also the case for the ^{13}C{^{1}H} NMR spectrum of **3.8** that also exhibits two resonances, at 5.49 and 70.12 ppm, assignable to the methyl groups of the silylamide ligands and the 18-crown-6 moiety, respectively.

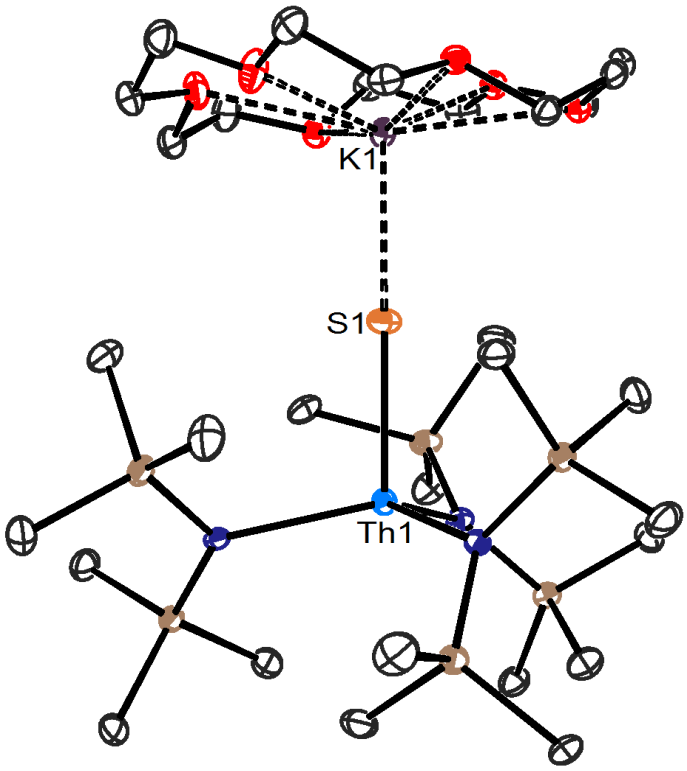

Figure 3.7. ORTEP diagram of [K(18-crown-6)][Th(S)$(NR_2)_3$] (**3.8**) with 50% probability ellipsoids. One molecule of **3.8** and hydrogen atoms are omitted for clarity. Selected bond lengths (Å) and angles (deg): Th1-S1 = 2.519(1), Th2-S2 = 2.513(1), S1-K1 = 3.122(2), S2-K2 = 3.039(2), Th-N (av.) = 2.363, N-Th-N (av.) = 116.6.

Complex **3.8** crystallizes in the triclinic spacegroup $P\bar{1}$, with two independent molecules in the asymmetric unit, and its solid state molecular structure is shown in Figure 3.7. Complex **3.8** is structurally identical to its uranium congener, [K(18-crown-6)][U(S)$(NR_2)_3$] (**2.1**), as well as its oxo analogue, complex **3.6**. **3.8** features a pseudotetrahedral geometry about thorium (av. N-Th-N = 116.6° and av. N-Th-S = 100.8°). The Th-S bond lengths in **3.8** (2.519(1) and 2.513(1) Å) are significantly shorter than what has been previously reported for Th-S single bonds, (*ca*. 2.74 Å)[24,50,51] suggestive of the multiple bond character in these interactions. Additionally, the Th-S bond distances of complex **3.8** are 0.07 Å longer than the analogous bonds of uranium complex **2.1**, which is consistent with the expected differences

in the ionic radii.[48] Lastly, the long S-K bond distances in **3.8** (3.122(1) and 3.039(2) Å) are similar to those of **2.1**, and are consistent with these being dative interactions.

3.2.7 DFT Analysis of [K(18-crown-6)][M(E)(NR$_2$)$_3$] (M =U, Th; E = O, S)

To gain greater insight into the electronic structures and bonding of these actinide terminal chalcogenides, the thorium complexes, **3.6** and **3.8**, along with their uranium analogues, **2.3** and **2.1**, were subjected to DFT analysis. This analysis was performed by Prof. Nikolas Kaltsoyannis at the University of Manchester. The geometries were optimized utilizing the PBE functional, and there was excellent agreement observed between the experimentally and computationally determined structures. The electronic structures of these complexes were investigated using Natural Bond Orbital (NBO) and the Quantum Theory of Atoms-in-Molecules (QTAIM) analyses, previously used to study actinide-covalency[2,4] and bond strengths.[52,53] NBO analysis determined that the M-E and M-N bonds for all four complexes

Table 3.1. NBO Composition (%) of the M-E π NLMOs and QTAIM Delocalization indices (DI) of [K(18-crown-6)][M(E)(NR$_2$)$_3$] (M = U, Th; E = O, S)[a]

	M (%)	E (%)	DI
M = U, E = O (**2.3**)	15.18 (51.73 f)	83.72	1.575
M = U, E = S (**2.1**)	18.89 (48.78 f)	79.44	1.372
M = Th, E = O (**3.6**)	11.75 (34.48 f)	86.86	1.387
M = Th, E = S (**3.8**)	16.67 (38.41 f)	81.69	1.184

[a]All calculations performed by Prof. Nikolas Kaltsoyannis.

are formally triple and double bonds, respectively. The M-E bond consists of one σ and two π components. The composition of the π NLMOs, and the f-orbital contributions to these molecular orbitals, as determined from NBO analysis, for all four complexes are listed in

Table 3.1. In addition, the natural localized molecular orbitals (NLMOs), representing these components, for the Th-O interaction of complex **3.6** are shown in Figure 3.8. NBO analysis demonstrates that there is a small percent increase in the metal based character for the uranium complexes versus their thorium analogues. In addition, there is greater amount of metal character seen in the sulfides than the oxos, for both metal systems. Most notable, is the calculated increase in the f-orbital contribution to the metal based character for the uranium complexes (**2.1** and **2.3**) versus their thorium counterparts (**3.6** and **3.8**).

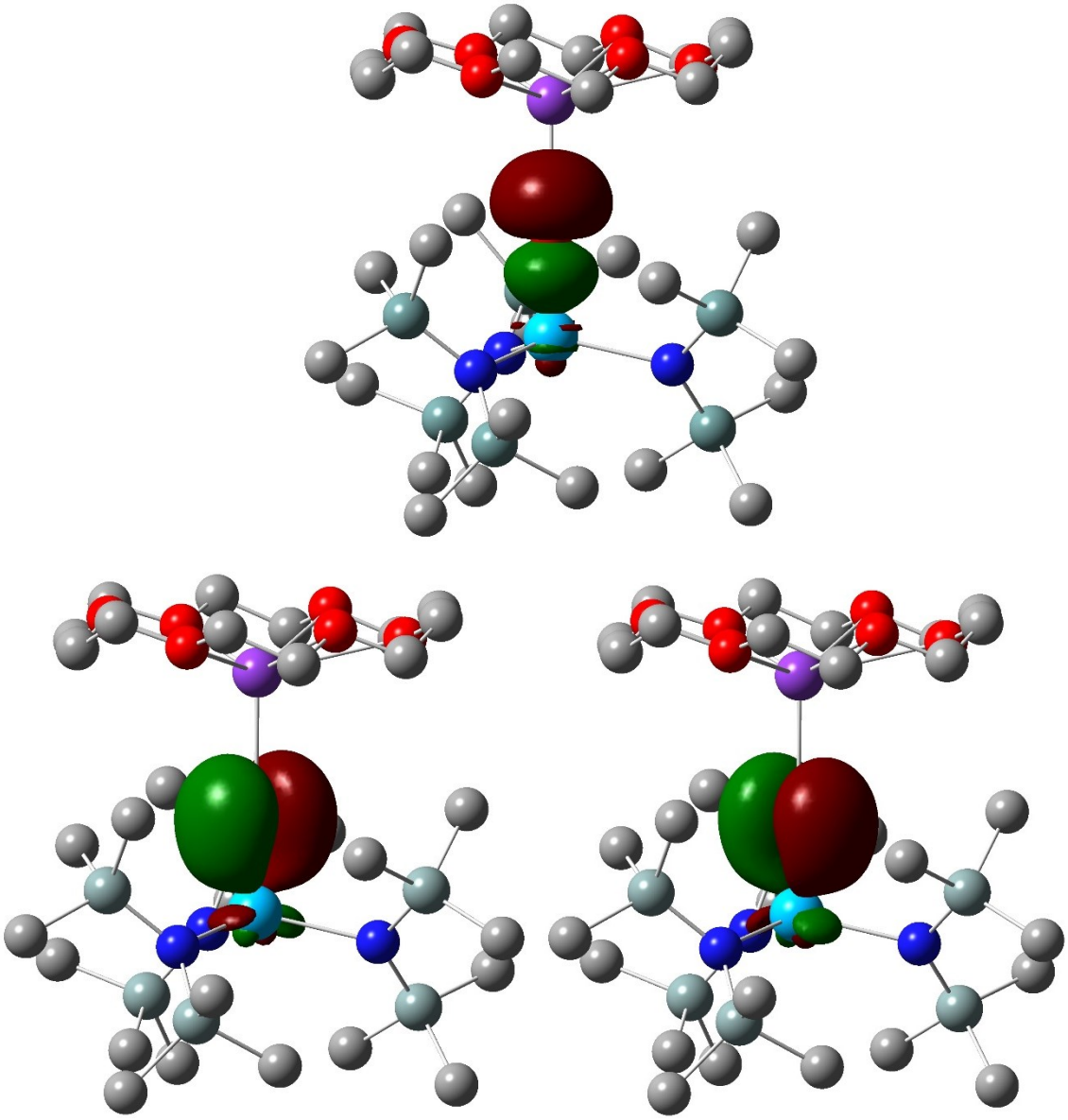

Figure 3.8. σ and π Natural Localized Molecular Orbitals (NLMO) for the Th-O bond of [K(18-crown-6)][Th(O)(NR_2)$_3$] (**3.6**). Hydrogen atoms are omitted for clarity. Isosurface = 0.04.

QTAIM analysis also indicates triple bond, and double bond character for the M-E and M-N interactions, respectively, consistent with the NBO analysis. Furthermore, the calculated delocalization indices (DI), the QTAIM measure of bond order, for the uranium complexes, **2.1** and **2.3**, are greater than those of their thorium analogues, **3.6** and **3.8** (Table 3.1), which argues for a greater degree of covalency in the uranium systems. Taken together with the results of the NBO analysis these data indicate that there is greater covalency in the uranium complexes than the thorium analogues, and in the sulfides than their oxo counterparts.

3.3 Summary

In summary, reaction of the thorium iodide [Th(I)(NR_2)$_3$] (**3.3**) with either $KOCPh_3$ or $KSCPh_3$ yields the thorium chalcogenates [Th($ECPh_3$)(NR_2)$_3$] (**3.4**, E = O; **3.7**, E = S). Application of the reductive deprotection protocol discussed in Chapter 2 to these complexes, via reaction with KC_8 in the presence of 18-crown-6 affords the new thorium terminal chalcogenides [K(18-crown-6)][Th(E)(NR_2)$_3$] (**3.6**, E = O; **3.8**, E = S), via cleavage of the triphenylmethyl protecting group. Structural characterization, via X-ray crystallography reveals short Th-E bond distances, suggestive of multiple bond character. This is also supported by DFT calculations performed on complexes **3.6** and **3.8**. The electronic structures of complexes **3.6** and **3.8**, and their uranium analogues, **2.1** and **2.3** were studied using NBO and QTAIM analyses. Taken together theory and experiment both suggest greater covalency in the uranium complexes versus thorium, and in the sulfides versus oxos, consistent with the predicted trends.

These results are another example of the reductive deprotection protocol discussed in Chapter 2 that utilizes homolytic bond cleavage, a $1e^-$ process, coupled with a metal centered oxidation, to remove the triphenylmethyl protecting group. In contrast, this work details the use of heterolytic bond cleavage, $2e^-$ processes, for which no metal based redox chemistry is required. This is extremely useful for systems, like thorium, for which metal based redox chemistry is inaccessible. The ability to install metal-ligand multiple bonds via both these pathways, exemplifies the broad scope of this methodology, and suggest that it will be extremely useful for systems that only undergo $1e^-$ redox chemistry, or those with none at all.

3.4 Experimental

3.4.1 General Methods

All reactions and subsequent manipulations were performed under anaerobic and anhydrous conditions under an atmosphere of nitrogen. Hexanes, Et_2O, THF, and toluene were dried using a Vacuum Atmospheres DRI-SOLV Solvent Purification system and stored over 3Å sieves for 24 h prior to use. Benzene-d_6 was dried over 3Å molecular sieves for 24 h prior to use. $ThCl_4(DME)_2$ was synthesized according to the previously reported procedure.[54] All other reagents were purchased from commercial suppliers and used as received.

NMR spectra were recorded on a Varian UNITY INOVA 400, a Varian UNITY INOVA 500 spectrometer, a Varian UNITY INOVA 600 MHz spectrometer, or an Agilent Technologies 400-MR DD2 400 MHz Spectrometer. ^1H and $^{13}C\{^1H\}$ NMR spectra were referenced to external $SiMe_4$ using the residual protio solvent peaks as internal standards. IR spectra were recorded on a Nicolet 6700 FT-IR spectrometer. Elemental analyses were performed by the Micro-Analytical Facility at the University of California, Berkeley.

Raman spectra were recorded on a LabRam Aramis microRaman system (Horiba Jobin Yvon) equipped with 1200 grooves/mm holographic gratings, and Peltier-cooled CCD camera. The 633 nm output of a Melles Griot He-Ne laser was used to excite the spectra, which were collected in a back scattering geometry using a confocal Raman Microscope (high stability BX40) equipped with Olympus objectives (MPlan 50x). Sample preparation was performed inside the glovebox: Pure crystalline solid samples were placed between a glass microscope slide and coverslip, sealed with a bead of silicone grease, and removed from the glovebox for spectral acquisition.

3.4.2 Synthesis of [Th(Cl)(NR$_2$)$_3$] (3.1)

To a colorless, cold (-25 °C), solution of $ThCl_4(DME)_2$ (385.7 mg, 0.70 mmol), in THF (4 mL) was added a cold (-25 °C) solution of $NaN(SiMe_3)_2$ (381.6 mg, 2.08 mmol) in THF (4 mL). This mixture was allowed to stir for 18 h, whereupon the solvent was removed in vacuo to afford a colorless solid. This solid was triturated with hexanes (3 × 4 mL) to yield a colorless powder. The resulting powder was extracted with diethyl ether (10 mL) and filtered through a Celite column supported on glass wool (0.5 cm × 3 cm). The cloudy filtrate was again filtered through a Celite column supported on glass wool (0.5 cm × 3 cm) to give a clear colorless filtrate. The volume of this filtrate was reduced in vacuo to 4 mL and layered with hexanes (5 mL). Storage of this mixture at -25 °C for 24 h resulted in the deposition of colorless crystals, which were isolated by decanting off the supernatant (167 mg, 32%). The supernatant was then dried in vacuo to afford a colorless solid. This solid was then extracted with diethyl ether (5 mL) and filtered through a Celite column supported on glass wool (0.5 cm × 3 cm) to afford a colorless filtrate. The volume of this filtrate was reduced to 2 mL in vacuo and layered with hexanes (4 mL). Storage of this mixture at -25 °C for 24 h resulted in

the deposition of an additional batch of colorless crystals, which were isolated by decanting off the supernatant. Total yield: 294.2 mg, 56%. Crystals suitable for X-ray crystallographic analysis were grown from a concentrated Et_2O solution stored at -25 °C for 24 h. Melting point: 208-210 °C (lit. value = 210-212 °C).[38] ^{1}H NMR (400 MHz, 25 °C, benzene-d_6): δ 0.41 (s, 54H, NSiCH_3). ^{13}C{^{1}H} NMR (100 MHz, 25 °C, benzene-d_6): δ 4.26 (NSiCH$_3$). IR (KBr pellet, cm^{-1}): 611 (s), 657 (m), 678 (m), 771 (s), 830 (s), 850 (s), 923 (s), 1073 (m), 1182 (w), 1248 (s), 1406 (m).

3.4.3 Synthesis of [Na(THF)$_{4.5}$][Th(Cl)$_2$(NR$_2$)$_3$] (3.2)

This procedure was adapted from the previously reported synthesis.[38] To a cold (-25 °C), stirring solution of $ThCl_4(DME)_2$[54] (465.5 mg, 0.84 mmol) in THF (6 mL) was added a cold (-25 °C) solution of $NaNR_2$ (462.0 mg, 2.52 mmol) in THF (6 mL). This mixture was allowed to stir for 72 h, during which time the deposition of a fine white solid was observed. The solvent was then removed in vacuo, and the resulting white solid triturated with diethyl ether (4 mL) and pentane (4 mL). The white powder was then extracted with THF (6 mL) and filtered through a Celite column supported on a glass frit (2 cm × 3 cm). The volume of this filtrate was reduced in vacuo to 5 mL and layered with pentane (8 mL). Storage of this mixture at -25 °C for 24 h resulted in the deposition of colorless needles (595.2 mg, 63%). Melting point = 196-199 °C. ^{1}H NMR (400 MHz, 25 °C, benzene-d_6): δ 0.41 (s, NSiCH_3), 1.41 (m, OCH$_2$CH_2), 3.59 (m, OCH_2CH$_2$). ^{13}C{^{1}H} NMR (100 MHz, 25 °C, benzene-d_6): δ 4.26 (NSiCH$_3$), 25.81 (OCH$_2$$CH_2$), 68.00 (O$CH_2CH_2$). IR (KBr pellet, cm^{-1}): 612 (s), 657 (m), 678 (m), 772 (s), 832 (s), 850 (s), 922 (s), 1073 (m), 1183 (w), 1248 (s), 1407 (m).

3.4.4 Synthesis of [Th(I)(NR_2)$_3$] (3.3)

To a stirring suspension of **3.1** (852.3 mg, 1.14 mmol) in hexanes (8 mL) was added TMSI (2 mL, 14.05 mmol). This mixture was allowed to stir for 96 h, whereupon the solvent was removed in vacuo to afford a white solid. The solid was triturated with pentane (2 × 3 mL) to yield a white powder (908.2 mg, 95%). Crystals suitable for X-ray crystallographic analysis were grown from a concentrated CH_2Cl_2 solution stored at -25 °C for 24 h. Anal. Calcd for $C_{18}H_{54}IN_3Si_6Th$: C, 25.73; H, 6.48; N, 5.00. Found: C, 25.34; H, 6.32; N, 5.24. ^{1}H NMR (400 MHz, 25 °C, benzene-d_6): δ 0.45 (s, 54H, NSiCH_3). ^{13}C{^{1}H} NMR (100 MHz, 25 °C, benzene-d_6): δ 5.13 (NSiCH$_3$). IR (KBr pellet, cm^{-1}): 612 (m), 657 (m), 676 (m), 772 (m), 830 (s), 850 (s), 909 (s), 1073 (m), 1249 (s), 1408 (w).

3.4.5 Synthesis of [Th($OCPh_3$)(NR_2)$_3$] (3.4)

To a colorless, stirring suspension of **3.3** (231.4 mg, 0.28 mmol) in toluene (4 mL) was added a cold (-25 °C) solution of $KOCPh_3$ (84.7 mg, 0.28 mmol) in toluene (4 mL), in two portions over the course of 1 h. This mixture was allowed to stir for another hour, resulting in the deposition of a fine white powder. An aliquot (0.25 mL) of the reaction mixture was taken, the solvent was removed in vacuo, and a ^{1}H NMR spectrum in benzene-d_6 was recorded. This spectrum indicated the presence of starting material, complex **3.4**, and a small amount of complex **3.5**. The amount of remaining starting material was estimated from relative area of its silylamide resonance, whereupon an additional portion of $KOCPh_3$ (13.4 mg, 0.045 mmol) was added to the reaction mixture. After 1 h of stirring, this mixture was filtered through a Celite column supported on glass wool (0.5 cm × 3 cm) to afford a colorless filtrate. The solvent was then removed in vacuo to yield a colorless oil. Storage of this oil at -25 °C for 24 h resulted in the formation of crystals within the matrix of the oil. The crystalline

material was isolated by decanting off the remaining oil and then washed with cold (-25 °C) pentane (2 mL). This material consisted mostly of complex **3.5** and was discarded. The oil and the pentane washings were combined and the solvent was removed in vacuo to yield a colorless oil. Storage of this oil at -25 °C for 24 h resulted in the deposition of colorless crystals, which were isolated by decanting off the remaining oil. 88.0 mg, 33%. Anal. Calcd for $C_{37}H_{69}N_3OSi_6Th$: C, 45.70; H, 7.15; N, 4.32. Found: C, 45.55; H, 7.24; N, 4.09. ^{1}H NMR (400 MHz, 25 °C, benzene-d_6): δ 0.39 (s, 54H, NSiCH_3), 7.09 (t, 3H, J_{HH} = 7.2 Hz, *p*-C*H*), 7.18 (t, 6H, J_{HH} = 7.6 Hz, *m*-C*H*), 7.39 (d, 6H, J_{HH} = 7.6 Hz, *o*-C*H*). ^{13}C{^{1}H} NMR (100 MHz, 25 °C, benzene-d_6): δ 5.53 (NSi*C*H$_3$), 96.13 (*C*(C$_6$H$_5$)$_3$), 127.56 (*p*-*C*), 127.88 (*o*-*C*), 129.90 (*m*-*C*), 148.16 (C_{ipso}). IR (KBr pellet, cm^{-1}): 475 (w), 610 (m), 639 (w), 662 (m), 700 (m), 759 (m), 773 (m), 849 (s), 882 (w), 901 (s), 1012 (m), 1035 (m), 1051 (m), 1090 (w), 1151 (w), 1159 (w), 1184 (w), 1201 (w), 1252 (s), 1445 (w), 1491 (w).

3.4.6 Synthesis of [Th(OCPh$_3$)$_2$(NR$_2$)$_2$] (3.5)

To a colorless, stirring solution of **3.1** (118.5 mg, 0.16 mmol) in benzene (3 mL) was added a colorless solution of KOCPh$_3$ (134.0 mg, 0.45 mmol) in benzene (3 mL). This was allowed to stir for 12 h, whereupon the solvent was removed in vacuo to afford a white solid. The solid was triturated with pentane (2 × 3 mL). The resulting white powder was extracted with hexanes (9 mL) and filtered through a Celite column supported on glass wool (0.5 cm × 3 cm) to afford a colorless filtrate. The volume of this filtrate was reduced to 3 mL in vacuo. Storage of this solution at -25 °C for 24 h resulted in the deposition of colorless crystals, which were isolated by decanting off the supernatant (56.9 mg, 34%). Anal. Calcd for $C_{49}H_{66}N_2O_2Si_4Th$: C, 55.55; H, 6.28; N, 2.64. Found: C, 55.64; H, 6.58; N, 2.68. ^{1}H NMR (400 MHz, 25 °C, benzene-d_6): δ 0.26 (s, 36H, NSiCH_3), 7.05-7.07 (m, 18H, *m*-C*H* and *p*-

C*H*), 7.36-7.40 (m, 12H, *o*-C*H*). $^{13}C\{^{1}H\}$ NMR (100 MHz, 25 °C, benzene-d_6): δ 4.18 (NSi*C*H$_3$), 94.87 (*C*(C$_6$H$_5$)$_3$), 127.25 (*p*-*C*), 129.26 (*m*-*C*), 149.12 (C_{ipso}). The resonance assignable to the *o*-*C* was not observed due to overlap with the benzene-d_6 resonance. IR (KBr Pellet, cm^{-1}): 475 (m), 503 (w), 604 (m), 639 (m), 654 (m), 675 (m), 699 (s), 764 (s), 786 (s), 830 (s), 844 (s), 870 (s), 902 (m), 941 (s), 1012 (s), 1034 (m), 1051 (s), 1088 (m), 1158 (m), 1183 (w), 1208 (w), 1250 (s), 1316 (w), 1398 (w), 1445 (s), 1490 (m), 1598 (m).

3.4.7 Synthesis of [K(18-crown-6)][Th(O)(NR$_2$)$_3$] (3.6)

To a colorless, cold (-25 °C), stirring solution of **3.4** (189.9 mg, 0.20 mmol) in THF (3 mL) was added KC$_8$ (56.1 mg, 0.42 mmol), which immediately yielded a dark red mixture. After 2 min, a cold (-25 °C), colorless solution of 18-crown-6 (104.3 mg, 0.39 mmol) in THF (3 mL) was added to this mixture. The solution was allowed to stir for 30 min, whereupon it was filtered through a Celite column supported on glass wool (0.5 cm × 3 cm) to provide a vibrant red filtrate. The filtrate was dried in vacuo to provide a red solid that was triturated with diethyl ether (3 × 3 mL). The resulting red powder was extracted with diethyl ether (5 mL) and filtered through a Celite column supported on glass wool (0.5 cm × 3 cm) to afford a large plug of bright red solid and a pale orange-red filtrate. The volume of the filtrate was reduced to 1 mL in vacuo. Storage of this solution at -25 °C for 24 h resulted in the deposition of colorless crystals, which were isolated by decanting off the supernatant (47.0 mg, 23%). Anal. Calcd for C$_{30}$H$_{78}$KN$_3$O$_7$Si$_6$Th·0.5C$_4$H$_{10}$O: C, 35.93; H, 7.82; N, 3.93. Found: C, 36.53; H, 7.82; N, 3.89. ^{1}H NMR (400 MHz, 25 °C, benzene-d_6): δ 0.64 (s, 54H, NSiC*H*$_3$), 3.09 (s, 24H, 18-crown-6). $^{13}C\{^{1}H\}$ NMR (100 MHz, 25 °C, benzene-d_6): 5.47 (NSi*C*H$_3$), 70.30 (18-crown-6). IR (KBr pellet, cm^{-1}): 599 (m), 665 (m), 677 (m), 724 (w), 755 (m), 770 (m), 832

(s), 867 (s), 966 (s), 986 (s), 1116 (s), 1182 (w), 1243 (s), 1285 (w), 1353 (m), 1455 (w), 1474 (w). Raman (neat solid, cm^{-1}): 389 (w), 615 (s), 678 (m).

3.4.8 Synthesis of [Th(SCPh$_3$)(NR$_2$)$_3$] (3.7)

To a stirring suspension of $KSCPh_3$ (51.4 mg, 0.16 mmol) in toluene (5 mL) was added **3.3** (137.4 mg, 0.16 mmol). This solution was allowed to stir for 1 h, whereupon the solvent was removed in vacuo. The resulting white solid was extracted with hexanes (10 mL) and filtered through a Celite column supported on glass wool (0.5 cm × 3 cm), to provide a colorless filtrate. The volume of the filtrate was reduced to 3 mL in vacuo. Storage of this solution for 48 h resulted in the deposition of colorless crystals, which were isolated by decanting off the supernatant (92.3 mg, 57%). Anal. Calcd for $C_{37}H_{69}N_3SSi_6Th$: C, 44.95; H, 7.04; N, 4.25. Found: C, 44.83; H, 6.90; N, 4.15. ^{1}H NMR (400 MHz, 25 °C, benzene-d_6): δ 0.42 (s, 54H, NSiCH_3), 7.02 (t, 3H, J_{HH} = 7.4 Hz, *p*-C*H*), 7.16 (t, 6H, J_{HH} = 7.6 Hz, *m*-C*H*), 7.66 (d, 6H, J_{HH} = 7.6 Hz, *o*-C*H*). ^{13}C{^{1}H} NMR (100 MHz, 25 °C, benzene-d_6): δ 5.21 (NSi*C*H$_3$), 80.70 (*C*(C$_6$H$_5$)$_3$), 126.78 (*p-C*), 130.97 (*m-C*), 149.57 (C_{ipso}). The resonance assignable to the *o-C* was not observed due to overlap with the benzene-d_6 resonance. IR (KBr pellet, cm^{-1}): 614 (m), 662 (m), 700 (m), 742 (m), 759 (m), 773 (m), 834 (s), 844 (s), 852 (s), 898 (s), 1034 (w), 1184 (w), 1254 (s), 1443 (w), 1484 (w).

3.4.9 Synthesis of [K(18-crown-6)][Th(S)(NR$_2$)$_3$] (3.8)

To a colorless, cold (-25 °C), stirring solution of **3.7** (144.7 mg, 0.15 mmol) in THF (3 mL) was added KC_8 (41.2 mg, 0.30 mmol), which immediately yielded a dark red mixture. After 2 min, a cold (-25 °C), colorless solution of 18-crown-6 (76.5 mg, 0.29 mmol) in THF (3 mL) was added to this mixture. This solution was allowed to stir for 15 min, whereupon it

was filtered through a Celite column supported on glass wool (0.5 cm × 3 cm) to provide a vibrant red filtrate. The filtrate was dried in vacuo to provide a red solid that was triturated with diethyl ether (8 mL). The resulting red powder was extracted with diethyl ether (8 mL) and filtered through a Celite column supported on glass wool (0.5 cm × 3 cm) to afford a large plug of bright red solid and a pale orange-red filtrate. The volume of the filtrate was reduced to 2 mL in vacuo. Storage of this solution at -25 °C for 24 h resulted in the deposition of colorless crystals, which were isolated by decanting off the supernatant (48.7 mg, 32%). Subsequent concentration of the mother liquor and storage at -25 °C for 24 h resulted in the deposition of additional crystals. Total yield: 95.6 mg, 62%. Anal. Calcd for $C_{30}H_{78}KN_3O_6SSi_6Th$: C, 34.36; H, 7.50; N, 4.01. Found: C, 34.85; H, 7.94; N, 3.64. ^{1}H NMR (400 MHz, 25 °C, benzene-d_6): δ 0.74 (s, 54H, NSiCH_3), 3.17 (s, 24H, 18-crown-6). ^{13}C{^{1}H} NMR (100 MHz, 25 °C, benzene-d_6): 5.49 (NSiCH$_3$), 70.12 (18-crown-6). IR (KBr pellet, cm^{-1}): 605 (m), 664 (m), 685 (w), 699 (w), 785 (sh), 771 (m), 842 (s), 882 (sh), 936 (s), 963 (s), 1108 (s), 1182 (m), 1252 (s), 1285 (w), 1352 (m), 1455 (w), 1474 (w). Raman (neat solid, cm^{-1}): 385 (w), 578 (s), 630 (s), 682 (s), 843 (m), 883 (m), 1014 (s).

3.4.10 X-ray Crystallography

Data for **3.1**, **3.2**, **3.3**, **3.5**, **3.6**, **3.7**, and **3.8** were collected on a Bruker KAPPA APEX II diffractometer equipped with an APEX II CCD detector using a TRIUMPH monochromator with a Mo Kα X-ray source (α = 0.71073 Å). The crystals were mounted on a cryoloop under Paratone-N oil, and all data were collected at 100(2) K using an Oxford nitrogen gas cryostream. Data were collected using ω scans with 0.5° frame widths. Frame exposures of 2 s were used for **3.1** and **3.2**. Frame exposures of 5 s were used for **3.3**. Frame exposures of 10 s were used for **3.7** and **3.8**. Frame exposures of 5 s (low angle) and 10 s (high angle) were

used for **3.5** and **3.6**. Data collection and cell parameter determination were conducted using the SMART program.[55] Integration of the data frames and final cell parameter refinement were performed using SAINT software.[56] Absorption correction of the data was carried out using the multi-scan method SADABS.[57] Subsequent calculations were carried out using SHELXTL.[58] Structure determination was done using direct or Patterson methods and difference Fourier techniques. All hydrogen atom positions were idealized, and rode on the atom of attachment. Structure solution, refinement, graphics, and creation of publication materials were performed using SHELXTL.[58]

For **3.2**, one sodium atom and its coordinated THF molecules exhibited positional disorder and were modelled over two positions in a 50:50 ratio. The C-C and C-O bond were constrained to 1.5 and 1.4 Å, respectively, using the DFIX command. In addition, the diethyl ether solvate of **3.6** exhibited positional disorder; one of the carbon atoms of this molecule was modelled over two positions in a 50:50 ratio. The anisotropic parameters of the disordered carbon atoms were constrained using the EADP command. Hydrogen atoms were not added to disordered carbon atoms.

Table 3.2. X-ray Crystallographic Data for Complexes **3.1**, **3.2**, and **3.3**

	3.1	**3.2**	**3.3**
empirical formula	$C_{18}H_{54}ClN_3Si_6Th$	$C_{36}H_{82}Cl_2N_3NaO_{4.5}Si_6Th$	$C_{18}H_{54}IN_3Si_6Th$
crystal habit, color	block, colorless	needle, colorless	block, colorless
crystal size (mm)	0.1 × 0.1 × 0.1	0.2 × 0.05 × 0.02	0.2 × 0.1 × 0.1
space group	*R*3c	$R\bar{3}$	*R*3c
volume (Å^3)	4953.5(6)	8690(3)	5049(3)
a (Å)	18.430(1)	18.404(4)	18.328(5)
b (Å)	18.430(1)	18.404(4)	18.328(5)
c (Å)	16.840(1)	29.626(7)	17.356(5)
α (deg)	90	90	90
β (deg)	90	90	90
γ (deg)	120	120	120
Z	6	6	6
formula weight (g/mol)	748.67	1131.59	840.10
density (calculated) (Mg/m^3)	1.506	1.288	1.658
absorption coefficient (mm^{-1})	4.825	2.831	5.572
F_{000}	2244	3444	2460
total no. reflections	20265	8328	9620
unique reflections	3383	5914	3344
R_{int}	0.0485	0.0316	0.0324
final R indices (I >2σ(I)]	R_1 = 0.0176 wR_2 = 0.0417	R_1 = 0.0503 wR_2 = 0.1166	R_1 = 0.0295 wR_2 = 0.0681
largest diff. peak and hole (e$^-$ A^{-3})	0.531 and -0.634	1.321 and -1.575	5.273 and -0.996
GOF	1.047	1.000	0.891

Table 3.3. X-ray Crystallographic Data for Complexes **3.5** and **3.6**

	3.5·0.5C_6H_{14}	**3.6**·0.5OC_4H_{10}
empirical formula	$C_{53}H_{73}N_2O_2Si_4Th$	$C_{32}H_{83}KN_3O_{7.5}Si_6Th$
crystal habit, color	plate, colorless	block, colorless
crystal size (mm)	0.1 × 0.1 × 0.05	0.1 × 0.1 × 0.1
space group	$P\bar{1}$	*P*bca
volume (Å^3)	2725.4(7)	10534(2)
a (Å)	12.955(2)	20.457(3)
b (Å)	13.025(2)	20.307(3)
c (Å)	16.867(2)	25.358(3)
α (deg)	85.654(3)	90
β (deg)	77.178(3)	90
γ (deg)	79.336(3)	90
Z	2	8
formula weight (g/mol)	1114.53	1069.69
density (calculated) (Mg/m^3)	1.358	1.349
absorption coefficient (mm^{-1})	2.862	3.086
F_{000}	1134	4392
total no. reflections	56153	51408
unique reflections	11192	13650
R_{int}	0.0655	0.1158
final R indices (I >2σ(I)]	R_1 = 0.0310 wR_2 = 0.0612	R_1 = 0.1001 wR_2 = 0.1885
largest diff. peak and hole (e$^-$ A^{-3})	1.598 and -0.757	6.017 and -3.222
GOF	1.013	1.207

Table 3.4. X-ray Crystallographic Data for Complexes **3.7** and **3.8**

	3.7	**3.8**
empirical formula	$C_{37}H_{69}N_3SSi_6Th$	$C_{30}H_{78}KN_3O_6SSi_6Th$
crystal habit, color	needle, colorless	needle, colorless
crystal size (mm)	0.1 × 0.05 × 0.01	0.1 × 0.02 × 0.02
space group	$P\bar{1}$	$P\bar{1}$
volume (Å^3)	2372.5(4)	5044.9(11)
a (Å)	10.594(1)	12.748 (2)
b (Å)	11.587(1)	18.891(2)
c (Å)	19.595(2)	21.817(3)
α (deg)	96.883(2)	91.554(2)
β (deg)	91.006(2)	105.863(2)
γ (deg)	96.270(2)	92.564(2)
Z	2	4
formula weight (g/mol)	988.59	1048.68
density (calculated) (Mg/m^3)	1.388	1.381
absorption coefficient (mm^{-1})	3.365	3.258
F_{000}	1010	2144
total no. reflections	19192	63038
unique reflections	10322	24802
R_{int}	0.0440	0.0408
final R indices (I >2σ(I)]	R_1 = 0.0350 wR_2 = 0.0702	R_1 = 0.0387 wR_2 = 0.1126
largest diff. peak and hole (e$^-$ A^{-3})	1.992 and -1.407	4.482 and -1.860
GOF	0.957	0.870

3.4.11 Computational Details

Density functional theory calculations were carried out using the PBE functional,[59,60] as implemented in the Gaussian 09 Rev. D.01 quantum chemistry code.[61] Dispersion corrections (D3) due to Grimme *et al*.[62] were included, as discussed. (14s 13p 10d 8f)/[10s 9p 5d 4f] segmented valence basis sets with Stuttgart-Bonn variety relativistic pseudopotentials were used for Th and U.[63] For the geometry optimizations, the 6-31G** basis sets were used for all other atoms. The ultrafine integration grid was employed in all calculations, as were the SCF convergence criteria. The default RMS force geometry convergence criterion was relaxed to 0.000667 a.u. using IOP 1/7; the maximum force at each converged geometry is given in the ESI. The electronic structures at the PBE+D3 geometries were recalculated using improved basis sets for the ligands; 6-311G** for O, S, N, K; 6-31G** for C and H. Natural Bond Orbital calculations were performed using the NBO6 code, interfaced with Gaussian.[64] QTAIM analyses were performed using the AIMAll program package,[65] with .wfx files generated in Gaussian used as input.

3.5 Appendix

3.5.1 Synthesis and Characterization of [Th(NHCPh$_3$)(NR$_2$)$_3$] (3.9)

Similar to the synthesis of the U(IV) amide, [U(NHCPh$_3$)(NR$_2$)$_3$] (**2.8**), an analogous thorium complex can be made. Thus, reaction of 1 equiv of [Li(NHCPh$_3$)(THF)] (**2.6**) with complex **3.1**, in benzene-d_6, affords the Th(IV) amide, [Th(NHCPh$_3$)(NR$_2$)$_3$] (**3.9**) as colorless plates after crystallization from diethyl ether (Scheme 3.6). Complete characterization of this species was not done and as such is only included here for completeness.

Scheme 3.6 Synthesis of [Th(NHCPh$_3$)(NR$_2$)$_3$]

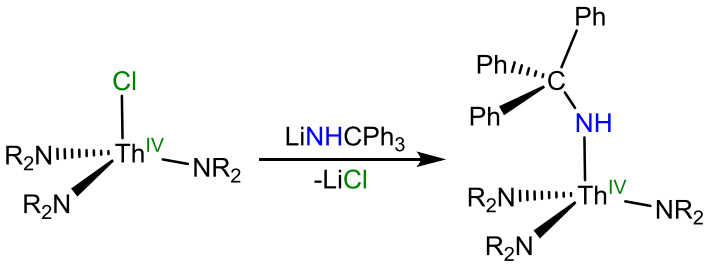

[Th(NHCPh$_3$)(NR$_2$)$_3$] (**3.9**) crystallizes in the triclinic spacegroup $P\bar{1}$, and its solid state molecular structure is shown in Figure A3.1. It is isostructural to its uranium analogue, and features a pseudotetrahedral geometry about thorium. In addition, the Th-N$_{trityl}$ (2.277(3) Å) and Th-N$_{NR_2}$ (av. 2.324 Å) bond distances are longer than the analogous U-N bonds of complex **2.8**, consistent with the increased ionic radius of Th^{4+} vs. U^{4+}.[48]

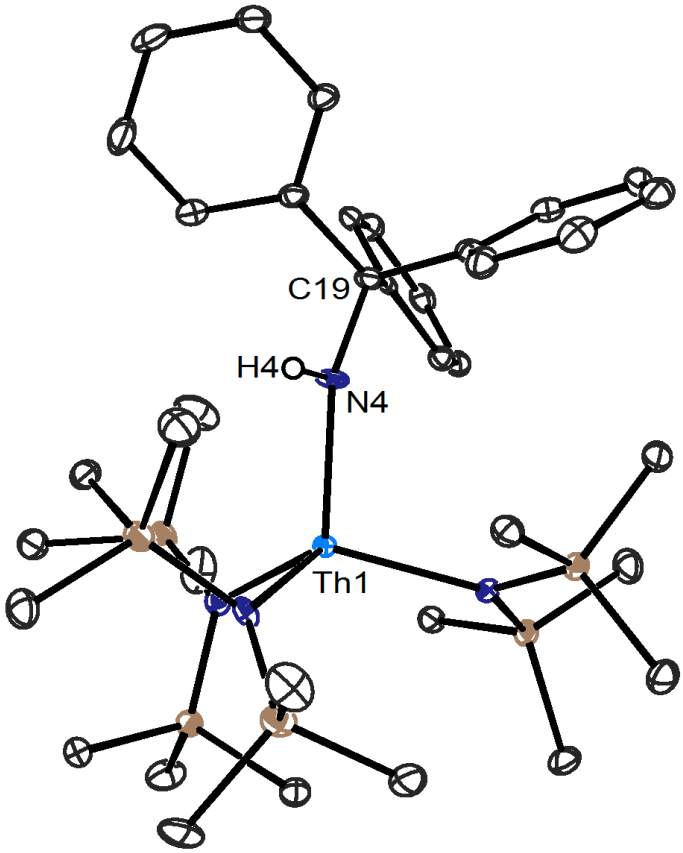

Figure A3.1. ORTEP diagram of [Th(NHCPh$_3$)(NR$_2$)$_3$] (**3.9**) with 50% probability ellipsoids. Hydrogen atoms, except the N-H proton, are omitted for clarity. Selected bond lengths (Å) and angles (deg): Th1-N4 = 2.277(3), Th1-N$_{NR_2}$ (av.) = 2.324; Th1-N4-C19 = 150.7(3), N-Th-N (av.) = 110.3.

3.5.2 Synthesis and Characterization of [Li(12-crown-4)$_2$][Th(NCPh$_3$)(NR$_2$)$_3$] (3.10)

Recently Arnold and co-workers reported the synthesis of thorium imido complexes [K(18-crown-6)][Th(NR´)(NR$_2$)$_3$] (R´ = 2,6-^{i}Pr$_2$C$_6$H$_3$, 2,4,6-Me$_3$C$_6$H$_3$, 2,6-Ph$_2$C$_6$H$_3$) via the protonation of the Th(IV) metallacycle [Th(*C*H$_2$SiMe$_2$*N*SiMe$_3$)(NR$_2$)$_2$] with the corresponding amide salt KNHR.[23] This route was then explored as a means to access a triphenylmethyl-imido complex, which could then be subjected to the reductive deprotection protocol to synthesize a thorium nitrido complex. Thus, addition of 1 equiv of complex **2.6**

to a solution of [Th(*C*H$_2$SiMe$_2$*N*SiMe$_3$)(NR$_2$)$_2$] in THF along with 2 equiv of 12-crown-4 affords the Th(IV) imido complex, [Li(12-crown-4)$_2$][Th(NCPh$_3$)(NR$_2$)$_3$] (**3.10**), as colorless crystals in 31% yield, after crystallization from diethyl ether (Scheme 3.7).

Scheme 3.7 Synthesis of [Li(12-crown-4)$_2$][Th(NCPh$_3$)(NR$_2$)$_3$] (**3.10**)

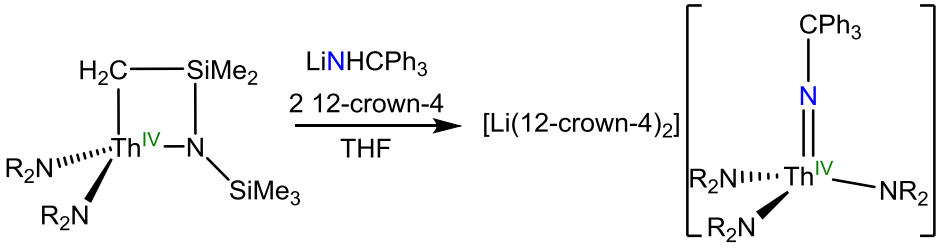

Complex **3.10** crystallizes in the triclinic spacegroup $P\bar{1}$ with two molecules in the asymmetric unit, and its solid state molecular structure is shown in Figure A3.2. The Th-N_{imido} bond distances in complex **3.10** (av. 2.036 Å) are comparable to those of other Th(IV) imido complexes,[21-23] and shorter than the Th-N_{trityl} bond distance of complex **3.9**, suggestive of the multiple bond character of this interaction. Furthermore the Th-N_{imido} and Th-N_{NR_2} (av. = 2.45 Å) bond lengths are longer than corresponding bond lengths of [K][U(NCPh$_3$)(NR$_2$)$_3$] (U-N_{imido} = 1.993(1), U-N_{NR_2} (av.) = 2.387 Å)[66] consistent with the increased ionic radius of Th^{4+} versus U^{4+}.[48]

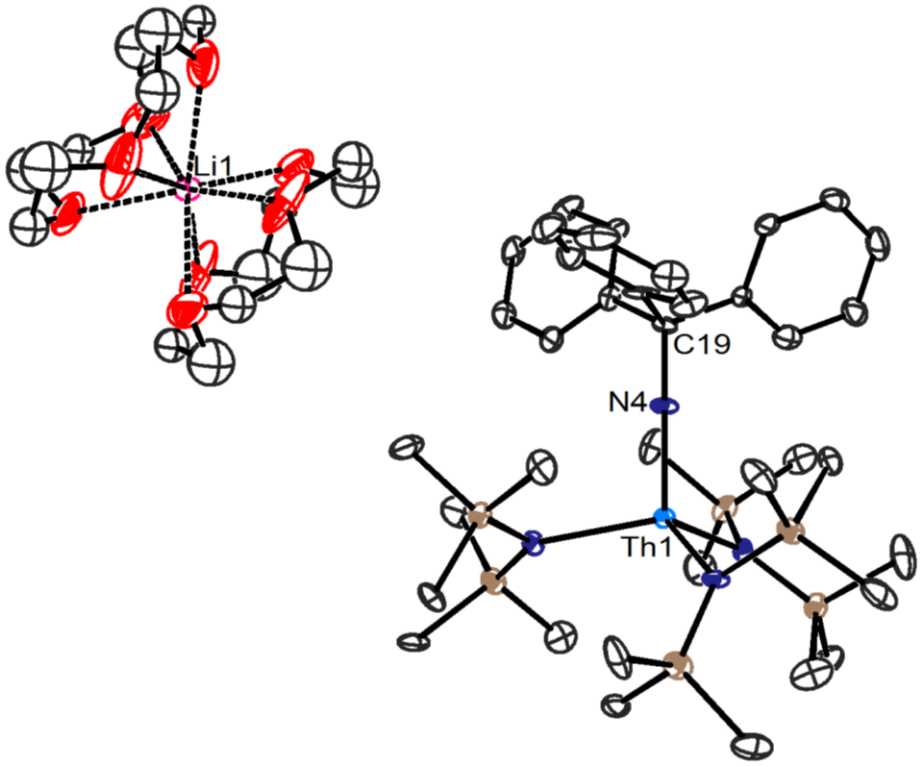

Figure A3.2. ORTEP diagram of $[Li(12\text{-crown-4})_2][Th(NCPh_3)(NR_2)_3]$ (**3.10**) with 50% probability ellipsoids. One molecule of **3.10** and hydrogen atoms are omitted for clarity. Selected bond lengths (Å) and angles (deg): Th1-N4 = 2.030(8), Th2-N8 = 2.041(8), Th-N_{NR_2} (av.) = 2.45, N_{imido}-C (av.) = 1.45, N-Th-N (av.) = 109.5, Th-N-C (av.) = 178.3.

The ^{1}H NMR spectrum of complex **3.10**, in benzene-d_6, features two sharp singlets at 0.65 and 3.11 ppm, attributable to the methyl groups of the silylamide ligands and the methylene groups of the 12-crown-4 moieties, respectively (Figure A3.3). Three additional resonances at 7.08, 7.30, and 7.99 ppm, consisting of two triplets and a doublet, are observed and are assignable to the *p*-, *m*-, and *o*-aryl proton environments of the triphenylmethyl ligand, respectively. In addition, the ^{7}Li{^{1}H} spectrum of **3.10**, in benzene-d_6, exhibits one resonance at -1.40 ppm (Figure A3.4).

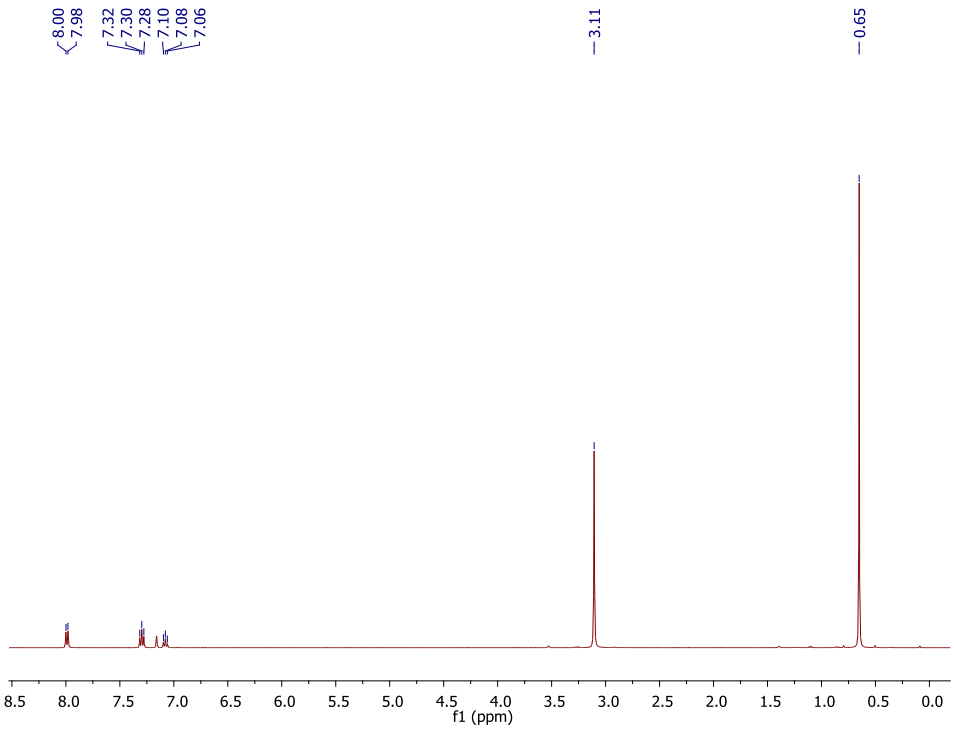

Figure A3.3. ^{1}H NMR spectrum of [Li(12-crown-4)$_2$][Th(NCPh$_3$)(NR$_2$)$_3$] (**3.10**) in benzene-d_6

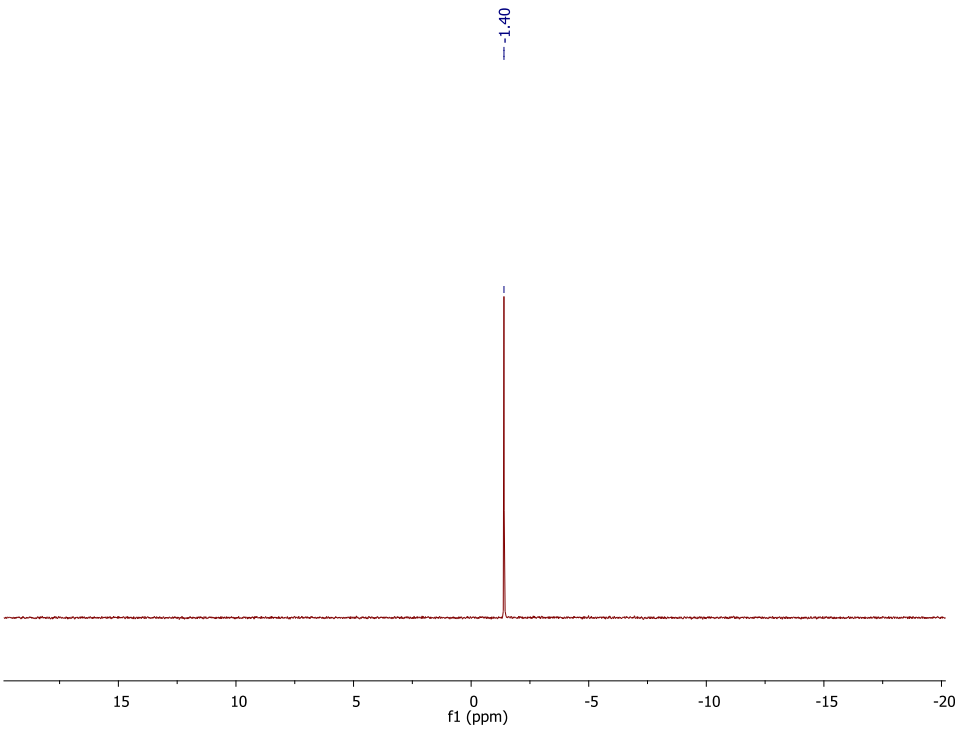

Figure A3.4. $^{7}Li\{^{1}H\}$ NMR spectrum of $[Li(12\text{-crown-4})_2][Th(NCPh_3)(NR_2)_3]$ (**3.10**) in benzene-d_6.

3.5.3 Synthesis and Characterization of [K(18-crown-6)][Th(NTs)(NR$_2$)$_3$] (3.11)

The inability to cleave the C-N bond of complex **3.10** led to the investigation of other protecting groups. The synthesis of $[K(18\text{-crown-6})][U(NTs)(NR_2)_3]$ (**2.9**) from the U(IV) metallacycle $[U(CH_2SiMe_2NSiMe_3)(NR_2)_2]$, suggested that an analogous thorium complex could be accessed via the identical route. Thus, addition of 1 equiv of KNHTs[67] to a THF solution of $[Th(CH_2SiMe_2NSiMe_3)(NR_2)_2]$ and 18-crown-6 affords the Th(IV) imido $[K(18\text{-crown-6})][Th(NTs)(NR_2)_3]$ (**3.11**) as a pale orange powder in 80% yield upon workup (Scheme 3.8).

Scheme 3.8 Synthesis of [K(18-crown-6)][Th(NTs)(NR$_2$)$_3$] (**3.11**)

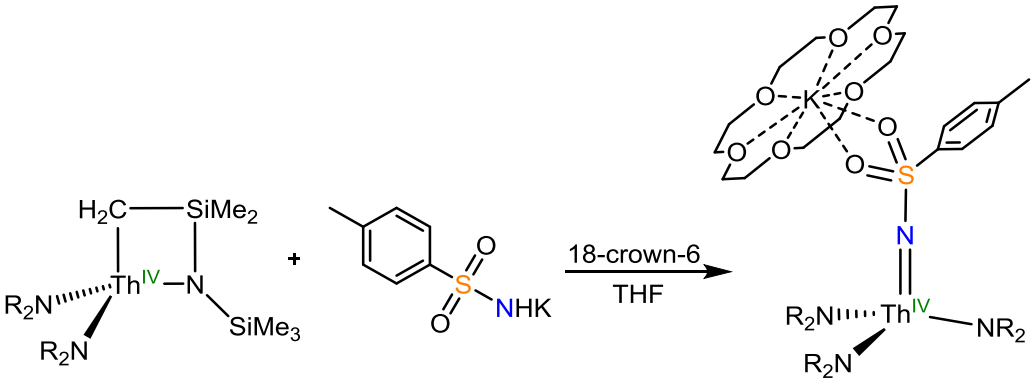

Complex **3.11** crystallizes in the triclinic spacegroup $P\bar{1}$, and its solid state molecular structure is shown in Figure A3.5. **3.11** is isostructural to its uranium analogue, complex **2.9**, and features a pseudotetrahedral geometry about thorium (av. N-Th-N = 109.1°). The Th-N_{imido} (2.149(7) Å) bond distance of **3.11** is slightly longer than those of other structurally characterized Th(IV) imido complexes,[21-23] but still considerably shorter than the Th-N_{NR_2} (av. = 2.36 Å) bond distances. In addition, the Th-N_{imido} and Th-N_{NR_2} bond distances of **3.11** are longer than the corresponding bond lengths of the analogous uranium complex (**2.9**), consistent with the increased ionic radius of Th^{4+} versus U^{4+}.[48]

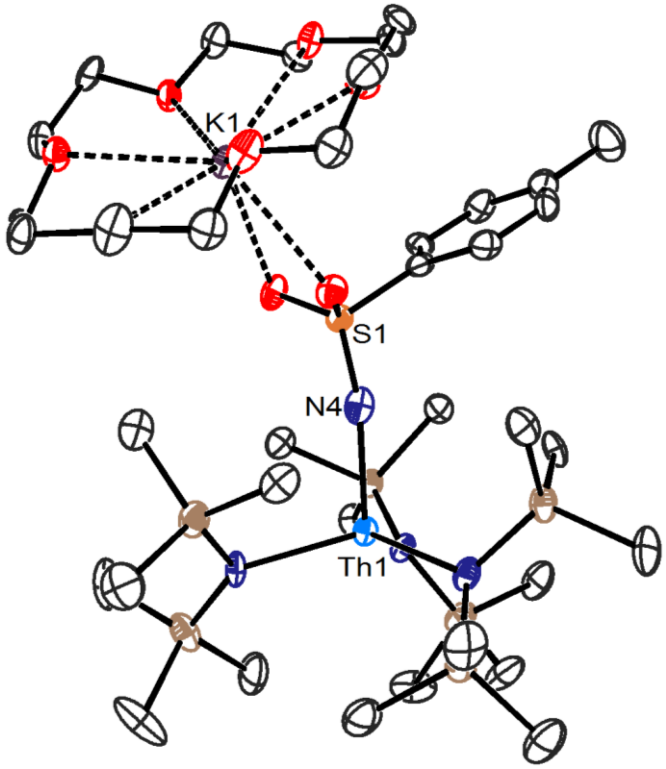

Figure A3.5. ORTEP diagram of [K(18-crown-6)][Th(NTs)(NR_2)$_3$] (**3.11**) with 50% probability ellipsoids. Hydrogen atoms are omitted for clarity. Selected bond lengths (Å) and angles (deg): Th1-N4 = 2.149(7), Th-N_{NR_2} (av.) = 2.36, N4-S1 = 1.543(8), N-U-N (av.) = 109.1, Th1-N4-S1 = 168.2(4).

The ^{1}H NMR spectrum of complex **3.11** exhibits five resonances in benzene-d_6, in a 54:3:24:2:2 ratio (Figure A3.6). These resonances consist of two singlets at 0.64 ppm and 3.12 ppm, assignable to the methyl groups of the silylamide ligands and the methylene groups of the 18-crown-6 moiety, as well as, one singlet and two doublets at 2.13, 7.06 and 8.16 ppm, assignable to the methyl group and two distinct aryl proton environments of the tosyl moiety.

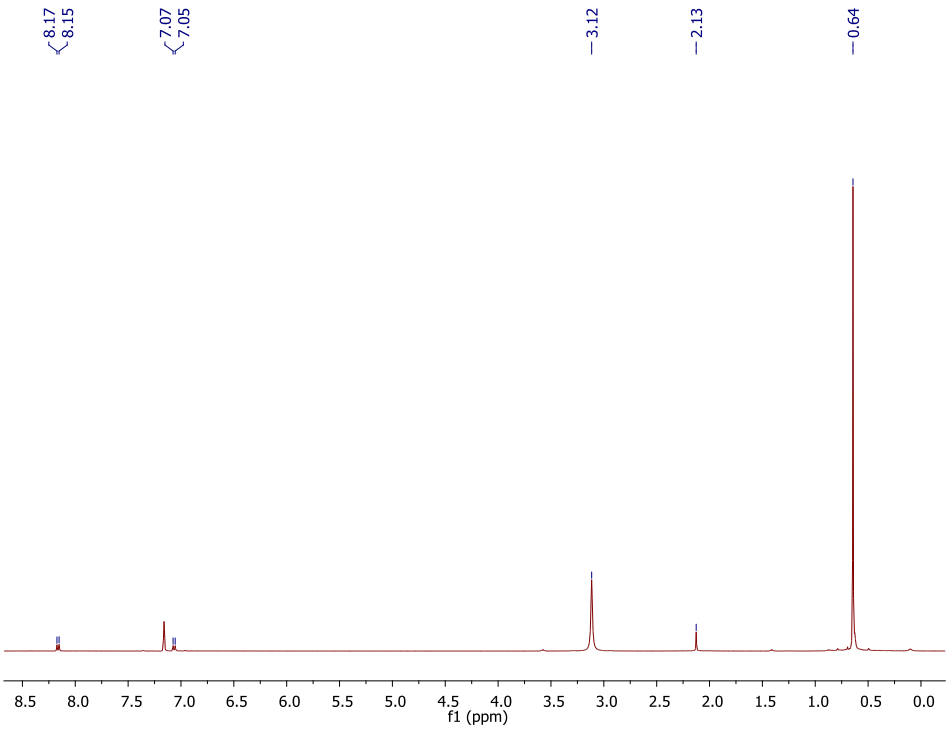

Figure A3.6. ^{1}H NMR spectrum of [K(18-crown-6)][Th(NTs)(NR_2)$_3$] (**3.11**) in benzene-d_6.

3.6 References

(1) Neidig, M. L.; Clark, D. L.; Martin, R. L. *Coord. Chem. Rev.* **2013**, *257*, 394.
(2) Kaltsoyannis, N. *Inorg. Chem.* **2013**, *52*, 3407.
(3) Minasian, S. G.; Krinsky, J. L.; Arnold, J. *Chem. Eur. J.* **2011**, *17*, 12234.
(4) Kirker, I.; Kaltsoyannis, N. *Dalton Trans.* **2011**, *40*, 124.
(5) Jensen, M. P.; Bond, A. H. *J. Am. Chem. Soc.* **2002**, *124*, 9870.
(6) Ingram, K. I. M.; Tassell, M. J.; Gaunt, A. J.; Kaltsoyannis, N. *Inorg. Chem.* **2008**, *47*, 7824.
(7) Hayton, T. W. *Chem. Commun.* **2013**, *49*, 2956.
(8) Hayton, T. W. *Dalton Trans.* **2010**, *39*, 1145.
(9) Fortier, S.; Brown, J. L.; Kaltsoyannis, N.; Wu, G.; Hayton, T. W. *Inorg. Chem.* **2012**, *51*, 1625.
(10) Fortier, S.; Kaltsoyannis, N.; Wu, G.; Hayton, T. W. *J. Am. Chem. Soc.* **2011**, *133*, 14224.
(11) Zi, G.; Jia, L.; Werkema, E. L.; Walter, M. D.; Gottfriedsen, J. P.; Andersen, R. A. *Organometallics* **2005**, *24*, 4251.
(12) Bart, S. C.; Anthon, C.; Heinemann, F. W.; Bill, E.; Edelstein, N. M.; Meyer, K. *J. Am. Chem. Soc.* **2008**, *130*, 12536.
(13) Hayton, T. W.; Boncella, J. M.; Scott, B. L.; Palmer, P. D.; Batista, E. R.; Hay, P. J. *Science* **2005**, *310*, 1941.
(14) Anderson, N. H.; Odoh, S. O.; Yao, Y.; Williams, U. J.; Schaefer, B. A.; Kiernicki, J. J.; Lewis, A. J.; Goshert, M. D.; Fanwick, P. E.; Schelter, E. J.; Walensky, J. R.; Gagliardi, L.; Bart, S. C. *Nat. Chem.* **2014**, *6*, 919.
(15) King, D. M.; McMaster, J.; Tuna, F.; McInnes, E. J. L.; Lewis, W.; Blake, A. J.; Liddle, S. T. *J. Am. Chem. Soc.* **2014**, *136*, 5619.
(16) King, D. M.; Tuna, F.; McInnes, E. J. L.; McMaster, J.; Lewis, W.; Blake, A. J.; Liddle, S. T. *Science* **2012**, *337*, 717.
(17) King, D. M.; Liddle, S. T. *Coord. Chem. Rev.* **2014**, *266–267*, 2.
(18) Fortier, S.; Wu, G.; Hayton, T. W. *J. Am. Chem. Soc.* **2010**, *132*, 6888.
(19) Fox, A. R.; Creutz, S. E.; Cummins, C. C. *Dalton Trans.* **2010**, *39*, 6632.
(20) Zi, G. *Sci. China Chem.* **2014**, *57*, 1064.
(21) Haskel, A.; Straub, T.; Eisen, M. S. *Organometallics* **1996**, *15*, 3773.
(22) Ren, W.; Zi, G.; Walter, M. D. *Organometallics* **2012**, *31*, 672.
(23) Bell, N. L.; Maron, L.; Arnold, P. L. *J. Am. Chem. Soc.* **2015**, *137*, 10492.
(24) Ren, W.; Zi, G.; Fang, D.-C.; Walter, M. D. *J. Am. Chem. Soc.* **2011**, *133*, 13183.
(25) Ma, G.; Ferguson, M. J.; McDonald, R.; Cavell, R. G. *Inorg. Chem.* **2011**, *50*, 6500.
(26) Simpson, S. J.; Turner, H. W.; Andersen, R. A. *J. Am. Chem. Soc.* **1979**, *101*, 7728.
(27) Ren, W.; Deng, X.; Zi, G.; Fang, D.-C. *Dalton Trans.* **2011**, *40*, 9662.
(28) Lu, E.; Lewis, W.; Blake, A. J.; Liddle, S. T. *Angew. Chem. Int. Ed.* **2014**, *53*, 9356.
(29) Bursten, B. E.; Strittmatter, R. J. *Angew. Chem. Int. Ed.* **1991**, *30*, 1069.
(30) Ortu, F.; Formanuik, A.; Innes, J. R.; Mills, D. P. *Dalton Trans.* **2016**, *45*, 7537.
(31) Nugent, L. J.; Baybarz, R. D.; Burnett, J. L.; Ryan, J. L. *J. Phys. Chem.* **1973**, *77*, 1528.

(32) Blake, P. C.; Lappert, M. F.; Atwood, J. L.; Zhang, H. *J. Chem. Soc. Chem. Commun.* **1986**, 1148.
(33) Blake, P. C.; Edelstein, N. M.; Hitchcock, P. B.; Kot, W. K.; Lappert, M. F.; Shalimoff, G. V.; Tian, S. *J. Organomet. Chem.* **2001**, *636*, 124.
(34) Parry, J. S.; Cloke; Coles, S. J.; Hursthouse, M. B. *J. Am. Chem. Soc.* **1999**, *121*, 6867.
(35) Arney, D. S. J.; Burns, C. J. *J. Am. Chem. Soc.* **1993**, *115*, 9840.
(36) Ren, W.; Song, H.; Zi, G.; Walter, M. D. *Dalton Trans.* **2012**, *41*, 5965.
(37) Bradley, D. C.; Ghotra, J. S.; Hart, F. A. *Inorg. Nucl. Chem. Lett.* **1974**, *10*, 209.
(38) Turner, H. W.; Andersen, R. A.; Zalkin, A.; Templeton, D. H. *Inorg. Chem.* **1979**, *18*, 1221.
(39) Williams, U. J.; Carroll, P. J.; Schelter, E. J. *Inorg. Chem.* **2014**, *53*, 6338.
(40) Pyykkö, P. *J. Phys. Chem. A* **2015**, *119*, 2326.
(41) Yang, L.; Powell, D. R.; Houser, R. P. *Dalton Trans.* **2007**, 955.
(42) Barnhart, D. M.; Clark, D. L.; Gordon, J. C.; Huffman, J. C.; Watkin, J. G. *Inorg. Chem.* **1994**, *33*, 3939.
(43) Korobkov, I.; Arunachalampillai, A.; Gambarotta, S. *Organometallics* **2004**, *23*, 6248.
(44) Beshouri, S. M.; Fanwick, P. E.; Rothwell, I. P.; Huffman, J. C. *Organometallics* **1987**, *6*, 2498.
(45) Barnhart, D. M.; Clark, D. L.; Gordon, J. C.; Huffman, J. C.; Watkin, J. G.; Zwick, B. D. *Inorg. Chem.* **1995**, *34*, 5416.
(46) Berg, J. M.; Clark, D. L.; Huffman, J. C.; Morris, D. E.; Sattelberger, A. P.; Streib, W. E.; Van Der Sluys, W. G.; Watkin, J. G. *J. Am. Chem. Soc.* **1992**, *114*, 10811.
(47) Clark, D. L.; Watkin, J. G. *Inorg. Chem.* **1993**, *32*, 1766.
(48) Shannon, R. D. *Acta Crystallogr. Sect. A* **1976**, *A32*, 751.
(49) Barnhart, D. M.; Burns, C. J.; Sauer, N. N.; Watkin, J. G. *Inorg. Chem.* **1995**, *34*, 4079.
(50) Lin, Z.; Brock, C. P.; Marks, T. J. *Inorg. Chim. Acta* **1988**, *141*, 145.
(51) Evans, W. J.; Miller, K. A.; Kozimor, S. A.; Ziller, J. W.; DiPasquale, A. G.; Rheingold, A. L. *Organometallics* **2007**, *26*, 3568.
(52) Mountain, A. R. E.; Kaltsoyannis, N. *Dalton Trans.* **2013**, *42*, 13477.
(53) Huang, Q.-R.; Kingham, J. R.; Kaltsoyannis, N. *Dalton Trans.* **2015**, *44*, 2554.
(54) Cantat, T.; Scott, B. L.; Kiplinger, J. L. *Chem. Commun.* **2010**, *46*, 919.
(55) *SMART Apex II*, Version 2.1. 2005
(56) *SAINT Software User's Guide*, Version 7.34a. 2005
(57) *SADABS*, 2005
(58) *SHELXTL PC*, Version 6.12. 2005
(59) Perdew, J. P.; Burke, K.; Ernzerhof, M. *Phys. Rev. Lett.* **1997**, *78*, 1396.
(60) Perdew, J. P.; Burke, K.; Ernzerhof, M. *Phys. Rev. Lett.* **1996**, *77*, 3865.
(61) *Gaussian 09, Revision D.01*, 2009
(62) Grimme, S.; Antony, J.; Ehrlich, S.; Krieg, H. *J. Chem. Phys.* **2010**, *132*, 154104.
(63) Cao, X.; Dolg, M. *J. Mol. Struct. THEOCHEM* **2004**, *673*, 203.
(64) *NBO 6.0*, 2013
(65) *AIMAll*, 14.11.23. 2014
(66) Mullane, K. C.; Lewis, A. J.; Yin, H.; Carroll, P. J.; Schelter, E. J. *Inorg. Chem.* **2014**, *53*, 9129.
(67) Breugst, M.; Tokuyasu, T.; Mayr, H. *J. Org. Chem.* **2010**, *75*, 5250.

Chapter 4 Synthesis of Uranium Selenides and Tellurides Utilizing Polychalcogenides as Chalcogen Atom Transfer Reagents

Portions of this work were published in:

Danil E. Smiles, Guang Wu, Trevor W. Hayton

Inorg. Chem. **2014**, *53*, 10240-10247.

Table of Contents

4.1 Introduction

There have been considerable advances made in the synthesis of complexes containing actinide-ligand multiple bonds.[1-3] However, while numerous examples of oxos,[4-7] imidos,[8-10] and nitridos,[11-14] and carbenes[15-21] have been reported, examples of complexes of the heavier chalcogenides (S, Se, Te) are much more uncommon.[3,22,23] This is due in part to the absence of kinetic control over chalcogen atom transfer, which gives rise to mixtures of products and unpredictable reaction outcomes. These problems occur with a variety of different chalcogen atom transfer reagents and are observed in both transition metal and actinide systems. For example, Kubas and co-workers reported that the reaction of $[CpFe(CO)_2]_2$ with Et_2S_3 yields a mixture of $[Cp_2Fe_2(S_2)(SEt)_2]$, $[Cp_3Fe_3(S_2)(SEt)]$, $[Cp_4Fe_4S_4]$, $[Cp_4Fe_4S_5]$, and $[Cp_4Fe_4S_6]$.[24] The lack of control is also observed when using more traditional chalcogen atom transfer reagents like elemental sulfur, as seen by Heck and co-workers, who reported that heating the

Scheme 4.1 Reaction of $[Me_2Si(\eta^5\text{-}C_5H_4)_2Fe_2(CO)_4]$ with S_8

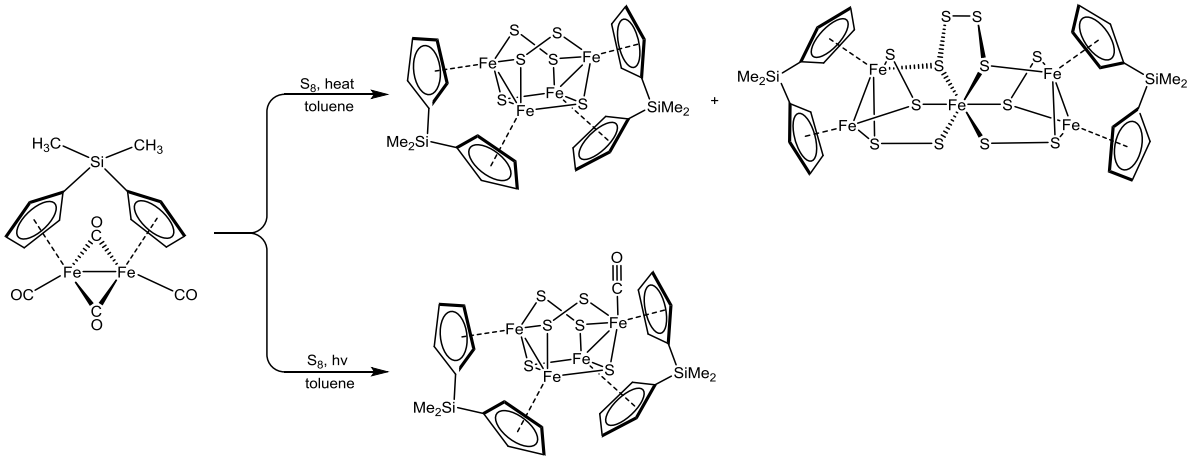

reaction of $[Me_2Si(\eta^5\text{-}C_5H_4)_2Fe_2(CO)_4]$ with S_8 in toluene gives a mixture of $[Me_2Si(\eta^5\text{-}C_5H_4)_2]_2Fe_5S_{12}$ and $[Me_2Si(\eta^5\text{-}C_5H_4)_2]_2Fe_4S_6$, while photolysis of this same reaction yields $[Me_2Si(\eta^5\text{-}C_5H_4)_2]_2Fe_4S_6(CO)$ (Scheme 4.1).[25,26] In actinide systems, installation of a terminal

chalcogenide ligand can be very difficult, as most of reactions tend to result in the formation of bimetallic chalcogen-bridged complexes.[27-31] For example, Meyer and co-workers reported that reaction of [((^{Ad}ArO)$_3$N)U(DME)] with elemental Se gave either [((^{Ad}ArO)$_3$N)U(DME)]$_2$(μ-Se), [((^{Ad}ArO)$_3$N)U]$_2$(μ-η^2:η^2-Se$_2$)(μ-DME), or [((^{Ad}ArO)$_3$N)U(DME)]$_2$(μ-η^3:η^3-Se$_4$), depending upon the stoichiometry.[27,28] Alternatively, Mazzanti and co-workers reported that reaction of [U((SiMe$_2$NPh)$_3$-tacn)] with elemental Se exclusively generates the bimetallic bridged complex, [U((SiMe$_2$NPh)$_3$-tacn)]$_2$(μ-Se), regardless of the stoichiometry.[29] Lastly, Hayton and co-workers reported that reaction of [U(NR$_2$)$_3$] with either Se or Te gave the corresponding bimetallic bridged monochalcogenides, [U(NR$_2$)$_3$](μ-E) (E = Se, Te), irrespective of the stoichiometry.[31]

The examples above illustrate the need for new synthetic strategies to access these complexes. In this regard, Hayton and co-workers recently reported that reaction of elemental chalcogen with the U(III) ylide adduct, [U(H$_2$CPPh$_3$)(NR$_2$)$_3$],[15] allows for isolation of a series uranium terminal chalcogenides, [Ph$_3$PCH$_3$][U(E)(NR$_2$)$_3$] (E = S, Se, Te).[23] Importantly, during this reaction the ylide ligand is believed to slow the rate of comproportionation, thus preventing the formation of a bimetallic bridged complex. The use of KSCPh$_3$ as a chalcogen atom transfer reagent, a strategy discussed in chapter 2, has also been shown to be an effective way to install these ligands (Scheme 2.2). The effectiveness of KSCPh$_3$ is due in part to its ability to function as a 1e$^-$ oxidant, whereas other chalcogen sources, like the elemental chalcogens and R$_3$P=E (E = S, Se, Te), function as 2e$^-$ oxidants. This is an extremely important observation because the actinides prefer 1e$^-$ redox chemistry.

Extending this strategy, of using of a triphenylmethyl protecting group, to include the heavier chalcogens was not possible due to the absence of Se and Te analogues of KSCPh$_3$.

This led to a search for other chalcogen sources that would perform the $1e^-$ redox chemistry favored by the actinides. In this regard, the polychalcogenides, $[E_n]^{2-}$ (E = Se, Te), specifically the dichalcogenides, $[E_2]^{2-}$, for which both chalcogen atoms are in a formally -1 oxidation state, are perfect for these reactions.[32-38] While these species have been known for over a hundred years, they are usually synthesized by reducing elemental chalcogen with an alkali metal either in liquid ammonia, or under solventothermal conditions.[32,37-50] These methods can be complicated and hazardous, and routinely use solvents that are not amenable to the highly air and moisture sensitive starting materials that are typically utilized in inorganic actinide chemistry.

As a result, alternative synthetic methods were sought. This chapter details these efforts, including the creation of a synthetic procedure that allows access to these polychalcogenide moieties, including a ditelluride and tetraselenide dianion. These polychalcogenides are generated under ambient temperatures and pressures and utilizing common organic solvents. Furthermore, these polychalcogenides are shown to be excellent chalcogen atom transfer reagents to both U(III) and U(IV), and are used to synthesis a series of new uranium terminal selenides and tellurides. These complexes are characterized both structurally and spectroscopically, and compared with their oxo and sulfido analogues.

4.2 Results and Discussion

4.2.1 Synthesis and Characterization of $[K(18\text{-crown-6})]_2[Te_2]$ (4.1) and $[K(2,2,2\text{-cryptand})]_2[Te_2]$ (4.2)

Reaction of elemental tellurium with 1 equiv of KH, in the presence of 1 equiv of 18-crown-6 or 2,2,2-cryptand, in THF, results in the formation of a violet-blue suspension, along with gas evolution, over the course of 18 h. The violet-blue powders, $[K(18\text{-crown-6})]_2[Te_2]$

(**4.1**) and $[K(2,2,2\text{-crpytand})]_2[Te_2]$ (**4.2**), can be isolated in 72% and 56% yield, respectively, after collection on a glass frit (Scheme 4.2). It should be noted that both complexes **4.1** and **4.2** were also prepared by Dehnen and co-workers, by mixing KPbTe with either 18-crown-6 or 2,2,2-cryptand in ethylenediamine, however, isolated yields of these reactions were low (*ca*. 10-15%).[51]

Scheme 4.2 Synthesis of $[K(L)]_2[Te_2]$ (**4.1**, L = 18-crown-6; **4.2**, L = 2,2,2-cryptand).

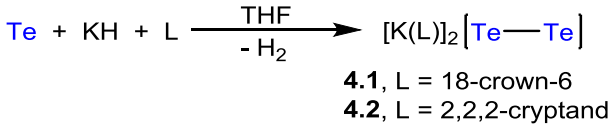

Crystals of **4.1** suitable for X-ray diffraction were grown from a dilute MeCN solution layered with diethyl ether. Complex **4.1** crystallizes in the monoclinic spacegroup *C*2/*c*, and its solid state molecular structure is shown in Figure 4.1. Complex **4.1** sits on a crystallographically imposed C_2 axis that results in one half of the molecule being generated by symmetry. In the solid state, **4.1** features a $[\mu\text{-}\eta^2\text{:}\eta^2\text{-}Te_2]^{2-}$ anion coordinated by two $[K(18\text{-crown-6})]^+$ moieties. Its Te-Te distance (2.7877(6) Å) is similar to the Te-Te distances (av. 2.78 Å) in other structurally characterized complexes containing the $[Te_2]^{2-}$ anion.[37,52-55] In addition, the Te-K distances are 3.483(1) and 3.6327(9) Å, and are similar to those observed in the Zintl phase, K_2Te_2 (av. K-Te = 3.57 Å).[37] It should also be noted that this structure is identical to that determined by Dehnen and co-workers.[51]

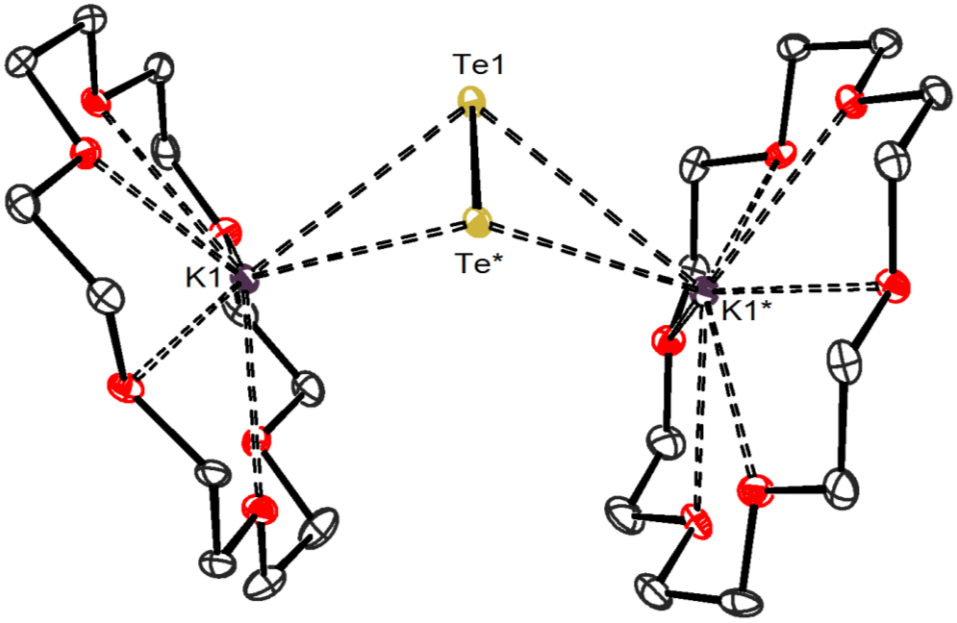

Figure 4.1. ORTEP diagram of $[K(18\text{-crown-6})]_2[Te_2]$ (4.1) with 50% probability ellipsoids. Hydrogen atoms are omitted for clarity. Selected bond lengths (Å): Te1-Te1* = 2.7877(6), K1-Te1 = 3.483(1), K1-Te1* = 3.6327(9).

Complex **4.1** is insoluble in non-polar or ethereal solvents, but is soluble in acetonitrile and pyridine. The violet-blue color in the solid-state is indicative of the presence of the $[Te_2]^{2-}$ anion.[46,52,56-58] Upon dissolution of **4.1** in MeCN, a red-violet solution is generated, which is consistent with the presence of both the $[Te_2]^{2-}$ and $[Te_3]^{2-}$ anions. All attempts to recrystallize **4.1** result in the co-precipitation of both violet-blue crystals, indicative of the presence of **4.1**, and violet-red crystals, which we suggest are $[K(18\text{-crown-6})]_2[Te_3]$.[46,52,56-58] This hypothesis is further supported by the UV-Vis spectrum of **4.1** in MeCN, which exhibits a broad peak centered at 550 nm and a peak at 298 nm (Figure A4.5), consistent with the presence of both $[Te_2]^{2-}$ and $[Te_3]^{2-}$ anions.[46,57] The formation of $[Te_3]^{2-}$ can be rationalized by invoking the disproportionation of $[Te_2]^{2-}$, a process that is known to occur for the $[Te_2]^{2-}$ anion in a variety of solvents.[46,52,56-58] This is also expected to be occur for solutions of complex **4.2**. While not ideal from a synthetic standpoint, as the $[Te_3]^{2-}$ anion contains an

extra Te atom in the 0 oxidation state, this does not appear to adversely affect the use of these species as Te transfer reagents, as seen by their reactivity described below.

4.2.2 Synthesis and Characterization of [K(18-crown-6)][U(Te)(NR$_2$)$_3$] (4.3) and [K(2,2,2-cryptand)][U(Te)(NR$_2$)$_3$] (4.4)

To test the atom transfer abilities of complexes **4.1** and **4.2**, these ditelluride salts were reacted with [U(NR$_2$)$_3$]. Accordingly, addition of 0.5 equiv of **4.1** to a solution of [U(NR$_2$)$_3$] in THF results in the formation of a black solution, that affords [K(18-crown-6)][U(Te)(NR$_2$)$_3$] (**4.3**), as black plates, in 51% yield, after crystallization from diethyl ether (Scheme 4.3). Likewise, addition of 0.5 equiv of **4.2** to a solution of [U(NR$_2$)$_3$] in pyridine results again in the formation of a black solution, that affords [K(2,2,2-cryptand)][U(Te)(NR$_2$)$_3$] (**4.4**), as black crystals, in 32% yield, upon crystallization from diethyl ether (Scheme 4.3). The ^{1}H NMR spectrum of complex **4.3**, in pyridine-d_5, exhibits

Scheme 4.3 Synthesis of [K(L)][U(Te)(NR$_2$)$_3$] (**4.3**, L = 18-crown-6; **4.4** L = 2,2,2-cryptand).

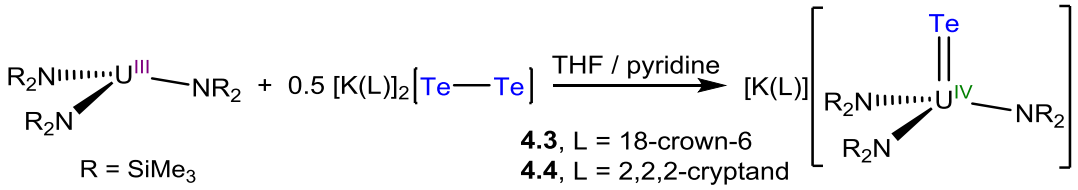

two broad resonances at -1.48 and 3.23 ppm, in a 54:24 ratio, assignable to the methyl groups of the silylamide ligands and the methylene groups of the 18-crown-6. The ^{1}H NMR spectrum of complex **4.4** exhibits four resonances, including a broad resonance at -1.48 ppm assignable to the methyl groups of the silylamide, in addition to two triplets and a singlet, at 2.06, 3.05 and 3.09 ppm, respectively, attributable to the three distinct proton environments of the 2,2,2-cryptand moiety.

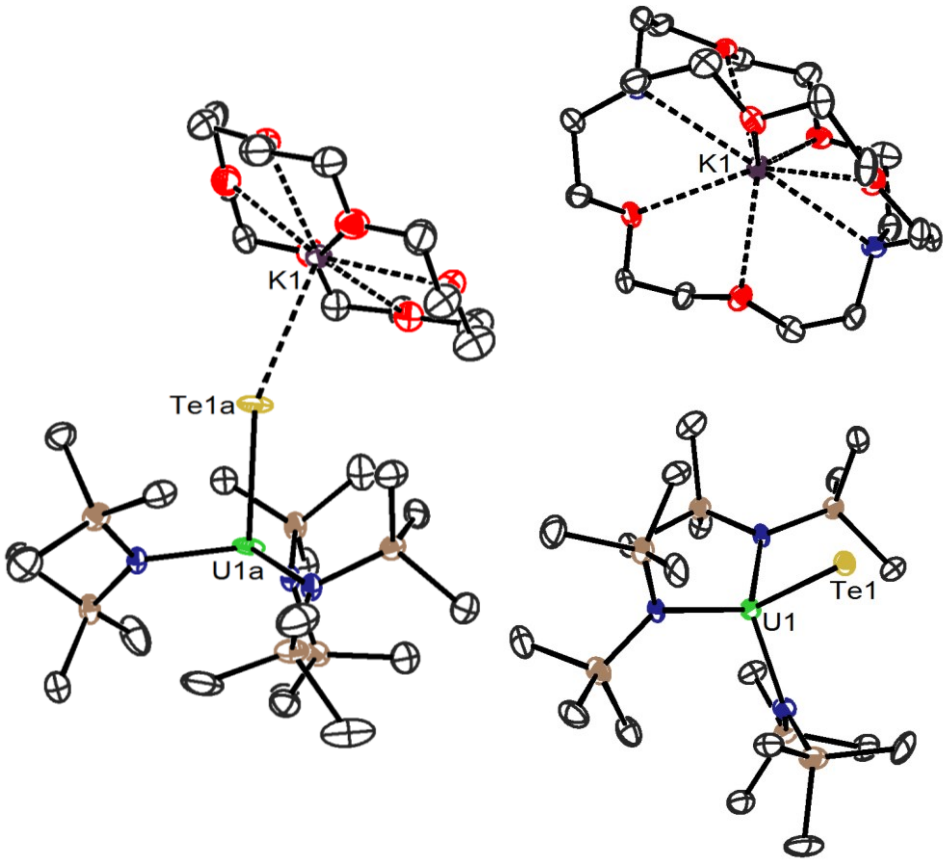

Figure 4.2. ORTEP diagram of [K(18-crown-6)][U(Te)(NR_2)$_3$] (**4.3**·0.5Et_2O) and [K(2,2,2-cryptand)][U(Te)(NR_2)$_3$] (**4.4**·Et_2O) with 50% probability ellipsoids. Three molecules of **4.3**, diethyl ether solvates, and hydrogen atoms omitted for clarity. Selected bond lengths (Å) and angles (deg): **4.3**, U1a-Te1a = 2.917(3), U1b-Te1b = 2.88(2), U2-Te2 = 2.879(2), U3-Te3 = 2.881(2), U4a-Te4a = 2.885(2), U4b-Te4b = 2.94(2), Te1a-K1 = 3.507(9), Te1b-K1 = 3.48(2), Te2-K2 = 3.467(2), Te3-K3 = 3.598(5), Te4a-K4 = 3.508(5); **4.4**, U1-Te1 = 2.854(1), Te1-K1 = 3.88(2), U-N (av.) = 2.30, N-U-N (av.) = 115.6.

Complex **4.3** crystallizes in the triclinic spacegroup $P\bar{1}$, as a diethyl ether solvate, **4.3**·0.5Et_2O, with four molecules in its asymmetric unit. Complex **4.4** crystallizes in the monoclinic spacegroup $P2_1/c$, also as a diethyl ether solvate, **4.4**·Et_2O. Their solid state molecular structures are shown in Figure 4.2 and selected metrical parameters can be found in Table 4.1. Both **4.3** and **4.4** feature pseudotetrahedral geometries about uranium, comparable to what has been previously observed for the [U(Te)(NR_2)$_3$]$^-$ moiety.[23] The U-

Te bond distances of **4.3** (av. = 2.90 Å) and **4.4** (2.854(1) Å) are similar to that of the one other U(IV) terminal telluride, $[Ph_3PCH_3][U(Te)(NR_2)_3]$ (2.866(2) Å).[23] In addition, these bond are significantly shorter than typical U(IV)-Te single bonds (av. = 3.12 Å),[31,59,60] suggestive of the multiple bond character of these linkages. The long Te-K bond lengths of **4.3** (av. 3.51 Å) are consistent with a dative interaction between the telluride ligand and the K^+ ion of the $[K(18\text{-crown-6})]^+$ moiety. Furthermore, the E-K bond lengths of **4.3** are longer than those of the structurally related oxo (**2.3**) (O-K = 2.640(5) Å) and sulfido (**2.1**) (av. S-K = 3.112 Å) complexes, consistent with the increase in ionic radii of Te^{2-} (2.21 Å) vs. O^{2-} (1.35 Å) and S^{2-} (1.84 Å).[61] The long distance between the Te^{2-} ligand of complex **4.4** and the nearest C atom of the $[K(2,2,2\text{-cryptand})]^+$ moiety (Te1-C34 = 3.892 Å) is comparable to the interaction between the Te^{2-} and the C of the methyl group of the $[Ph_3PCH_3]^+$ moiety in $[Ph_3PCH_3][U(Te)(NR_2)_3]$ (Te1-C1 = 3.853(2) Å).[23]

Table 4.1. Selected Bond Distances (Å) and Angles (deg) of Uranium Tellurides

Complex	**4.3**	**4.4**	$[Ph_3PCH_3][U(Te)(NR_2)_3]$[a]
U-Te	(av.) 2.90	2.854(1)	2.866(2)
Te-cation$^+$	(av.) 3.51	3.892	3.853(2)
U-N (av.)	2.33	2.30	2.28
N-U-N (av.)	112.2	115.6	115.7

[a] Taken from Ref [23]

4.2.3 Synthesis and Characterization of $[K(18\text{-crown-6})][U(\eta^2\text{-}Te_2)(NR_2)_3]$ (4.5) and $[K(2,2,2\text{-cryptand})][U(\eta^2\text{-}Te_2)(NR_2)_3]$ (4.6)

The syntheses of complexes **4.3** and **4.4** demonstrated the efficacy of the ditelluride salts **4.1** and **4.2** to act as single tellurium atom transfer reagents. The reactivity of these salts were

then probed with $[U(I)(NR_2)_3]$ to determine if they could also function as a source of $[Te_2]^{2-}$. Accordingly, addition of 1 equiv of complex **4.1** or **4.2** to a solution $[U(I)(NR_2)_3]$ in pyridine or 1:1 THF/pyridine, respectively, affords a black solution. Subsequent workup and crystallization from diethyl ether affords $[K(18\text{-crown-6})][U(\eta^2\text{-}Te_2)(NR_2)_3]$ (**4.5**) and $[K(2,2,2\text{-cryptand})][U(\eta^2\text{-}Te_2)(NR_2)_3]$ (**4.6**), as black crystalline solids, in 38% and 52% yields, respectively (Scheme 4.4). The ^{1}H NMR spectrum of complex **4.5** in benzene-d_6 exhibits one extremely broad resonance at -4.98 ppm, assignable to the methyl groups of the silylamide ligands, in addition to one broad resonance at 2.35 ppm, assignable to the 18-crown-6 moiety. These resonances shift to -6.40 and 3.45 ppm, respectively, in pyridine-d_5. In solution, similar to its solid state structure, complex **4.5** exists as a contact ion pair, with the $[K(18\text{-crown-6})]^+$ cation directly interacting with the $[U(\eta^2\text{-}Te_2)(NR_2)_3]^-$ anion, specifically in non-polar solvents such as benzene-d_6. When dissolved in a more polar coordinating solvent, such as pyridine-d_5, resonance attributed to the 18-crown-6 moiety shifts upfield towards free 18-crown-6 (3.39 ppm in benzene-d_6). The observed shift is indicative of the formation of a solvent separated cation/anion pair, similar to the behavior observed for complexes **2.1** and **2.2**. The ^{1}H NMR spectrum of complex **4.6**, in pyridine-d_5, is very similar to that of **4.5**, exhibiting an extremely broad resonance at -6.26 ppm, assignable to the methyl groups of the silylamide ligands, as well as three resonances at 2.35, 3.33, and 3.37 ppm, assignable to the three distinct proton environments of the 2,2,2-cryptand moiety (Figure A4.2).

Scheme 4.4 Synthesis of $[K(L)][U(\eta^2\text{-}Te_2)(NR_2)_3]$ (**4.5**, L = 18-crown-6; **4.6**, L = 2,2,2-cryptand)

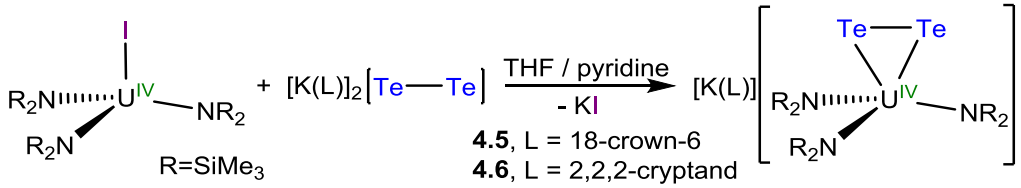

Complex **4.5** and **4.6** both crystallize in the triclinic spacegroup $P\bar{1}$. Complex **4.5** crystallizes as a diethyl ether solvate **4.5**·0.5Et_2O. Their solid state molecular structures are shown in Figure 4.3. Both complexes feature distorted pseudotetrahedral geometries about uranium, with N-U-N angles (e.g., **4.5**: 99.60(8)°, 107.78(8)°, and 127.19(8)°) that deviate substantially from what is to be expected for an idealized tetrahedron. This distortion is due to the presence of the larger $[\eta^2\text{-}Te_2]^{2-}$ ligand alongside the three sterically bulky $[N(SiMe_3)_2]^-$ ligands. This distortion is also manifested in the asymmetry exhibited by the U-Te bond distances of both complexes **4.5** (U1-Te1 = 3.1650(3) Å, U1-Te2 = 3.0506(3) Å) and **4.6** (U1-Te1 = 3.050(2) Å, U1-Te2 = 3.144(2) Å). The U-Te bond lengths are comparable to those previously reported for U-Te single bonds,[27,31,59,60,62,63] and appreciably longer than those of their monotelluride analogues, **4.3** and **4.4**. The Te-Te bond distances in **4.5** (Te1-Te2 = 2.7456(4) Å) and **4.6** (Te1-Te2 = 2.741(2) Å) are slightly longer than the range of Te-Te bond distances (2.665(2)–2.703(2) Å) in previously structurally characterized complexes with a terminal $[\eta^2\text{-}Te_2]^{2-}$ ligand,[64-73] but are similar to those of their ditelluride precursors, **4.1** (2.7877(6) Å) and **4.2** (2.764(1) Å).[51] In the solid state the $[Te_2]^{2-}$ ligand of **4.5** possesses dative interactions with the K^+ cation of the of the $[K(18\text{-crown-6})]^+$ moiety that results in an overall $[\mu\text{-}\eta^2\text{:}\eta^2]$ binding mode, a feature also seen in complex **4.1**. The asymmetric Te-K bond lengths of **4.5** (Te1-K1 = 3.7635(7) and Te2-K1 = 3.6344(7) Å) are longer than those of **4.1**, but similar to those of K_2Te_2.[37]

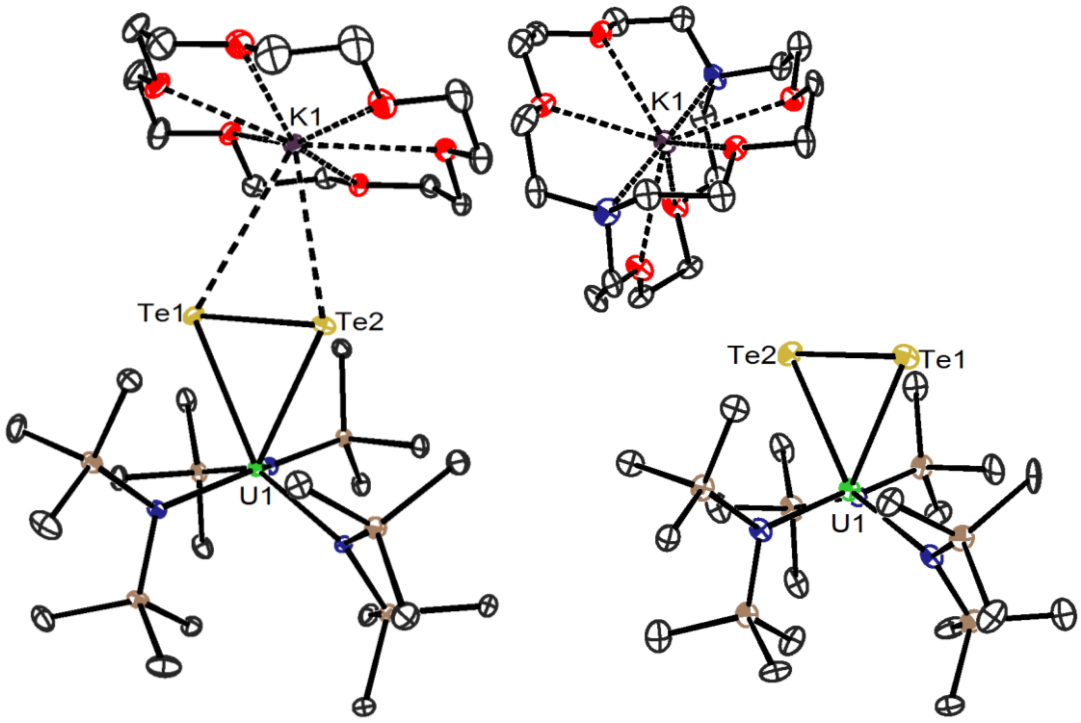

Figure 4.3. ORTEP diagram of [K(18-crown-6)][U(η^2-Te_2)(NR_2)$_3$] (**4.5**·0.5Et_2O) and [K(2,2,2-cryptand)][U(η^2-Te_2)(NR_2)$_3$] (**4.6**) with 50% probability ellipsoids. Hydrogen atoms and a diethyl ether solvate are omitted for clarity. Selected bond lengths (Å) and angles (deg): **4.5**, U1-Te1 = 3.1650(3), U1-Te2 = 3.0506(3), Te1-K1 = 3.7635(7), Te2-K1 = 3.6344(7), Te1-Te2 = 2.7456(4), N1-U1-N2 = 99.60(8), N1-U1-N3 = 107.78(8), N2-U1-N3 = 127.19(8); **4.6**, U1-Te1 = 3.050(2), U1-Te2 = 3.144(2), Te1-Te2 = 2.741(2), N1-U1-N2 = 107.2(4), N1-U1-N3 = 122.6(4), N2-U1-N3 = 99.7(4).

Complexes **4.5** and **4.6** are the first, and only, examples of uranium complexes with a terminal [η^2-Te_2]$^{2-}$ ligand, and their syntheses are achieved via simple salt metatheses. This method stands in stark contrast to the various routes used to synthesize the numerous transition metal examples, which usually utilize elemental tellurium, as the source of tellurium, and whose outcome can be extremely difficult to predict.[64,68,72,73]

4.2.4 Synthesis and Characterization of $[K(18\text{-crown-6})]_2[Se_4]$ (4.7)

The success had with ditellurides, **4.1** and **4.2**, spurred the investigation towards development of a selenium analogue. Thus, reaction of 1 equiv of elemental selenium with 0.5 equiv of KH, in the presence of 0.5 equiv of 18-crown-6 in THF, results in the formation of a brown suspension, along with gas evolution, over the course of 18 h. The brown powder, $[K(18\text{-crown-6})]_2[Se_4]$ (**4.7**), can be isolated in 72% yield after collection on a glass frit (Scheme 4.5).

Scheme 4.5 Synthesis of $[K(18\text{-crown-6})]_2[Se_4]$ (**4.7**)

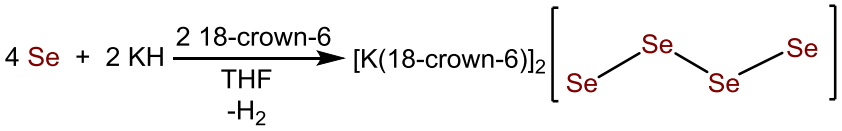

Complex **4.7** exhibits identical solubility to complexes **4.1** and **4.2**; it is insoluble in nonpolar solvents, but soluble in acetonitrile and pyridine. Upon dissolution of **4.7** in MeCN, a dark green solution is generated that is indicative of the presence of the $[Se_3]^{2-}$ anion.[43,58,74] Similar to what has been observed for the polytelluride anions, $[Se_4]^{2-}$ readily disproportionates in solution, forming a complex mixture of polyselenides, including $[Se_3]^{2-}$.[45,52,74-78] This is further evidenced by the UV-Vis spectrum of **4.7** in MeCN, which displays two bands at 434 and 598 nm, as well as a shoulder at 390 nm (Figure A4.5). These features are consistent with the presence of both the $[Se_3]^{2-}$ and $[Se_4]^{2-}$ anions.[74,79] It should be noted that all attempts to synthesize a species with a $[Se_2]^{2-}$ anion, similar to complexes **4.1** and **4.2** were unsuccessful. Reaction of elemental Se with KH and 18-crown-6, in a 1:1:1 molar ratio, in THF, generates a brown powder, consistent with the formation of an $[Se_4]^{2-}$ anion, not a red material, which would be indicative of the formation of an $[Se_2]^{2-}$ anion.[74] These results suggest that either KH is not capable of reducing elemental selenium to $[Se_2]^{2-}$

under these conditions, or that any $[Se_2]^{2-}$ formed is not stable under these conditions and readily forms other polyselenide anions.[47,52,58,80-82]

Crystals of **4.7** suitable for X-ray diffraction were grown from an MeCN solution layered with diethyl ether. Complex **4.7** crystallizes in the orthorhombic spacegroup *P*bcn as an acetonitrile solvate **4.7**·2MeCN and its solid state molecular structure is shown in Figure 4.4. **4.7** also sits on a crystallographically imposed C_2 axis that results in one half of the molecule being generated by symmetry. In the solid state, **4.7** features an $[Se_4]^{2-}$ anion that bridges two $[K(18\text{-crown-}6)]^+$ moieties via independent η^2 interactions. The long K-Se bond distances (K1-Se1 = 3.208(2), K1-Se2 = 3.486(2) Å) feature a notable asymmetry and are indicative of weak dative interactions. Additionally, the Se-Se bond distances (Se1-Se2 = 2.333(1), Se2-Se2* = 2.332(2) Å) are similar to those of other structurally characterized complexes with an $[Se_4]^{2-}$ moiety.[83-87]

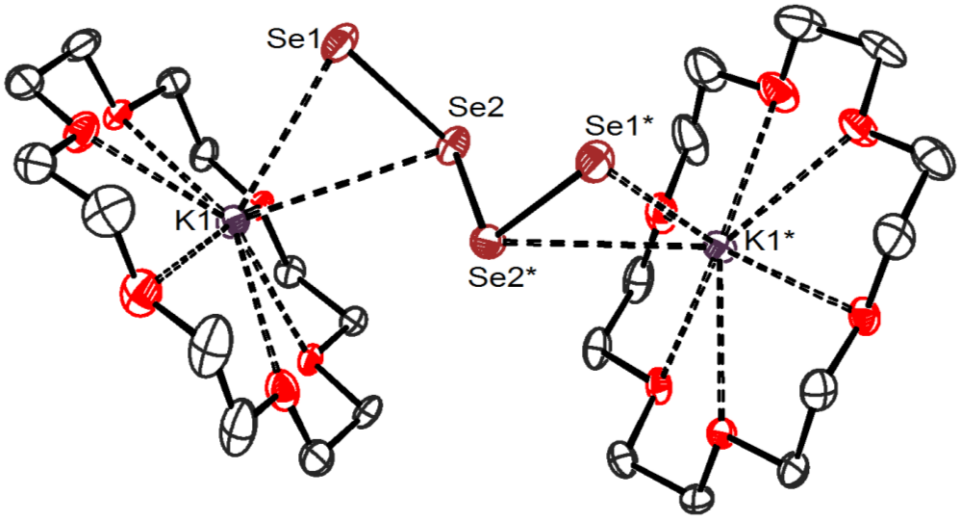

Figure 4.4. ORTEP diagram of $[K(18\text{-crown-}6)]_2[Se_4]$ (**4.7**·2MeCN) with 50% probability ellipsoids. Hydrogen atoms and acetonitrile solvates are omitted for clarity. Selected bond distances (Å): Se1-Se2 = 2.333(1), Se2-Se2* = 2.332(2), Se1-K1 = 3.208(2), Se2-K1 = 3.486(2).

4.2.5 Synthesis and Characterization of [K(18-crown-6)][(U(η^2-Se$_2$)(NR$_2$)$_3$] (4.8)

With complex **4.7** in hand, its atom transfer abilities were then investigated in a similar fashion to those of **4.1** and **4.2**. Accordingly, addition of 0.5 equiv of **4.7** to a solution of [U(NR$_2$)$_3$] in 2:1 THF/pyridine results in the formation of an orange-red solution. Removal of the solvent and subsequent crystallization from diethyl ether affords [K(18-crown-6)][(U(η^2-Se$_2$)(NR$_2$)$_3$] (**4.8**) as orange-red plates in 74% yield (Scheme 4.6). The [Se$_4$]$^{2-}$ anion is formally acting as a 2e$^-$ oxidant during which two U(III) centers reduce the [Se$_4$]$^{2-}$ anion and break the central Se-Se bond, which results in the formation of the two U(IV) η^2-diselenide moieties. The ^{1}H NMR spectrum of complex **4.8**, in pyridine-d_5, features two broad resonances at -7.65 and 3.47 ppm, assignable to the methyl groups of the silylamide ligands and the methylene groups of the 18-crown-6 moiety, respectively. In addition, the NIR spectrum of the **4.8** is consistent with the presence of a U(IV) metal center (Figure A4.4).[4,23,31,88]

Scheme 4.6 Synthesis of [K(18-crown-6)][U(η^2-Se$_2$)(NR$_2$)$_3$] (**4.8**)

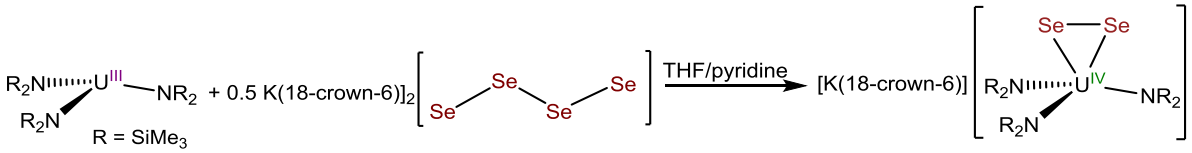

Complex **4.8** crystallizes in the monoclinic spacegroup $P2_1$, with two molecules in the asymmetric unit, and its solid state molecular structure is shown in Figure 4.5. Complex **4.8** is nearly structurally identical to complex **4.5**, differing only in the coordination of the K$^+$ cation, η^1 in **4.8** versus η^2 in **4.5**, to the dichalcogenide ligand. The Se-K bond distances (Se1-K1 = 3.261(2), Se3-K2 = 3.257(2) Å) are similar to those of complex **4.7**, and are shorter than the Te-K bond distances of complex **4.5**, consistent with the smaller ionic radius of Se^{2-} vs. Te^{2-}.[61] Complex **4.8** again features a distorted pseudotetrahedral geometry about uranium

(N1-U1-N2 = 100.7(2), N1-U1-N3 = 106.6(2), N2-U1-N3 = 129.4(2) Å) that is attributable to the presence of the more sterically demanding $[\eta^2\text{-}Se_2]^{2-}$ ligand in addition to the three bulky $[N(SiMe_3)_2]^-$ ligands. The U-Se bond distances of **4.8** exhibit a distinct asymmetry (U1-Se1 = 2.7897(7), U1-Se2 = 2.8597(8), U2-Se3 = 2.7833(7), U2-Se4 = 2.8614(8) Å) due to this steric crowding, identical to what is seen for complex **4.5**, its telluride analogue. The U-Se bond distances are comparable to those of other structurally characterized uranium species with a terminal diselenide ligand, such as $[Tp^*_2U(\eta^2\text{-}Se_2)]$ (Tp^* = hydrotris(3,5-dimethylpyrazolyl)borate) (U-Se = 2.8147(5) and 2.7745(5) Å) reported by Bart and co-workers in 2013,[89] and $[K]_4[U(Se_2)_4]$ (U-Se = 2.840(3), 2.903(3), 2.923(3), and 2.920(3) Å) reported by Kanatzidis and co-workers in 1991.[90] Finally, the Se-Se bond lengths in **4.8** (Se1-Se2 = 2.368(1), Se3-Se4 = 2.366(1) Å) are comparable to those of complex **4.7**, as well as to those of other structurally characterized complexes containing a terminal $[\eta^2\text{-}Se_2]^{2-}$ ligand (av. 2.375 Å).[68,80,91-109]

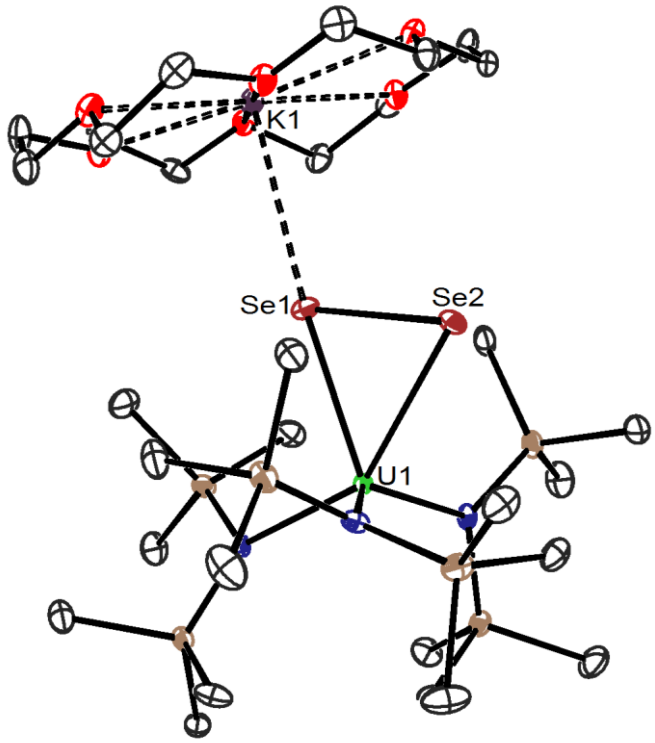

Figure 4.5. ORTEP diagram of [K(18-crown-6)][U(η^2-Se_2)(NR_2)$_3$] (4.8) with 50% probability ellipsoids. One molecule of **4.8** and hydrogen atoms are omitted for clarity. Selected bond distances (Å) and angles (deg): U1-Se1 = 2.7897(7), U1-Se2 = 2.8597(8), U2-Se3 = 2.7833(7), U2-Se4 = 2.8614(8), Se1-K1 = 3.261(2), Se3-K2 = 3.257(2), Se1-Se2 = 2.368(1), Se3-Se4 = 2.366(1), N1-U1-N2 = 100.7(2), N1-U1-N3 = 106.6(2), N2-U1-N3 = 129.4(2), N4-U2-N5 = 131.3(2), N4-U2-N6 = 100.3(2), N5-U2-N6 = 106.1(2).

4.2.6 Synthesis and Characterization of [K(18-crown-6)][U(Se)(NR_2)$_3$] (4.9)

While complex **4.8** was not the monoselenide complex originally sought, it was believed that it could be a viable precursor to a terminal monoselenide complex, via the removal of one Se atom. Thus, the reaction of 1 equiv of **4.8** with Ph_3P, in pyridine-d_5, was monitored by ^{1}H and ^{31}P{^{1}H} NMR spectroscopies. The in situ ^{1}H NMR spectrum of this reaction, after 5 min, revealed the complete consumption of **4.8** in addition to the appearance of a new broad resonance at -1.76 ppm, which was tentatively assigned to the new monoselenide complex,

[K(18-crown-6)][U(Se)$(NR_2)_3$] (**4.9**). Additionally, the $^{31}P\{^1H\}$ NMR spectrum obtained after 5 min features a new resonance at 34.31 ppm, assignable to the formation $Ph_3P{=}Se$.[110,111]

On a preparative scale, addition of 1 equiv of PPh_3 to a solution of **4.8**, in diethyl ether, affords [K(18-crown-6)][U(Se)$(NR_2)_3$] (**4.9**) as an orange-red crystalline solid, in 70% yield, upon crystallization (Scheme 4.7). The ^1H NMR spectrum of **4.9**, in pyridine-d_5, features two broad resonances at -1.76 and 3.07 ppm, assignable to the methyl groups of the silylamide ligands and the methylene groups of the 18-crown-6 moiety, respectively. Importantly, the NIR spectrum of complex **4.9** is consistent with a U(IV) metal center,[4,23,31,88] and demonstrates that no change in the uranium oxidation state takes place during this reaction (Figure A4.4).

Scheme 4.7 Synthesis of [K(18-crown-6)][U(Se)$(NR_2)_3$] (**4.9**)

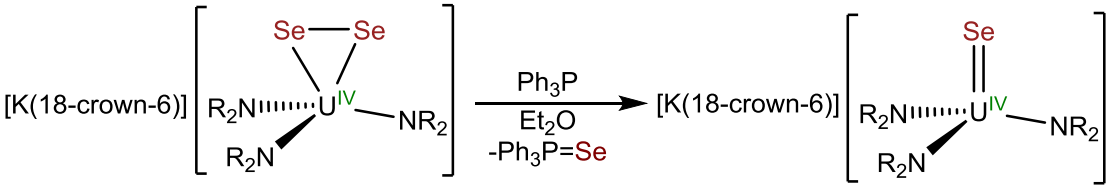

Complex **4.9** crystallizes in the triclinic space group $P\bar{1}$, features two molecules in the asymmetric unit, and its solid state molecular structure is shown in Figure 4.6. Complex **4.9** is structurally identical to its oxo (**2.3**), sulfido (**2.1**), and tellurido (**4.3**) congeners, featuring a pseudotetrahedral geometry about the uranium center (av. N-U-N = 116.8°, av. Se-U-N = 100.5°). The U-Se bond lengths in **4.9** (U1-Se1 = 2.585(1), U2-Se2 = 2.595(1) Å) are shorter than those observed in complex **4.8**, and are suggestive of multiple bond character in the U-Se interaction. These bond lengths are also slightly shorter than the U-Se bond length in the only other reported U(IV) terminal selenide, [Ph_3PCH_3][U(Se)$(NR_2)_3$] (2.6463(7) Å).[23] Finally, The E-K distances in **4.9** (Se1-K1 = 3.150(6), Se2-K2 = 3.234(3), Å) are shorter than those observed for telluride complex **4.3** (see above) and longer than those of the analogous

oxide (**2.3**, O1-K1 = 2.640(5) Å) and sulfide (**2.1**, av. S-K = 3.112 Å) complexes, consistent with the trend of increasing ionic radii as one moves down the group.[61]

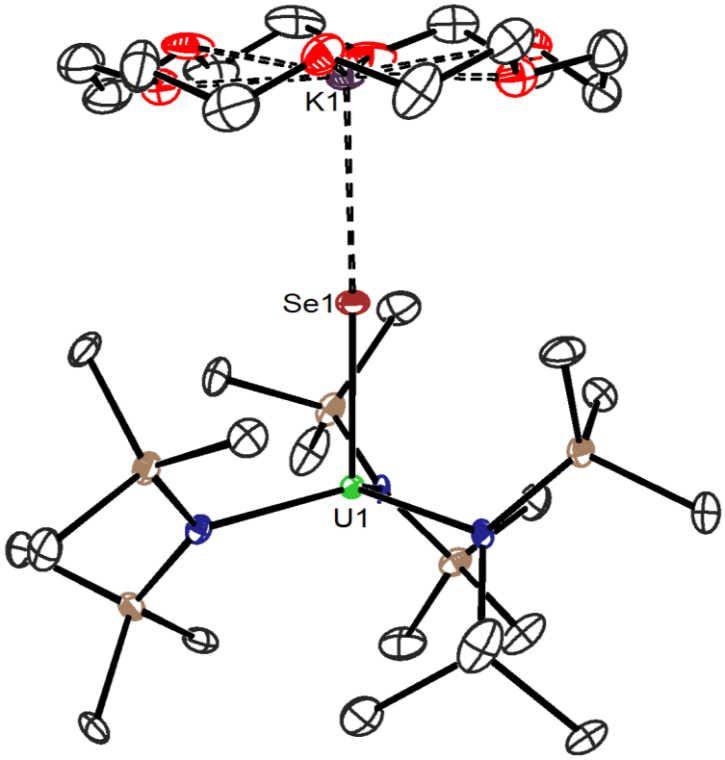

Figure 4.6. ORTEP diagram of [K(18-crown-6)][U(Se)(NR_2)$_3$] (**4.9**) with 50% probability ellipsoids. One molecule of **4.9** and hydrogen atoms are omitted for clarity. Selected bond distances (Å) and angles (deg): U1-Se1 = 2.585(1), U2-Se2 = 2.595(1), Se1-K1 = 3.150(6), Se2-K2 = 3.234(3), U-N (av.) = 2.29, N-U-N (av.) = 116.8°, Se-U-N (av.) = 100.5°.

4.2.7 Reaction of [U(NR_2)$_3$] with 0.25 equiv of [K(18-crown-6)]$_2$[Se_4] (4.7)

Addition of 0.25 equiv of **4.7** to a solution [U(NR_2)$_3$], in diethyl ether, results in the formation of an orange-red mixture. The ^{1}H NMR spectrum of this crude mixture, in benzene-d_6, reveals the formation of complexes **4.8**, **4.9**, and the previously reported bridged monoselenide, [U(NR_2)$_3$]$_2$(μ-Se),[31] in an approximately 1:1:1 ratio (Figure A4.3). Under these conditions, [U(NR_2)$_3$] is present in excess and Se atom transfer from **4.8** likely gives rise to the formation of [U(NR_2)$_3$]$_2$(μ-Se). The mixture of products obtained from this

experiment further demonstrates the need for controlled chalcogen atom transfer reagents that are better suited to match the $1e^-$ U(III)/U(IV) redox couple, and illustrates the utility of the polychalcogenides for installation of these ligands.

4.3 Summary

In summary, the ditelluride salts, $[K(L)]_2[Te_2]$ (**4.1**, L = 18-crown-6; **4.2**, L = 2,2,2-cryptand), can be prepared from elemental Te, KH, and 18-crown-6. This provides a rational route to the inorganic polychalcogenide salts that does not require elevated temperatures or pressures, nor does it require any specialized glassware. Reaction of $[U(NR_2)_3]$ with 0.5 equiv of **4.1** or **4.2** affords the U(IV) terminal monotelluride complexes, $[K(L)][U(Te)(NR_2)_3]$ (**4.3**, L = 18-crown-6; **4.4**, L = 2,2,2-cryptand) in moderate yields. These feature short U-Te bond distances, indicative of the multiple bond character of these interactions. In addition, reaction of the U(IV) iodide, $[U(I)(NR_2)_3]$, with 1 equiv of **4.1** and **4.2** affords the U(IV) terminal ditellurides, $[K(L)][U(\eta^2\text{-}Te_2)(NR_2)_3]$ (**4.5**, L = 18-crown-6; **4.6**, L = 2,2,2-cryptand). These complexes feature severely distorted pseudotetrahedral geometries evinced by asymmetric U-Te bond lengths and N-U-N angles, attributed to the presence of the larger $[\eta^2\text{-}Te_2]^{2-}$ ligand.

A similar synthetic procedure provides the tetraselenide salt, $[K(18\text{-crown-}6)]_2[Se_4]$ (**4.7**), in good yield. This complex has proven to be competent for Se atom transfer as well. Reaction of 0.5 equiv of **4.7** with $[U(NR_2)_3]$ affords the U(IV) terminal diselenide, $[K(18\text{-crown-}6)][U(\eta^2\text{-}Se_2)(NR_2)_3]$ (**4.8**) that is structurally identical to its Te analogue. Complex **4.8** readily reacts with phosphines to give the U(IV) terminal monoselenide, $[K(18\text{-crown-}6)][U(Se)(NR_2)_3]$ (**4.9**). Complex **4.9** is structurally identical to its O, S, and Te analogues, and features short U-Se bond distances indicative of multiple bond character.

The synthesis of these uranium chalcogenides demonstrate the utility of these polychalcogenide salts for installation of $[E]^{2-}$ and $[E_2]^{2-}$ ligands. Additionally, the differing redox pathways used suggest that these complexes could also be useful in systems that are resistant to the typical $2e^-$ chemistry of the chalcogens, or those resistant to any redox chemistry at all. Furthermore, analogous polysulfides should be both accessible and provide a similar route for the installation of sulfide ligands, an area of investigation that is discussed in Chapter 6.

4.4 Experimental

4.4.1 General Methods

All reactions and subsequent manipulations were performed under anaerobic and anhydrous conditions under an atmosphere of nitrogen. Hexanes, diethyl ether (Et_2O), and toluene were dried using a Vacuum Atmospheres DRI-SOLV Solvent Purification system and stored over 3Å sieves for 24 h prior to use. Tetrahydrofuran (THF) was distilled twice, first from calcium hydride and then from sodium benzophenone ketyl and stored over 3Å molecular sieves for 24 h prior to use. Dimethoxyethane (DME) was distilled from sodium benzophenone ketyl and stored over 3Å molecular sieves for 24 h prior to use. Pyridine, benzene-d_6, pyridine-d_5, and tetrahydrofuran-d_8 were dried over 3Å molecular sieves for 24 h prior to use. $[U(NR_2)_3]$,[112] $[U(I)(NR_2)_3]$,[4] were synthesized according to the previously reported procedures. All other reagents were purchased from commercial suppliers and used as received.

NMR spectra were recorded on a Varian UNITY INOVA 400, a Varian UNITY INOVA 500 spectrometer, or a Varian UNITY INOVA 600 MHz spectrometer. ^1H NMR spectra were referenced to external $SiMe_4$ using the residual protio solvent resonances as internal standards.

$^{31}P\{^{1}H\}$ NMR spectra were referenced to external 85% H_3PO_4 in D_2O. IR spectra were recorded on a Nicolet 6700 FT-IR spectrometer with a NXR FT Raman Module. UV-Vis / NIR experiments were performed on a UV-3600 Shimadzu spectrophotometer. Elemental analyses were performed by the Micro-Mass Facility at the University of California, Berkeley.

4.4.2 Synthesis of $[K(18\text{-crown-}6)]_2[Te_2]$ (4.1)

To a mixture of Te powder (200.8 mg, 1.57 mmol) and 18-crown-6 (422.0 mg, 1.60 mmol) in tetrahydrofuran (4 mL) was added KH (63.8 mg, 1.59 mmol). This mixture was allowed to stir for 18 h, during which time gas evolution was observed, concomitant with the deposition of a violet-blue powder. This material was collected by filtration through a glass frit, and subsequently rinsed with Et_2O (5 mL) to provide a violet-blue powder (488.5 mg, 72% yield). This material was used in subsequent reactions without further purification. Anal. Calcd for $C_{24}H_{48}K_2O_{12}Te_2$: C, 33.44; H, 5.61. Found: C, 26.27; H, 4.39. The low carbon % is attributed to the incomplete solvation of the K^+ cations by 18-crown-6. ^1H NMR (600 MHz, 25 °C, CD_3CN): δ 3.58 (s, 18-crown-6). IR (KBr Pellet, cm^{-1}): 529 (w). 614 (w), 730 (w), 839 (m), 965 (s), 1106 (s), 1251 (m), 1283 (m), 1351 (s), 1433 (w), 1452 (m), 1473 (m), 2744 (w), 2822 (m), 2882 (s). UV-Vis/NIR (CH_3CN, 0.174 mM, 25 °C, $L \cdot mol^{-1} \cdot cm^{-1}$): 298 (ε = 10661), 550 (ε = 3140). Crystals of **4.1** suitable for X-ray crystallography were grown from a dilute acetonitrile solution layered with diethyl ether.

4.4.3 Synthesis of $[K(2,2,2\text{-cryptand})]_2[Te_2]$ (4.2)

To a mixture of Te powder (32.4 mg, 0.25 mmol) and 2,2,2-cryptand (97.9 mg, 0.26 mmol) in tetrahydrofuran (4 mL) was added KH (10.4 mg, 0.26 mmol). This mixture was allowed to stir for 48 h, during which time gas evolution was observed, concomitant with the

deposition of a violet-blue powder. This material was collected by filtration through a glass frit, and subsequently rinsed with Et_2O (5 mL) to provide a violet-blue powder (76.8 mg, 56% yield). This material was used in subsequent reactions without further purification.

4.4.4 Synthesis of [K(18-crown-6)][U(Te)(NR$_2$)$_3$] (4.3)

To a deep purple, cold (-25 °C), stirring solution of [U(N(SiMe$_3$)$_2$)$_3$] (120.2 mg, 0.17 mmol) in THF (2 mL) was added dropwise a cold (-25 °C), red-violet solution of **4.1** (72.1 mg, 0.083 mmol) in pyridine (2 mL). This solution was allowed to stir for 30 min, whereupon the solvent was removed in vacuo and the resulting black solid was triturated with hexanes (5 mL). The resulting black powder was extracted with diethyl ether (6 mL) and filtered through a Celite column supported on glass wool (0.5 cm × 3 cm). The volume of the filtrate was reduced to 1 mL in vacuo. Storage of this solution at -25 °C for 24 h resulted in the deposition of black crystals, which were isolated by decanting off the supernatant (98.0 mg, 51%). It should be noted that complex **4.1** likely undergoes disproportionation to the higher polychalcogenides upon dissolution in pyridine, as indicated by the violet-red solution that it forms in this solvent. Anal. Calcd for $C_{30}H_{78}KN_3O_6Si_6TeU \cdot 0.5C_4H_{10}O$: C, 32.37; H, 7.05; N, 3.54. Found: C, 32.37; H, 6.58; N, 3.48. ^{1}H NMR (400 MHz, 25 °C, pyridine-d_5): δ -1.48 (br s, 54H, NSiCH_3), 3.23 (br s, 24H, 18-crown-6). IR (KBr Pellet, cm^{-1}): 609 (m), 662 (m), 688 (m), 723 (m), 841 (s), 883 (m), 934 (m), 964 (m), 1109 (s), 1183 (w), 1251 (m), 1284 (w), 1352 (m), 1454 (w), 1473 (w), 2894 (m), 2953 (m). UV-Vis/NIR (C_4H_8O, 5.17 mM, 25 °C, L·mol^{-1}·cm^{-1}): 1016 (ε = 16.3), 1098 (ε = 31.9), 1198 (ε = 26.5), 1500 (ε = 12.8), 1650 (ε = 14.7), 1794 (ε = 13.5), 2060 (ε = 23.8), 2166 (ε = 29.2).

4.4.5 Synthesis of [K(2,2,2-cryptand)][U(Te)(NR$_2$)$_3$] (4.4)

To a cold (-25 °C), stirring solution of [U(N(SiMe$_3$)$_2$)$_3$] (54.8 mg, 0.076 mmol) in pyridine (2 mL) was added dropwise a cold (-25 °C) solution of **4.2** (42.3 mg, 0.039 mmol) in pyridine (3 mL). This solution was allowed to stir for 15 min, whereupon the solvent was removed in vacuo. The resulting black solid was extracted with diethyl ether (4 mL) and filtered through a Celite column supported on glass wool (0.5 cm × 3 cm). The volume of the filtrate was reduced to 2 mL in vacuo. Storage of this solution at -25 °C for 24 h resulted in the deposition of black crystals, which were isolated by decanting off the supernatant (20.4 mg, 21%). The supernatant was further concentrated to 1 mL in vacuo and storage of this solution at -25 °C for 24 h resulted in the deposition of additional black crystals (total yield: 25%). This solution was then transferred to a 4 mL scintillation vial that was place inside a 20 mL scintillation vial. Toluene (6 mL) was then added to the outer vial. Storage of this two vial system for 48 h resulted in the deposition of additional black crystals (total yield: 32%). Anal. Calcd for $C_{36}H_{90}KN_5O_6Si_6TeU$: C, 34.25; H, 7.19; N, 5.55. Found: C, 33.84; H, 7.05; N, 5.28. ^{1}H NMR (400 MHz, 25 °C, pyridine-d_5): δ -1.48 (br s, 54H, NSiCH_3), 2.06 (t, 12H, J_{HH} = 4.6 Hz, NCH_2), 3.05 (t, 12H, J_{HH} = 4.6 Hz, OCH_2CH$_2$N), 3.09 (s, 12H, OCH_2CH_2O). IR (KBr Pellet, cm^{-1}): 669 (w), 752 (w), 845 (m), 887 (m), 933 (m), 1103 (s), 1130 (m), 1180 (m), 1257 (m), 1296 (w), 1356 (m), 1446 (w), 1475 (w), 2812 (m), 2875 (s), 2954 (s).

4.4.6 Synthesis of [K(18-crown-6)][U(η^2-Te$_2$)(NR$_2$)$_3$] (4.5)

To a cold (-25 °C), stirring mixture of [U(I)(N(SiMe$_3$)$_2$)$_3$] (61.5 mg, 0.073 mmol) in pyridine (3 mL) was added dropwise a cold (-25 °C) solution of **4.1** (64.0 mg, 0.074 mmol) in pyridine (3 mL). This mixture was allowed to stir for 20 min, whereupon the solvent was removed in vacuo and the resulting black solid was triturated with hexanes (3 × 5 mL). The

black powder was then extracted with diethyl ether (8 mL) and filtered through a Celite column supported on glass wool (0.5 cm × 3 cm). The volume of the filtrate was reduced to 1 mL in vacuo. Storage of this solution at -25 °C for 24 h resulted in the deposition of black crystals, which were isolated by decanting off the supernatant (34.9 mg, 38%). Anal. Calcd for $C_{30}H_{78}KN_3O_6Si_6Te_2U$: C, 28.20; H, 6.15; N, 3.29. Found: C, 28.49; H, 6.29; N, 3.04. ^{1}H NMR (400 MHz, 25 °C, benzene-d_6): δ -4.98 (br s, 54H, NSiCH_3), 2.35 (br s, 24H, 18-crown-6). ^{1}H NMR (400 MHz, 25 °C, pyridine-d_5): δ -6.40 (br s, 54H, NSiCH_3), 3.45 (br s, 24H, 18-crown-6). IR (KBr Mull, cm^{-1}): 610 (w), 662 (w), 688 (w), 773 (w), 842 (s), 885 (m), 934 (m), 936 (m), 1108 (s), 1182 (w), 1251 (m), 1284 (w), 1352 (w), 1454 (w), 1473 (w), 2894 (m), 2954 (m). UV-Vis/NIR (C_4H_8O, 4.41 mM, 25 °C, L·mol^{-1}·cm^{-1}): 1020 (ε = 33.3), 1078 (ε = 40.5), 1136 (ε = 34.0), 1318 (ε = 17.9), 1440 (ε = 10.4), 1500 (ε = 13.8), 1658 (ε = 11.3), 1804 (ε = 18.6), 2054 (ε = 63.4), 2180 (ε = 76.8).

4.4.7 Synthesis of [K(2,2,2,-cryptand)][U(η^2-Te$_2$)(NR$_2$)$_3$] (4.6)

To a cold (-25 °C), stirring solution of [U(I)(N(SiMe$_3$)$_2$)$_3$] (31.3 mg, 0.037 mmol) in THF (3 mL) was added a cold (-25 °C) mixture of **4.2** (41.2 mg, 0.038 mmol) in 1:1 THF / pyridine (3 mL). This mixture was allowed to stir for 30 min, whereupon the solvent was removed in vacuo and the resulting black solid was triturated with hexanes (1 × 5 mL). The black powder was then extracted with diethyl ether (4 mL) and filtered through a Celite column supported on glass wool (0.5 cm × 3 cm). The volume of the filtrate was reduced to 1 mL in vacuo. Storage of this solution at -25 °C for 24 h resulted in the deposition of black crystals, which were isolated by decanting off the supernatant (26.7 mg, 52%). Anal. Calcd for $C_{36}H_{90}KN_5O_6Si_6Te_2U$: C, 31.11; H, 6.53; N, 5.04. Found: C, 31.37; H, 6.65; N, 4.98. ^{1}H NMR (400 MHz, 25 °C, pyridine-d_5): δ -6.26 (br s, 54H, NSiCH_3), 2.35 (t, 12H, J_{HH} = 4.6 Hz,

NCH_2), 3.33-3.37 (m, 12H, OCH_2CH_2N), 3.38 (s, 12H, OCH_2CH_2O). IR (KBr Pellet, cm^{-1}): 611 (m), 663 (m), 673 (m), 754 (m), 773 (m), 845 (s), 891 (s), 901 (s), 912 (s), 933 (s), 957 (s), 1080 (m), 1105 (s), 1134 (m), 1182 (m), 1250 (s), 1298 (m), 1354 (m), 1356 (m), 1444 (w), 1458 (w), 1477 (w), 2812 (m), 2889 (s), 2956 (s).

4.4.8 Synthesis of [K(18-crown-6)]$_2$[Se$_4$] (4.7)

To a mixture of Se powder (34.2 mg, 0.43 mmol) and 18-crown-6 (57.2 mg, 0.22 mmol) in tetrahydrofuran (4 mL) was added KH (8.7 mg, 0.22 mmol). This mixture was allowed to stir for 18 h, during which time gas evolution was observed, concomitant with the deposition of a brown powder. This material was collected by filtration through a glass frit, and subsequently rinsed with Et_2O (5 mL) to provide a brown powder (78.6 mg, 72% yield). This material was used in subsequent reactions without further purification. Anal. Calcd for $C_{24}H_{48}K_2O_{12}Se_4$: C, 31.24; H, 5.24; N, 0.0. Found: C, 29.76; H, 4.73; N, 0.29. The low carbon % is attributed to the incomplete solvation of the K^+ cations by 18-crown-6. ^{1}H NMR (500 MHz, 25 °C, CD_3CN): δ 3.58 (s, 18-crown-6). IR (KBr Mull, cm^{-1}): 530 (w), 838 (m), 964 (s), 1106 (s), 1250 (m), 1285 (m), 1351 (m), 1454 (m), 1473 (m), 2824 (m), 2894 (s). UV-Vis/NIR (CH_3CN, 0.323 mM, 25 °C, $L \cdot mol^{-1} \cdot cm^{-1}$): 390 (sh) (ε = 5280), 434 (ε = 6721), 598 (ε = 1401). Crystals of **4.7** suitable for X-ray crystallography were grown from a dilute acetonitrile solution layered with diethyl ether.

4.4.9 Synthesis of [K(18-crown-6)][U(η^2-Se$_2$)(NR$_2$)$_3$] (4.8)

To a deep green, cold (-25 °C), stirring mixture of **4.7** (89.9 mg, 0.097 mmol) dissolved in a 2:1 mixture of tetrahydrofuran and pyridine (4 mL) was added a deep purple, cold (-25 °C) solution of [U(N(SiMe$_3$)$_2$)$_3$] (132.9 mg, 0.18 mmol) in tetrahydrofuran (2 mL). This

solution was allowed to stir for 20 min, whereupon the solvent was removed in vacuo and the resulting orange-red solid was triturated with Et_2O (5 mL) and hexanes (2 × 5 mL). The orange-red powder was then extracted with diethyl ether (10 mL) and filtered through a Celite column supported on glass wool (0.5 cm × 2 cm). The volume of the orange-red filtrate was reduced in vacuo to 1 mL. This solution was then transferred to a 4 mL scintillation vial that was placed inside a 20 mL scintillation vial. Toluene (6 mL) was then added to the outer vial. Storage of this two vial system for 72 h resulted in the deposition of orange-red crystalline solid, which was isolated by decanting the supernatant (161.0 mg, 74%). Anal. Calcd for $C_{30}H_{78}KN_3O_6Se_2Si_6U$: C, 30.52; H, 6.66; N, 3.56. Found: C, 30.60; H, 6.86; N, 3.62. ^{1}H NMR (600 MHz, 25 °C, pyridine-d_5): δ -7.65 (br s, 54H, NSiCH_3), 3.47 (br s, 24H, 18-crown-6). IR (KBr Mull, cm^{-1}): 610 (m), 663 (m), 772 (m), 845 (s), 897 (m), 921 (s), 964 (m), 1111 (s), 1182 (w), 1249 (s), 1284 (w), 1352 (m), 1454 (w), 1473 (w), 2826 (w), 2894 (s), 2951 (s). UV-Vis/NIR (C_4H_8O, 3.92 mM, 25 °C, $L \cdot mol^{-1} \cdot cm^{-1}$): 1020 (ε = 45.6), 1080 (ε = 51.0), 1134 (ε = 43.1), 1322 (ε = 25.7), 1450 (ε = 16.8), 1508 (ε =18.9), 1626 (ε =15.8), 1806 (ε = 17.6), 2062 (ε = 60.7), 2160 (ε = 68.8).

4.4.10 Synthesis of [K(18-crown-6)][U(Se)(NR$_2$)$_3$] (4.9)

To a deep orange-red, cold (-25 °C), stirring solution of **4.8** (102.5 mg, 0.087 mmol), in diethyl ether (3 mL) was added a cold (-25 °C) solution of Ph_3P (22.2 mg, 0.085 mmol) in diethyl ether (2 mL). The solution was allowed to stir for 15 min, during which time a white precipitate was deposited in the reaction vial. The reaction mixture was filtered through a Celite column supported on glass wool (0.5 cm × 2 cm). The volume of the orange-red filtrate was reduced in vacuo to 3 mL. Storage of this solution at -25 °C for 24 h resulted in the further deposition of colorless crystals, subsequently identified as Ph_3P=Se by $^{31}P\{^1H\}$ NMR

spectroscopy. These were isolated by decanting the supernatant. The volume of the supernatant was reduced in vacuo to 2 mL. This solution was then transferred to a 4 mL scintillation vial that was place inside a 20 mL scintillation vial. Toluene (6 mL) was then added to the outer vial. Storage of this two vial system for 48 h resulted in the deposition of an orange-red crystalline solid, which was isolated by decanting the supernatant (67.0 mg, 70%). Anal. Calcd for $C_{30}H_{78}KN_3O_6SeSi_6U$: C, 32.71; H, 7.14; N, 3.81. Found: C, 32.93; H, 6.87; N, 3.75. ^{1}H NMR (600 MHz, 25 °C, pyridine-d_5): δ -1.77 (br s, 54H, NSiCH_3), 3.12 (br s, 24H, 18-crown-6). IR (KBr pellet, cm^{-1}): 689 (w), 756 (w), 844 (s), 886 (m), 935 (s), 1046 (w), 1105 (s), 1182 (m), 1252 (s), 1285 (w), 1352 (m), 2896 (s), 2955 (s). UV-Vis/NIR (C_4H_8O, 4.77 mM, 25 °C, L·mol^{-1}·cm^{-1}): 700 (ε = 33.9), 720 (ε = 32.0), 928 (ε = 6.9), 1112 (ε = 26.0), 1208 (ε = 32.5).

4.4.11 Reaction of [U(NR$_2$)$_3$] with (4.1)

To a deep blue solution of [U(NR$_2$)$_3$] (15.9 mg, 0.022 mmol), in pyridine-d_5 (0.75 mL) was added a violet suspension of **4.1** (9.6 mg, 0.011 mmol) in pyridine-d_5 (0.75 mL). A color change to black was observed immediately upon addition. After 5 min, a ^{1}H NMR spectrum was obtained, revealing the clean formation of **4.3**. ^{1}H NMR (400 MHz, 25 °C, pyridine-d_5): δ -1.48 (br s, 54H, NSiCH_3), 3.12 (br s, 24H, 18-crown-6).

4.4.12 Reaction of [U(NR$_2$)$_3$] with 0.25 equiv of (4.7)

To a stirring, deep purple solution of [U(NR$_2$)$_3$] (38.4 mg, 0.053 mmol) in Et$_2$O (2 mL) was added **4.7** (13.4 mg, 0.015 mmol) as a solid. A color change to orange-brown was observed immediately upon addition. After 10 min, the volatiles were removed in vacuo. The resulting brown solid was dissolved in C_6D_6 (0.75 mL), and a ^{1}H NMR spectrum was

recorded. ^{1}H NMR (400 MHz, 25 °C, C_6D_6): δ –7.07 (br s, 54H, **4.8**), -6.55 (br s, 108H, $[U(NR_2)_3]_2(\mu\text{-Se})$), -1.63 (br s, 54H, **4.9**), 0.38 (br s, 24H, 18-crown-6). The resonance at -6.55 ppm was assigned to $[U(NR_2)_3]_2(\mu\text{-Se})$ by comparison with the ^{1}H NMR spectrum of authentic material.[31]

4.4.13 Reaction of [K(18-crown-6)][U(η^2-Se$_2$)(NR$_2$)$_3$] (4.8) with PPh$_3$

To an orange-red solution of **4.8** (30.0 mg, 0.025 mmol) in pyridine-d_5 (0.75 mL) was added a solution of PPh_3 (6.8 mg, 0.026 mmol) in pyridine-d_5 (0.5 mL). The color lightened upon addition. After 5 min, ^{1}H NMR and ^{31}P NMR spectra were obtained, revealing the clean formation of **4.9** and Ph_3P=Se. ^{1}H NMR (600 MHz, 25 °C, pyridine-d_5): δ -1.76 (br s, 54H, **4.9** NSiCH_3), 3.04 (br s, 24H, **4.9** 18-crown-6), 7.35-7.39 (m, 9H, Ph_3P overlapping resonances from *m*-C*H* and *p*-C*H*), 7.40-7.44 (m, 6H, Ph_3P=Se *m*-C*H*), 7.45-7.51 (m, 9H, overlapping resonances from *o*-C*H* of Ph_3P and *p*-C*H* of Ph_3P=Se), 7.92-8.00 (m, 6H, Ph_3P=Se, *o*-C*H*). ^{31}P{^{1}H} NMR (161.92 MHz, 25 °C, pyridine-d_5): δ -6.73 (s, Ph_3P), 34.31 (s, Ph_3P=Se).

4.4.14 X-ray Crystallography

Data for **4.1**, **4.3**, **4.4**, **4.5**, **4.6**, **4.7**, **4.8**, **4.9** were collected on a Bruker KAPPA APEX II diffractometer equipped with an APEX II CCD detector using a TRIUMPH monochromator with a Mo Kα X-ray source (α = 0.71073 Å). The crystals were mounted on a cryoloop under Paratone-N oil, and all data were collected at 100(2) K using an Oxford nitrogen gas cryostream. Data were collected using ω scans with 0.5° frame widths. Frame exposures of 10 s (low angle), and 15 s (high angle) were used for **4.1**. Frame exposures of 10 s were used for **4.3** and **4.9**. Frame exposures of 2 s were used for **4.5**. Frame exposures of 60 s were used

for **4.7**. Frame exposures of 5 s (low angle) and 10 s (high angle) were used for **4.8**. Data collection and cell parameter determination were conducted using the SMART program.[113] Integration of the data frames and final cell parameter refinement were performed using SAINT software.[114] For complexes **4.1**, **4.3-4.7** and **4.9**, the absorption correction was performed using SADABS,[115] while for complex **4.8**, which crystallized as a racemic twin in a ratio of 46:54, the absorption correction was performed with TWINABS.[116] Subsequent calculations were carried out using SHELXTL.[117] Structure determination was done using direct or Patterson methods and difference Fourier techniques. All hydrogen atom positions were idealized, and rode on the atom of attachment. Structure solution, refinement, graphics, and creation of publication materials were performed using SHELXTL.[117]

Complex **4.3** crystallizes in the triclinic space group $P\bar{1}$ with four independent molecules in the asymmetric unit. The four molecules of **4.3** differ significantly in their U-Te-K angles (e.g., U1a-Te1a-K1 = 155.4(1)°, U1b-Te1b-K1 = 133.8(8), U2-Te2-K2 = 162.1(1)°, U3-Te3-K3 = 132.96(9)°, U4a-Te4a-K4 = 149.2(1)°), which disrupts any possible symmetry operations that could interrelate the four molecules, and results in the observed low symmetry space group. For this structure, U1, Te1, U4, and Te4 exhibited positional disorder, wherein each atom was modeled over two sites in a 90:10 ratio. In addition, the anisotropic displacement parameters of the K, Si, N, O and C atoms among four molecules in the asymmetric unit were constrained with the EADP command, while for the U and Te atoms, only the thermal parameters of the disordered pairs were constrained. Finally, one of the diethyl ether solvate molecules in **4.3** exhibited positional disorder; one carbon of this molecule was modeled over two positions in a 50:50 ratio. The C-C and C-O bond distances of all the diethyl ether solvate molecules were constrained to 1.54 and 1.45 Å, respectively,

using the DFIX command. Hydrogen atoms were not assigned to disordered carbon atoms. The diethyl ether solvate molecule in **4.5** exhibited positional disorder. One carbon atom was modeled over two positions in a 50:50 ratio. The C-C and C-O bond distances of the diethyl ether solvate were constrained to 1.54 and 1.45 Å, respectively, using the DFIX command. The C-C and C-N bond distances of the acetonitrile solvate molecule of **4.7** were constrained to 1.45 and 1.1 Å, respectively, using the DFIX command.

Table 4.2. X-ray Crystallographic Data for Complexes **4.1**, **4.3**, and **4.4**

	4.1	**4.3**·0.5$C_4H_{10}O$	**4.4**·$C_4H_{10}O$
empirical formula	$C_{24}H_{48}K_2O_{12}Te_2$	$C_{32}H_{83}KN_3O_{6.5}Si_6TeU$	$C_{40}H_{100}KN_5O_7Si_6TeU$
crystal habit, color	block, blue	plate, black	plate, black
crystal size (mm)	0.2 × 0.1 × 0.1	0.2 × 0.2 × 0.01	0.4× 0.2 × 0.05
space group	*C*2/*c*	$P\bar{1}$	$P2_1/c$
volume (Å^3)	3510.4(6)	10907(11)	6271.7(14)
a (Å)	22.801(3)	11.589(7)	21.127(2)
b (Å)	8.5162(8)	22.75(1)	13.435(2)
c (Å)	19.626(2)	43.62(3)	22.543(3)
α (deg)	90	102.440(8)	90
β (deg)	112.904(4)	93.421(6)	101.418(6)
γ (deg)	90	102.200(7)	90
Z	4	8	4
formula weight (g/mol)	862.02	1187.28	1336.52
density (calculated) (Mg/m^3)	1.631	1.446	1.415
absorption coefficient (mm^{-1})	1.950	3.745	3.267
F_{000}	1720	4760	2712
total no. reflections	7576	140939	27721
unique reflections	3603	46966	11648
R_{int}	0.0399	0.0922	0.1307
final R indices (I >2σ(I)]	R_1 = 0.0351 wR_2 = 0.0707	R_1 = 0.1425 wR_2 = 0.2828	R_1 = 0.0758 wR_2 = 0.1782
largest diff. peak and hole (e$^-$ A^{-3})	0.970 and -0.910	6.663 and -8.717	3.032 and -3.787
GOF	0.960	1.645	0.997

Table 4.3. X-ray Crystallographic Data for Complexes **4.5**, **4.6**, and **4.7**

	4.5·0.5$C_4H_{10}O$	**4.6**	**4.7**·2CH_3CN
empirical formula	$C_{32}H_{83}KN_3O_{6.5}Si_6Te_2U$	$C_{36}H_{88}KN_5O_6Si_6Te_2U$	$C_{28}H_{54}K_2N_2O_{12}Se_4$
crystal habit, color	plate, black	plate, black	plate, orange
crystal size (mm)	0.2 × 0.1 × 0.05	0.2 × 0.1 × 0.05	0.4 × 0.2 × 0.01
space group	$P\bar{1}$	$P\bar{1}$	*P*bcn
volume (Å^3)	2736.1(5)	2960.9(16)	4285(1)
a (Å)	11.1133(12)	11.613(4)	8.338(1)
b (Å)	14.6606(17)	15.142(5)	23.532(4)
c (Å)	17.909(2)	17.673(6)	21.837(3)
α (deg)	88.872	90.094(8)	90
β (deg)	88.828	95.903(8)	90
γ (deg)	69.715	106.581(7)	90
Z	2	2	4
formula weight (g/mol)	1314.88	1387.98	1004.77
density (calculated) (Mg/m^3)	1.596	1.557	1.558
absorption coefficient (mm^{-1})	4.256	3.937	3.671
F_{000}	1294	1372	2024
total no. reflections	38729	23445	14999
unique reflections	16824	10161	4496
R_{int}	0.0285	0.0941	0.0869
final R indices (I >2σ(I)]	R_1 = 0.0272 wR_2 = 0.0562	R_1 = 0.0872 wR_2 = 0.2159	R_1 = 0.0748 wR_2 = 0.1995
largest diff. peak and hole (e$^-$ A^{-3})	1.380 and -0.988	7.256 and -3.801	2.350 and -1.185
GOF	1.008	0.874	1.053

Table 4.4. X-ray Crystallographic Data for Complexes **4.8** and **4.9**

	4.8	**4.9**
empirical formula	$C_{30}H_{78}KN_3O_6Se_2Si_6U$	$C_{30}H_{78}KN_3O_6SeSi_6U$
crystal habit, color	plate, red-orange	plate, red
crystal size (mm)	0.3 × 0.2 × 0.1	0.2 × 0.1 × 0.1
space group	$P2_1$	$P\bar{1}$
volume (Å^3)	5119.9(4)	5036(1)
a (Å)	13.2894(6)	12.817(2)
b (Å)	17.7878(8)	18.780(3)
c (Å)	22.4872(8)	21.833(3)
α (deg)	90	91.640(2)
β (deg)	105.602(2)	106.308(2)
γ (deg)	90	92.187(2)
Z	4	4
formula weight (g/mol)	1180.54	1101.58
density (calculated) (Mg/m^3)	1.532	1.453
absorption coefficient (mm^{-1})	4.850	4.207
F_{000}	2360	2224
total no. reflections	25138	54763
unique reflections	20231	22070
R_{int}	0.0319	0.0375
final R indices (I >2σ(I)]	R_1 = 0.0408 wR_2 = 0.0916	R_1 = 0.0748 wR_2 = 0.1894
largest diff. peak and hole (e$^-$ A^{-3})	2.654 and -1.635	5.223 and -2.877
GOF	0.998	1.561

4.5 Appendix

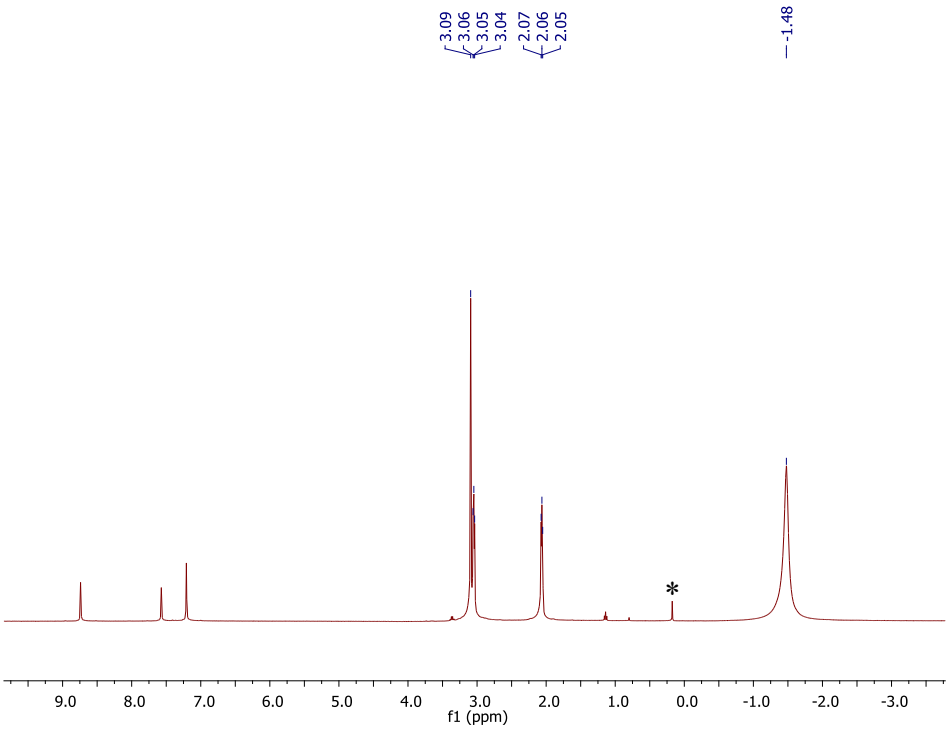

Figure A4.1. ^{1}H NMR spectrum of [K(2,2,2-cryptand)][U(Te)(NR_2)$_3$] (**4.4**) in pyridine-d_5. (*) indicates the presence of $HN(SiMe_3)_2$.

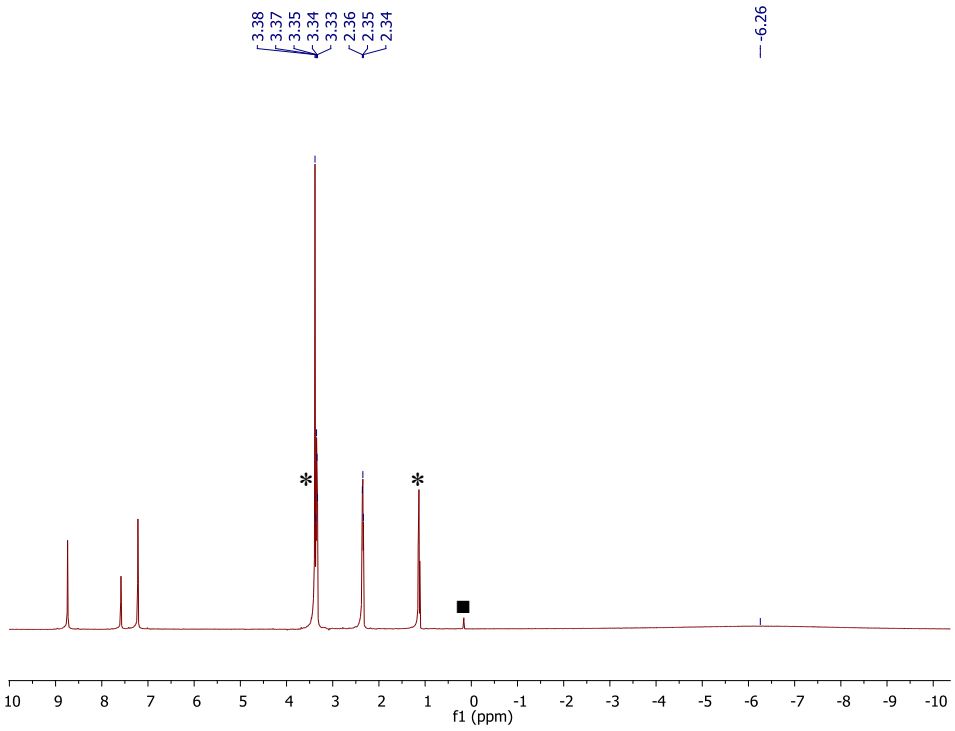

Figure A4.2. ^{1}H NMR spectrum of [K(2,2,2-crytpand)][U(η^2-Te_2)(NR_2)$_3$] (**4.6**) in pyridine-d_5. (*) indicates the presence of diethyl ether, (■) indicates the presence of $HN(SiMe_3)_2$.

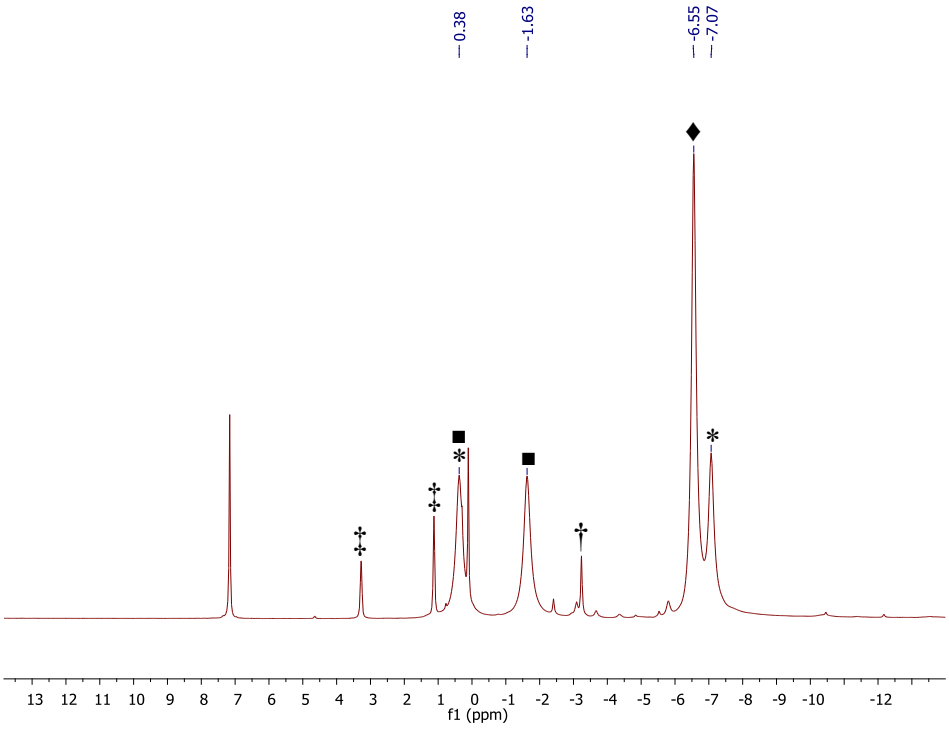

Figure A4.3. ^{1}H NMR spectrum of the reaction of $[U(NR_2)_3]$ with 0.25 equiv of $[K(18\text{-crown-6})]_2[Se_4]$ (**4.7**). (*) indicates the presence of complex **4.8**, (■) indicates the presence of complex **4.9**, (♦) indicates the presence of $[U(NR_2)_3]_2(\mu\text{-Se})$, (‡) indicates the presence of Et_2O, (†) indicates the presence of $HN(SiMe_3)_2$, and (•) indicates the presence of $[U(NR_2)_4]$,[118] an impurity in the starting material.

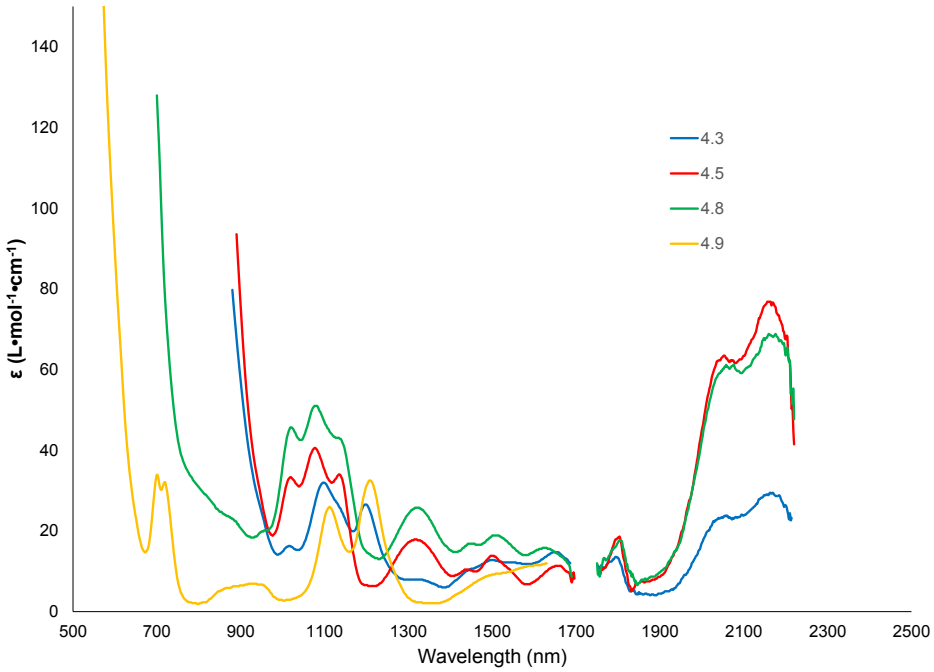

Figure A4.4. NIR spectra of complexes **4.3**, **4.5**, **4.8**, and **4.9**. Concentration (mM) in C_4H_8O: **4.3**, 5.17; **4.5**, 4.41; **4.8**, 3.92; **4.9**, 4.77.

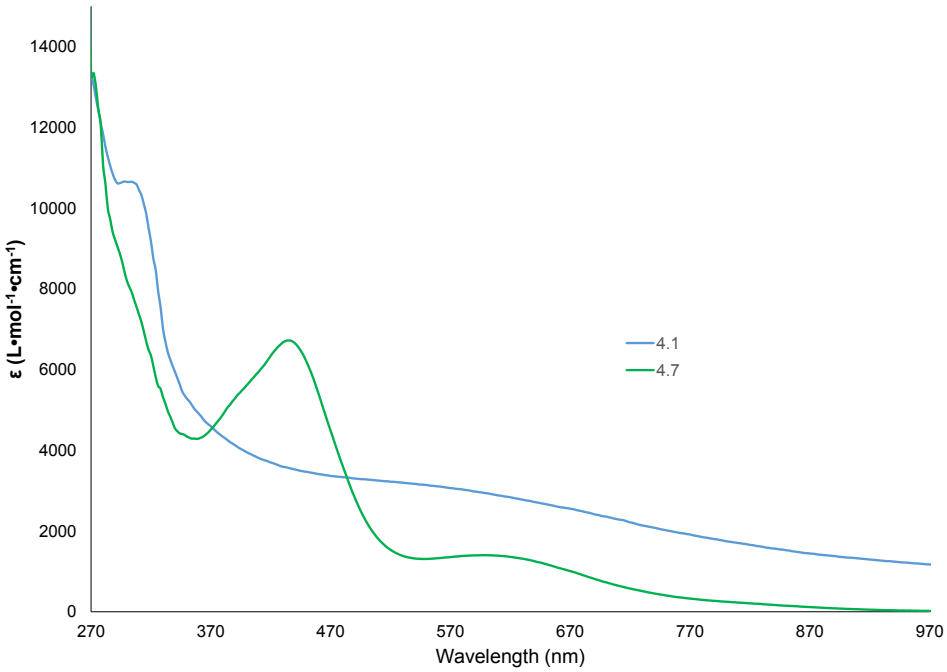

Figure A4.5. UV-Vis Spectra of complexes **4.1** and **4.7**. Concentration (mM) in CH_3CN: **4.1**, 0.174; **4.7**, 0.323.

4.6 References

(1) Hayton, T. W. *Chem. Commun.* **2013**, *49*, 2956.
(2) Hayton, T. W. *Dalton Trans.* **2010**, *39*, 1145.
(3) *Cambridge Structural Database*, version 1.18. 2015
(4) Fortier, S.; Brown, J. L.; Kaltsoyannis, N.; Wu, G.; Hayton, T. W. *Inorg. Chem.* **2012**, *51*, 1625.
(5) Fortier, S.; Kaltsoyannis, N.; Wu, G.; Hayton, T. W. *J. Am. Chem. Soc.* **2011**, *133*, 14224.
(6) Zi, G.; Jia, L.; Werkema, E. L.; Walter, M. D.; Gottfriedsen, J. P.; Andersen, R. A. *Organometallics* **2005**, *24*, 4251.
(7) Bart, S. C.; Anthon, C.; Heinemann, F. W.; Bill, E.; Edelstein, N. M.; Meyer, K. *J. Am. Chem. Soc.* **2008**, *130*, 12536.
(8) Hayton, T. W.; Boncella, J. M.; Scott, B. L.; Palmer, P. D.; Batista, E. R.; Hay, P. J. *Science* **2005**, *310*, 1941.
(9) Anderson, N. H.; Odoh, S. O.; Yao, Y.; Williams, U. J.; Schaefer, B. A.; Kiernicki, J. J.; Lewis, A. J.; Goshert, M. D.; Fanwick, P. E.; Schelter, E. J.; Walensky, J. R.; Gagliardi, L.; Bart, S. C. *Nat. Chem.* **2014**, *6*, 919.
(10) King, D. M.; McMaster, J.; Tuna, F.; McInnes, E. J. L.; Lewis, W.; Blake, A. J.; Liddle, S. T. *J. Am. Chem. Soc.* **2014**, *136*, 5619.
(11) King, D. M.; Tuna, F.; McInnes, E. J. L.; McMaster, J.; Lewis, W.; Blake, A. J.; Liddle, S. T. *Science* **2012**, *337*, 717.
(12) King, D. M.; Liddle, S. T. *Coord. Chem. Rev.* **2014**, *266–267*, 2.
(13) Fortier, S.; Wu, G.; Hayton, T. W. *J. Am. Chem. Soc.* **2010**, *132*, 6888.
(14) Fox, A. R.; Creutz, S. E.; Cummins, C. C. *Dalton Trans.* **2010**, *39*, 6632.
(15) Fortier, S.; Walensky, J. R.; Wu, G.; Hayton, T. W. *J. Am. Chem. Soc.* **2011**, *133*, 6894.
(16) Cramer, R. E.; Bruck, M. A.; Edelmann, F.; Afzal, D.; Gilje, J. W.; Schmidbaur, H. *Chem. Ber.* **1988**, *121*, 417.
(17) Cramer, R. E.; Maynard, R. B.; Paw, J. C.; Gilje, J. W. *J. Am. Chem. Soc.* **1981**, *103*, 3589.
(18) Cramer, R. E.; Maynard, R. B.; Paw, J. C.; Gilje, J. W. *Organometallics* **1983**, *2*, 1336.
(19) Cantat, T.; Arliguie, T.; Noel, A.; Thuery, P.; Ephritikhine, M.; Le Floch, P.; Mezailles, N. *J. Am. Chem. Soc.* **2009**, *131*, 963.
(20) Tourneux, J.-C.; Berthet, J.-C.; Cantat, T.; Thuery, P.; Mezailles, N.; Ephritikhine, M. *J. Am. Chem. Soc.* **2011**, *133*, 6162.
(21) Tourneux, J.-C.; Berthet, J.-C.; Cantat, T.; Thuery, P.; Mezailles, N.; Le Floch, P.; Ephritikhine, M. *Organometallics* **2011**, *30*, 2957.
(22) Ventelon, L.; Lescop, C.; Arliguie, T.; Leverd, P. C.; Lance, M.; Nierlich, M.; Ephritikhine, M. *Chem. Commun.* **1999**, 659.
(23) Brown, J. L.; Fortier, S.; Lewis, R. A.; Wu, G.; Hayton, T. W. *J. Am. Chem. Soc.* **2012**, *134*, 15468.
(24) Kubas, G. J.; Vergamini, P. J. *Inorg. Chem.* **1981**, *20*, 2667.

(25) van den Berg, W.; Boot, L.; Joosen, H.; van der Linden, J. G. M.; Bosman, W. P.; Smits, J. M. M.; de Gelder, R.; Beurskens, P. T.; Heck, J.; Gal, A. W. *Inorg. Chem.* **1997**, *36*, 1821.
(26) van den Berg, W.; Boot, C. E.; van der Linden, J. G. M.; Bosman, W. P.; Smits, J. M. M.; Beurskens, P. T.; Heck, J. *Inorg. Chim. Acta* **1994**, *216*, 1.
(27) Lam, O. P.; Heinemann, F. W.; Meyer, K. *Chem. Sci.* **2011**, *2*, 1538.
(28) Franke, S. M.; Heinemann, F. W.; Meyer, K. *Chem. Sci.* **2014**, *5*, 942.
(29) Camp, C.; Antunes, M. A.; Garcia, G.; Ciofini, I.; Santos, I. C.; Pecaut, J.; Almeida, M.; Marcalo, J.; Mazzanti, M. *Chem. Sci.* **2014**, *5*, 841.
(30) Brennan, J. G.; Andersen, R. A.; Zalkin, A. *Inorg. Chem.* **1986**, *25*, 1761.
(31) Brown, J. L.; Wu, G.; Hayton, T. W. *Organometallics* **2013**, *32*, 1193.
(32) Sheldrick, W. S. In *Handbook of Chalcogen Chemistry: New Perspectives in Sulfur, Selenium and Tellurium*; The Royal Society of Chemistry: 2007, p 543.
(33) Kolis, J. W. *Coord. Chem. Rev.* **1990**, *105*, 195.
(34) Ansari, M. A.; Ibers, J. A. *Coord. Chem. Rev.* **1990**, *100*, 223.
(35) Smith, D. M.; Ibers, J. A. *Coord. Chem. Rev.* **2000**, *200–202*, 187.
(36) Zintl, E., Goubeau, J., Dullenkopf, W. *Z. Physik. Chem.* **1931**, *154*, 1.
(37) Böttcher, P.; Getzschmann, J.; Keller, R. *Z. Anorg. Allg. Chem.* **1993**, *619*, 476.
(38) Kanatzidis, M. G.; Huang, S.-P. *Coord. Chem. Rev.* **1994**, *130*, 509.
(39) Hugot, M. C. *C. R. Hebd. Acad. Sci.* **1899**, *129*, 299.
(40) Hugot, M. C. *C. R. Hebd. Acad. Sci.* **1899**, *129*, 388.
(41) Mathewson, C. H. *J. Am. Chem. Soc.* **1907**, *29*, 867.
(42) Kraus, C. A.; Chiu, C. Y. *J. Am. Chem. Soc.* **1922**, *44*, 1999.
(43) Bergstrom, F. W. *J. Am. Chem. Soc.* **1926**, *48*, 146.
(44) Böttcher, P. *Z. Anorg. Allg. Chem.* **1977**, *432*, 167.
(45) Sheldrick, W. S.; Wachhold, M. *Angew. Chem. Int. Ed.* **1997**, *36*, 206.
(46) Schultz, L. D. *Inorg. Chim. Acta* **1990**, *176*, 271.
(47) Klemm, W.; Sodomann, H.; Langmesser, P. *Z. Anorg. Allg. Chem.* **1939**, *241*, 281.
(48) Bacher, A.-D.; Ulrich, M.; Ruhlandt-Senge, K. *Z. Naturforsch. B* **1992**, *47*, 1673.
(49) Müller, V.; Frenzen, G.; Dehnicke, K.; Fenske, D. *Z. Naturforsch. B* **1992**, *47*, 205.
(50) Bacher, A.-D.; Ulrich, M. *Z. Naturforsch. B* **1992**, *47*, 1063.
(51) Thiele, G.; Lichtenberger, N.; Tonner, R.; Dehnen, S. *Z. Anorg. Allg. Chem.* **2013**, *639*, 2809.
(52) Batchelor, R. J.; Einstein, F. W. B.; Gay, I. D.; Jones, C. H. W.; Sharma, R. D. *Inorg. Chem.* **1993**, *32*, 4378.
(53) Thiele, K. H.; Steinicke, A.; Dümichen, U.; Neumüller, B. *Z. Anorg. Allg. Chem.* **1996**, *622*, 231.
(54) Yanagisawa, S.; Tashiro, M.; Anzai, S. *J. Inorg. Nucl. Chem* **1969**, *31*, 943.
(55) Li, J.; Guo, H.-Y.; Carey, J. R.; Mulley, S.; Proserpio, D. M.; Sironi, A. *Mater. Res. Bull.* **1994**, *29*, 1041.
(56) McAfee, J. L.; Andreatta, J. R.; Sevcik, R. S.; Schultz, L. D. *J. Mol. Struct.* **2012**, *1022*, 68.
(57) Schultz, L. D.; Koehler, W. H. *Inorg. Chem.* **1987**, *26*, 1989.
(58) Bjoergvinsson, M.; Schrobilgen, G. J. *Inorg. Chem.* **1991**, *30*, 2540.
(59) Evans, W. J.; Miller, K. A.; Ziller, J. W.; DiPasquale, A. G.; Heroux, K. J.; Rheingold, A. L. *Organometallics* **2007**, *26*, 4287.

(60) Evans, W. J.; Takase, M. K.; Ziller, J. W.; DiPasquale, A. G.; Rheingold, A. L. *Organometallics* **2009**, *28*, 236.
(61) Shannon, R. D. *Acta Crystallogr. Sect. A* **1976**, *A32*, 751.
(62) Graves, C. R.; Scott, B. L.; Morris, D. E.; Kiplinger, J. L. *Chem. Commun.* **2009**, 776.
(63) Franke, S. M.; Rosenzweig, M. W.; Heinemann, F. W.; Meyer, K. *Chem. Sci.* **2015**, *6*, 275.
(64) Howard, W. A.; Parkin, G.; Rheingold, A. L. *Polyhedron* **1995**, *14*, 25.
(65) Fischer, J. M.; Piers, W. E.; MacGillivray, L. R.; Zaworotko, M. J. *Inorg. Chem.* **1995**, *34*, 2499.
(66) Rabinovich, D.; Parkin, G. *J. Am. Chem. Soc.* **1993**, *115*, 9822.
(67) Rabinovich, D.; Parkin, G. *Inorg. Chem.* **1995**, *34*, 6341.
(68) Shin, J. H.; Churchill, D. G.; Bridgewater, B. M.; Pang, K.; Parkin, G. *Inorg. Chim. Acta* **2006**, *359*, 2942.
(69) Shin, J. H.; Parkin, G. *Organometallics* **1994**, *13*, 2147.
(70) Murphy, V. J.; Rabinovich, D.; Halkyard, S.; Parkin, G. *J. Chem. Soc. Chem. Comm.* **1995**, 1099.
(71) Di Vaira, M.; Peruzzini, M.; Stoppioni, P. *Angew. Chem. Int. Ed.* **1987**, *26*, 916.
(72) Steigerwald, M. L.; Siegrist, T.; Gyorgy, E. M.; Hessen, B.; Kwon, Y. U.; Tanzler, S. M. *Inorg. Chem.* **1994**, *33*, 3389.
(73) Piers, W. E.; Ziegler, T.; Fischer, J. M.; Macgillivray, L. R.; Zaworotko, M. J. *Chem. Eur. J.* **1996**, *2*, 1221.
(74) Sharp, K. W.; Koehler, W. H. *Inorg. Chem.* **1977**, *16*, 2258.
(75) Raymond, C. C.; Dick, D. L.; Dorhout, P. K. *Inorg. Chem.* **1997**, *36*, 2678.
(76) Goldbach, A.; Saboungi, M.-L.; Johnson, J. A.; Cook, A. R.; Meisel, D. *J. Phys. Chem. A* **2000**, *104*, 4011.
(77) Licht, S.; Forouzan, F. *J. Electrochem. Soc.* **1995**, *142*, 1546.
(78) Cusick, J.; Dance, I. *Polyhedron* **1991**, *10*, 2629.
(79) Ahrika, A.; Paris, J. *New J. Chem.* **1999**, *23*, 1177.
(80) Gea, Y.; Greaney, M. A.; Coyle, C. L.; Stiefel, E. I. *J. Chem. Soc. Chem. Comm.* **1992**, 160.
(81) Föppl, H.; Busmann, E.; Frorath, F. K. *Z. Anorg. Allg. Chem.* **1962**, *314*, 12.
(82) Cordier, G.; Cook, R.; Schäfer, H. *Angew. Chem. Int. Ed.* **1980**, *19*, 324.
(83) Wang, X.; Wang, H. H.; Makarenko, B.; Jacobson, A. J. *Z. Anorg. Allg. Chem.* **2012**, *638*, 2538.
(84) Menezes, P. W.; Fässler, T. F. *Z. Anorg. Allg. Chem.* **2012**, *638*, 1109.
(85) König, T.; Eisenmann, B.; Schäfer, H. *Z. Anorg. Allg. Chem.* **1983**, *498*, 99.
(86) König, T.; Eisenmann, B.; Schäfer, H. *Z. Naturforsch. B* **1982**, *37b*, 1245.
(87) Kim, K.-W.; Kanatzidis, M. G. *J. Am. Chem. Soc.* **1998**, *120*, 8124.
(88) Smiles, D. E.; Wu, G.; Hayton, T. W. *J. Am. Chem. Soc.* **2014**, *136*, 96.
(89) Matson, E. M.; Goshert, M. D.; Kiernicki, J. J.; Newell, B. S.; Fanwick, P. E.; Shores, M. P.; Walensky, J. R.; Bart, S. C. *Chem. Eur. J.* **2013**, *19*, 16176.
(90) Sutorik, A. C.; Kanatzidis, M. G. *J. Am. Chem. Soc.* **1991**, *113*, 7754.
(91) Ginsberg, A. P.; Lindsell, W. E.; Sprinkle, C. R.; West, K. W.; Cohen, R. L. *Inorg. Chem.* **1982**, *21*, 3666.
(92) Mathur, P.; Ahmed, M. O.; Dash, A. K.; Kaldis, J. H. *Organometallics* **2000**, *19*, 941.
(93) Wardle, R. W. M.; Chau, C. N.; Ibers, J. A. *J. Am. Chem. Soc.* **1987**, *109*, 1859.

(94) Chau, C. N.; Wardle, R. W. M.; Ibers, J. A. *Inorg. Chem.* **1987**, *26*, 2740.
(95) Wardle, R. W. M.; Bhaduri, S.; Chau, C. N.; Ibers, J. A. *Inorg. Chem.* **1988**, *27*, 1747.
(96) Rohrmann, J.; Herrmann, W. A.; Herdtweck, E.; Riede, J.; Ziegler, M.; Sergeson, G. *Chem. Ber.* **1986**, *119*, 3544.
(97) Adel, J.; Weller, F.; Dehnicke, K. *J. Organomet. Chem.* **1988**, *347*, 343.
(98) Eichhorn, B. W.; Gardner, D. R.; Nichols-Ziebarth, A.; Ahmed, K. J.; Bott, S. G. *Inorg. Chem.* **1993**, *32*, 5412.
(99) Guo, G.-C.; Mak, T., C. W. *J. Chem. Soc. Dalton Trans.* **1997**, 709.
(100) Ansari, M. A.; Chau, C. N.; Mahler, C. H.; Ibers, J. A. *Inorg. Chem.* **1989**, *28*, 650.
(101) Saito, M.; Tokitoh, N.; Okazaki, R. *J. Am. Chem. Soc.* **1997**, *119*, 11124.
(102) Mandimutsira, B. S.; Chen, S. J.; Reynolds III, R. A.; Coucouvanis, D. *Polyhedron* **1997**, *16*, 3911.
(103) Liao, J. H.; Hill, L.; Kanatzidis, M. G. *Inorg. Chem.* **1993**, *32*, 4650.
(104) Nagao, S.; Seino, H.; Hidai, M.; Mizobe, Y. *Inorg. Chim. Acta* **2004**, *357*, 4618.
(105) Shin, J. H.; Savage, W.; Murphy, V. J.; Bonanno, J. B.; Churchill, D. G.; Parkin, G. *J. Chem. Soc. Dalton Trans.* **2001**, 1732.
(106) Farrar, D. H.; Grundy, K. R.; Payne, N. C.; Roper, W. R.; Walker, A. *J. Am. Chem. Soc.* **1979**, *101*, 6577.
(107) Suzuki, T.; Tsuji, N.; Kashiwabara, K.; Tatsumi, K. *Inorg. Chem.* **2000**, *39*, 3938.
(108) Nagata, K.; Takeda, N.; Tokitoh, N. *Angew. Chem. Int. Ed.* **2002**, *41*, 136.
(109) Liao, J.-H.; Li, J.; Kanatzidis, M. G. *Inorg. Chem.* **1995**, *34*, 2658.
(110) Montilla, F.; Galindo, A.; Rosa, V.; Aviles, T. *Dalton Trans.* **2004**, 2588.
(111) Allen, D. W.; Nowell, I. W.; Taylor, B. F. *J. Chem. Soc. Dalton Trans.* **1985**, 2505.
(112) Avens, L. R.; Bott, S. G.; Clark, D. L.; Sattelberger, A. P.; Watkin, J. G.; Zwick, B. D. *Inorg. Chem.* **1994**, *33*, 2248.
(113) *SMART Apex II*, Version 2.1. 2005
(114) *SAINT Software User's Guide*, Version 7.34a. 2005
(115) *SADABS*, 2005
(116) *TWINABS*, 2008/4. 2008
(117) *SHELXTL PC*, Version 6.12. 2005
(118) Lewis, A. J.; Williams, U. J.; Carroll, P. J.; Schelter, E. J. *Inorg. Chem.* **2013**, *52*, 7326.

Chapter 5 Synthesis of Thorium Selenides and Tellurides Utilizing Polychalcogenides as Chalcogen Atom Transfer Reagents

Portions of this work were published in:

Danil E. Smiles, Guang Wu, Peter Hrobárik, Trevor W. Hayton

J. Am. Chem. Soc. **2016**, *138*, 814-825.

Table of Contents

5.1 Introduction

Despite the considerable progress made in the study of actinide ligand bonding, several important areas remain underdeveloped.[1-7] The study of actinide ligand multiple bonds is one such area, and even though there has been a surge in the synthesis of these complexes in recent years, the vast majority are uranium complexes.[8-11] Examples of actinide ligand multiple bonds involving other actinides, like thorium are significantly more uncommon.[12,13]

While there have been a handful of examples of thorium imidos[14-16] and carbenes[17-19] reported in the last two decades, with respect to the chalcogenides, the number of complexes with thorium ligand multiple bonds drops dramatically. Zi and co-workers reported the synthesis of the first thorium oxo complex, $[(\eta^5\text{-}1,2,4\text{-}^t\text{Bu}_3\text{C}_5\text{H}_2)_2\text{Th(O)(dmap)}]$ (dmap = dimethylaminopyridine), in 2011.[20] The only other examples are the thorium oxo and sulfido, $[\text{K(18-crown-6)}][\text{Th(E)(NR}_2)_3]$ (**3.6**, E = O; **3.8**, E = S), described in Chapter 3, isolated via reductive deprotection of the corresponding chalcogenate complexes.[21] There have been no reported examples of thorium selenides or tellurides. Furthermore, structurally characterized coordination complexes with Th-Se bonds are extremely uncommon (Figure 5.1),[15,22-24] and coordination complexes with Th-Te bonds are completely non-existent.[13]

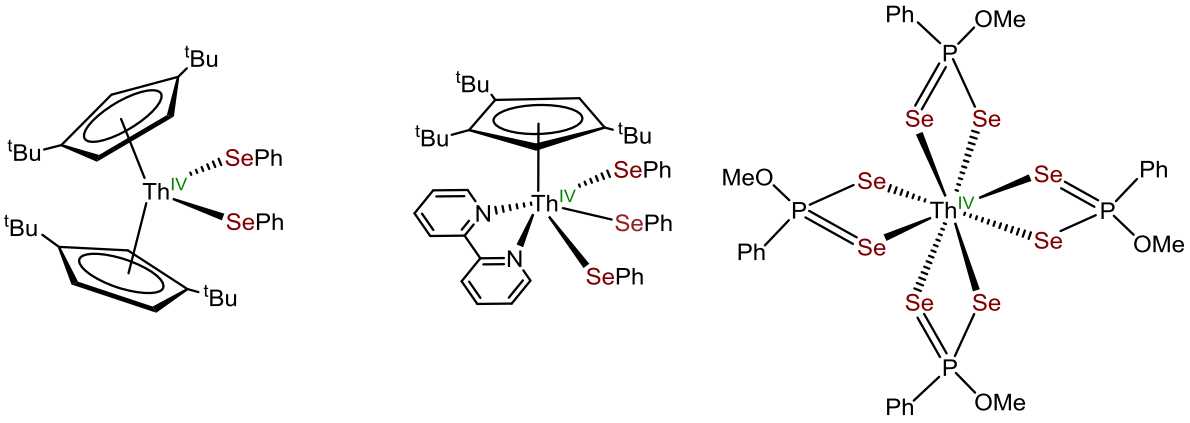

Figure 5.1. Previously reported complexes with Th-Se bonds. $[(\eta^5\text{-}1,3\text{-}{}^t\mathrm{Bu}_3\mathrm{C}_5\mathrm{H}_3)_2\mathrm{Th}(\mathrm{SePh})_2]$ (left),[22] $[(\eta^5\text{-}1,2,4\text{-}{}^t\mathrm{Bu}_3\mathrm{C}_5\mathrm{H}_2)\mathrm{Th}(\mathrm{SePh})_3(\mathrm{bipy})]$ (center),[15] $\mathrm{Th}[\mathrm{Se}_2\mathrm{P}(\mathrm{C}_6\mathrm{H}_5)(\mathrm{OMe})]_4$ (right).[23]

The polychalcogenides detailed in Chapter 4 have been demonstrated to be useful in the synthesis of uranium chalcogenides, including the synthesis of the U(IV) ditelluride, $[\mathrm{K}(18\text{-crown-6})][\mathrm{U}(\eta^2\text{-}\mathrm{Te}_2)(\mathrm{NR}_2)_3]$ (**4.5**), which was generated via the reaction of $[\mathrm{U(I)}(\mathrm{NR}_2)_3]$ with $[\mathrm{K}(18\text{-crown-6})]_2[\mathrm{Te}_2]$ (**4.1**). Importantly, no metal based redox chemistry is required in this reaction, and suggests that these polychalcogenides should also be amenable to use in the analogous thorium based systems. The synthesis of thorium selenides and tellurides also provides the opportunity to probe the f-orbital participation and bonding of these complexes using $^{77}\mathrm{Se}$ and $^{125}\mathrm{Te}$ NMR spectroscopies. A similar approach was previously employed by Hayton and co-workers, and Hrobárik and co-workers, in the study of actinide hydride and alkyl complexes using $^{1}\mathrm{H}$ and $^{13}\mathrm{C}$ NMR spectroscopies.[25,26]

This chapter describes the synthesis of the first thorium terminal selenides and tellurides. These complexes are all accessed utilizing the polychalcogenide salts described in Chapter 4. This series of complexes is characterized structurally and spectroscopically, including $^{77}\mathrm{Se}$ and $^{125}\mathrm{Te}$ NMR spectroscopies. DFT calculations were performed, in collaboration with Dr.

Peter Hrobárik at the Technical University of Berlin, to analyze the electronic structures of these complexes, along with their oxo and sulfido analogues. In addition, the previously reported uranium oxy selenide, $[Cp^*_2Co][U(O)(Se)(NR_2)_3]$,[27] was characterized by ^{77}Se NMR spectroscopy as well, and the chemical shifts of all these complexes are calculated using DFT. Experimental and computational data are used in concert to discuss differences in bonding among the actinides.

5.2 Results and Discussion

5.2.1 Synthesis and Characterization of $[K(18\text{-crown-6})][Th(\eta^2\text{-}Se_2)(NR_2)_3]$ (5.1).

The success had with $[K(18\text{-crown-6})]_2[Se_4]$ (**4.7**) and other polychalcogenides discussed in Chapter 4 suggested that these species could be used in other actinide systems, for which analogous starting materials are available. Thus, addition of 1 equiv of $[K(18\text{-crown-6})]_2[Se_4]$ (**4.7**) to a suspension of $[Th(I)(NR_2)_3]$ (**3.3**) in THF, generates an orange solution and a black precipitate. Crystallization from diethyl ether affords $[K(18\text{-crown-6})][Th(\eta^2\text{-}Se_2)(NR_2)_3]$ (**5.1**), as orange crystals in 63% yield (Scheme 5.1). The black precipitate is postulated to be Se^0 that is ejected due to steric crowding between the bulky $[N(SiMe_3)_2]^-$ ligands and the larger polychalcogenide moiety, and gives rise to the observed diselenide.

Scheme 5.1 Synthesis of $[K(18\text{-crown-6})][Th(\eta^2\text{-}Se_2)(NR_2)_3]$ (**5.1**)

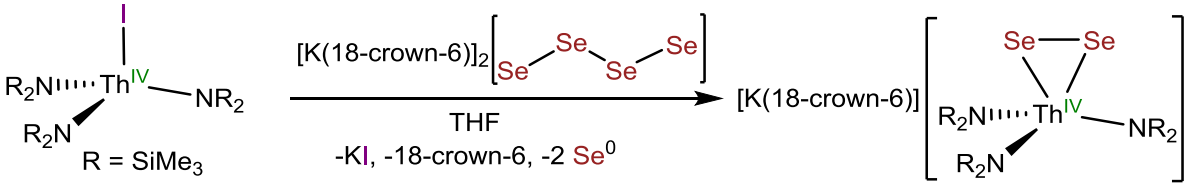

The ^{1}H NMR spectrum of complex **5.1** exhibits two sharp resonances at 0.74 and 3.17 ppm, in benzene-d_6, and 0.74 and 3.47 ppm, in pyridine-d_5, assignable to the methyl groups of the silylamide ligands and the methylene groups of the 18-crown-6 moiety, respectively. Similarly, the ^{13}C{^{1}H} NMR spectrum features two resonances at 6.05 and 70.18 ppm, in benzene-d_6, and 6.56 and 70.87 ppm, in pyridine-d_5, again attributable to the methyl groups of the silylamide ligands and the methylene groups of the 18-crown-6 moiety, respectively. Complex **5.1** was also characterized by ^{77}Se{^{1}H} NMR spectroscopy. Its ^{77}Se{^{1}H} NMR spectrum, in benzene-d_6, features one resonance at 246 ppm, assignable to the $[\eta^2\text{-Se}_2]^{2-}$ ligand. Importantly, this resonance shifts downfield to 302 ppm in pyridine-d_5, consistent with the formation of a solvent separated cation/anion pair. Both chemical shifts are within the range for previously reported complexes with an $[\eta^2\text{-Se}_2]^{2-}$ ligand (-408–1252).[28-35] Furthermore, the only other reported ^{77}Se chemical shift of a complex with Th-Se bonds is for $Th[Se_2P(C_6H_5)(OMe)]_4$, which features a single resonance at 222 ppm in its ^{77}Se NMR spectrum.[23]

Complex **5.1** crystallizes in the triclinic spacegroup $P\bar{1}$, as a diethyl ether solvate **5.1**·0.5Et$_2$O, and its solid state molecular structure is shown in Figure 5.2. Complex **5.1** is structurally identical to its uranium analogue, $[K(18\text{-crown-6})][U(\eta^2\text{-Se}_2)(NR_2)_3]$ (**4.8**). It features a distorted pseudotetrahedral geometry about thorium (N1-Th1-N2 = 99.8(2)°, N2-Th1-N3 = 110.1(2)°, N1-Th1-N3 = 125.4(2)°), again attributable to the presence of the larger $[\eta^2\text{-Se}_2]^{2-}$ ligand in addition to the sterically demanding $[N(SiMe_3)_3]^-$ ligands. The Th-Se bond lengths (Th1-Se1 = 2.8750(7), Th1-Se2 = 2.9555(7) Å) are comparable to those of previously reported complexes with Th-Se single bonds,[15,22,23] including $[Th(Se_2P(C_6H_5)(OMe))_4]$ (av. Th-Se = 3.027 Å),[23] and $[(\eta^5\text{-1,3-}(Me_3C)_2C_5H_3)_2Th(SePh)_2]$

(av. Th-Se = 2.88 Å).[22] Furthermore, the Th-Se bond distances of **5.1** are also similar to those of the solid state selenide, $ThSe_2$, which features an average Th-Se bond distance of 3.06 Å (range 2.85–3.27 Å).[36] The asymmetry observed in the Th-Se bond distances is similar to

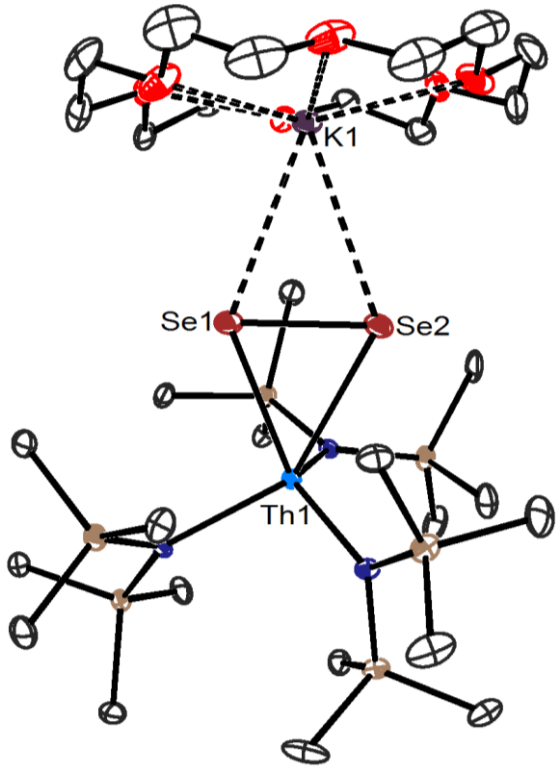

Figure 5.2. ORTEP diagram of [K(18-crown-6)][Th(η^2-Se_2)(NR_2)$_3$] (**5.1**·0.5Et_2O) with 50% probability ellipsoids. Diethyl ether solvate and hydrogen atoms are omitted for clarity. Selected bond distances (Å) and angles (deg): Th1-Se1 = 2.8750(7), Th1-Se2 = 2.9555(7), Se1-K1 = 3.425(2), Se2-K1 = 3.441(2), Se1-Se2 = 2.397(1), Th-N (av.) = 2.354, N1-Th1-N2 = 99.8(2), N2-Th1-N3 = 110.1(2), N1-Th1-N3 = 125.4(2).

what is seen for its uranium analogue, [K(18-crown-6)][U(η^2-Se_2)(NR_2)$_3$] (**4.8**), and likely a result of the aforementioned steric crowding around the metal center. The Se-K bond distances (Se1-K1 = 3.425(2), Se2-K1 = 3.441(2) Å) are comparable to those of the polyselenide salt (**4.7**) and the uranium congener (**4.8**). Finally, the Se-Se bond distance of **5.1** (Se1-Se2 = 2.397(1) Å) is comparable to that of complex **4.8**, as well as those of other

structurally characterized complexes with an $[\eta^2\text{-}Se_2]^{2-}$ ligand (av. Se-Se = 2.327 Å).[29-31,33,35,37-51]

5.2.2 Synthesis and Characterization of [K(18-crown-6)][Th(η²-Te₂)(NR₂)₃] (5.2)

The utility of $[K(18\text{-crown-6})]_2[Te_2]$ (**4.1**) as a tellurium atom transfer reagent was then applied towards the synthesis of a new thorium ditelluride. Accordingly, addition of 1 equiv of $[K(18\text{-crown-6})]_2[Te_2]$ (**4.1**) to a diethyl ether suspension of $[Th(I)(NR_2)_3]$ (**3.3**) affords a green mixture. Subsequent crystallization from diethyl ether affords $[K(18\text{-crown-6})][Th(\eta^2\text{-}Te_2)(NR_2)_3]$ (**5.2**), as a green crystalline solid in 36% yield (Scheme 5.2). Like the synthesis of its uranium analogue (**4.5**), complex **5.2** is formed via a simple salt metathesis that further demonstrates the versatility of **4.1** and reinforces the synthetic utility of these polychalcogenide salts.

Scheme 5.2 Synthesis of $[K(18\text{-crown-6})][Th(\eta^2\text{-}Te_2)(NR_2)_3]$ (**5.2**)

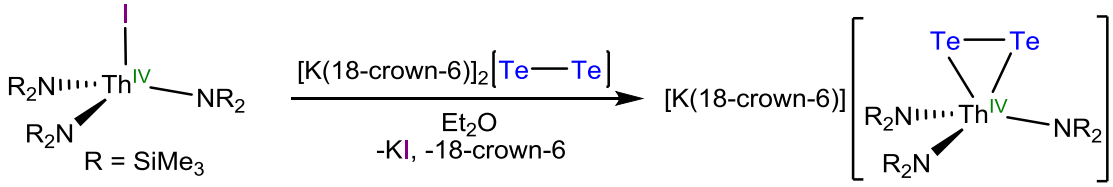

The ^1H NMR spectra of **5.2**, in benzene-d_6 and pyridine-d_5, are nearly identical to those of its selenide analogue, complex **5.1**. The spectra feature two sharp resonances at 0.79 and 3.14 ppm, in benzene-d_6, and at 0.76 and 3.58 ppm, in pyridine-d_5, in both cases assignable to the methyl groups of the silylamide ligands and the methylene groups of the 18-crown-6 moiety, respectively. The $^{13}C\{^1H\}$ NMR spectra are also extremely similar, exhibiting two resonances at either 6.28 and 70.13 ppm (benzene-d_6) or 6.74 and 71.18 ppm (pyridine-d_5), again assignable to the methyl groups of the silylamide ligands and the methylene groups of

the 18-crown-6 moiety, respectively. Complex **5.2** was also characterized by $^{125}Te\{^{1}H\}$ NMR spectroscopy. The $^{125}Te\{^{1}H\}$ NMR spectrum of complex **5.2** features a singlet at -351 ppm, in benzene-d_6, or -272 ppm, in pyridine-d_5, attributable to the $[\eta^2\text{-}Te_2]^{2-}$ ligand. Both resonances are within the known chemical shift range for complexes with a $[\eta^2\text{-}Te_2]^{2-}$ ligand.[28-30,52-55] The downfield shift observed in pyridine-d_5 is again consistent with the formation of a solvent separated cation/anion pair, identical to what has been seen for complex **5.1**.

Complex **5.2** crystallizes in the triclinic spacegroup $P\bar{1}$, as a diethyl ether solvate **5.2**·0.5Et_2O, and its solid state molecular structure is shown in Figure 5.3. Complex **5.2** is isostructural to its uranium analogue, **4.5**, as well as its selenide congener, **5.1**. It exhibits a distorted pseudotetrahedral geometry about thorium, with N-U-N angles (N1-Th1-N2 = 126.8(1)°, N2-Th1-N3 = 108.9(1)°, N1-Th1-N3 = 100.8(1)°) that deviate considerably from what would be expected for idealized tetrahedral, a consequence of accommodating the larger $[\eta^2\text{-}Te_2]^{2-}$ ligand. The asymmetric Th-Te bond distances of **5.2** (Th1-Te1 = 3.1076(4), Th1-Te2 = 3.2375(4) Å), a feature again attributed to the steric crowding around Th, are longer than the U-Te bonds distances of complex **4.5** and the Th-Se bonds distances of complex **5.1**, consistent with the increased ionic radii of Th^{4+} vs. U^{4+} and Te^{2-} vs. Se^{2-}.[56,57] Complex **5.2** is the first structurally characterized coordination complex with Th-Te bonds,[13] however solid state thorium tellurides are known.[58-64] For example, KTh_2Te_6,[62] $ThTe_2I_2$,[61] and Th_7Te_{12}[63] have all been structurally characterized, and the range of Th-Te bond distances (3.137(2)–3.483(1) Å) exhibited by these materials are comparable to the those in complex **5.2**. In addition, the Te-Te bond distance in **5.2** (Te1-Te2 = 2.7525(5) Å) is slightly longer than those

of other structurally characterized complexes with an $[\eta^2\text{-}Te_2]^{2-}$ ligand (av. 2.69 Å),[28,29,52,53,55,65-69] but similar to that of its uranium analogue, **4.5**.

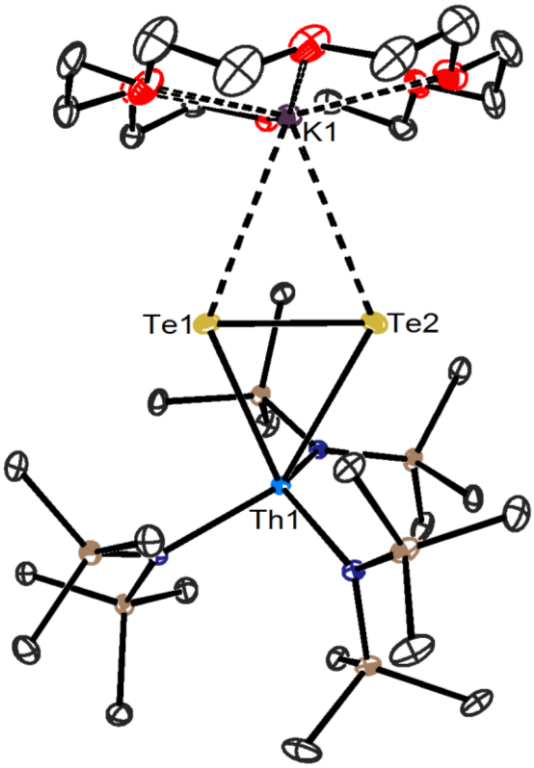

Figure 5.3. ORTEP diagram of $[K(18\text{-crown-6})][Th(\eta^2\text{-}Te_2)(NR_2)_3]$ (**5.2**·0.5Et_2O) with 50% probability ellipsoids. Diethyl ether solvate and hydrogen atoms are omitted for clarity. Selected bond distances (Å) and angles (deg): Th1-Te1 = 3.1076(4), Th1-Te2 = 3.2375(4), Te1-K1 = 3.6534(9), Te2-K1 = 3.6682(9), Th-N (av.) = 2.345, Te1-Te2 = 2.7525(5), N1-Th1-N2 = 126.8(1), N2-Th1-N3 = 108.9(1), N1-Th1-N3 = 100.8(1).

5.2.3 Synthesis and Characterization of $[K(18\text{-crown-6})][Th(Se)(NR_2)_3]$ (5.3)

Diselenide **5.1** was then used as a precursor to a terminal monoselenide complex, via reaction with a phosphine. Thus, addition of 1 equiv of Et_3P to an orange solution of **5.1** in diethyl ether results in a bleaching of the color. Upon work-up and crystallization from diethyl ether, $[K(18\text{-crown-6})][Th(Se)(NR_2)_3]$ (**5.3**) was isolated as a colorless crystalline solid, in 53% yield (Scheme 5.3). The other expected byproduct of this reaction, Et_3P=Se, can be

identified by $^{31}P\{^{1}H\}$ and $^{77}Se\{^{1}H\}$ NMR spectroscopies and isolated as an off-white solid in 97% yield. A similar strategy has been employed previously for the synthesis of monochalcogenide complexes, including the synthesis of the uranium monoselenide, [K(18-crown-6)][Th(Se)$(NR_2)_3$] (**4.9**).[51,69-71]

Scheme 5.3 Synthesis of [K(18-crown-6)][Th(Se)$(NR_2)_3$] (**5.3**)

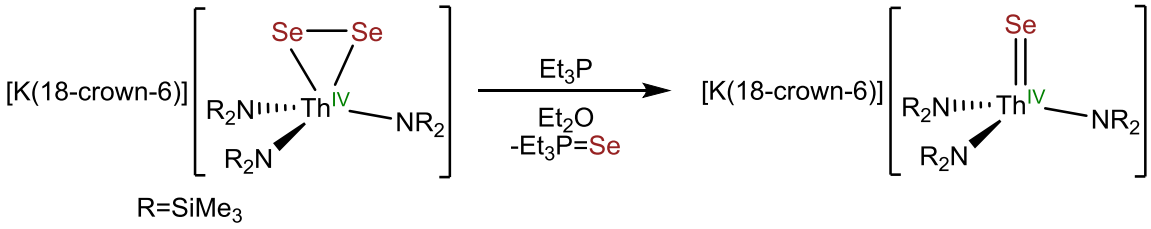

Complex **5.3** crystallizes in the triclinic spacegroup $P\bar{1}$, with two molecules in the asymmetric unit, and its solid state molecular structure is shown in Figure 5.4. Complex **5.3** is structurally identical to its uranium analogue, **4.9**, as well as its oxo (**3.6**) and sulfido (**3.8**) congeners. It exhibits an identical pseudotetrahedral geometry about thorium. This is evidenced by N-Th-N (av. 116.4°) and N-Th-Se (av. 101.0°) angles close to the established values for an idealized tetrahedral molecule. The Th-Se bond distances of **5.3** (Th1-Se1 = 2.6497(7), Th2-Se2 = 2.6566(7) Å) are notably shorter than those of complex **5.1**, suggestive of the multiple bond character in these interactions. And while the Se-K bond distances of **5.3** (Se1-K1 = 3.125(2), Se2-K2 = 3.201(2) Å) are shorter than those of **5.1**, they are similar to those of the corresponding uranium complex (**4.9**).

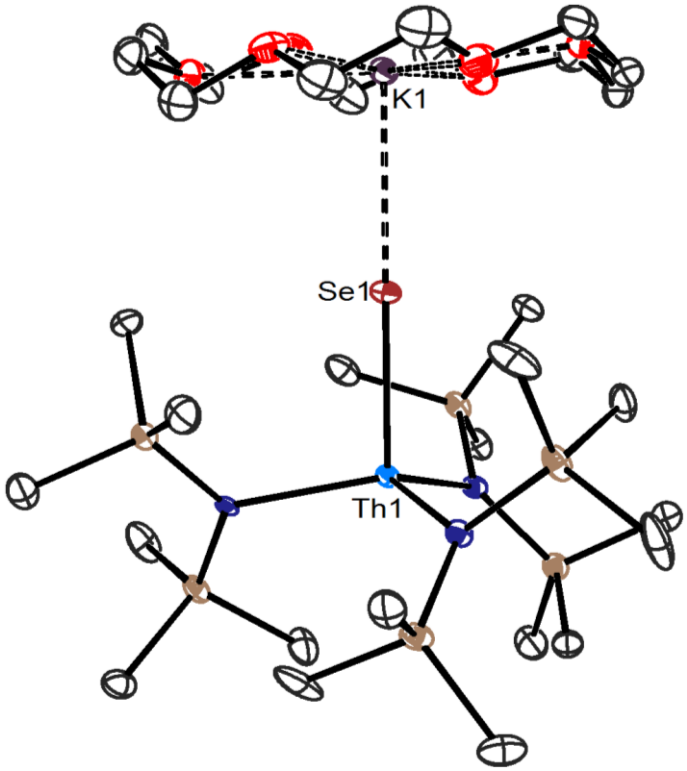

Figure 5.4. ORTEP diagram of [K(18-crown-6)][Th(Se)(NR_2)$_3$] (**5.3**) with 50% probability ellipsoids. One molecule of **5.3** and hydrogen atoms are omitted for clarity. Selected bond distances (Å) and angles (deg): Th1-Se1 = 2.6497(7), Th2-Se2 = 2.6566(7), Se1-K1 = 3.125(2), Se2-K2 = 3.201(2), Th-N (av.) = 2.35, N-Th-N (av.) = 116.4, N-Th-Se (av.) = 101.0.

The ^{1}H NMR and ^{13}C{^{1}H} NMR spectra of **5.3**, in benzene-d_6, are extremely similar to those of complex **5.1**, each featuring two resonances, 0.76 and 3.17 ppm and 5.75 and 70.11 ppm, which correspond to the methyl groups of the silylamide ligands and the methylene groups of the 18-crown-6 moiety, respectively. The spectra in pyridine-d_5 are almost identical, the most notable difference being the downfield shift of the resonance attributable to the 18-crown-6 moiety in the ^{1}H NMR spectrum to 3.53 ppm. This downfield shift is also observed in the ^{77}Se{^{1}H} NMR spectrum of complex **5.3**, which features a single resonance at 885 ppm, when dissolved in benzene-d_6, that shifts to 992 ppm, when dissolved in pyridine-d_5. This shift results from breaking up the contact between the [K(18-crown-6)]$^{+}$ cation and

the $[Th(Se)(NR_2)_3]^-$ anion upon dissolution in the more polar coordinating solvent. Additionally, both chemical shifts are within the range (700–2400 ppm) for complexes with a terminal $[Se]^{2-}$ ligand that have been previously reported.[32,53,54,72-75]

5.2.4 Synthesis and Characterization of [K(18-crown-6)][Th(Te)(NR$_2$)$_3$] (5.4)

The synthetic procedure used to generate complex **5.3** was then applied to the tellurium system. However, addition of 1 equiv of Et_3P to a benzene-d_6 solution of **5.2** results in no reaction after 24 h, as determined by both ^1H and $^{31}P\{^1H\}$ NMR spectroscopies. Parkin and co-workers reported, in 1994, that conversion of a ditelluride complex, $[Cp^*_2Ta(\eta^2\text{-}Te_2)(H)]$, into the corresponding monotelluride complex, $[Cp^*_2Ta(Te)(H)]$, could be achieved via reaction with Et_3P and Hg.[52] This alternative route was then investigated as a means to synthesize a thorium monotelluride complex. Thus, addition of Et_3P and Hg, both in excess, to a green solution of **5.2**, in diethyl ether, produces a colorless solution, along with a black precipitate, after 24 h. Upon work-up, [K(18-crown-6)][Th(Te)(NR$_2$)$_3$] (**5.4**) can be isolated as a colorless powder in 78% yield (Scheme 5.4). Whereas formation of a P-Te bond was insufficient to drive abstraction of the Te atom, addition of Hg and formation of the Hg-Te bond likely provides the necessary thermodynamic sink.[76]

Scheme 5.4 Synthesis of [K(18-crown-6)][Th(Te)(NR$_2$)$_3$] (**5.4**)

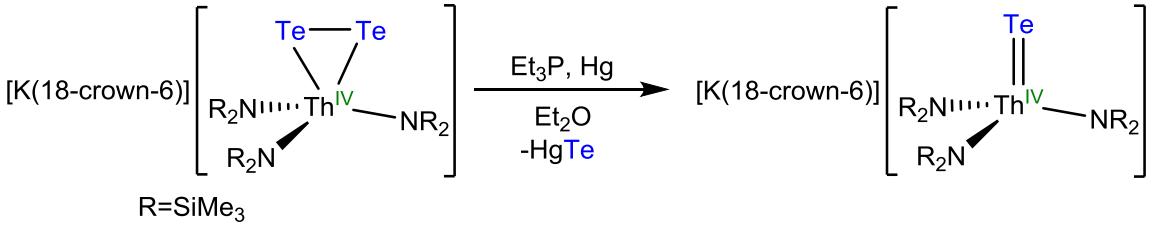

Crystals of complex **5.4** suitable for X-ray crystallography can be grown from a concentrated diethyl ether solution. **5.4** crystallizes in the triclinic spacegroup $P\bar{1}$ as a diethyl

ether solvate, **5.4**·0.5Et_2O, with four molecules in the asymmetric unit, and its solid state molecular structure is shown in Figure 5.5. Complex **5.4** is isostructural to its uranium analogue, [K(18-crown-6)][U(Te)$(NR_2)_3$] (**4.3**), and features a pseudotetrahedral geometry about thorium (av. N-Th-N = 112.9°, av. N-Th-Te = 107.0°), comparable to what is observed for complex **5.3**. The Th-Te bond distances of **5.4** (av. 2.933 Å) are significantly shorter than those of ditelluride **5.2**, and are actually the shortest Th-Te bonds reported,[58-64,77-79] suggestive of the multiple bond character of these interactions. In addition, the Te-K bond lengths of **5.4** (av. 3.437 Å) are longer than the corresponding O-K (2.645(7) Å), S-K (av. 3.081 Å), and Se-K (av. 3.163 Å) bond distances of the structurally identical oxo (**3.6**), sulfido (**3.8**), and selenido (**5.3**) complexes, consistent with the increased ionic radius of Te^{2-} vs. O^{2-}, S^{2-}, and Se^{2-}.[56]

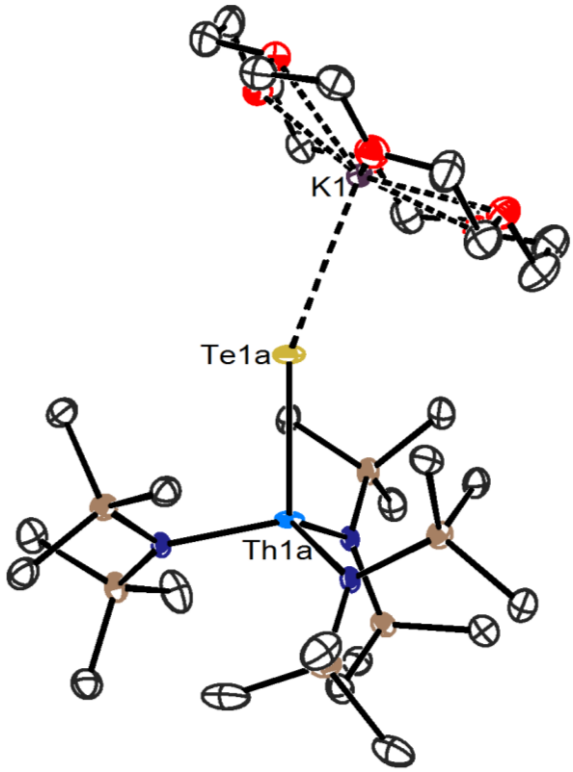

Figure 5.5. ORTEP diagram of [K(18-crown-6)][Th(Te)$(NR_2)_3$] (**5.4**·0.5Et_2O) with 50% probability ellipsoids. Three molecules of **5.4**, diethyl ether solvates, and hydrogen atoms are

omitted for clarity. Selected bond distances (Å) and angles (deg): Th1a-Te1a = 2.953(2), Th1b-Te1b = 2.95(2), Th2a-Te2a = 2.933(1), Th2b-Te2b = 2.94(2), Th3a-Te3a = 2.930(2), Th3b-Te3b = 2.86(2), Th4a-Te4a = 2.933(1), Th4b-Te4b = 2.96(1), Te1a-K1 = 3.448(4), Te1b-K1 = 3.44(2), Te2a-K2 = 3.437(4), Te2b-K2 = 3.28(1), Te3a-K3 = 3.518(4), Te3b-K3 = 3.49(2), Te4a-K4 = 3.453(4), Th-N (av.) = 2.37, N-Th-N (av.) = 112.9, N-Th-Te (av.) = 107.0.

The ^{1}H NMR spectrum of **5.4** in benzene-d_6 and pyridine-d_5 both exhibit a sharp resonance at 0.81 ppm, assignable to the methyl groups of the silylamide ligands. The only difference between the two is, again, the downfield shift of the resonance attributed to the 18-crown-6 moiety in the more polar solvent, 3.15 ppm (benzene-d_6) vs. 3.47 ppm (pyridine-d_5). This shift is also observed in the ^{125}Te{^{1}H} NMR spectrum, which features a single resonance at 481 ppm, in benzene-d_6, and at 628 ppm, in pyridine-d_5. Both values are well within the range reported for complexes with a terminal $[Te]^{2-}$ ligand.[28-30,52-54,72,80]

5.2.5 DFT Analysis of the Electronic Structures of [K(18-crown-6)][Th(η^2-E$_2$)(NR$_2$)$_3$] and K(18-crown-6)][Th(E)(NR$_2$)$_3$] (E = Se, Te)

The electronic structures of complexes **5.1**, **5.2**, **5.3**, and **5.4** were investigated using DFT, including Natural Bond Order (NBO) and Quantum Theory of Atoms-in-Molecules (QTAIM). This analysis was conducted by Dr. Peter Hrobárik at the Technical University of Berlin. Also investigated were the oxo, [K(18-crown-6)][Th(O)(NR$_2$)$_3$] (**3.6**) and sulfido, [K(18-crown-6)][Th(S)(NR$_2$)$_3$] (**3.8**) analogues, in addition to the previously reported uranium(VI) complex, [Cp$^*_2$Co][U(O)(Se)(NR$_2$)$_3$].[27] There is excellent agreement between the computationally and X-ray determined structural parameters for all the complexes studied. The Th-E interactions are calculated to be formal triple bonds, with a single σ and two π components, as determined by both NBO and QTAIM analyses. The σ and 2π NLMOs for

the Th-Se interaction of complex **5.3** are shown in Figure 5.6. These analyses also indicate that the Th-N bonds possess double bond character. Similar results are seen for the uranium complex, $[U(O)(Se)(NR_2)_3]^-$, as well. The percent composition of the natural localized

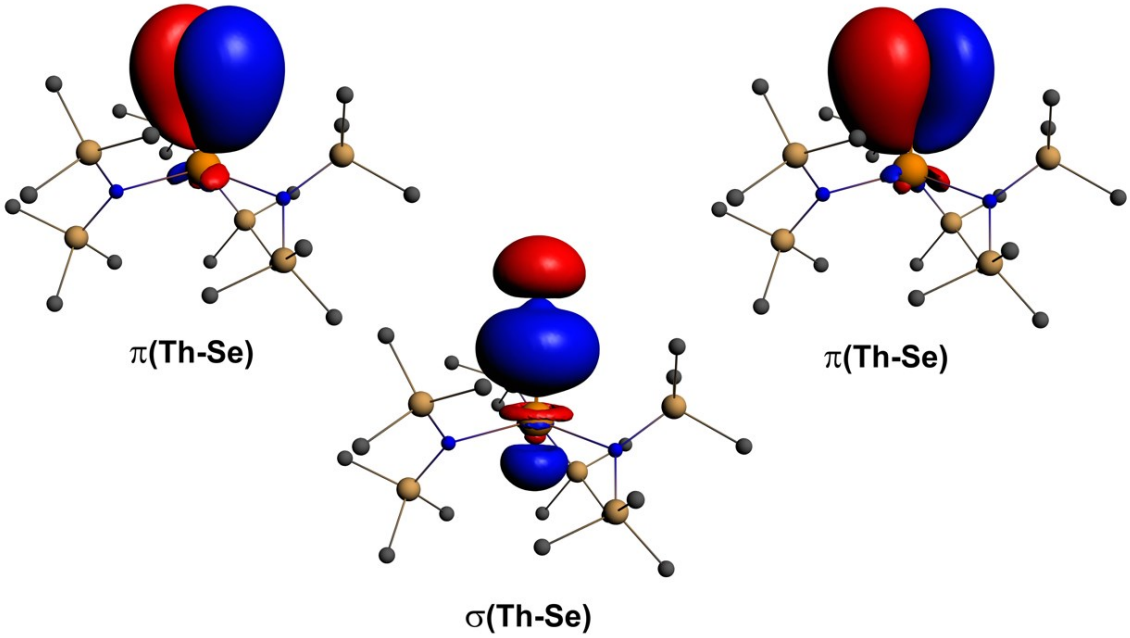

Figure 5.6. σ and π Natural Localized Molecular Orbitals (NLMO) for the Th-Se bond of $[Th(Se)(NR_2)_3]^-$ (**5.3**). Hydrogen atoms are omitted for clarity. Isosurface = 0.03.

molecular orbitals (NLMOs), and the f-orbital contribution to these bonds, for both the thorium and uranium complexes are collected in Table 5.1. Notably, there is a slight increase in the metal character to the Th-E bonds as the chalcogen becomes heavier. Furthermore, there is a considerably greater amount of metal contribution seen in the U-E interaction in addition to a marked increase in the f orbital character to the uranium contribution. These results are consistent with previous computational analyses of related actinide chalcogenides, including those discussed in Chapter 3,[27] and suggest greater covalency in the uranium(VI) complexes versus structurally similar thorium(IV) complexes.[81]

Table 5.1. Composition (%) and f-orbital contribution of the M-E NLMOs of $[Th(E)(NR_2)_3]^-$ and $[U(O)(Se)(NR_2)_3]^-$ (E = O, S, Se, Te)

		M (%)	E (%)
$[Th(E)(NR_2)_3]^-$			
E = O (**3.6**)	σ	6.9 (22)	93.0
	π	11.3 (30)	88.0
E = S (**3.8**)	σ	18.8 (11)	80.5
	π	18.5 (33)	80.2
E = Se (**5.3**)	σ	21.1 (10)	78.1
	π	19.8 (35)	78.8
E= Te (**5.4**)	σ	24.8 (9)	74.1
	π	20.3 (38)	78.0
$[U(O)(Se)(NR_2)_3]^-$	σ	35.8 (68)	62.4
	π	26.0 (57)	72.3

5.2.6 DFT Analysis of the ^{77}Se and ^{125}Te NMR Chemical Shifts of [K(18-crown-6)][Th(η^2-E_2)$(NR_2)_3$] and K(18-crown-6)][Th(E)$(NR_2)_3$] (E = Se, Te)

Electronic structure analysis is limited by the experimental data to which it is correlated, and typically the only experimental data used is that from X-ray crystallography. The ability to include other spectroscopic data would allow for greater insight into the bonding of these complexes and provide a way to corroborate the results of the electronic structure analyses in the previous section. Thus, the ^{77}Se and ^{125}Te chemical shifts of complexes **5.1**–**5.4** are an excellent set of experimental data to which theory can be applied. In collaboration with Dr. Peter Hrobárik at the Technical University of Berlin the ^{77}Se and ^{125}Te NMR chemical shifts (δ) of complexes **5.1**–**5.4** were calculated using DFT. These calculations were performed at the two-component ZORA-SO relativistic level including spin-orbit coupling, in conjunction with a PBE0 hybrid functional and TZ2P basis set. The theoretically determined chemical shifts agree very closely with the experimental values. Importantly, the calculations also

support the formation of different solution state structures, solvent separated cation / anion pairs and contact ion pairs, in polar and non-polar solvents, respectively, a phenomenon first evidenced by ^{1}H NMR spectroscopy.

In order to expand the scope of these studies the previously reported U(VI) complex, $[Cp^{*}_{2}Co][U(O)(Se)(NR_{2})_{3}]$,[27] was also characterized by $^{77}Se\{^{1}H\}$ NMR spectroscopy. This exhibits a single resonance at 4905 ppm in its $^{77}Se\{^{1}H\}$ NMR spectrum (Figure 5.7). This ^{77}Se NMR chemical shift is the largest downfield shift reported for a diamagnetic complex, and more than double that of the previous downfield limit, 2434 ppm, reported for the triselenido-substituted aromatic dication[82]. Most importantly, the calculated chemical shift for this complex agrees very well with the experimental data.

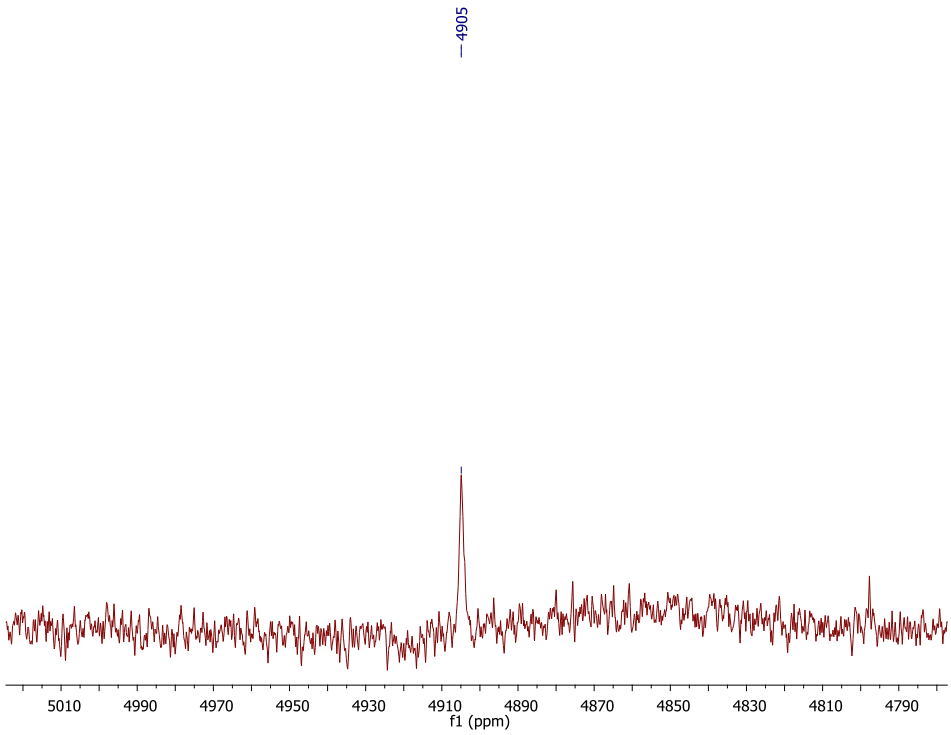

Figure 5.7. $^{77}Se\{^{1}H\}$ NMR spectrum of $[Cp^{*}_{2}Co][U(O)(Se)(NR_{2})_{3}]$ in pyridine-d_5.

The delocalization indices (DI), the QTAIM measure of bond order, were also calculated for the complexes under investigation, and a linear relationship was found between these

values and the corresponding ^{77}Se or ^{125}Te chemical shifts (δ) of complexes **5.1**–**5.4**. It is important to note that the increase in bond strength of the Th-E interactions that could be expected upon forming a solvent separated cation / anion pair is not only consistent with what is predicted by the DFT calculations, as evinced by an increase in the DI values, but also is echoed by the downfield shift observed for the δ values as well. The data obtained for $[Cp^*_2Co][U(O)(Se)(NR_2)_3]$, however, does not fit well with that of the thorium complexes, due in part to its dramatically large δ value. This discrepancy can be ascribed to the major differences in the bonding between U(VI), which is expected be exhibit greater covalency, and Th(IV). As reflected in NBO analysis and composition of the NLMOs (Table 5.1), the uranium-chalcogen bond is more covalent then its thorium counterparts, and there is significantly more 5f-orbital participation, which results in the striking increase in δ value that is observed.

5.3 Summary

In summary, conversion of $[Th(Cl)(NR_2)_3]$ (**3.1**) into the corresponding iodide, $[Th(I)(NR_2)_3]$ (**3.3**), via reaction with excess TMSI. Reaction of complex **3.3** with 1 equiv of the polychalcogenides, $[K(18\text{-crown-6})]_2[Se_4]$ (**4.7**) and $[K(18\text{-crown-6})]_2[Te_2]$ (**4.1**), affords the Th(IV) terminal dichalcogenides, $[K(18\text{-crown-6})][Th(\eta^2\text{-}E_2)(NR_2)_3]$ (**5.1**, E = Se; **5.2**, E = Te), in moderate yields. Similar to their uranium analogues, complexes **5.1** and **5.2** feature asymmetric Th-E bond lengths and N-Th-N angles. Reaction of **5.1** and **5.2** with Et_3P or Et_3P and Hg, respectively, yields the Th(IV) terminal monochalcogenides, $[K(18\text{-crown-6})][Th(E)(NR_2)_3]$ (**5.3**, E = Se; **5.4**, E = Te). These feature the shortest Th-E bond distances reported to date suggestive of the multiple bond character of these interactions. These

syntheses are another example of the usefulness of the polychalcogenides as a means to install terminal chalcogenide ligands.

Complexes **5.1**–**5.4** were characterized by ^{77}Se and ^{125}Te NMR spectroscopies. Additionally, characterization of $[Cp^*_2Co][U(O)(Se)(NR_2)_3]$ by ^{77}Se NMR spectroscopy reveals an unprecedentedly downfield resonance. The electronic structures and ^{77}Se or ^{125}Te NMR chemical shifts of complexes **5.1**–**5.4** and $[Cp^*_2Co][U(O)(Se)(NR_2)_3]$ were also calculated by DFT using NBO and QTAIM analyses. These analyses agree well with experiment, predicting both multiple bond character for the Th-E bonds of **5.3** and **5.4** and the extreme ^{77}Se δ value of $[Cp^*_2Co][U(O)(Se)(NR_2)_3]$. Furthermore, the considerable difference in δ between the thorium and uranium complexes is attributed directly to the increased covalency and f-orbital participation in the latter. These results illustrate the benefits of combining experimental and theoretical analyses to gain insight into actinide-ligand bonding, and demonstrate that NMR spectroscopy can be used to probe the bonding of actinide systems. The simplicity and ubiquity of NMR spectroscopy should allow for the application of this methodology to other actinide or transition metal systems.

5.4 Experimental

5.4.1 General Methods

All reactions and subsequent manipulations were performed under anaerobic and anhydrous conditions under an atmosphere of nitrogen. Hexanes, Et_2O, tetrahydrofuran (THF), and toluene were dried using a Vacuum Atmospheres DRI-SOLV Solvent Purification system and stored over 3Å sieves for 24 h prior to use. Benzene-d_6 and pyridine-d_5 were dried over 3Å molecular sieves for 24 h prior to use. **3.3**,[83] **4.1**,[84] **4.7**,[84] and $[Cp^*_2Co][U(O)(Se)(NR_2)_3]$,[27] were synthesized according to the previously reported

procedures. Thorium(IV) nitrate hydrate was purchased from Strem Chemicals, while elemental Se, elemental Te, and $NaNR_2$ were purchased from Acros Organics. Unless noted, all reagents were used as received.

NMR spectra were recorded on a Varian UNITY INOVA 400 MHz spectrometer, a Varian UNITY INOVA 500 MHz spectrometer, a Varian UNITY INOVA 600 MHz spectrometer, or an Agilent Technologies 400-MR DD2 400 MHz Spectrometer. ^{1}H NMR spectra were referenced to external $SiMe_4$ using the residual protio solvent peaks as internal standards. $^{13}C\{^{1}H\}$, $^{31}P\{^{1}H\}$, $^{77}Se\{^{1}H\}$, and $^{125}Te\{^{1}H\}$ NMR spectra were referenced indirectly with the ^{1}H resonance of $SiMe_4$ at 0 ppm, according to IUPAC standard,[85,86] using the residual solvent peaks as internal standards. ^{77}Se and ^{125}Te NMR spectra were recorded at an operating frequency of 76.28 MHz and 126.20 MHz, respectively. IR spectra were recorded on a Nicolet 6700 FT-IR spectrometer. Raman spectra were recorded on a LabRam Aramis microRaman system (Horiba Jobin Yvon) equipped with 1200 grooves/mm holographic gratings, and Peltier-cooled CCD camera. The 633 nm output of a Melles Griot He-Ne laser was used to excite the samples, which were collected in a back scattering geometry using a confocal Raman Microscope (high stability BX40) equipped with Olympus objectives (MPlan 50x). Sample preparation was performed inside the glovebox: Pure crystalline solid samples were placed between a glass microscope slide and coverslip, sealed with a bead of silicone grease, and removed from the glovebox for spectral acquisition. Elemental analyses were performed by the Micro-Analytical Facility at the University of California, Berkeley.

5.4.2 Synthesis of [K(18-crown-6)][Th(η^2-Se_2)(NR_2)$_3$] (5.1)

To a colorless, cold (-25 °C), stirring mixture of [Th(I)(NR_2)$_3$] (**3.3**) (40.7 mg, 0.048 mmol) in THF (3 mL) was added [K(18-crown-6)]$_2$[Se_4] (**4.7**) (47.9 mg, 0.052 mmol). The

color of the solution became pale orange upon addition. This mixture was allowed to stir for 20 min, whereupon the deposition of a black precipitate was observed. This mixture was filtered through a Celite column supported on glass wool (0.5 cm × 3 cm) to afford an orange solution. The solvent was then removed in vacuo to afford an orange solid. The solid was triturated with pentane (2 mL) to afford an orange powder. This powder was extracted with diethyl ether (5 mL) and filtered through a Celite column supported on glass wool (0.5 cm × 3 cm) to afford an orange solution. The volume of the filtrate was reduced to 2 mL in vacuo, and then the solution was transferred to a 4 mL scintillation vial that was placed inside a 20 mL scintillation vial. Toluene (6 mL) was then added to the outer vial. Storage of this two vial system at -25 °C for 48 h resulted in the deposition of an orange crystalline solid, which was isolated by decanting the supernatant (37.0 mg, 63%). Anal. Calcd for $C_{30}H_{78}KN_3O_6Se_2Si_6Th \cdot 0.5C_4H_{10}O$: C, 31.72; H, 6.91; N, 3.47. Found: C, 31.38; H, 6.64; N, 3.27. ^{1}H NMR (400 MHz, 25 °C, benzene-d_6): δ 0.74 (s, 54H, NSiCH_3), 3.17 (s, 24H, 18-crown-6). ^{13}C{^{1}H} NMR (100 MHz, 25 °C, benzene-d_6): δ 6.05 (NSiCH$_3$), 70.18 (18-crown-6). ^{77}Se{^{1}H} (76.28 MHz, 25 °C, benzene-d_6): δ 246 (s, $\nu_{1/2}$ = 8 Hz). ^{1}H NMR (400 MHz, 25 °C, pyridine-d_5): δ 0.74 (s, 54H, NSiCH_3), 3.47 (s, 24H, 18-crown-6). ^{13}C{^{1}H} NMR (100 MHz, 25 °C, pyridine-d_5): δ 6.56 (NSiCH$_3$), 70.87 (18-crown-6). ^{77}Se{^{1}H} (76.28 MHz, 25 °C, pyridine-d_5): δ 302 (s, $\nu_{1/2}$ = 9 Hz). IR (KBr pellet, cm^{-1}): 608 (m), 665 (m), 774 (m), 847 (s), 930 (s), 964 (m), 1020 (w), 1057 (w), 1112 (s), 1182 (w), 1250 (s), 1284 (w), 1351 (m), 1400 (w), 1453 (w), 1472 (w).

5.4.3 Synthesis of [K(18-crown-6)][Th(Se)(NR$_2$)$_3$] (5.2)

To an orange, cold (-25 °C), stirring solution of **5.1** (136.7 mg, 0.12 mmol) in diethyl ether (4 mL) was added Et$_3$P (18 μL, 0.12 mmol). The color of this solution became light yellow

upon addition. This solution was allowed to stir for 90 min, whereupon the deposition of a white precipitate was observed. This mixture was then filtered through a Celite column supported on glass wool (0.5 cm × 3 cm) to afford a light yellow solution. The volume of this filtrate was reduced to 2 mL in vacuo. Storage of this solution at -25 °C for 24 h resulted in the deposition of an off-white solid, subsequently identified as $Et_3P{=}Se$ by $^{31}P\{^1H\}$ and $^{77}Se\{^1H\}$ NMR spectroscopies (19.7 mg, 97%).[87] The solid was isolated by decanting the supernatant. The volume of the supernatant was reduced in vacuo to 1 mL. This solution was then transferred to a 4 mL scintillation vial that was placed inside a 20 mL scintillation vial. Toluene (6 mL) was then added to the outer vial. Storage of this two vial system at -25 °C for 48 h resulted in the deposition of colorless crystals, which were isolated by decanting off the supernatant (28.8 mg, 22%). The supernatant was then transferred to a 4 mL scintillation vial that was placed inside a 20 mL scintillation vial. Toluene (6 mL) was then added to the outer vial. Storage of this two vial system at -25 °C for 48 h resulted in the deposition of additional colorless crystals. Total yield: 67.8 mg, 53%. Anal. Calcd for $C_{30}H_{78}KN_3O_6SeSi_6Th$: C, 32.89; H, 7.18; N, 3.84. Found: C, 33.20; H, 7.28; N, 4.00. ^1H NMR (400 MHz, 25 °C, benzene-d_6): δ 0.76 (s, 54H, NSiCH_3), 3.17 (s, 24H, 18-crown-6). $^{13}C\{^1H\}$ NMR (100 MHz, 25 °C, benzene-d_6): δ 5.75 (NSiCH$_3$), 70.11 (18-crown-6). $^{77}Se\{^1H\}$ (76.28 MHz, 25 °C, benzene-d_6): δ 885 (s, $\nu_{1/2}$ = 10 Hz). ^1H NMR (400 MHz, 25 °C, pyridine-d_5): δ 0.75 (s, 54H, NSiCH_3), 3.53 (s, 24H, 18-crown-6). $^{13}C\{^1H\}$ NMR (100 MHz, 25 °C, pyridine-d_5): δ 6.31 (NSiCH$_3$), 70.01 (18-crown-6). $^{77}Se\{^1H\}$ (76.28 MHz, 25 °C, pyridine-d_5): δ 992 (s, $\nu_{1/2}$ = 16 Hz). IR (KBr pellet, cm^{-1}): 500 (w), 606 (m), 667 (m), 758 (m), 771 (m), 836 (s), 843 (s), 862 (s), 1111 (s), 1182 (w), 1250 (s), 1285 (w), 1352 (m),

1402 (w), 1454 (w), 1474 (w). Raman (neat solid, cm^{-1}): 179 (m), 253 (m), 570 (m), 622 (m), 674 (m), 750 (w), 833 (m), 874 (w), 1145 (w), 1250 (w), 1277 (w), 1413 (w), 1478 (m).

5.4.4 Synthesis of [K(18-crown-6)][Th(η^2-Te_2)(NR_2)$_3$] (5.3)

To a colorless, cold (-25 °C), stirring mixture of [Th(I)(NR_2)$_3$] (**3.3**) (102.4 mg, 0.12 mmol) in diethyl ether (4 mL) was added [K(18-crown-6)]$_2$[Te_2] (**4.1**) (106.9 mg, 0.12 mmol). The color of the solution became green upon addition. This mixture was allowed to stir for 30 min, whereupon the deposition of a black precipitate was observed. This mixture was then filtered through a Celite column supported on glass wool (0.5 cm × 3 cm) to afford a green solution. The volume of the filtrate was reduced to 1 mL in vacuo. Storage of this solution at -25 °C for 24 h resulted in the deposition of green crystals, which were isolated by decanting off the supernatant (58.2 mg, 36%). Anal. Calcd for $C_{30}H_{78}KN_3O_6Si_6Te_2Th \cdot 0.5C_4H_{10}O$: C, 29.37; H, 6.39; N, 3.21. Found: C, 29.78; H, 6.34; N, 3.06. ^{1}H NMR (400 MHz, 25 °C, benzene-d_6): δ 0.79 (s, 54H, NSiCH_3), 3.14 (s, 24H, 18-crown-6). ^{13}C{^{1}H} NMR (100 MHz, 25 °C, benzene-d_6): δ 6.28 (NSi*C*H$_3$), 70.13 (18-crown-6). ^{125}Te{^{1}H} NMR (126.20 MHz, 25 °C, benzene-d_6): δ -351 (s, $\nu_{1/2}$ = 16 Hz). ^{1}H NMR (400 MHz, 25 °C, pyridine-d_5): δ 0.76 (s, 54H, NSiCH_3), 3.58 (s, 24H, 18-crown-6). ^{13}C{^{1}H} NMR (100 MHz, 25 °C, pyridine-d_5): δ 6.74 (NSi*C*H$_3$), 71.18 (18-crown-6). ^{125}Te{^{1}H} NMR (126.20 MHz, 25 °C, pyridine-d_5): δ -272 (s, $\nu_{1/2}$ = 28 Hz). IR (KBr pellet, cm^{-1}): 610 (m), 664 (m), 687 (m), 760 (m), 773 (m), 844 (s), 900 (s), 919 (s), 964 (m), 1059 (w), 1110 (s), 1183 (w), 1249 (s), 1283 (w), 1351 (m), 1454 (w), 1472 (w).

5.4.5 Synthesis of [K(18-crown-6)][Th(Te)(NR_2)$_3$] (5.4)

To a green, cold (-25 °C), stirring solution of **5.3** (43.3 mg, 0.034 mmol) in diethyl ether (3 mL) was added Et_3P (30 μL, 0.20 mmol) and Hg (737.5 mg, 3.67 mmol). This mixture was allowed to stir for 24 h, whereupon the color of the solution bleached to colorless, concomitant with the deposition of a black precipitate. This mixture was filtered through a Celite column supported on glass wool (0.5 cm × 3 cm) to afford a colorless solution. The volatiles were then removed in vacuo to give a colorless solid (31.4 mg, 78%). Crystals suitable for X-ray crystallographic analysis were grown from a concentrated Et_2O solution stored at -25 °C for 24 h. Anal. Calcd for $C_{30}H_{78}KN_3O_6Si_6TeTh$: C, 31.49; H, 6.87; N, 3.67. Found: C, 31.66, H, 7.03, N, 3.52. ^{1}H NMR (400 MHz, 25 °C, benzene-d_6): δ 0.81 (s, 54H, NSiCH_3), 3.15 (s, 24H, 18-crown-6). ^{13}C{^{1}H} NMR (100 MHz, 25 °C, benzene-d_6): δ 6.45 (NSiCH$_3$), 70.16 (18-crown-6). ^{125}Te{^{1}H} NMR (126.20 MHz, 25 °C, benzene-d_6): δ 481 (s, $\nu_{1/2}$ = 60 Hz). ^{1}H NMR (400 MHz, 25 °C, pyridine-d_5): δ 0.81 (s, 54H, NSiCH_3), 3.47 (s, 24H, 18-crown-6). ^{13}C{^{1}H} NMR (100 MHz, 25 °C, pyridine-d_5): δ 6.95 (NSiCH$_3$), 70.89 (18-crown-6). ^{125}Te{^{1}H} NMR (126.20 MHz, 25 °C, pyridine-d_5): δ 628 (s, $\nu_{1/2}$ = 70 Hz). IR (KBr pellet, cm^{-1}): 609 (m), 664 (m), 687 (m), 759 (m), 773 (m), 837 (s), 930 (s), 963 (s), 1110 (s), 1181 (w), 1251 (s), 1285 (w), 1352 (m), 1454 (w), 1474 (w). Raman (neat solid, cm^{-1}): 176 (s), 260 (w), 280 (w), 388 (m), 627 (s), 676 (m), 747 (w), 791 (w), 835 (m), 876 (m), 1007 (w), 1143 (w), 1252 (m), 1277 (m), 1412 (m), 1476 (m).

5.4.6 X-ray Crystallography

Data for **5.1**, **5.2**, **5.3**, and **5.4** were collected on a Bruker KAPPA APEX II diffractometer equipped with an APEX II CCD detector using a TRIUMPH monochromator with a Mo Kα X-ray source (α = 0.71073 Å). The crystals were mounted on a cryoloop under Paratone-N

oil, and all data were collected at 100(2) K using an Oxford nitrogen gas cryostream. Data were collected using ω scans with 0.5° frame widths. Frame exposures of 20 s were used for **5.1**. Frame exposures of 5 s were used for **5.2** and **5.3**. Frame exposures of 10 s were used for **5.4**. Data collection and cell parameter determination were conducted using the SMART program.[88] Integration of the data frames and final cell parameter refinement were performed using SAINT software.[89] Absorption correction of the data was carried out using the multi-scan method SADABS.[90] Subsequent calculations were carried out using SHELXTL.[91] Structure determination was done using direct or Patterson methods and difference Fourier techniques. All hydrogen atom positions were idealized, and rode on the atom of attachment. Structure solution, refinement, graphics, and creation of publication materials were performed using SHELXTL.[91]

The diethyl ether solvate molecule in **5.1** and **5.2** exhibited positional disorder. One carbon atom was modeled over two positions in a 50:50 ratio. The C-C and C-O bond distances of the diethyl ether solvate were constrained to 1.54 and 1.45 Å, respectively, using the DFIX command. The Th and Te atoms of **5.4** exhibited positional disorder and were modeled over two positions in a 90:10 ratio. In addition, the anisotropic displacement parameters of the Th, Te, K, Si, O, N, and C atoms among the four molecules in the asymmetric unit were constrained with the EADP command. Two of the diethyl ether solvate molecules in **5.4** exhibited positional disorder; one carbon of each molecule was modeled over two positions in a 50:50 ratio. The C-C and C-O bond distances of the diethyl ether solvates were constrained to 1.54 and 1.45 Å, respectively, using the DFIX command. Hydrogen atoms were not assigned to disordered carbon atoms.

Table 5.2. X-ray Crystallographic Data for Complexes **5.1** and **5.2**

	5.1	**5.2**
empirical formula	$C_{32}H_{83}KN_3O_6Se_2Si_6Th$	$C_{32}H_{83}KN_3O_6Si_6Te_2Th$
crystal habit, color	plate, orange	plate, green
crystal size (mm)	0.1 × 0.1 × 0.01	0.1 × 0.085 × 0.02
space group	$P\bar{1}$	$P\bar{1}$
volume (Å^3)	2704.5(7)	2755.4(6)
a (Å)	11.268(2)	11.184(2)
b (Å)	14.392(2)	14.689(2)
c (Å)	17.841(3)	17.923(2)
α (deg)	87.899(4)	88.665(3)
β (deg)	88.397(5)	89.012(3)
γ (deg)	69.307(4)	69.407(3)
Z	2	2
formula weight (g/mol)	1216.65	1313.93
density (calculated) (Mg/m^3)	1.494	1.584
absorption coefficient (mm^{-1})	4.350	3.987
F_{000}	1228	1300
total no. reflections	23030	31551
unique reflections	11801	13139
R_{int}	0.0466	0.0446
final R indices (I >2σ(I)]	R_1 = 0.0433 wR_2 = 0.1003	R_1 = 0.0303 wR_2 = 0.0715
largest diff. peak and hole (e$^-$ A^{-3})	4.155 and -1.550	1.403 and -0.589
GOF	1.010	1.018

Table 5.3. X-ray Crystallographic Data for Complexes **5.3** and **5.4**

	5.3	**5.4**
empirical formula	$C_{30}H_{78}KN_3O_6SeSi_6Th$	$C_{32}H_{83}KN_3O_6Si_6TeTh$
crystal habit, color	plate, colorless	plate, colorless
crystal size (mm)	0.2 × 0.1 × 0.02	0.4 × 0.2 × 0.03
space group	$P\bar{1}$	$P\bar{1}$
volume (Å^3)	5084.4(9)	10743.3(1)
a (Å)	12.864(1)	11.5257(8)
b (Å)	18.914(2)	22.587(2)
c (Å)	21.813(2)	43.507(3)
α (deg)	91.704(3)	102.717(3)
β (deg)	106.371(3)	93.748(3)
γ (deg)	92.124(3)	101.784(3)
Z	4	8
formula weight (g/mol)	1095.59	1178.77
density (calculated) (Mg/m^3)	1.431	1.458
absorption coefficient (mm^{-1})	3.907	3.556
F_{000}	2216	4724
total no. reflections	42768	214801
unique reflections	22209	48048
R_{int}	0.0500	0.0601
final R indices (I >2σ(I)]	R_1 = 0.0484 wR_2 = 0.1093	R_1 = 0.1231 wR_2 = 0.2716
largest diff. peak and hole (e$^-$ A^{-3})	3.071 and -1.608	8.203 and -8.491
GOF	1.001	1.073

5.4.7 Computational Details

All investigated structures were fully optimized at the PBE0 level of theory,[92-94] including an atom-pairwise correction for dispersion forces via Grimme's D3 model[95] with Becke-Johnson (BJ)[96] damping in the Turbomole program.[97] Quasirelativistic energy-consistent small-core pseudopotentials (effective-core potentials, ECP)[98,99] were used for the metal centers, with (8s7p6d1f)/[6s4p3d1f] and (14s13p10d8f1g)/[10s9p5d4f1g] Gaussian-type orbital valence basis sets for the transition-metal and actinide atoms, respectively. Ligand atoms were treated with an all-electron def2-TZVP basis set.[100] Relativistic all-electron DFT calculations of the nuclear shieldings were performed using the Amsterdam Density Functional (ADF) program suite,[101] employing the PBE0 exchange-correlation functional in conjunction with Slater-type orbital basis sets of triple-zeta doubly polarized (TZ2P) quality and an integration accuracy of 5. Both scalar and spin-orbit relativistic effects were treated by the two-component zeroth-order regular approximation (ZORA).[102,103] The calculated NMR shieldings have been broken down into MO contributions using the analysis tools in the ADF code. Bulk solvent effects in selected complexes were simulated by the conductor-like screening model (COSMO) as implemented self-consistently in ADF.[104] The computed ^{77}Se and ^{125}Te nuclear shieldings were converted to chemical shifts (δ, in ppm) relative to the shieldings of Me_2Se and Me_2Te, respectively, computed at the same level (in the case of di- and polychalcogenide complexes, the shieldings were averaged over the magnetically equivalent nuclei).

Natural population analyses (NPA) and analysis of natural localized molecular orbitals (NLMOs)[105] were carried out at the PBE0/def2-TZVP/ECP level using the NBO6 code, interfaced with Gaussian 09.[106,107] Bader's quantum theory of atoms-in-molecules

(QTAIM)[108,109] analyses of the Kohn-Sham wavefunctions (generated in Gaussian at the same level as used for NLMO analysis and stored as .wfx files) were performed using the Multiwfn program.[110,111] The actinide-ligand bond covalency was also studied using a quantitative energy decomposition analysis (EDA) of the total bonding energy into electrostatic interaction, Pauli-repulsive orbital interactions and attractive orbital interactions, as implemented in the ADF code.[101,112]

5.5 Appendix

5.6 References

(1) Minasian, S. G.; Krinsky, J. L.; Arnold, J. *Chem. Eur. J.* **2011**, *17*, 12234.
(2) Neidig, M. L.; Clark, D. L.; Martin, R. L. *Coord. Chem. Rev.* **2013**, *257*, 394.
(3) Ingram, K. I. M.; Tassell, M. J.; Gaunt, A. J.; Kaltsoyannis, N. *Inorg. Chem.* **2008**, *47*, 7824.
(4) Ingram, K. I. M.; Kaltsoyannis, N.; Gaunt, A. J.; Neu, M. P. *J. Alloys Compd.* **2007**, *444–445*, 369.
(5) Jensen, M. P.; Bond, A. H. *J. Am. Chem. Soc.* **2002**, *124*, 9870.
(6) Kozimor, S. A.; Yang, P.; Batista, E. R.; Boland, K. S.; Burns, C. J.; Clark, D. L.; Conradson, S. D.; Martin, R. L.; Wilkerson, M. P.; Wolfsberg, L. E. *J. Am. Chem. Soc.* **2009**, *131*, 12125.
(7) Minasian, S. G.; Keith, J. M.; Batista, E. R.; Boland, K. S.; Clark, D. L.; Conradson, S. D.; Kozimor, S. A.; Martin, R. L.; Schwarz, D. E.; Shuh, D. K.; Wagner, G. L.; Wilkerson, M. P.; Wolfsberg, L. E.; Yang, P. *J. Am. Chem. Soc.* **2012**, *134*, 5586.
(8) Hayton, T. W. *Chem. Commun.* **2013**, *49*, 2956.
(9) Hayton, T. W. *Dalton Trans.* **2010**, *39*, 1145.
(10) Gardner, B. M.; Liddle, S. T. *Chem. Commun.* **2015**, *51*, 10589.
(11) King, D. M.; Liddle, S. T. *Coord. Chem. Rev.* **2014**, *266–267*, 2.
(12) Zi, G. *Sci. China Chem.* **2014**, *57*, 1064.
(13) *Cambridge Structural Database*, version 1.18. 2015
(14) Haskel, A.; Straub, T.; Eisen, M. S. *Organometallics* **1996**, *15*, 3773.
(15) Ren, W.; Zi, G.; Walter, M. D. *Organometallics* **2012**, *31*, 672.
(16) Bell, N. L.; Maron, L.; Arnold, P. L. *J. Am. Chem. Soc.* **2015**, *137*, 10492.
(17) Ma, G.; Ferguson, M. J.; McDonald, R.; Cavell, R. G. *Inorg. Chem.* **2011**, *50*, 6500.
(18) Lu, E.; Lewis, W.; Blake, A. J.; Liddle, S. T. *Angew. Chem. Int. Ed.* **2014**, *53*, 9356.
(19) Ren, W.; Deng, X.; Zi, G.; Fang, D.-C. *Dalton Trans.* **2011**, *40*, 9662.
(20) Ren, W.; Zi, G.; Fang, D.-C.; Walter, M. D. *J. Am. Chem. Soc.* **2011**, *133*, 13183.
(21) Smiles, D. E.; Wu, G.; Kaltsoyannis, N.; Hayton, T. W. *Chem. Sci.* **2015**, *6*, 3891.
(22) Ren, W.; Song, H.; Zi, G.; Walter, M. D. *Dalton Trans.* **2012**, *41*, 5965.
(23) Behrle, A. C.; Barnes, C. L.; Kaltsoyannis, N.; Walensky, J. R. *Inorg. Chem.* **2013**, *52*, 10623.
(24) Behrle, A. C.; Levin, J. R.; Kim, J. E.; Drewett, J. M.; Barnes, C. L.; Schelter, E. J.; Walensky, J. R. *Dalton Trans.* **2015**, *44*, 2693.
(25) Seaman, L. A.; Hrobárik, P.; Schettini, M. F.; Fortier, S.; Kaupp, M.; Hayton, T. W. *Angew. Chem. Int. Ed.* **2013**, *52*, 3259.
(26) Hrobarik, P.; Hrobarikova, V.; Greif, A. H.; Kaupp, M. *Angew. Chem. Int. Ed.* **2012**, *51*, 10884.
(27) Brown, J. L.; Fortier, S.; Wu, G.; Kaltsoyannis, N.; Hayton, T. W. *J. Am. Chem. Soc.* **2013**, *135*, 5352.
(28) Piers, W. E.; Ziegler, T.; Fischer, J. M.; Macgillivray, L. R.; Zaworotko, M. J. *Chem. Eur. J.* **1996**, *2*, 1221.

(29) Shin, J. H.; Churchill, D. G.; Bridgewater, B. M.; Pang, K.; Parkin, G. *Inorg. Chim. Acta* **2006**, *359*, 2942.
(30) Shin, J. H.; Savage, W.; Murphy, V. J.; Bonanno, J. B.; Churchill, D. G.; Parkin, G. *J. Chem. Soc. Dalton Trans.* **2001**, 1732.
(31) Mathur, P.; Ahmed, M. O.; Dash, A. K.; Kaldis, J. H. *Organometallics* **2000**, *19*, 941.
(32) Wardle, R. W. M.; Bhaduri, S.; Chau, C. N.; Ibers, J. A. *Inorg. Chem.* **1988**, *27*, 1747.
(33) Eichhorn, B. W.; Gardner, D. R.; Nichols-Ziebarth, A.; Ahmed, K. J.; Bott, S. G. *Inorg. Chem.* **1993**, *32*, 5412.
(34) Ansari, M. A.; Ibers, J. A. *Coord. Chem. Rev.* **1990**, *100*, 223.
(35) Wardle, R. W. M.; Chau, C. N.; Ibers, J. A. *J. Am. Chem. Soc.* **1987**, *109*, 1859.
(36) D'Eye, R. W. M. *J. Chem. Soc.* **1953**, 1670.
(37) Ginsberg, A. P.; Lindsell, W. E.; Sprinkle, C. R.; West, K. W.; Cohen, R. L. *Inorg. Chem.* **1982**, *21*, 3666.
(38) Rohrmann, J.; Herrmann, W. A.; Herdtweck, E.; Riede, J.; Ziegler, M.; Sergeson, G. *Chem. Ber.* **1986**, *119*, 3544.
(39) Adel, J.; Weller, F.; Dehnicke, K. *J. Organomet. Chem.* **1988**, *347*, 343.
(40) Ansari, M. A.; Chau, C. N.; Mahler, C. H.; Ibers, J. A. *Inorg. Chem.* **1989**, *28*, 650.
(41) Mandimutsira, B. S.; Chen, S. J.; Reynolds III, R. A.; Coucouvanis, D. *Polyhedron* **1997**, *16*, 3911.
(42) Liao, J. H.; Hill, L.; Kanatzidis, M. G. *Inorg. Chem.* **1993**, *32*, 4650.
(43) Nagao, S.; Seino, H.; Hidai, M.; Mizobe, Y. *Inorg. Chim. Acta* **2004**, *357*, 4618.
(44) Guo, G.-C.; Mak, T., C. W. *J. Chem. Soc. Dalton Trans.* **1997**, 709.
(45) Farrar, D. H.; Grundy, K. R.; Payne, N. C.; Roper, W. R.; Walker, A. *J. Am. Chem. Soc.* **1979**, *101*, 6577.
(46) Gea, Y.; Greaney, M. A.; Coyle, C. L.; Stiefel, E. I. *J. Chem. Soc. Chem. Comm.* **1992**, 160.
(47) Fedin, V. P.; Mironov, Y. V.; Virovets, A. V.; Podberezskaya, N. V.; Fedorov, V. Y. *Polyhedron* **1992**, *11*, 1959.
(48) Suzuki, T.; Tsuji, N.; Kashiwabara, K.; Tatsumi, K. *Inorg. Chem.* **2000**, *39*, 3938.
(49) Nagata, K.; Takeda, N.; Tokitoh, N. *Angew. Chem. Int. Ed.* **2002**, *41*, 136.
(50) Liao, J.-H.; Li, J.; Kanatzidis, M. G. *Inorg. Chem.* **1995**, *34*, 2658.
(51) Howard, W. A.; Trnka, T. M.; Parkin, G. *Organometallics* **1995**, *14*, 4037.
(52) Shin, J. H.; Parkin, G. *Organometallics* **1994**, *13*, 2147.
(53) Rabinovich, D.; Parkin, G. *Inorg. Chem.* **1995**, *34*, 6341.
(54) Parkin, G. In *Prog. Inorg. Chem.*; John Wiley & Sons, Inc.: 2007, p 1.
(55) Murphy, V. J.; Rabinovich, D.; Halkyard, S.; Parkin, G. *J. Chem. Soc. Chem. Comm.* **1995**, 1099.
(56) Shannon, R. D. *Acta Crystallogr. Sect. A* **1976**, *A32*, 751.
(57) Pyykkö, P. *J. Phys. Chem. A* **2015**, *119*, 2326.
(58) Benz, R.; Zachariasen, W. H. *Acta Cryst. Sect. B.* **1970**, *26*, 823.
(59) Cody, J. A.; Ibers, J. A. *Inorg. Chem.* **1996**, *35*, 3836.
(60) Narducci, A. A.; Ibers, J. A. *Inorg. Chem.* **1998**, *37*, 3798.
(61) Rocker, F.; Tremel, W. *Z. Anorg. Allg. Chem.* **2001**, *627*, 1305.
(62) Wu, E. J.; Pell, M. A.; Ibers, J. A. *J. Alloys Compd.* **1997**, *255*, 106.
(63) Tougait, O.; Potel, M.; Noël, H. *Inorg. Chem.* **1998**, *37*, 5088.
(64) D'Eye, R. W. M.; Sellman, P. G. *J. Chem. Soc.* **1954**, 3760.

(65) Di Vaira, M.; Peruzzini, M.; Stoppioni, P. *Angew. Chem. Int. Ed.* **1987**, *26*, 916.
(66) Rabinovich, D.; Parkin, G. *J. Am. Chem. Soc.* **1993**, *115*, 9822.
(67) Steigerwald, M. L.; Siegrist, T.; Gyorgy, E. M.; Hessen, B.; Kwon, Y. U.; Tanzler, S. M. *Inorg. Chem.* **1994**, *33*, 3389.
(68) Fischer, J. M.; Piers, W. E.; MacGillivray, L. R.; Zaworotko, M. J. *Inorg. Chem.* **1995**, *34*, 2499.
(69) Howard, W. A.; Parkin, G.; Rheingold, A. L. *Polyhedron* **1995**, *14*, 25.
(70) Brunner, H.; M. Kubicki, M.; Leblanc, J.-C.; Meier, W.; Moïse, C.; Sadorge, A.; Stubenhofer, B.; Wachter, J.; Wanninger, R. *Eur. J. Inorg. Chem.* **1999**, *1999*, 843.
(71) Seikel, E.; Oelkers, B.; Sundermeyer, J. *Inorg. Chem.* **2012**, *51*, 2709.
(72) Christou, V.; Arnold, J. *Angew. Chem. Int. Ed.* **1993**, *32*, 1450.
(73) Shin, J. H.; Parkin, G. *Organometallics* **1995**, *14*, 1104.
(74) Rabinovich, D.; Parkin, G. *Inorg. Chem.* **1994**, *33*, 2313.
(75) Johnson, A. R.; Davis, W. M.; Cummins, C. C.; Serron, S.; Nolan, S. P.; Musaev, D. G.; Morokuma, K. *J. Am. Chem. Soc.* **1998**, *120*, 2071.
(76) Capps, K. B.; Wixmerten, B.; Bauer, A.; Hoff, C. D. *Inorg. Chem.* **1998**, *37*, 2861.
(77) Hahn, H.; Stocks, K. *Naturwissenschaften* **1968**, *55*, 389.
(78) Hulliger, F. *J. Less-Common Met.* **1968**, *16*, 113.
(79) Beck, H. P.; Dausch, W. *Z. Anorg. Allg. Chem.* **1989**, *571*, 162.
(80) Howard, W. A.; Waters, M.; Parkin, G. *J. Am. Chem. Soc.* **1993**, *115*, 4917.
(81) Smiles, D. E.; Wu, G.; Hrobárik, P.; Hayton, T. W. *J. Am. Chem. Soc.* **2016**, *138*, 814.
(82) Awere, E. G.; Passmore, J.; White, P. S. *J. Chem. Soc. Dalton Trans.* **1993**, 299.
(83) Smiles, D. E.; Wu, G.; Kaltsoyannis, N.; Hayton, T. W. *Chem. Sci.* **2015**, *6*, 3891.
(84) Smiles, D. E.; Wu, G.; Hayton, T. W. *Inorg. Chem.* **2014**, *53*, 10240.
(85) Harris, R. K.; Becker, E. D.; Cabral De Menezes, S. M.; Goodfellow, R.; Granger, P. *Pure Appl. Chem.* **2001**, *73*, 1795.
(86) Harris, R. K.; Becker, E. D.; Cabral De Menezes, S. M.; Granger, P.; Hoffman, R. E.; Zilm, K. W. *Pure Appl. Chem.* **2008**, *80*, 59.
(87) Kuhn, N.; Henkel, G.; Schumann, H.; Frohlich, R. *Z. Naturforsch. B* **1990**, *45*, 1010.
(88) *SMART Apex II*, Version 2.1. 2005
(89) *SAINT Software User's Guide*, Version 7.34a. 2005
(90) *SADABS*, 2005
(91) *SHELXTL PC*, Version 6.12. 2005
(92) Perdew, J. P.; Burke, K.; Ernzerhof, M. *Phys. Rev. Lett.* **1996**, *77*, 3865.
(93) Perdew, J. P.; Burke, K.; Ernzerhof, M. *Phys. Rev. Lett.* **1997**, *78*, 1396.
(94) Adamo, C.; Barone, V. *Chem. Phys. Lett.* **1998**, *298*, 113.
(95) Grimme, S.; Antony, J.; Ehrlich, S.; Krieg, H. *J. Chem. Phys.* **2010**, *132*, 154104.
(96) Grimme, S.; Ehrlich, S.; Goerigk, L. *J. Comput. Chem.* **2011**, *32*, 1456.
(97) *Turbomole*, version 6.3.1, University of Karlsruhe and Forschungszentrum Karlsruhe, GmbH, 1989-2007, TURBOMOLE GmbH since 2007; http://www.turbomole.com.
(98) Cao, X.; Dolg, M. *J. Mol. Struct. THEOCHEM* **2004**, *673*, 203.
(99) Andrae, D.; Häußermann, U.; Dolg, M.; Stoll, H.; Preuß, H. *Theo. Chim. Acta* **1990**, *77*, 123.
(100) Weigend, F.; Ahlrichs, R. *Phys. Chem. Chem. Phys.* **2005**, *7*, 3297.
(101) *Amsterdam Density Functional (ADF)*, version 2014.07; SCM, Theoretical Chemistry, Vrije Univeriteit: Amsterdam, Netherlands, 2015; http://www.scm.com.

(102) Wolff, S. K.; Ziegler, T. *J. Chem. Phys.* **1998**, *109*, 895.
(103) Wolff, S. K.; Ziegler, T.; van Lenthe, E.; Baerends, E. J. *J. Chem. Phys.* **1999**, *110*, 7689.
(104) Klamt, A.; Schuurmann, G. *J. Chem. Soc. Perk. T. 2* **1993**, 799.
(105) Reed, A. E.; Curtiss, L. A.; Weinhold, F. *Chem. Rev.* **1988**, *88*, 899.
(106) Glendening, E. D.; Badenhoop, J. K.; Reed, A. E.; Carpenter, J. E.; Bohmann, J. A.; Morales, C. M.; Landis, C. R.; Weinhold, F. *NBO 6.0*; Theoretical Chemistry Institute, University of Wisconsin: Madison, WI, 2013; http://nbo6.chem.wisc.edu/.
(107) Frisch, M. J. et. al. *Gaussian 09*, revision D.01; Gaussian, Inc.: Wallingford, CT, 2009.
(108) Matta, C. F.; Boyd, R. J. In *The quantum theory of atoms in molecules*; Matta, C. F., Boyd, R. J., Eds.; Wiley-VCH: Weinheim, Germany, 2007, p 1.
(109) Bader, R. F. W. *Atoms in Molecules: A Quantum Theory*; Oxford University Press: Oxford, U.K., 1990.
(110) Lu, T. *Multiwfn: A Multifunctional Wave Function Analyzer*, version 3.3.7; 2015; http://multiwfn.codeplex.com.
(111) Lu, T.; Chen, F. *J. Comput. Chem.* **2012**, *33*, 580.
(112) te Velde, G.; Bickelhaupt, F. M.; Baerends, E. J.; Fonseca Guerra, C.; van Gisbergen, S. J. A.; Snijders, J. G.; Ziegler, T. *J. Comput. Chem.* **2001**, *22*, 931.

Chapter 6 Reversible Chalcogen Atom Transfer to Uranium Terminal Sulfides

Portions of this work were published in:

Danil E. Smiles, Guang Wu, Trevor W. Hayton

Inorg. Chem. **2014**, *53*, 12683-12685.

Table of Contents

6.1 Introduction

The ability to transfer sulfur in a controlled manner is key to incorporating sulfur into organic compounds, and to the synthesis of wide variety of sulfur containing products.[1-6] Of the various sulfur sources that are typically employed elemental sulfur, S_8, stands out as especially useful. This is due not only to its inexpensiveness, but also the fact that using S_8 in these transformations is highly atom economical. Even with these benefits, many examples of sulfur atom transfer catalysis utilize other sulfur sources, and the few that do use S_8 exhibit narrow substrate scopes.[4-12] For example, Bargon and co-workers reported that $[((EtO)_2PS_2)_2Mo(O)]$ catalyzes the formation of thiiranes from a handful of activated olefins and S_8. One active species in this transformation is believed to be the disulfide complex, $[((EtO)_2PS_2)_2Mo(O)(\eta^2\text{-}S_2)]$. This disulfide can transfer a sulfur atom to generate the monosulfide, $[((EtO)_2PS_2)_2Mo(O)(S)]$, which also can act as a sulfur transfer reagent. Formation of the oxo complex is followed by reaction with S_8 to regenerate the active disulfide.[10,11] This process is similar to that of $[Cp^*_2Ti(\eta^2\text{-}S_2)]$, reported by Bergman and co-workers. The titanium disulfide readily reacts with phosphines, R_3P (R = Me, Ph), to generate the corresponding phosphine sulfide, and the titanium monosulfide complex, $[Cp^*_2Ti(S)]$. Addition of elemental sulfur to this monosulfide will regenerate the disulfide species. Notably, reaction of this disulfide with additional S_8 affords the trisulfide complex, $[Cp^*_2Ti(\kappa^2\text{-}S_3)]$ (Scheme 6.1).[13,14]

Scheme 6.1 Reversible and Irreversible sulfur transfer to [$Cp^*Ti(\eta^2\text{-}S_2)$] using S_8

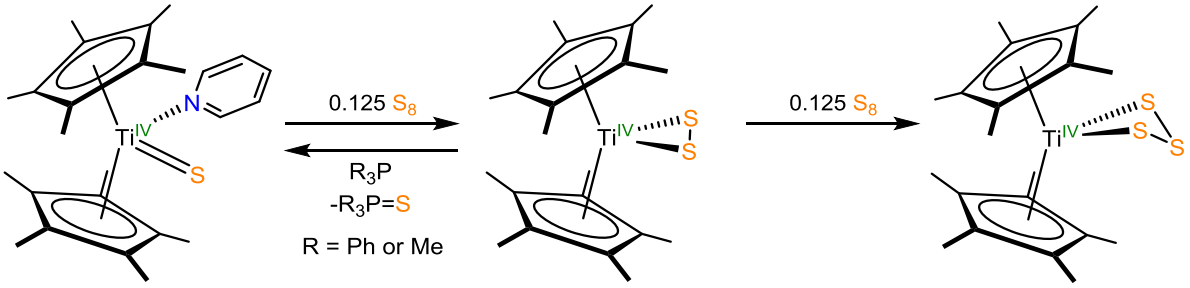

Chalcogen atom transfer is also known for actinide systems; however, none of the reactions have been reported to be reversible. For example, Mazzanti and co-workers reported that [U((SiMe$_2$NPh)$_3$-tacn)(η^2-S$_2$)], transfers sulfur to Ph$_3$P to give Ph$_3$P=S, however the uranium containing portion of the reaction proved to be an intractable mixture.[15] Additionally, Meyer and co-workers reported that [((^{Ad}ArO)$_3$N)U(DME)]$_2$(μ-Se) reacts with 1 and 3 equiv of elemental Se to give [((^{Ad}ArO)$_3$N)U]$_2$(μ-η^2:η^2-Se$_2$)(μ-DME) and [((^{Ad}ArO)$_3$N)U(DME)]$_2$(μ-η^3:η^3-S$_4$), respectively. In this instance, the reverse reaction, Se atom abstraction, was not described.[16,17]

The lack of examples of reversible chalcogen atom transfer and the disadvantages associated with reported systems demonstrates the need to further develop this area. This chapter describes the investigation of chalcogen atom transfer to and from the terminal uranium monosulfide, [K(18-crown-6)][U(S)(NR$_2$)$_3$] (**2.1**),[18] using elemental sulfur and selenium. The isolation of new U(IV) terminal chalcogenide complexes is described, and these complexes are all characterized both structurally and spectroscopically. The synthesis of a polysulfide salt, similar to the polychalcogenides discussed in Chapter 4, and its use as an alternative route to synthesize uranium sulfides, is also detailed.

6.2 Results and Discussion

6.2.1 Synthesis and Characterization of [K(18-crown-6)][U(η²-S₂)(NR₂)₃] (6.1)

Addition of 0.125 equiv of S_8 to a THF solution of the uranium monosulfide, [K(18-crown-6)][U(S)(NR₂)₃] (**2.1**), yields a red-orange solution, from which the new U(IV) disulfide, [K(18-crown-6)][U(η²-S₂)(NR₂)₃] (**6.1**), can be isolated as red-orange crystals in 59% yield, after crystallization from diethyl ether / pentane (Scheme 6.2).

The ^{1}H NMR spectrum of complex **6.1**, in pyridine-d_5, features two broad resonances at -8.20 and 3.52 ppm, attributable to the methyl groups of the silylamide ligands and the methylene groups of the 18-crown-6 moiety, respectively. In addition, the NIR spectrum of complex **6.1** matches those of other complexes with U(IV) metal centers (Figure A6.6),[18-22] and it indicates that no metal based redox chemistry has occurred during this transformation.

Scheme 6.2. Synthesis of [K(18-crown-6)][U(η²-S₂)(NR₂)₃] (**6.1**)

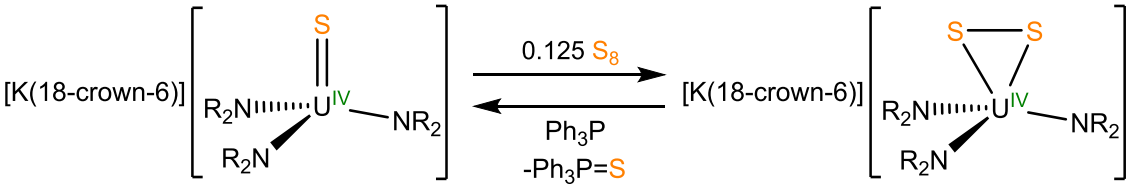

Complex **6.1** crystallizes in the monoclinic spacegroup $P2_1/n$, and its solid state molecular structure is shown in Figure 6.1. Complex **6.1** is structurally identical to its selenide analogue, [K(18-crown-6)][U(η²-Se₂)(NR₂)₃] (**4.8**), and features a considerable deviation from idealized tetrahedral geometry around uranium. This results not only in distorted N-U-N angles (N1-U1-N2 = 102.4(3)°, N2-U1-N3 = 108.1(3)°, N1-U1-N3 = 128.4(3)°), but also a notable asymmetry in the U-S bond distances (U1-S1 = 2.589(4), U1-S2 = 2.747(3) Å). The U-S bond distances of **6.1** are within the range known for U-S single bonds[23] and are comparable to those of other uranium disulfides.[15,16,22,24-27] Furthermore, the S-S bond distance of complex

6.1 (S1-S2 = 2.160(7) Å) is slightly longer than those of other structurally characterized uranium disulfides,[15,16,22,24-27] which is believed to be a consequence of the coordination of the $[K(18\text{-crown-6})]^+$ moiety to $[S_2]^{2-}$ ligand. The E-K bond length in **6.1** (S1-K1 = 3.176(5) Å) is similar to that of complex **2.1** and shorter than the corresponding E-K bond lengths of the structurally identical selenide (**4.8**) (av. Se-K = 3.260 Å) and telluride (**4.3**) (av. Te-K = 3.704 Å), consistent with the smaller ionic radius of S^{2-} versus Se^{2-} and Te^{2-}.[28]

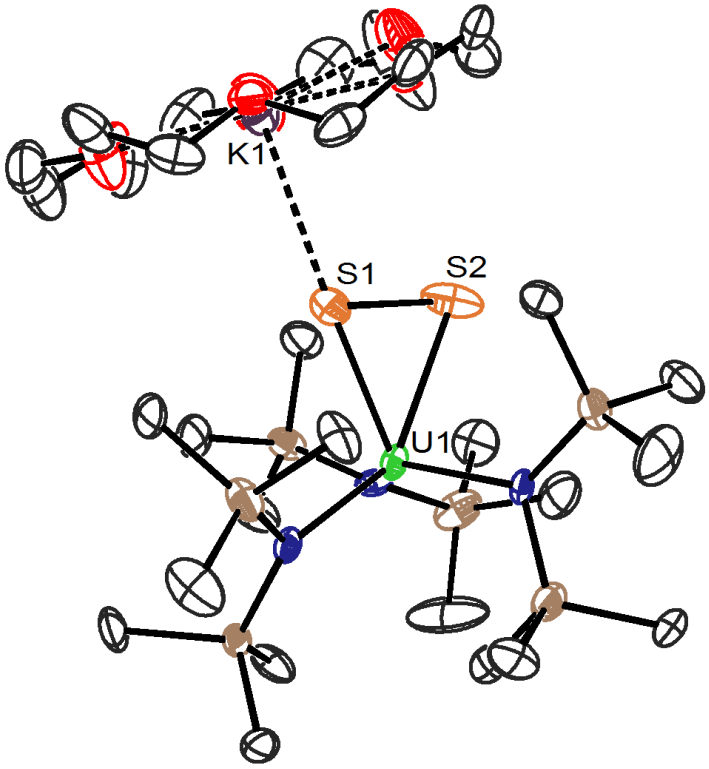

Figure 6.1. ORTEP diagram of $[K(18\text{-crown-6})][U(\eta^2\text{-}S_2)(NR_2)_3]$ (**6.1**) with 50% probability ellipsoids. Hydrogen atoms are omitted for clarity. Selected bond distances (Å) and angles (deg): U1-S1 = 2.589(4), U1-S2 = 2.747(3), S1-K1 = 3.176(5), S1-S2 = 2.160(7), N1-U1-N2 = 102.4(3), N2-U1-N3 = 108.1(3), N1-U1-N3 = 128.4(3).

Remarkably, the formation of complex **6.1** is reversible, and it can be readily converted back into the starting monosulfide, complex **2.1**, via addition of a phosphine (Scheme 6.2). Thus, addition of 1 equiv of Ph_3P to a solution of **6.1** in pyridine-d_5 results in the reformation

of complex **2.1** as determined by in situ ^{1}H NMR spectroscopy (Figure 6.2). Also observed during this reaction is the formation of $Ph_3P{=}S$, as determined by in situ ^{1}H and $^{31}P\{^{1}H\}$ NMR spectroscopies (Figure 6.2 and Figure A6.1).

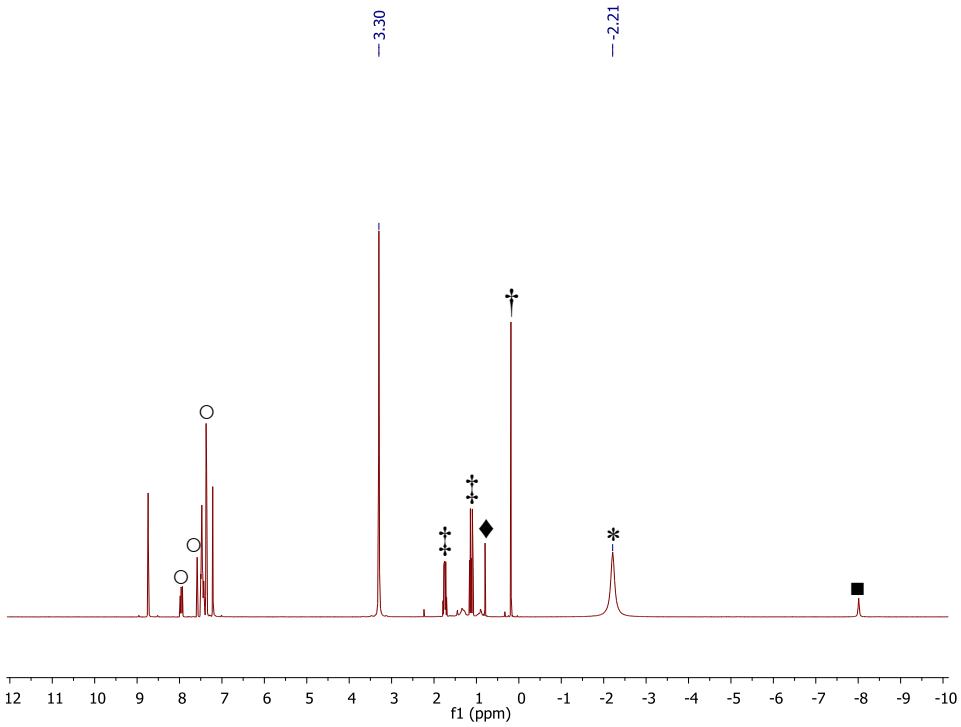

Figure 6.2. In situ ^{1}H NMR spectrum of the reaction of [K(18-crown-6)][U(η^2-S_2)(NR_2)$_3$] (**6.1**) with Ph_3P in pyridine-d_5. (*) indicates the presence of **2.1**, (■) indicates the presence of unreacted **6.1**, (○) Ph_3P and $Ph_3P{=}S$, (†) indicates the presence of $HN(SiMe_3)_2$, (‡) indicates the presence of Et_2O, and (♦) indicates the presence of hexanes.

6.2.2 Synthesis and Characterization of [K(18-crown-6)][U(η^3-S_3)(NR_2)$_3$] (6.2)

Complex **6.1** also exhibits reactivity with elemental sulfur, similar to that observed for complex **2.1**. Reaction **6.1** with 0.125 equiv of S_8 in THF affords the U(IV) trisulfide, [K(18-crown-6)][U(η^3-S_3)(NR_2)$_3$] (**6.2**), as orange crystals, in 34% yield after crystallization from diethyl ether (Scheme 6.3). The ^{1}H NMR spectrum of complex **6.2** is very similar to that of complex **6.1**, featuring two resonances at -7.05 and 3.56 ppm, assignable to methyl groups of

the silylamide ligands the methylene groups of the 18-crown-6 moiety. The only major difference is that the resonance attributable to the silylamide ligands is extremely broad (FWHM = 2150 Hz) (Figure A6.2). Additionally, the NIR spectrum of **6.2** is consistent with the presence of a U(IV) metal center (Figure A6.6),[18-22] again indicating that no metal based redox chemistry has occurred. The formation of complex **6.2** is reversible, and addition of 1 equiv of Et_3P to a solution of **6.2** results in the formation of Et_3P=S in addition to regenerating complex **6.1**.

Scheme 6.3 Synthesis of [K(18-crown-6)][U(η^3-S_3)(NR_2)$_3$] (**6.2**)

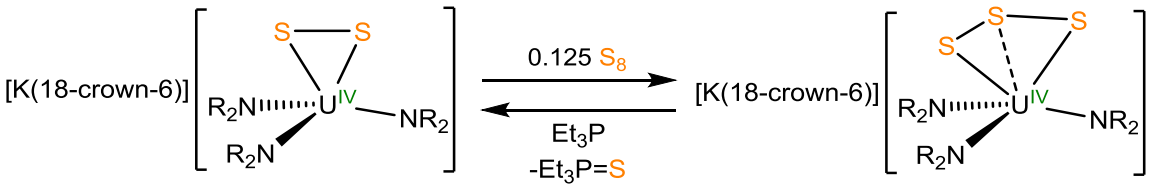

Complex **6.2** crystallizes in the triclinic spacegroup $P\bar{1}$ as a diethyl ether solvate, **6.2**·Et_2O, and its solid state molecular structure is shown in Figure 6.3. Complex **6.2** possesses a terminal $[\eta^3\text{-}S_3]^{2-}$ ligand, which stands in contrast to the few structurally characterized complexes with a terminal $[S_3]^{2-}$ ligand that all feature a κ^2-coordination mode.[29-35] Furthermore, this is the only actinide example. Complex **6.2** features asymmetric U-S bond lengths (U1-S1 = 2.835(1), U1-S2 = 2.819(1), U1-S3 = 2.760(1) Å) and N-U-N angles (N1-U1-N2 = 121.8(1)°, N2-U1-N3 = 107.3(1)°, N1-U1-N3 = 95.8(1)°), both likely a consequence of the presence of the $[\eta^3\text{-}S_3]^{2-}$ ligand and the sterically demanding silylamide ligands, identical to what is observed for **6.1**. While the S-S bond distances (S1-S2 = 2.059(2), S2-S3 = 2.066(1) Å) are slightly shorter than those of complex **6.1**, they are comparable to those of other uranium disulfides.[15,24-27]

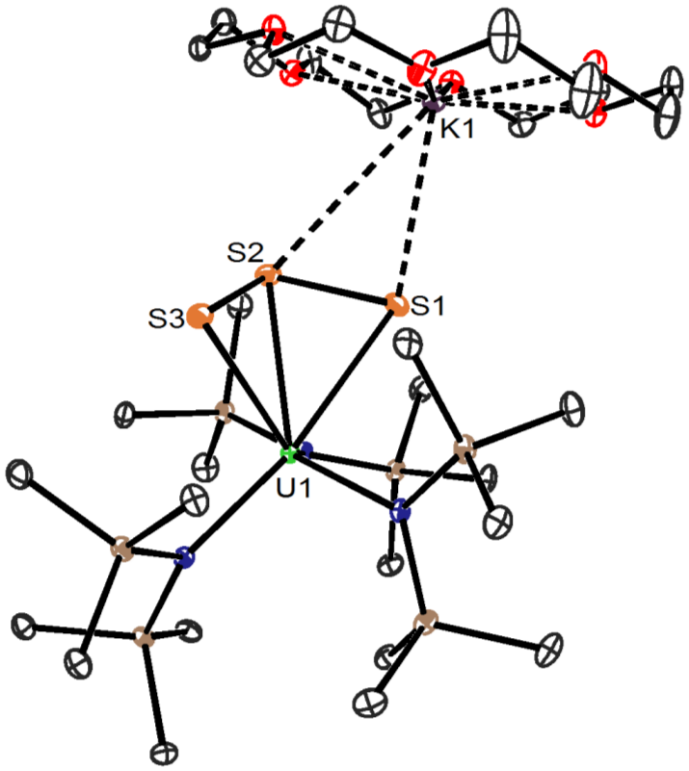

Figure 6.3. ORTEP diagram of [K(18-crown-6)][U(η^3-S_3)(NR_2)$_3$] (**6.2**·Et_2O) with 50% probability ellipsoids. Diethyl ether solvate and hydrogen atoms are omitted for clarity. Selected bond distances (Å) and angles (deg): U1-S1 = 2.835(1), U1-S2 = 2.819(1), U1-S3 = 2.760(1), S1-K1 = 3.196(1), S2-K1 = 3.747(1), S1-S2 = 2.059(2), S2-S3 = 2.066(1), N1-U1-N2 = 121.8(1), N2-U1-N3 = 107.3(1), N1-U1-N3 = 95.8(1).

6.2.3 Synthesis and Characterization of [K(18-crown-6)][U(η^2-SSe)(NR_2)$_3$] (6.3)

After the successful synthesis of complexes **6.1** and **6.2** the scope of chalcogen atom transfer was investigated. Thus, reaction of complex **2.1** with 1 equiv of elemental Se, in mixture of diethyl ether / THF, results in the formation of a dark orange-red solution. Upon crystallization from diethyl ether the selenosulfide complex, [K(18-crown-6)][U(η^2-SSe)(NR_2)$_3$] (**6.3**), can be isolated as a dark orange-red crystalline solid in 52% yield (Scheme 6.4). The ^{1}H NMR spectrum of complex **6.3** exhibits is nearly identical to that of complex **6.1**, and exhibits two broad resonances at -7.73 and 3.46 ppm, attributable to the methyl groups

of the silylamide ligands and the methylene groups of the 18-crown-6 moiety, respectively. In addition, the NIR spectrum of **6.3** confirms the presence of a U(IV) metal center (Figure A6.6) and that no redox chemistry has occurred at the metal center.

Scheme 6.4 Synthesis of [K(18-crown-6)][U(η^2-SSe)(NR_2)$_3$] (**6.3**)

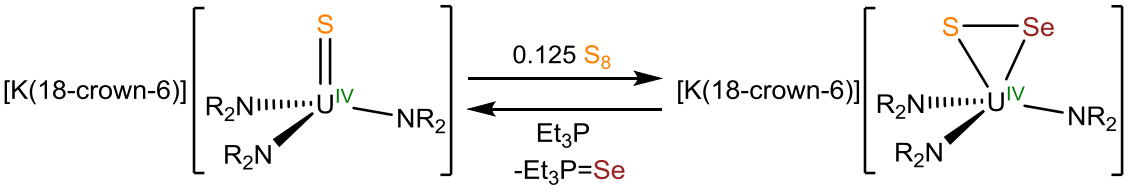

Identical to what is observed for complexes **6.1** and **6.2**, the synthesis of complex **6.3** is reversible. Thus, addition of 1 equiv of Et_3P to a solution of **6.3** in pyridine-d_5 results in regeneration of complex **2.1** and formation of Et_3P=Se as determined by in situ ^{1}H and ^{31}P{^{1}H} NMR spectroscopies (Figure 6.4 and Figure A6.3). Interestingly, the reaction proceeds with selective removal of the selenium atom, as no evidence for the formation of either [K(18-crown-6)][U(Se)(NR_2)$_3$] (**4.8**) or Et_3P=S is observed. This is unexpected as the formation of a P-S bond is thermodynamically favored over the analogous P-Se bond.[36] However, the longer U-Se versus U-S bond may suggest that the kinetic barrier to Se transfer is lower than that for S and account for the observed reactivity.

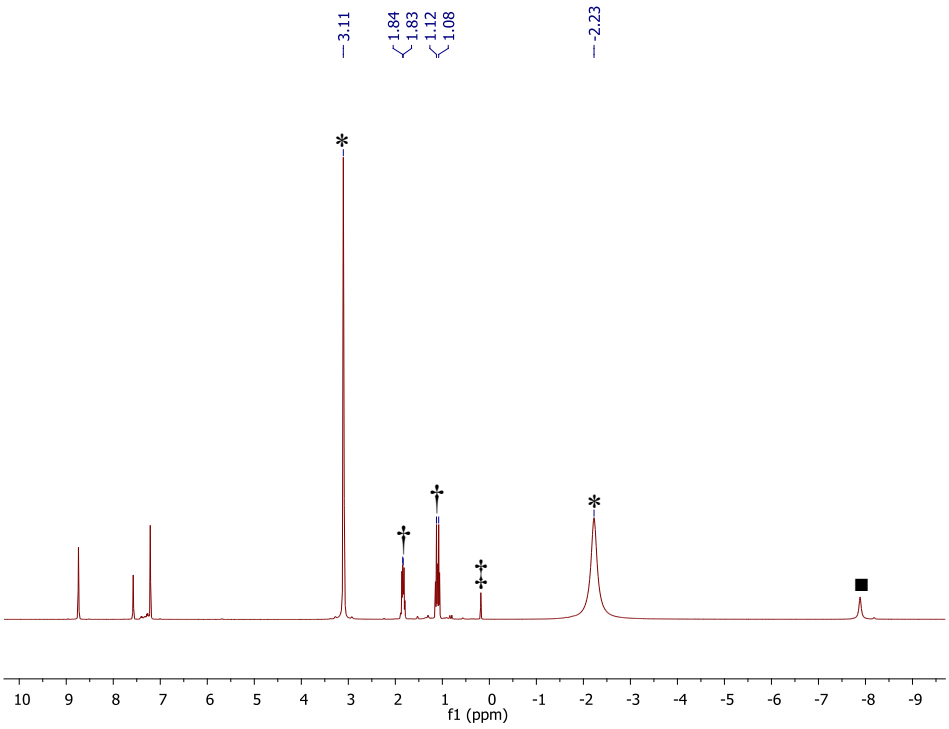

Figure 6.4. In situ ^{1}H NMR spectrum of the reaction of [K(18-crown-6)][U(η^2-SSe)$(NR_2)_3$] (**6.3**) with Et_3P in pyridine-d_5. (*) indicates the presence of **2.1**, (■) indicates the presence of unreacted (**6.3**), (†) indicates the presence of Et_3P=Se, and (‡) indicates the presence of $HN(SiMe_3)_2$.

Complex **6.3** crystallizes in the monoclinic spacegroup $P2_1$ with two independent molecules in the asymmetric unit, and its solid state molecular structure is shown in Figure 6.5. Complex **6.3** is isostructural to its disulfide (**6.1**) and diselenide (**4.8**) analogues, and selected metrical parameters for all three are collected in Table 6.1. While other complexes with a selenosulfide ligand, $[SSe]^{2-}$ have been made previously, all of these complexes feature a bridging [μ-η^2:η^2] motif,[37-44] whereas complex **6.3** features a terminal $[SSe]^{2-}$ ligand. The U-S (U1-S1 = 2.664(2), U2-S2 = 2.653(2) Å) and U-Se (U1-Se1 = 2.845(1), U2-Se2 = 2.851(1) Å) bond lengths of **6.3** are comparable to the U-S and U-Se bond lengths of **6.1** and **4.8**, respectively. In addition, the S-Se bond distances (S1-Se1 = 2.242(3), S2-Se2 = 2.240(3) Å) are longer than the S-S bond distances of **6.1** and shorter than the Se-Se bond distances of

4.8, as expected. The S-K bond distances of **6.3** (S1-K1 = 3.128(3), S2-K2 = 3.153(3) Å) are similar to those of complex **6.1**. Interestingly, in the solid state the $[K(18\text{-crown-6})]^+$ cation is exclusively interacting with the sulfur atom of the $[SSe]^{2-}$ ligand, and is believed to possibly play a role in the reactivity with Et_3P that is observed.

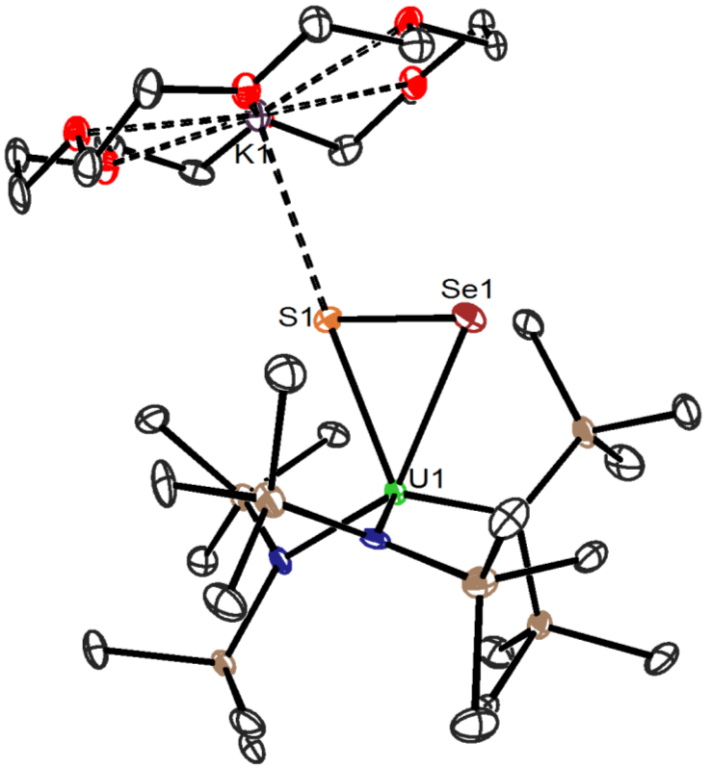

Figure 6.5. ORTEP diagram of $[K(18\text{-crown-6})][U(\eta^2\text{-SSe})(NR_2)_3]$ (**6.3**) with 50% probability ellipsoids. One molecule of **6.3** and hydrogen atoms are omitted for clarity. Selected bond distances (Å) and angles (deg): U1-S1 = 2.664(2), U2-S2 = 2.653(2), U1-Se1 = 2.845(1), U2-Se2 = 2.851(1), S1-K1 = 3.128(3), S2-K2 = 3.153(3), S1-Se1 = 2.242(3), S2-Se2 = 2.240(3), N1-U1-N2 = 100.9(3), N2-U1-N3 = 106.5(3), N1-U1-N3 = 129.7(3), N4-U2-N5 = 100.9(3), N5-U2-N6 = 106.1(3), N4-U2-N6 = 130.8(3).

It should be noted that all attempts to synthesize an analogous tellurosulfide complex were unsuccessful. No reaction was observed between complex **2.1** and elemental tellurium after 60 h, as determined by ^{1}H NMR spectroscopy. The lower oxidation potential of Te versus S and Se is likely responsible for the difference in observed reactivities.[45]

Table 6.1. Selected Bond Distances (Å) for Uranium Dichalcogenides

Complex	**6.1** (E = S)	**6.3** (E = S, Se)	**4.8** (E = Se)
U-E	U-S: 2.589(4), 2.747(3)	U-S: = 2.664(2), 2.653(2); U-Se = 2.845(1), 2.851(1)	U-Se: 2.7897(7), 2.8597(8), 2.7833(7), 2.8614(8)
E-K	S-K: 3.176(5)	S-K: 3.128(3), 3.153(3)	Se-K: 3.261(2), 3.257(2)
E-E	S-S: 2.160(7)	S-Se: 2.242(3), 2.240(3)	Se-Se: 2.368(1), 2.366(1)

6.2.4 Reaction of [K(18-crown-6)][U(S)(NR$_2$)$_3$] (2.1) with S$_8$ and Alkenes

The ability to reversibly add sulfur to the U(IV) monosulfide complex, [K(18-crown-6)][U(S)(NR$_2$)$_3$] (**2.1**) to afford complex **6.1** suggested that this complex could be competent for sulfur atom transfer catalysis. Accordingly, the reactivity of this species with alkenes was investigated as a way to catalytically prepare thiiranes (Scheme 6.5). Addition of excess S$_8$ and excess cyclohexene to a pyridine-d_5 solution of complex **2.1** results in conversion of **2.1** into the U(IV) trisulfide, **6.2** as determined by ^{1}H NMR spectroscopy (Figure A6.4). However, no evidence for the formation of cyclohexene sulfide is observed in this reactions. Similarly, reaction of complex **2.1** with excess S$_8$ and excess norbornene, in pyridine-d_5, results in no reaction after 72 h as determine by ^{1}H NMR spectroscopy (Figure A6.5). These results further illustrate the difficulties associated with sulfur atom transfer catalysis that utilizes S$_8$, and while initial attempts have been unsuccessful, further investigations are needed to discover the scope of this system.

Scheme 6.5 Proposed Sulfur Atom Transfer Catalysis Using [K(18-crown-6)][U(η^2-S_2)(NR_2)$_3$] (**6.1**)

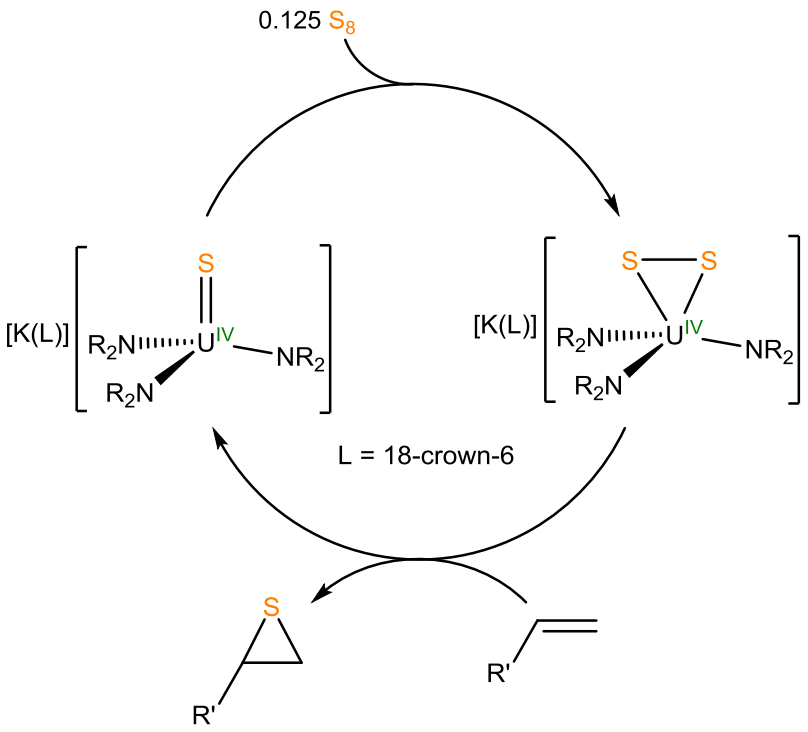

6.2.5 Synthesis and Characterization of [K(18-crown-6)]$_2$[S_4] (6.4)

The utility of the polytellurides and polyselenides discussed in Chapters 4 and 5 suggested that an analogous polysulfide might also prove synthetically useful. Modification of the procedure developed for the synthesis of [K(18-crown-6)]$_2$[Se_4] (**4.7**) allows access to the analogous tetrasulfide. Thus, reaction of KC_8 with elemental sulfur, in the presence of 18-crown-6, in THF affords the tetrasulfide salt, [K(18-crown-6)]$_2$[S_4] (**6.4**), which, after crystallization from acetonitrile / diethyl ether, can be isolated as orange crystals in 75% yield (Scheme 6.6).

Scheme 6.6 Synthesis of $[K(18\text{-crown-6})]_2[S_4]$ (**6.4**)

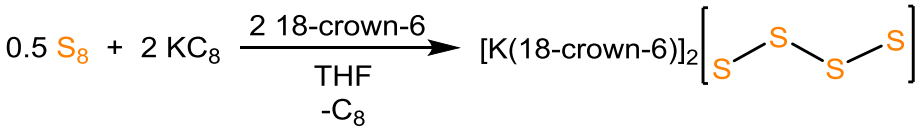

Complex **6.4** crystallizes in the monoclinic spacegroup $P2_1/n$, and its solid state molecular structure is shown in Figure 6.6. The S-S bond distances in **6.4** (av. 2.011 Å) are comparable to those of other structurally characterized alkali/alkaline earth metal complexes containing a $[S_4]^{2-}$ anion (av. 2.062 Å).[46,47] In addition, the S-K bond distances (av. 3.21 Å) of **6.4** are larger than the S-Li (av. 2.43 Å)[47] and shorter than the S-Rb (av. 3.671 Å)[46] bond distances of similar complexes with an $[S_4]^{2-}$ ligand, consistent with the differences in ionic radii between Li^+, K^+, and Rb^+.[28]

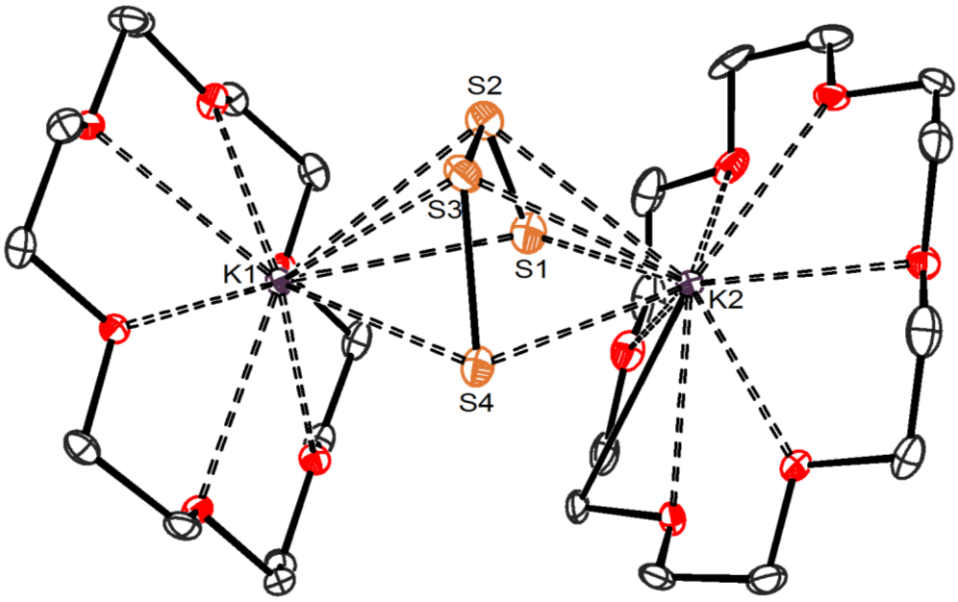

Figure 6.6. ORTEP diagram of $[K(18\text{-crown-6})]_2[S_4]$ (**6.4**) with 50% probability ellipsoids. Hydrogen atoms and disordered S atoms are omitted for clarity. Selected bond distances (Å): S1-S2 = 1.98(1), S2-S3 = 1.84(1), S3-S4 = 2.230(8), S1-K1 = 3.34(1), S2-K1 = 3.19(1), S3-K1 = 3.190(8), S4-K1 = 3.262(2).

6.2.6 Alternate Syntheses of Complexes 6.1 and 6.2

With complex **6.4** in hand its ability to act as a sulfur transfer reagent was investigated. Using this tetrasulfide salt, disulfide **6.1** can be prepared in an identical manner employed for the synthesis of complex **4.8**. Thus, reaction of 0.5 equiv of **6.4** with $[U(NR_2)_3]$ in diethyl ether / pyridine affords a red-orange solution. After crystallization from diethyl ether / pentane, complex **6.1** can be isolated as red-orange crystals in 42% yield (Scheme 6.7). During this reaction the $[S_4]^{2-}$ anion acts as a $2e^-$ oxidant. Two U(III) metal centers reduce the $[S_4]^{2-}$ anion, breaking the central S-S bond, and giving rise to the $[\eta^2\text{-}S_2]^{2-}$ ligands, all in an identical manner to what is observed for the analogous selenium reaction.

Scheme 6.7 Synthesis of $[K(18\text{-crown-6})][U(\eta^2\text{-}S_2)(NR_2)_3]$ (**6.1**) using $[K(18\text{-crown-6})]_2[S_4]$ (**6.4**)

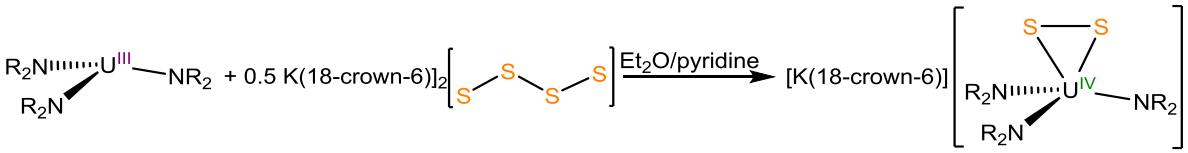

Complex **6.4** can also be used to synthesize trisulfide complex, **6.2**. The addition of 1 equiv of **6.4** to a mixture of $[U(I)(NR_2)_3]$[19] in THF results in the formation of a dark orange solution and the deposition of a white powder. Upon workup, complex **6.2** can be isolated as orange crystals in 64% yield (Scheme 6.8). The fourth sulfur of complex **6.4** is believed to be ejected as a result of the steric clash between the polysulfide ligand and the bulky silylamide ligands, giving rise to the observed $[S_3]^{2-}$ ligand and similar to what has been observed in the synthesis of $[K(18\text{-crown-6})][U(\eta^2\text{-}Se_2)(NR_2)_3]$ (**4.8**) using the tetraselenide salt, $[K(18\text{-crown-6})]_2[Se_4]$ (**4.7**).

Scheme 6.8 Synthesis of [K(18-crown-6)][U(η^3-S_3)(NR_2)$_3$] (**6.2**) using [K(18-crown-6)]$_2$[S_4] (**6.4**)

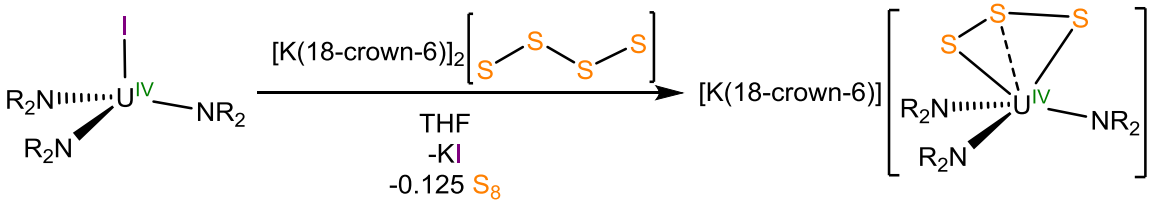

6.3 Summary

In summary, reaction of the U(IV) monosulfide, [K(18-crown-6)][U(S)(NR_2)$_3$] (**2.1**), with either elemental S or Se affords the U(IV) dichalcogenides, [K(18-crown-6)][U(η^2-S_2)(NR_2)$_3$] (**6.1**) and [K(18-crown-6)][U(η^2-SSe)(NR_2)$_3$] (**6.3**). Both transformations are reversible and the starting monosulfide is regenerated upon reaction with a phosphine. Addition of 0.125 equiv of S_8 to complex **6.1** generates the U(IV) trisulfide, [K(18-crown-6)][U(η^3-S_3)(NR_2)$_3$] (**6.2**), which contains the rare [η^3-S_3]$^{2-}$ ligand. This reaction is also reversible, and importantly all these interconversions occur with no change in the uranium oxidation state.

The tetrasulfide salt, [K(18-crown-6)]$_2$[S_4] (**6.4**), is synthesized by reducing S_8 with KC_8 in the presence of 18-crown-6. Complex **6.4** is shown to be a competent sulfur atom transfer source and provides alternative synthetic routes to complexes **6.1**, via reaction with [U(NR_2)$_3$], and **6.2**, via reaction with [U(I)(NR_2)$_3$]. The utility of this polysulfide, similar to its Se and Te analogues, suggests of its usefulness for other systems. Furthermore, the ability to do reversible chalcogen atom transfer opens up the possibility of catalysis. Preliminary experiments have been unsuccessful. The wide array of substrates available, in addition to the lack of progress in this field, however, suggest that more investigation is needed to fully take advantage of this system.

6.4 Experimental

6.4.1 General Methods

All reactions and subsequent manipulations were performed under anaerobic and anhydrous conditions under an atmosphere of nitrogen. Hexanes, Et_2O, and toluene were dried using a Vacuum Atmospheres DRI-SOLV Solvent Purification system and stored over 3Å sieves for 24 h prior to use. Tetrahydrofuran (THF) was distilled twice, first from calcium hydride and then from sodium benzophenone ketyl, and stored over 3Å molecular sieves for 24 h prior to use. Pyridine and pyridine-d_5 were dried over 3Å molecular sieves for 24 h prior to use. [K(18-crown-6)][U(S)$(NR_2)_3$] (**2.1**),[18] [U$(NR_2)_3$][48] and [U(I)$(NR_2)_3$][19] were synthesized according to the previously reported procedures. All other reagents were purchased from commercial suppliers and used as received.

NMR spectra were recorded on a Varian UNITY INOVA 400, a Varian UNITY INOVA 500 spectrometer, a Varian UNITY INOVA 600 MHz spectrometer, or an Agilent Technologies 400-MR DD2 400 MHz Spectrometer. ^{1}H NMR spectra were referenced to external $SiMe_4$ using the residual protio solvent peaks as internal standards. $^{31}P\{^1H\}$ NMR spectra were referenced indirectly with the ^{1}H resonance of $SiMe_4$ at 0 ppm, according to IUPAC standard,[49,50] using the residual solvent peaks as internal standards. IR spectra were recorded on a Nicolet 6700 FT-IR spectrometer with a NXR FT Raman Module. UV-Vis / NIR experiments were performed on a UV-3600 Shimadzu spectrophotometer. Elemental analyses were performed by the Micro-Analytical Facility at the University of California, Berkeley.

6.4.2 Synthesis of [K(18-crown-6)][U(η^2-S_2)(NR_2)$_3$] (6.1)

Method A. To an orange, cold (-25 °C), stirring solution of [K(18-crown-6)][U(S)(NR_2)$_3$] (**2.1**) (50.0 mg, 0.047 mmol) in a 2:1 mixture of Et_2O:tetrahydrofuran (3 mL) was added S_8 (1.6 mg 0.0062 mmol). The color of the solution became dark red-orange upon addition. The solution was allowed to stir for 15 min, whereupon the solvent was removed in vacuo to provide a red-orange solid. The solid was then extracted with Et_2O (4 mL), and the mixture was filtered through a Celite column supported on glass wool (0.5 cm × 3 cm) to provide a dark orange-red solution. The volume of the filtrate was reduced to 1 mL in vacuo. Storage of this solution at -25 °C for 24 h resulted in the deposition of red-orange crystals, which were isolated by decanting off the supernatant (15.3 mg, 30%). The volume of the supernatant was then reduced in vacuo to 0.5 mL, and the solution was transferred to a 4 mL scintillation vial that was placed inside a 20 mL scintillation vial. Toluene (4 mL) was then added to the outer vial. Storage of this two vial system for 48 h resulted in the deposition of more red-orange crystalline solid, which was isolated by decanting off the supernatant. Total yield: 30.5 mg, 59%. Anal. Calcd for $C_{30}H_{78}KN_3O_6S_2Si_6U$: C, 33.16; H, 7.23; N, 3.87. Found: C, 33.48; H, 7.12; N, 3.71. ^{1}H NMR (400 MHz, 25 °C, pyridine-d_5): δ -8.18 (br s, 54H, NSiCH_3), 3.53 (br s, 24H, 18-crown-6). IR (KBr Pellet, cm^{-1}): 489 (w), 528 (w), 608 (m), 663 (m), 772 (m), 842 (s), 932 (s), 964 (m), 1110 (s), 1182 (m), 1250 (s), 1285 (w), 1352 (m), 1454 (w), 1473 (w). UV-Vis/NIR (C_4H_8O, 3.65 mM, 25 °C, L·mol^{-1}·cm^{-1}): 1024 (ε = 51), 1080 (ε = 51), 1318 (ε = 22), 1450 (ε = 10), 1594 (ε = 9), 1804 (ε = 5), 2058 (ε = 34).

Method B. To an orange, cold (-25 °C), stirring solution of **6.2** (91.1 mg, 0.081 mmol) in Et_2O (3 mL) was added a cold (-25 °C) solution of Et_3P (12 μL, 0.081 mmol) in Et_2O (2 mL). The color of the solution became red-orange upon addition. After 1 h, the solution was

filtered through a Celite column supported on glass wool (0.5 cm × 3 cm) to provide a dark red-orange solution. Concentration of this solution in vacuo to 3 mL followed by storage at -25 °C for 24 h resulted in the deposition of colorless crystals, subsequently identified as $Et_3P{=}S$ by $^{31}P\{^1H\}$ NMR spectroscopy.[51] These were isolated by decanting off the supernatant. The volume of the supernatant was reduced in vacuo to 2 mL and then the solution was transferred to a 4 mL scintillation vial that was placed inside a 20 mL scintillation vial. Toluene (6 mL) was then added to the outer vial. Storage of this two vial system for 48 h resulted in the deposition of a red-orange crystalline solid, which was isolated by decanting the supernatant (52.2 mg, 59%). This material was subsequently identified as **6.1** by comparison of its ^1H NMR spectrum to that of independently prepared material. ^1H NMR (400 MHz, 25 °C, pyridine-d_5): δ -7.95 (br s, 54H, NSiCH_3), 3.52 (br s, 24H, 18-crown-6).

Method C. To a purple, cold (-25 °C), stirring solution of $[U(NR_2)_3]$ (129.4 mg, 0.18 mmol) in Et_2O (2 mL) was added a cold solution of **6.4** (66.9.0 mg, 0.09 mmol) in pyridine (2 mL). The color of the solution became dark red-orange upon addition. After 10 min the solvent was removed in vacuo and the resulting solids were triturated with pentane (3 × 3 mL) and Et_2O (3 × 3 mL). The red-orange powder was then extracted with Et_2O (5 mL) and filtered through a Celite column supported on glass wool (0.5 cm × 3 cm) to provide a dark red-orange solution. The filtrate was then concentrated in vacuo to 2 mL and layered with pentane (3 mL). Storage of this solution at -25 °C for 24 h resulted in the deposition of red-orange crystals, which were isolated by decanting off the supernatant (52.2 mg, 27%). Subsequent concentration of the mother liquor and storage at -25 °C for 24 h resulted in the deposition of additional crystals. Total yield: 82.9 mg, 42%. ^1H NMR (600 MHz, 25 °C, pyridine-d_5): δ -8.20 (br s, 54H, NSiCH_3), 3.52 (br s, 24H, 18-crown-6).

6.4.3 Synthesis of [K(18-crown-6)][U(η^3-S_3)(NR_2)$_3$] (6.2)

Method A. To a red-orange, cold (-25 °C), stirring solution of **6.1** (98.7 mg, 0.091 mmol) in tetrahydrofuran (3 mL) was added S_8 (3.6 mg, 0.014 mmol). This mixture was allowed to stir for 3 h, whereupon the solvent was removed in vacuo to provide a dark orange solid, which was triturated with Et_2O (4 mL). The resulting dark orange powder was extracted with Et_2O (4 mL) and filtered through a Celite column supported on glass wool (0.5 cm × 3 cm) to provide a dark orange solution. The volume of the filtrate was reduced in vacuo to 1 mL. The filtrate was then transferred to a 4 mL scintillation vial that was placed inside a 20 mL scintillation vial. Toluene (6 mL) was then added to the outer vial. Storage of this two vial system for 72 h resulted in the deposition of orange crystals, which were isolated by decanting off the supernatant (34.3 mg, 34%). Anal. Calcd for $C_{30}H_{78}KN_3O_6S_3Si_6U$: C, 32.21; H, 7.03; N, 3.76. Found: C, 32.79; H, 7.02; N, 3.79. ^{1}H NMR (400 MHz, 25 °C, pyridine-d_5): δ -7.20 (br s, 54H, NSiCH_3, FWHM = 2700 Hz), 3.65 (br s, 24H, 18-crown-6). IR (KBr Pellet, cm^{-1}): 497 (w), 608 (m), 665 (m), 773 (m), 844 (s), 891 (s), 917 (s), 964 (m), 1055 (w), 1112 (s), 1182 (w), 1249 (s), 1284 (w), 1352 (m), 1454 (w), 1473 (w). UV-Vis/NIR (C_4H_8O, 4.60 mM, 25 °C, L·mol^{-1}·cm^{-1}): 626 (ε = 74), 968 (ε = 36), 1044 (ε = 43), 1110 (ε = 40), 1262 (ε = 27), 1472 (ε = 25), 1586 (ε = 30), 1802 (ε = 29), 1938 (ε = 45).

Method B. To a cold (-25 °C), stirring mixture of [U(I)(NR_2)$_3$] (124.9 mg, 0.15 mmol) in tetrahydrofuran (3 mL) was added a cold solution of **6.4** (94.0 mg, 0.13 mmol) in pyridine (4 mL). The color of the solution became dark orange upon addition. The solution was allowed to stir for 30 min, whereupon the solvent was then removed in vacuo to provide a dark orange solid, which was then triturated with hexanes (5 mL), Et_2O (5 mL), hexanes (3 mL), and Et_2O (3 mL). The resulting dark orange powder was then extracted with Et_2O (10

mL), and the mixture was filtered through a Celite column supported on glass wool (0.5 cm × 3 cm) to provide a dark orange solution. The volume of the filtrate was reduced to 3 mL in vacuo. Storage of this solution at -25 °C for 24 h resulted in the deposition of orange crystals, which were isolated by decanting the supernatant (105.7 mg, 64%). The supernatant was further concentrated to 1 mL in vacuo and storage of this solution at -25 °C for 24 h resulted in the deposition of more orange crystals. Total yield: 111.2 mg, 67%. ^{1}H NMR (400 MHz, 25 °C, pyridine-d_5): δ -7.05 (br s, 54H, NSiCH_3, FWHM = 2150 Hz), 3.56 (br s, 24H, 18-crown-6).

6.4.4 Synthesis of [K(18-crown-6)][U(η^2-SSe)(NR$_2$)$_3$] (6.3)

To an orange, cold (-25 °C), stirring solution of [K(18-crown-6)][U(S)(NR$_2$)$_3$] (**2.1**) (124.5 mg, 0.12 mmol), in a 2:1 mixture of Et$_2$O:tetrahydrofuran (4 mL), was added Se powder (12.9 mg, 0.16 mmol). This mixture was allowed to stir for 2 h, whereupon the color darkened to orange-red. The solvent was removed in vacuo and triturated with pentane (4 mL), which afforded a dark orange-red powder. This powder was then extracted with Et$_2$O (4 mL) and filtered through a Celite column supported on glass wool (0.5 cm × 3 cm) to provide a dark orange-red solution. The volume of the filtrate was reduced to 2 mL in vacuo. The filtrate was then transferred to a 4 mL scintillation vial that was placed inside a 20 mL scintillation vial. Toluene (6 mL) was then added to the outer vial. Storage of this two vial system for 72 h resulted in the deposition of dark orange-red crystals, which were isolated by decanting the supernatant (70.0 mg, 52%). Anal. Calcd for $C_{30}H_{78}KN_3O_6SSeSi_6U$: C, 31.79; H, 6.94; N, 3.71. Found: C, 32.20; H, 7.01; N, 3.62. ^{1}H NMR (400 MHz, 25 °C, pyridine-d_5): δ -7.73 (br s, 54H, NSiCH_3), 3.46 (br s, 24H, 18-crown-6). IR (KBr Pellet, cm^{-1}): 608 (w), 662 (w), 685 (w), 772 (w), 843 (s), 885 (w), 931 (m), 963(w), 1109 (s), 1182 (w), 1250 (m), 1285 (w), 1352

(m), 1454 (w), 1473 (w). UV-Vis/NIR (C_4H_8O, 4.14 mM, 25 °C, $L \cdot mol^{-1} \cdot cm^{-1}$): 1026 (ε = 32), 1082 (ε = 34), 1328 (ε = 18), 1456 (ε = 12), 1506 (ε = 13), 1618 (ε = 11), 1808 (ε = 13).

6.4.5 Synthesis of [K(18-crown-6)$_2$][S_4] (6.4)

To a stirring mixture of S_8 (17.7 mg, 0.069 mmol) and 18-crown-6 (151.7 mg, 0.574 mmol), in tetrahydrofuran (4 mL), was added KC_8 (75.3 mg, 0.557 mmol). There was an immediate color change to red upon addition. After stirring for 5 min, the color of the mixture became a deep blue, concomitant with the deposition of a dark black precipitate. This mixture was allowed to stir overnight, whereupon it was filtered through a Celite column supported on glass wool (0.5 cm × 2 cm). This provided a black plug and a faint yellow filtrate. The filtrate was then discarded, while the black solid that remained on the Celite was rinsed with acetonitrile (5 mL) to provide a solution that appeared red to transmitted light and green to reflected light. The filtrate was then reduced in vacuo to 2 mL and layered with Et_2O (6 mL). Storage of this solution at -25 °C for 24 h resulted in the deposition of orange crystals (76.1 mg, 75%). Anal. Calcd for $C_{24}H_{48}K_2O_{12}S_4$: C, 39.22; H, 6.58. Found: C, 38.60; H, 6.60. ^{1}H NMR (600 MHz, 25 °C, CD_3CN): δ 3.60 (s, 18-crown-6). IR (KBr Pellet, cm^{-1}): 482 (m), 495 (w), 529 (w), 840 (m), 965 (s), 1108 (s), 1251 (m), 1285 (m), 1351 (s), 1435 (w), 1452 (w), 1472 (m). UV-Vis/NIR (CH_3CN, 0.353 mM, 25 °C, $L \cdot mol^{-1} \cdot cm^{-1}$): 270 (ε = 5809), 336 (sh) (ε = 1540), 438 (ε = 374), 612 (ε = 4192).

6.4.6 Reaction of [K(18-crown-6)][U(S)(NR_2)$_3$] (2.1) with Te

In a 20 mL scintillation vial, an orange solution of **2.1** (9.4 mg, 0.0089 mmol), in benzene-d_6 (0.75 mL), was added to Te powder (20.0 mg 0.16 mmol). This mixture was then transferred to an NMR tube fitted with a J-Young valve and the reaction was monitored by ^{1}H

NMR spectroscopy over the course of 60 h. No reaction was observed. ^{1}H NMR (400 MHz, 25 °C, benzene-d_6): δ -2.03 (br s, 54H, NSiCH_3, **2.1**), -1.06 (br s, 24H, 18-crown-6, **2.1**).

6.4.7 Reaction of [K(18-crown-6)][U(η^2-S$_2$)(NR$_2$)$_3$] (6.1) with PPh$_3$

To a solution of **6.1** (9.7 mg, 0.0089 mmol) in pyridine-d_5 (0.5 mL), in an NMR tube fitted with a J-Young valve, was added a solution of Ph_3P (3.3 mg, 0.013 mmol) in pyridine-d_5 (0.5 mL). The color of the solution immediately lightened upon addition. The reaction was monitored by ^{1}H and ^{31}P{^{1}H} NMR spectroscopies over the course of 72 h, which revealed the formation of **2.1** and Ph_3P=S.[51] The identity of **2.1** was confirmed by comparison of the ^{1}H spectrum with that of authentic material.[18] ^{1}H NMR (400 MHz, 25 °C, pyridine-d_5): δ -2.21 (br s, **2.1** 54H, NSiCH_3), 3.30 (br s, 24H, **2.1** 18-crown-6), 7.35-7.38 (m, 9H, Ph_3P overlapping resonances from *m*-C*H* and *p*-C*H*), 7.40-7.50 (m, 15H, overlapping resonances from *o*-C*H* of Ph_3P and *m*-CH and *p*-C*H* of Ph_3P=S), 7.92-7.99 (m, 6H, Ph_3P=S, *o*-C*H*). ^{31}P{^{1}H} NMR (161.92 MHz, 25 °C, pyridine-d_5): δ -5.40 (s, Ph_3P), 42.85 (s, Ph_3P=S).

6.4.8 Reaction of [K(18-crown-6)][U(η^2-SSe)(NR$_2$)$_3$] (6.3) with PEt$_3$

To a solution of **6.3** (21.9 mg, 0.019 mmol) in pyridine-d_5 (0.75 mL), in an NMR tube fitted with a J-Young valve, was added Et_3P (3 μL, 0.020 mmol). The color of the solution immediately lightened upon addition. After 5 min, ^{1}H and ^{31}P{^{1}H} spectra were recorded. These revealed the formation of **2.1** and Et_3P=Se.[52] The identity of **2.1** was confirmed by comparison of the ^{1}H NMR spectrum with of authentic material.[18] ^{1}H NMR (400 MHz, 25 °C, pyridine-d_5): δ -2.23 (br s, **2.1** 54H, N(Si(CH_3)$_3$)$_2$), 1.11 (dt, 9H, CH_3, $J_{P\text{-}H}$ = 18.8 Hz, $J_{H\text{-}H}$ = 8 Hz), 1.84 (dq, 6H, CH_2, $J_{P\text{-}H}$ = 11.6 Hz, $J_{H\text{-}H}$ = 7.6 Hz), 3.11 (s br, **2.1** 24H, 18-crown-

6). $^{31}P\{^{1}H\}$ NMR (161.92 MHz, 25 °C, pyridine-d_5): δ 46.77 (s with Se satellites, $Et_3P{=}Se$, $J_{P\text{-}Se}$ = 348 Hz).

6.4.9 Reaction of [K(18-crown-6)][U(S)(NR$_2$)$_3$] (2.1) with S$_8$ and cyclohexene

To a solution of **2.1** (19.0 mg, 0.018 mmol) in pyridine-d_5 (0.75 mL), in an NMR tube fitted with a J-Young valve, was added cyclohexene (20 μL, 0.20 mmol) and S_8 (7.1 mg, 0.027 mmol). This reaction was monitored by ^{1}H NMR spectroscopy over the course of 36 h, which revealed that no reaction with the cyclohexene had taken place in addition to decomposition of the starting material. ^{1}H NMR (400 MHz, 25 °C, pyridine-d_5): δ -8.20 (br s, **6.1**, 54H, $N(Si(CH_3)_3)_2$), -7.05 (br s, **6.2**, 54H, $N(Si(CH_3)_3)_2$), -2.21 (br s, **2.1**, 54H, $N(Si(CH_3)_3)_2$), 1.51 (s, cyclohexene, 4H, CH_2), 1.92 (s, cyclohexene, 4H, CH_2), 3.60 (br s, 18-crown-6), 5.68 (s, cyclohexene, 2H, C*H*).

6.4.10 Reaction of [K(18-crown-6)][U(S)(NR$_2$)$_3$] (2.1) with S$_8$ and norbornene

To a solution of **2.1** (22.2 mg, 0.021 mmol) in pyridine-d_5 (0.75 mL), in an NMR tube fitted with a J-Young valve, was added norbornene (16.4 mg, 0.17 mmol) and S_8 (5.4 mg, 0.021 mmol). This reaction was monitored by ^{1}H NMR spectroscopy over the course of 2 h, which revealed that no reaction had taken place. ^{1}H NMR (400 MHz, 25 °C, pyridine-d_5): δ -8.20 (br s, **6.1**, 54H, $N(Si(CH_3)_3)_2$), -7.02 (br s, **6.2**, 54H, $N(Si(CH_3)_3)_2$), -2.22 (br s, **2.1**, 54H, $N(Si(CH_3)_3)_2$), 0.89 (m, norbornene, 2H, C*H*), 0.98 (d, norbornene, 1H, C*H*), 1.29 (m, norbornene, 1H, C*H*), 1.51 (d, norbornene, 2H, C*H*), 2.75 (s, norbornene, 2H, C*H*), 5.98 (s, norbornene, 2H, C*H*).

6.4.11 X-ray Crystallography

Data for **6.1**, **6.2**, **6.3**, and **6.4** were collected on a Bruker KAPPA APEX II diffractometer equipped with an APEX II CCD detector using a TRIUMPH monochromator with a Mo Kα X-ray source (α = 0.71073 Å). The crystals were mounted on a cryoloop under Paratone-N oil, and all data were collected at 100(2) K using an Oxford nitrogen gas cryostream. Data were collected using ω scans with 0.5° frame widths. Frame exposures of 2 s (low angle), 10 s (medium angle), and 15 s (high angle) were used for **6.1**. Frame exposures of 2 s (low angle) and 5 s (high angle) were used for **6.2**. Frame exposures of 10 s (low angle) and 15 s (high angle) were used for **6.3** and **6.4**. Data collection and cell parameter determinations were conducted using the SMART program.[53] Integration of the data frames and final cell parameter refinements were performed using SAINT software.[54] Absorption corrections of the data were carried out using the multi-scan method SADABS.[55] Subsequent calculations were carried out using SHELXTL.[56] Structure determination was done using direct or Patterson methods and difference Fourier techniques. All hydrogen atom positions were idealized, and rode on the atom of attachment. Structure solution, refinement, graphics, and creation of publication materials were performed using SHELXTL.[56]

Three of the sulfur atoms (S1, S2, and S3) in complex **6.4** exhibited positional disorder and were modeled over two positions in an 80:20 ratio. The anisotropic displacement parameters of these disordered atoms were constrained with the EADP command, and the bond distances between pairs of atoms, e.g. S1-S2 and S1b-S2b, were constrained with the SADI command.

Table 6.2. X-ray Crystallographic Data for Complexes **6.1** and **6.2**

	6.1	**6.2**
empirical formula	$C_{30}H_{78}KN_3O_6S_2Si_6U$	$C_{34}H_{88}KN_3O_7S_3Si_6U$
crystal habit, color	block, red-orange	block, orange
crystal size (mm)	0.1 × 0.1 × 0.1	0.2 × 0.1 × 0.1
space group	$P2_1/n$	$P\bar{1}$
volume (Å^3)	5031.6(3)	2777.9(6)
a (Å)	12.9305(4)	11.255(1)
b (Å)	17.8735(5)	12.934(2)
c (Å)	22.5628(7)	20.934(3)
α (deg)	90	98.456(2)
β (deg)	105.223(2)	96.945(2)
γ (deg)	90	110.308(2)
Z	4	2
formula weight (g/mol)	1086.74	1192.92
density (calculated) (Mg/m^3)	1.435	1.426
absorption coefficient (mm^{-1})	3.571	3.279
F_{000}	2216	1224
total no. reflections	32568	31228
unique reflections	11110	12268
R_{int}	0.0418	0.0726
final R indices (I >2σ(I)]	R_1 = 0.0814 wR_2 = 0.2165	R_1 = 0.0345 wR_2 = 0.0853
largest diff. peak and hole (e$^-$ A^{-3})	8.120 and -3.889	3.638 and -2.427
GOF	1.053	1.040

Table 6.3. X-ray Crystallographic Data for Complexes **6.3** and **6.4**

	6.3	**6.4**
empirical formula	$C_{34}H_{78}KN_3O_6SSeSi_6U$	$C_{24}H_{48}K_2O_{12}S_4$
crystal habit, color	block, orange-red	block, orange-yellow
crystal size (mm)	0.2 × 0.1 × 0.1	0.1 × 0.1 × 0.1
space group	$P2_1$	$P2_1/n$
volume (Å^3)	5073.7(6)	3478.9(2)
a (Å)	13.1630(9)	11.9285(5)
b (Å)	17.804(1)	18.5061(6)
c (Å)	22.488(1)	16.5489(6)
α (deg)	90	90
β (deg)	105.691(4)	107.769(2)
γ (deg)	90	90
Z	2	4
formula weight (g/mol)	1133.65	735.06
density (calculated) (Mg/m^3)	1.484	1.403
absorption coefficient (mm^{-1})	4.218	0.566
F_{000}	2288	1560
total no. reflections	31505	19483
unique reflections	22136	7107
R_{int}	0.0514	0.0514
final R indices (I >2σ(I)]	R_1 = 0.0537 wR_2 = 0.1450	R_1 = 0.0792 wR_2 = 0.2091
largest diff. peak and hole (e$^-$ A^{-3})	6.095 and -2.458	3.392 and -3.781
GOF	0.851	1.124

6.5 Appendix

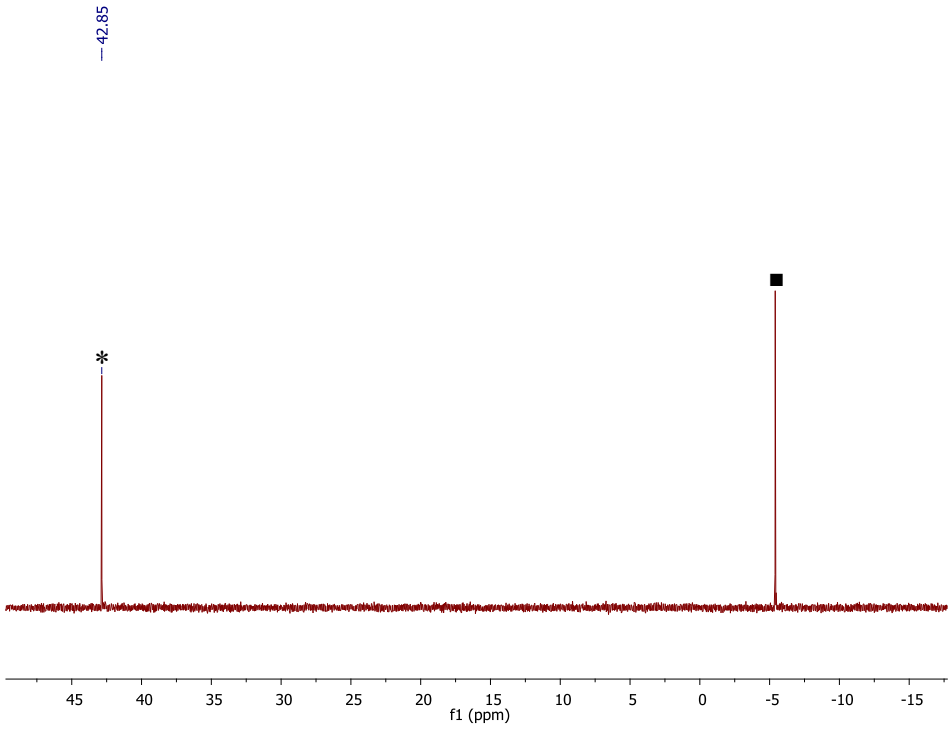

Figure A6.1. In situ $^{31}P\{^{1}H\}$ NMR spectrum of the reaction of [K(18-crown-6)][U(η^2-S_2)$(NR_2)_3$] (**6.1**) with Ph_3P in pyridine-d_5. (*) indicates the presence of Ph_3P=S, and (■) indicates the presence of unreacted Ph_3P.

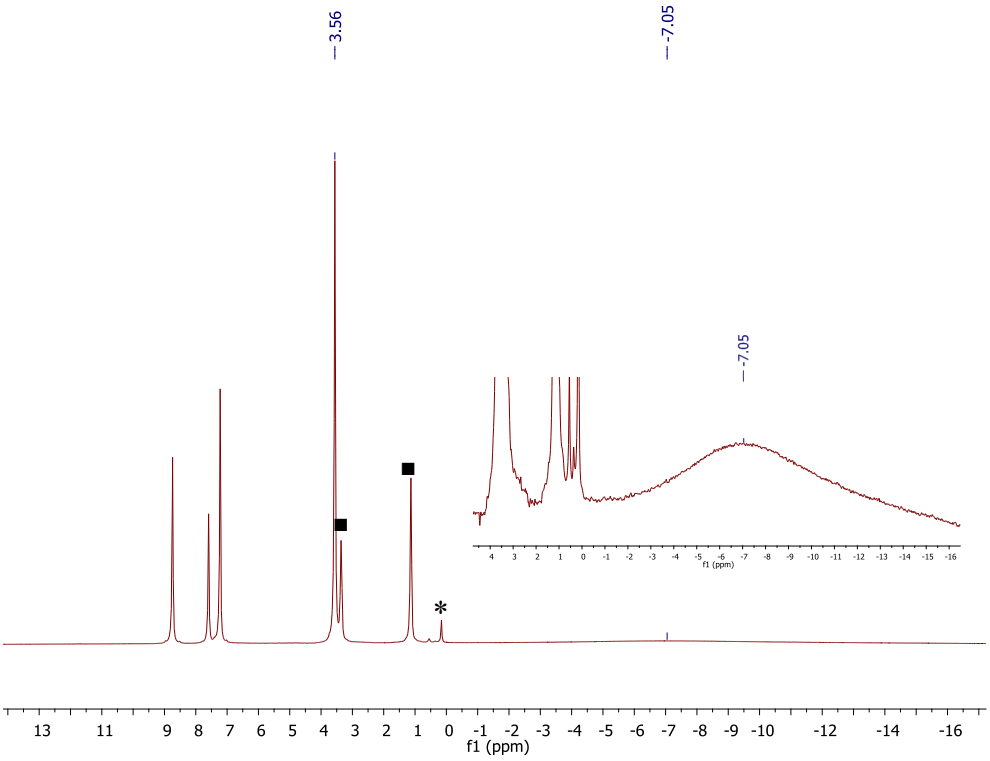

Figure A6.2. ^{1}H NMR spectrum of [K(18-crown-6][U(η^3-S_3)(NR_2)$_3$] (**6.2**) in pyridine-d_5. (*) indicates the presence of $HN(SiMe_3)_2$, and (■) indicates the presence of diethyl ether. Inset: portion of the spectrum showing the broad resonance at -7.05 ppm, assignable to the methyl groups of the silylamide ligands of **6.2**.

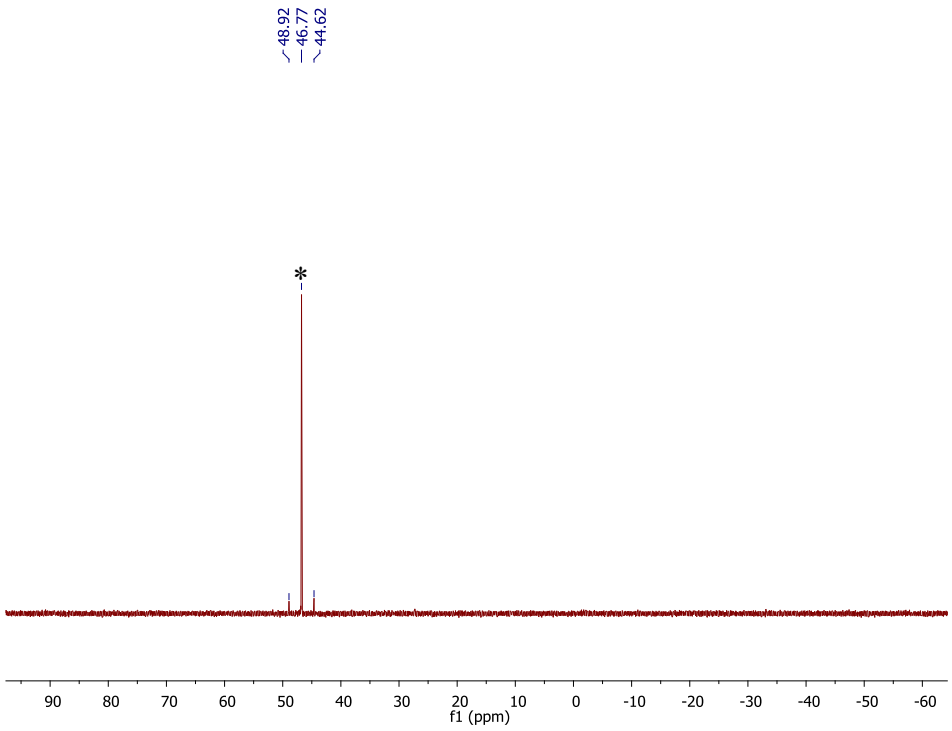

Figure A6.3. In Situ $^{31}P\{^{1}H\}$ NMR spectrum of the reaction of [K(18-crown-6)][U(η^2-SSe)$(NR_2)_3$] (**6.3**) with Et_3P in pyridine-d_5 (*) indicates the presence of Et_3P=Se.

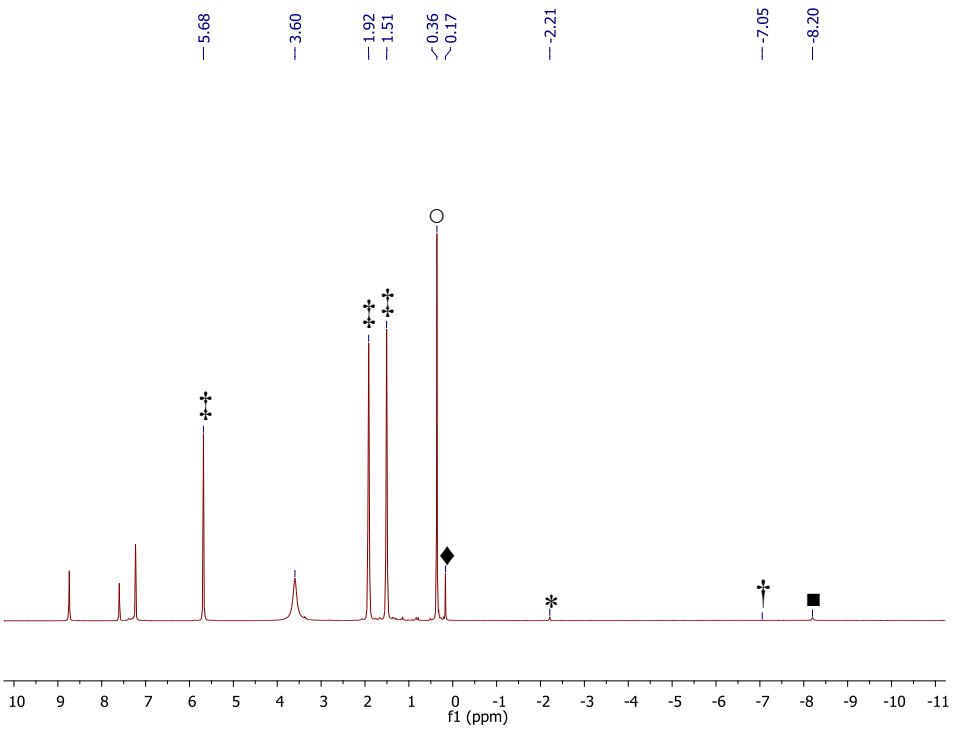

Figure A6.4. In situ ^{1}H NMR spectrum of the reaction of [K(18-crown-6)][U(S)(NR$_2$)$_3$] (**2.1**) with excess S_8 and excess cyclohexene, in pyridine-d_5, after 36 h. (*) indicates the presence of complex **2.1**, (■) indicates the presence of complex **6.1**, (†) indicates the presence of complex **6.2**, (‡) indicates the presence of cyclohexene, (♦) indicates the presence of HN(SiMe$_3$)$_2$, and (○) indicates the presence of an unidentified decomposition product that results from thermal decomposition over the course of the reaction

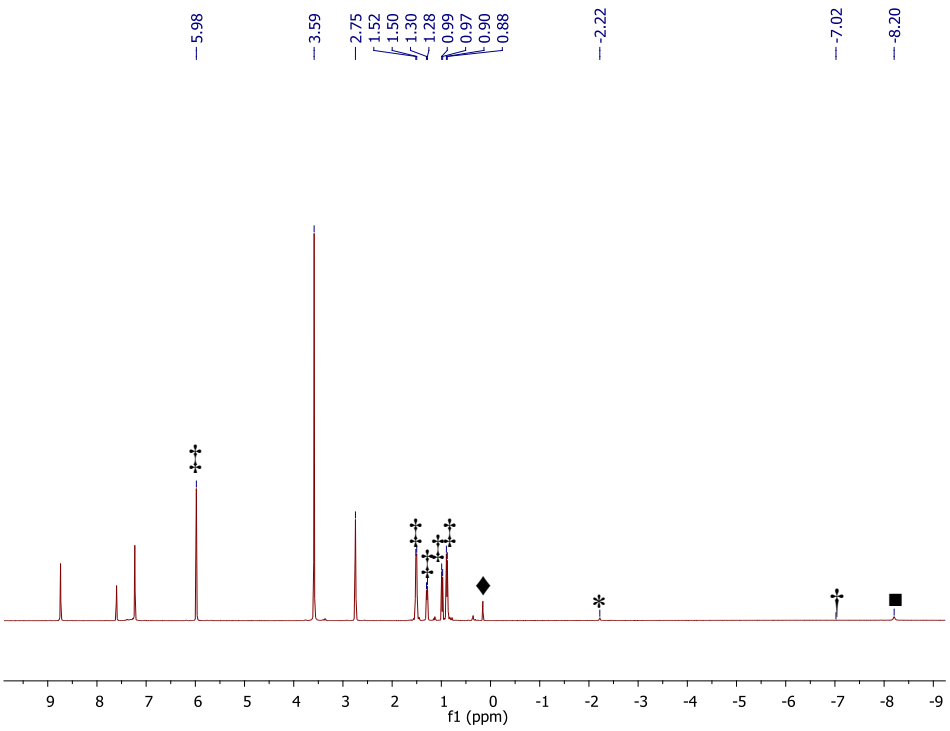

Figure A6.5. In situ ^{1}H NMR spectrum of the reaction of [K(18-crown-6)][U(S)(NR$_2$)$_3$] (**2.1**) with excess S_8 and excess norbornene, in pyridine-d_5, after 2 h. (*) indicates the presence of complex **2.1**, (■) indicates the presence of complex **6.1**, (†) indicates the presence of complex **6.2**, (‡) indicates the presence of norbornene, and (♦) indicates the presence of HN(SiMe$_3$)$_2$.

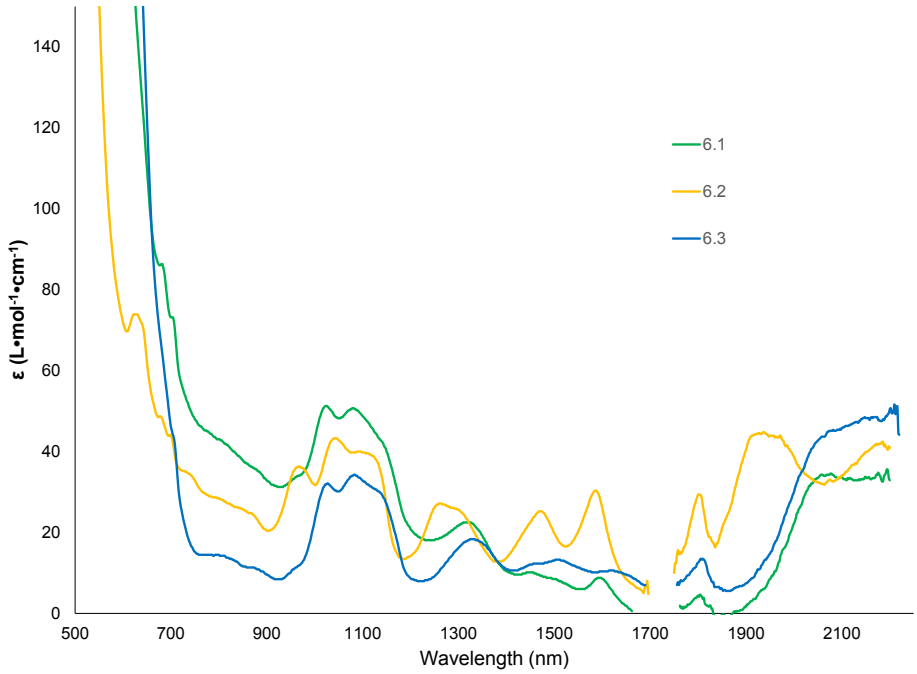

Figure A6.6. NIR Spectra of Complexes **6.1**, **6.2**, and **6.3**. Concentration (mM) in C_4H_8O: **6.1**, 3.65; **6.2**, 4.60; **6.3**, 4.14.

6.6 References

(1) Chauhan, P.; Mahajan, S.; Enders, D. *Chem. Rev.* **2014**, *114*, 8807.
(2) Clayden, J.; MacLellan, P. *Beilstein J. Org. Chem.* **2011**, *7*, 582.
(3) Sander, M. *Chem. Rev.* **1966**, *66*, 297.
(4) Adam, W.; Bargon, R. M. *Chem. Rev.* **2004**, *104*, 251.
(5) Donahue, J. P. *Chem. Rev.* **2006**, *106*, 4747.
(6) Saito, M.; Nakayama, J. *Sci. Synth.* **2008**, *39*, 589.
(7) Proulx, G.; Bergman, R. G. *Organometallics* **1996**, *15*, 133.
(8) Poulain, S.; Julien, S.; Duñach, E. *Tetrahedron Lett.* **2005**, *46*, 7077.
(9) Adam, W.; Bargon, R. M.; Bosio, S. G.; Schenk, W. A.; Stalke, D. *J. Org. Chem.* **2002**, *67*, 7037.
(10) Adam, W.; Bargon, R. M. *Chem. Commun.* **2001**, 1910.
(11) Adam, W.; Bargon, R. M.; Schenk, W. A. *J. Am. Chem. Soc.* **2003**, *125*, 3871.
(12) Arisawa, M.; Ashikawa, M.; Suwa, A.; Yamaguchi, M. *Tetrahedron Lett.* **2005**, *46*, 1727.
(13) Sweeney, Z. K.; Polse, J. L.; Andersen, R. A.; Bergman, R. G.; Kubinec, M. G. *J. Am. Chem. Soc.* **1997**, *119*, 4543.
(14) Sweeney, Z. K.; Polse, J. L.; Bergman, R. G.; Andersen, R. A. *Organometallics* **1999**, *18*, 5502.
(15) Camp, C.; Antunes, M. A.; Garcia, G.; Ciofini, I.; Santos, I. C.; Pecaut, J.; Almeida, M.; Marcalo, J.; Mazzanti, M. *Chem. Sci.* **2014**, *5*, 841.
(16) Franke, S. M.; Heinemann, F. W.; Meyer, K. *Chem. Sci.* **2014**, *5*, 942.
(17) Lam, O. P.; Heinemann, F. W.; Meyer, K. *Chem. Sci.* **2011**, *2*, 1538.
(18) Smiles, D. E.; Wu, G.; Hayton, T. W. *J. Am. Chem. Soc.* **2014**, *136*, 96.
(19) Fortier, S.; Brown, J. L.; Kaltsoyannis, N.; Wu, G.; Hayton, T. W. *Inorg. Chem.* **2012**, *51*, 1625.
(20) Smiles, D. E.; Wu, G.; Hayton, T. W. *Inorg. Chem.* **2014**, *53*, 10240.
(21) Brown, J. L.; Fortier, S.; Lewis, R. A.; Wu, G.; Hayton, T. W. *J. Am. Chem. Soc.* **2012**, *134*, 15468.
(22) Brown, J. L.; Wu, G.; Hayton, T. W. *Organometallics* **2013**, *32*, 1193.
(23) *Cambridge Structural Database*, version 1.18. 2015
(24) Matson, E. M.; Goshert, M. D.; Kiernicki, J. J.; Newell, B. S.; Fanwick, P. E.; Shores, M. P.; Walensky, J. R.; Bart, S. C. *Chem. Eur. J.* **2013**, *19*, 16176.
(25) Grant, D. J.; Weng, Z.; Jouffret, L. J.; Burns, P. C.; Gagliardi, L. *Inorg. Chem.* **2012**, *51*, 7801.
(26) Kwak, J.-e.; Gray, D. L.; Yun, H.; Ibers, J. A. *Acta Crystallogr. Sect. E* **2006**, *62*, i86.
(27) Sutorik, A. C.; Kanatzidis, M. G. *Polyhedron* **1997**, *16*, 3921.
(28) Shannon, R. D. *Acta Crystallogr. Sect. A* **1976**, *A32*, 751.
(29) Shaver, A.; McCall, J. M.; Bird, P. H.; Siriwardane, U. *Acta Crystallogr. Sect. C* **1991**, *47*, 659.
(30) Shaver, A.; McCall, J. M. *Organometallics* **1984**, *3*, 1823.
(31) Shaver, A.; Lopez, O.; N. Harpp, D. *Inorg. Chim. Acta* **1986**, *119*, 13.
(32) Hobert, S. E.; Noll, B. C.; Rakowski DuBois, M. *Organometallics* **2001**, *20*, 1370.
(33) Howard, W. A.; Parkin, G.; Rheingold, A. L. *Polyhedron* **1995**, *14*, 25.

(34) Maruyama, M.; Guo, J.-D.; Nagase, S.; Nakamura, E.; Matsuo, Y. *J. Am. Chem. Soc.* **2011**, *133*, 6890.
(35) Herberhold, M.; Jin, G.-X.; Milius, W. *Angew. Chem. Int. Ed.* **1993**, *32*, 85.
(36) Capps, K. B.; Wixmerten, B.; Bauer, A.; Hoff, C. D. *Inorg. Chem.* **1998**, *37*, 2861.
(37) Gushchin, A. L.; Llusar, R.; Vicent, C.; Abramov, P. A.; Gómez-Garcia, C. J. *Eur. J. Inorg. Chem.* **2013**, *2013*, 2615.
(38) Fedin, V. P.; Mironov, Y. V.; Sokolov, M. N.; Kolesov, B. A.; Federov, V. Y.; Yufit, D. S.; Struchkov, Y. T. *Inorg. Chim. Acta* **1990**, *174*, 275.
(39) Fedin, V. P.; Sokolov, M. N.; Fedorov, V. Y.; Yufit, D. S.; Struchkov, Y. T. *Inorg. Chim. Acta* **1991**, *179*, 35.
(40) Mathur, P.; Sekar, P.; L. Rheingold, A.; M. Liable-Sands, L. *J. Chem. Soc. Dalton Trans.* **1997**, 2949.
(41) Hernandez-Molina, R.; Sokolov, M.; Nunez, P.; Mederos, A. *J. Chem. Soc. Dalton Trans.* **2002**, 1072.
(42) Alberola, A.; Llusar, R.; Triguero, S.; Vicent, C.; Sokolov, M. N.; Gomez-Garcia, C. *J. Mater. Chem.* **2007**, *17*, 3440.
(43) Hu, J.; Zhuang, H.-H.; Liu, S.-X.; Huang, J.-L. *Trans. Met. Chem.* **1998**, *23*, 547.
(44) Fedin, V. P.; Sokolov, M. N.; Virovets, A. V.; Podberezskaya, N. V.; Fedorov, V. Y. *Polyhedron* **1992**, *11*, 2395.
(45) Bratsch, S. G. *J. Phys. Chem. Ref. Data* **1989**, *18*, 1.
(46) Meier, M.; Korber, N. *Z. Anorg. Allg. Chem.* **2009**, *635*, 764.
(47) Tatsumi, K.; Kawaguchi, H.; Inoue, K.; Tani, K.; Cramer, R. E. *Inorg. Chem.* **1993**, *32*, 4317.
(48) Avens, L. R.; Bott, S. G.; Clark, D. L.; Sattelberger, A. P.; Watkin, J. G.; Zwick, B. D. *Inorg. Chem.* **1994**, *33*, 2248.
(49) Harris, R. K.; Becker, E. D.; Cabral De Menezes, S. M.; Goodfellow, R.; Granger, P. *Pure Appl. Chem.* **2001**, *73*, 1795.
(50) Harris, R. K.; Becker, E. D.; Cabral De Menezes, S. M.; Granger, P.; Hoffman, R. E.; Zilm, K. W. *Pure Appl. Chem.* **2008**, *80*, 59.
(51) Baccolini, G.; Boga, C.; Mazzacurati, M. *J. Org. Chem.* **2005**, *70*, 4774.
(52) Kuhn, N.; Henkel, G.; Schumann, H.; Frohlich, R. *Z. Naturforsch. B* **1990**, *45*, 1010.
(53) *SMART Apex II*, Version 2.1. 2005
(54) *SAINT Software User's Guide*, Version 7.34a. 2005
(55) *SADABS*, 2005
(56) *SHELXTL PC*, Version 6.12. 2005

Chapter 7 Reactivity of a Uranium Metallacycle with Chalcogens

Portions of this work were published in:

Danil E. Smiles, Guang Wu, Trevor W. Hayton

New. J. Chem. **2015**, *39*, 7563-7566.

Table of Contents

7.1 Introduction

Separating lanthanides and actinides is extremely important to the nuclear energy community.[1,2] Complexation agents with soft donor atoms, like the heavier chalcogenides (S, Se, Te), have shown great promise at affording these separations.[3-5] In addition, the efficacy of these species is believed to be a direct result of the differences between the bonding of the chalcogens with the actinides versus the lanthanides.[6-11] This has motivated the study of actinide chalcogenide bonding,[12-14] which in turn has led to significant advances in the synthesis of complexes with actinide chalcogenide bonds.[15-25] While the most commonly used chalcogen sources are the elemental chalcogens,[23-27] a wide variety of other chalcogen sources have been utilized in these syntheses. These include the polychalcogenides,[16,17,19] such as Li_2S_5, which Ryan and co-workers employed to synthesis the thorium pentasulfide complex, $[Cp^*_2Th(\kappa^2\text{-}S_5)]$, from $[Cp^*_2ThCl_2]$.[28] The phosphine chalcogenides, $R_3P{=}E$ (E = S, Se, Te) are another common chalcogen transfer reagent.[20,21,24,29] For example, Mazzanti and co-workers reported that $Ph_3P{=}S$ reacts with $[K(U(OSi(O^tBu)_3)_4)]$, in the presence of 18-crown-6, to give the U(IV) terminal sulfide, $[K_2(U(S)(OSi(O^tBu)_3)_4)]_2(\mu\text{-}(18\text{-crown-6}))$.[20] There have even been report of using the hydrogen chalcogenides, H_2E (E = S, Se, Te), to install these types of ligands.[22,30]

Despite the success that has been had, there remain problems controlling chalcogen atom transfer in these syntheses, and complicated reaction mixtures are regularly obtained. The use of elemental sulfur, S_8, has proven to be especially problematic. For example, Meyer and co-workers reported that reaction of S_8 or $Ph_3P{=}S$ with $[((^{Ad,Me}ArO)_3tacn)U]$ resulted in either no reaction or in the formation of an intractable mixture of products, whereas the reaction with H_2S cleanly afforded a U(IV) hydrosulfide complex, which could then be deprotonated to give

a new U(IV) terminal sulfide.[22] In addition, Mazzanti and co-workers reported that reaction of [K(U(OSi(O^{t}Bu)$_3$)$_4$)] with S_8, in contrast to the results seen when using $Ph_3P{=}S$, gave a mixture of [K$_2$(U(η^2-S$_2$)(OSi(O^{t}Bu)$_3$)$_4$)]$_2$ and [K(U(OSi(O^{t}Bu)$_3$)$_3$)]$_2$(μ-S$_2$)(μ-S$_3$), as well as several other unidentifiable products.[20] Similarly, Hayton and co-workers reported that reaction of [U(NR$_2$)$_3$] with S_8 yields a mixture of [U(NR$_2$)$_3$]$_2$(μ-S) and [U(NR$_2$)$_3$]$_2$(μ-η^2:η^2-S$_2$) in unpredictable ratios (Scheme 7.1).[24]

Scheme 7.1 Reaction of [U(NR$_2$)$_3$] with S_8

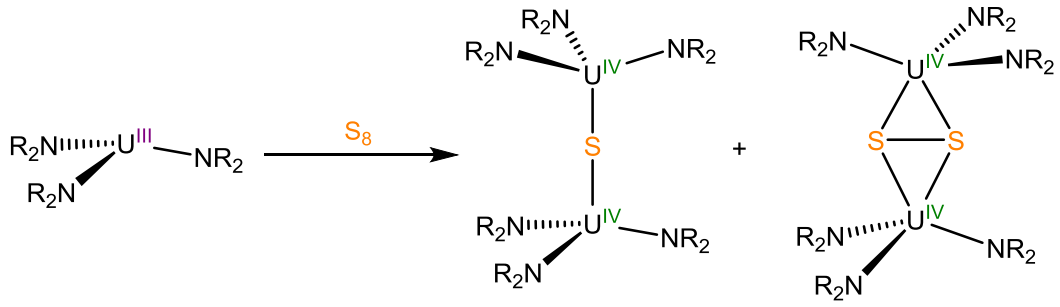

These reactions illustrate the need to improve understanding of chalcogen atom transfer, specifically in the synthesis of actinide chalcogenides. Meyer and co-workers demonstrated that reaction of [((Ad ArO)$_3$N)U(DME)] with S_8 gave either, [((Ad ArO)$_3$N)U(DME)]$_2$(μ-S) or [((Ad ArO)$_3$N)U]$_2$(μ-η^2:η^2-S$_2$)$_2$, depending upon the stoichiometry.[26,27] Interestingly, the monosulfide complex could be converted into the disulfide species via reaction with additional S_8. A similar stepwise mechanism was investigated for the formation of [U(NR$_2$)$_3$]$_2$(μ-η^2:η^2-S$_2$), however, reaction of [U(NR$_2$)$_3$]$_2$(μ-S) with various sulfur sources was reported to result in no change.[24] During the investigation of this reaction Hayton and co-workers noted that there existed a correlation between the formation of the U(IV) disulfide, [U(NR$_2$)$_3$]$_2$(μ-η^2:η^2-S$_2$), and the presence of the U(IV) metallacycle, [U(*C*H$_2$SiMe$_2$*N*SiMe$_3$)(NR$_2$)$_2$], an impurity in the [U(NR$_2$)$_3$] starting material. These observations, along with the reported reactivity of [U(*C*H$_2$SiMe$_2$*N*SiMe$_3$)(NR$_2$)$_2$], specifically insertion into the U-C bond,[31-37] suggest that a

sulfur containing metallacycle such as, [U(*S*$_2$CH$_2$SiMe$_2$*N*SiMe$_3$)(NR$_2$)$_2$], could be responsible for the formation of the observed disulfide via formal 'S_2' transfer. Elucidating the mechanism responsible for the formation of [U(NR$_2$)$_3$]$_2$(μ-η^2:η^2-S$_2$) may help explain the variable reactivity observed in reactions with the chalcogens, and could aid in designing better chalcogen atom transfer reagents for these systems.

This chapter describes the reaction of [U(*C*H$_2$SiMe$_2$*N*SiMe$_3$)(NR$_2$)$_2$] with chalcogen sources, and the isolation and characterization of a series of chalcogen containing U(IV) metallacycles. Furthermore, investigations into a rational route towards the synthesis of [U(NR$_2$)$_3$]$_2$(μ-η^2:η^2-S$_2$) are described. The chalcogen atom transfer capabilities of several different reagents, including KSCPh$_3$ and Ph$_3$CSSCPh$_3$, are investigated as means to access the aforementioned disulfide, as well as other actinide chalcogenides.

7.2 Results and Discussion

7.2.1 Synthesis and Characterization of [U(*S*CH$_2$SiMe$_2$*N*SiMe$_3$)(NR$_2$)$_2$] (7.1)

In order to test the mechanism for the formation of [U(NR$_2$)$_3$]$_2$(μ-η^2:η^2-S$_2$), the reactivity of the U(IV) metallacycle, [U(*C*H$_2$SiMe$_2$*N*SiMe$_3$)(NR$_2$)$_2$], with sulfur transfer reagents was investigated. Accordingly, addition of 0.125 equiv of S_8 to hexanes solution of [U(*C*H$_2$SiMe$_2$*N*SiMe$_3$)(NR$_2$)$_2$] results in the formation of a yellow-brown solution. Crystallization from hexanes affords the new U(IV) thiolate complex, [U(*S*CH$_2$SiMe$_2$*N*SiMe$_3$)(NR$_2$)$_2$] (**7.1**), as a yellow-brown crystalline solid in 62% yield (Scheme 7.2). The ^{1}H NMR spectrum of complex **7.1**, in benzene-d_6, is very similar to that of the parent metallacycle. It features four broad resonances at -11.44, -9.97, -4.22, and 3.38 ppm, in a 9:2:36:6 ratio, respectively, assignable to the one methylene environment and three independent methyl environments.

Scheme 7.2 Synthesis of [U(*S*CH$_2$SiMe$_2$*N*SiMe$_3$)(NR$_2$)$_2$] (**7.1**)

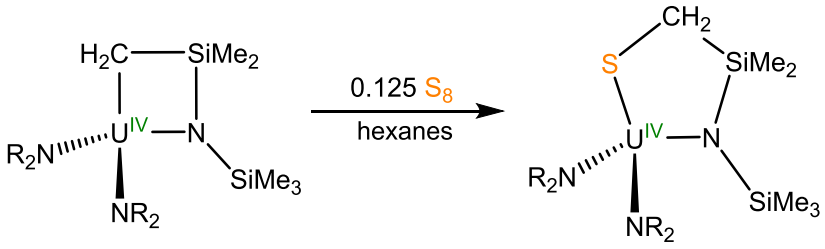

Complex **7.1** can also be synthesized using other sulfur sources, including ethylene sulfide. Monitoring the reaction of [U(*C*H$_2$SiMe$_2$*N*SiMe$_3$)(NR$_2$)$_2$] with 1 equiv of ethylene sulfide, in benzene-d_6, by ^{1}H NMR spectroscopy over the course of 24 h reveals both the consumption of [U(*C*H$_2$SiMe$_2$*N*SiMe$_3$)(NR$_2$)$_2$] and the formation of complex **7.1**. Additionally, a new resonance at 5.26 ppm is observed, and is consistent with the formation of ethylene (Figure 7.1). On a preparative scale, reaction of [U(*C*H$_2$SiMe$_2$*N*SiMe$_3$)(NR$_2$)$_2$] with 1 equiv of ethylene sulfide affords complex **7.1** as a yellow-brown powder in 93% yield after workup (Scheme 7.3). The NIR spectrum of complex **7.1** is consistent with the presence of a U(IV) metal center, and confirms that no metal based redox chemistry takes place upon chalcogen atom insertion (Figure A7.3).[16-18,23,24,38]

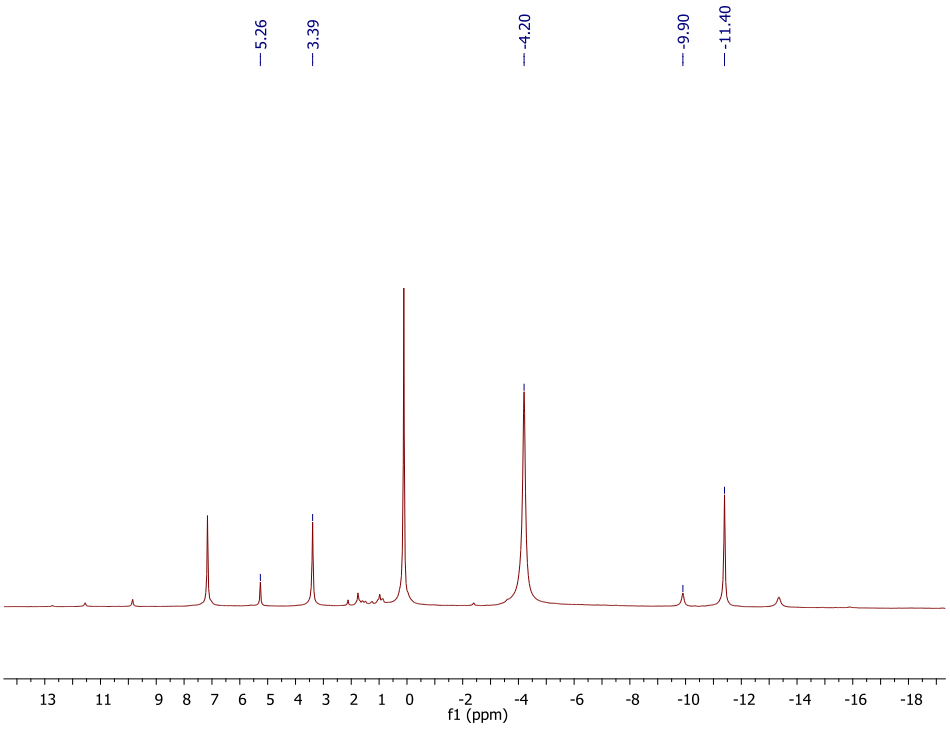

Figure 7.1. In situ ^{1}H NMR spectrum of the reaction of [U(*C*H$_2$SiMe$_2$*N*SiMe$_3$)(NR$_2$)$_2$] with ethylene sulfide, in benzene-d_6, after 24 h. (*) indicates the presence of HN(SiMe$_3$)$_2$, (■) indicates the presence of unreacted **2**, and (†) indicates the presence of ethylene.

Scheme 7.3 Reaction of [U(*C*H$_2$SiMe$_2$*N*SiMe$_3$)(NR$_2$)$_2$] with Ethylene Sulfide

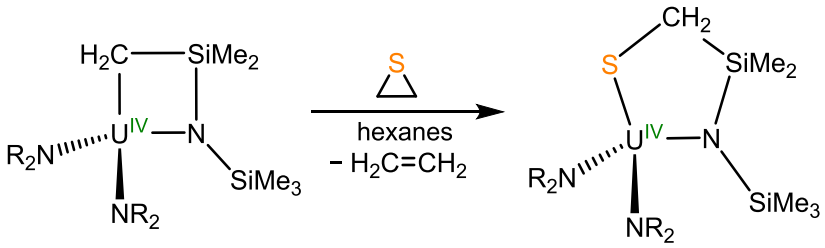

Crystals of complex **7.1** suitable for X-ray crystallographic analysis were grown from a concentrated hexanes solution. Complex **7.1** crystallizes in the trigonal spacegroup $P\bar{3}1c$. Due to in part to the high symmetry, the considerable positional disorder exhibited by complex **7.1** allows only for the confirmation of its connectivity.

7.2.2 Synthesis and Characterization of [U(*Se*CH_2SiMe_2*N*$SiMe_3$)$(NR_2)_2$] (7.2)

The U(IV) metallacycle, [U(*C*H_2SiMe_2*N*$SiMe_3$)$(NR_2)_2$], exhibits similar reactivity with elemental Se as it did with S. Thus, addition of 1 equiv of Se to a hexanes solution of [U(*C*H_2SiMe_2*N*$SiMe_3$)$(NR_2)_2$] also affords a yellow brown solution. Crystallization from hexanes affords the U(IV) selenate, [U(*Se*CH_2SiMe_2*N*$SiMe_3$)$(NR_2)_2$] (**7.2**), as yellow needles in 60% yield (Scheme 7.4). The ^{1}H NMR spectrum of **7.2**, in benzene-d_6, also features four broad resonances in a 9:2:36:6 ratio, at -12.24, -7.18, -3.69, and 4.67 ppm, respectively, corresponding to the three methyl and one methylene environments. The NIR spectrum of **7.2** is similar to that of **7.1** and is again consistent with the presence of a U(IV) metal center (Figure A7.3).[16-18,23,24,38] Like its sulfur analogue (**7.1**), complex **7.2** crystallizes in the trigonal spacegroup $P\bar{3}1c$, but due to severe positional disorder, only the connectivity of the complex could be determined.

Scheme 7.4 Synthesis of [U(*Se*CH_2SiMe_2*N*$SiMe_3$)$(NR_2)_2$] (**7.2**)

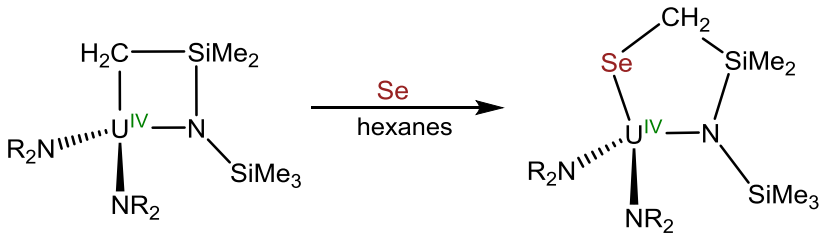

7.2.3 Synthesis and Characterization of [U(*Te*CH_2SiMe_2*N*$SiMe_3$)$(NR_2)_2$] (7.3)

In an identical manner to the synthesis of complexes **7.1** and **7.2**, reaction of 1 equiv of Te with [U(*C*H_2SiMe_2*N*$SiMe_3$)$(NR_2)_2$] in hexanes results in the formation of a red solution. Crystallization from hexanes affords the new tellurate complex, [U(*Te*CH_2SiMe_2*N*$SiMe_3$)$(NR_2)_2$] (**7.3**), as red needles in 51% yield (Scheme 7.5). The ^{1}H NMR spectrum of complex **7.3** is extremely similar to those of complexes **7.1** and **7.2**, again

featuring four broad resonances at -16.30, -3.22, -0.32, and 7.21 ppm, in a 9:36:2:6 ratio, respectively. Interestingly, the resonance attributable to the unique $SiMe_3$ moiety shifts upfield for this series of compounds as group 16 is descended. This stands in contrast to the downfield trend observed for the Cp^* resonances of $Cp^*_2U(EPh)_2$ (E = S, Se, Te).[39-41] Lastly, the NIR spectrum of complex **7.3** confirms the presence of a U(IV) metal center (Figure A7.3).[16-18,23,24,38]

Scheme 7.5 Synthesis of $[U(TeCH_2SiMe_2NSiMe_3)(NR_2)_2]$ (**7.3**)

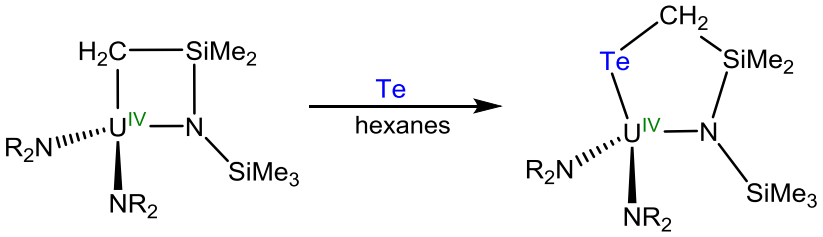

Complex **7.3** crystallizes in the triclinic spacegroup $P\bar{1}$, and does not exhibit the positional disorder observed for its sulfido and selenido analogues. Complex **7.3** features a distorted tetrahedral geometry about uranium, and its solid state molecular structure is shown in Figure 7.2. The most notable feature is the five membered ring that has now formed via insertion of a Te atom into the U-C bond. The U-Te (U1-Te1 = 3.0185(1) Å) bond distance is similar to those of other complexes with U-Te single bonds,[24,39,42] and the U-N bond distances (av. 2.250 Å) are also similar to the those of other U(IV) complexes with $[NR_2]^-$ ligands.[16-18,23,24]

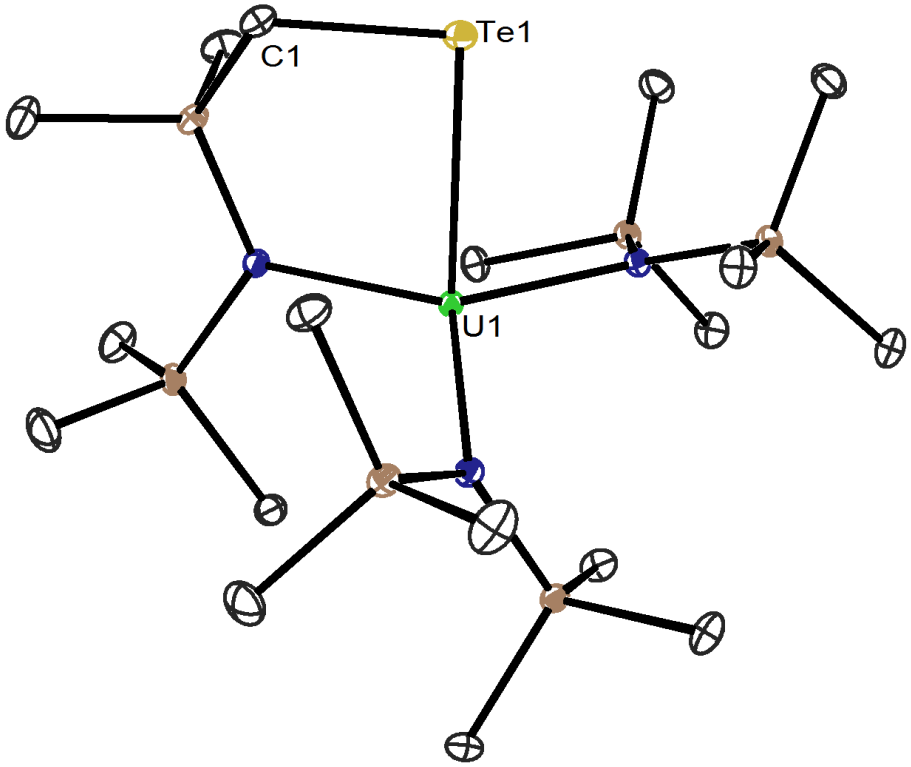

Figure 7.2. ORTEP diagram of [U(*Te*CH_2SiMe_2*N*$SiMe_3$)$(NR_2)_2$] (**7.3**) with 50% probability ellipsoids. Hydrogen atoms are omitted for clarity. Selected bond lengths (Å): U1-Te1 = 3.0185(1), Te1-C1 = 2.171(2), U-N (av.) = 2.250.

7.2.4 Reaction of [U(*E*CH_2SiMe_2*N*$SiMe_3$)$(NR_2)_2$] (E = S, Se, Te) with [U$(NR_2)_3$]

The chalcogen atom transfer capability of these chalcogen inserted metallacycles was then interrogated, in part to discover if complex **7.1** is responsible for the formation of [U$(NR_2)_3]_2(\mu\text{-}\eta^2\text{:}\eta^2\text{-}S_2)$. The reaction of complex **7.1** and [U$(NR_2)_3$] was monitored by ^{1}H NMR spectroscopy. Addition of 1 equiv of [U$(NR_2)_3$] to a benzene-d_6 solution of **7.1** results in the formation of an orange solution. The in situ ^{1}H NMR spectrum reveals the formation of the previously reported bridging monosulfide, [U$(NR_2)_3]_2(\mu\text{-}S)$,[24] the regeneration of [U(*C*H_2SiMe_2*N*$SiMe_3$)$(NR_2)_2$], and a corresponding decrease in the intensity of the resonances associated with complex **7.1** (Figure 7.3). Addition of a second equiv of [U$(NR_2)_3$]

to this reaction mixture results in complete consumption of complex **7.1** and an increase in the intensity of the resonances attributed to $[U(NR_2)_3]_2(\mu\text{-}S)$ and $[U(CH_2SiMe_2NSiMe_3)(NR_2)_2]$

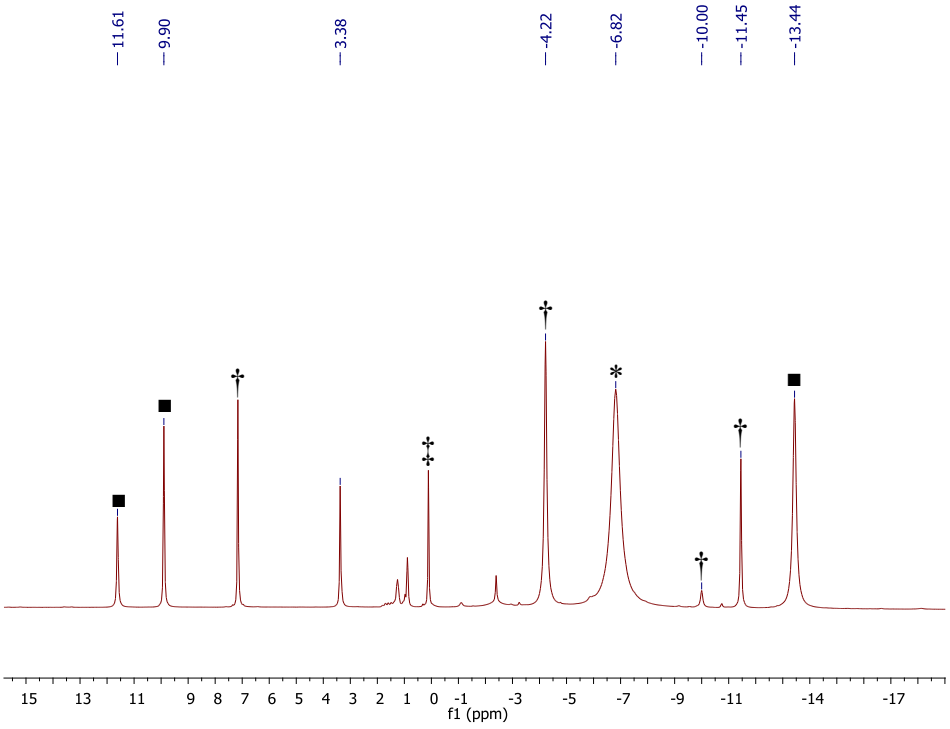

Figure 7.3. Portion of the in situ ^{1}H NMR spectrum of the reaction of **7.1** with 1 equiv of $[U(NR_2)_3]$ in benzene-d_6, after 2 h. (*) indicates the presence of $[U(NR_2)_3]_2(\mu\text{-}S)$, (■) indicates the presence of $[U(CH_2SiMe_2NSiMe_3)(NR_2)_2]$, (†) indicates the presence of unreacted 7.1, and (‡) indicates the presence of $HN(SiMe_3)_2$. (Not shown: resonance assignable to CH_2 of $[U(CH_2SiMe_2NSiMe_3)(NR_2)_2]$ at -118.8 ppm).

Complexes **7.2** and **7.3** also act as chalcogen atom transfer reagents, in an identical manner to complex **7.1**. Thus, reaction of either complex **7.2** or **7.3** with 2 equiv of $[U(NR_2)_3]$ affords the corresponding bridging monochalcogenide, $[U(NR_2)_3]_2(\mu\text{-}E)$ (E = Se, Te), and regenerates the four membered metallacycle, $[U(CH_2SiMe_2NSiMe_3)(NR_2)_2]$ (Scheme 7.6).

Scheme 7.6 Reaction of [U(*E*CH$_2$SiMe$_2$*N*SiMe$_3$)(NR$_2$)$_2$] (E = S, Se, Te) with [U(NR$_2$)$_3$]

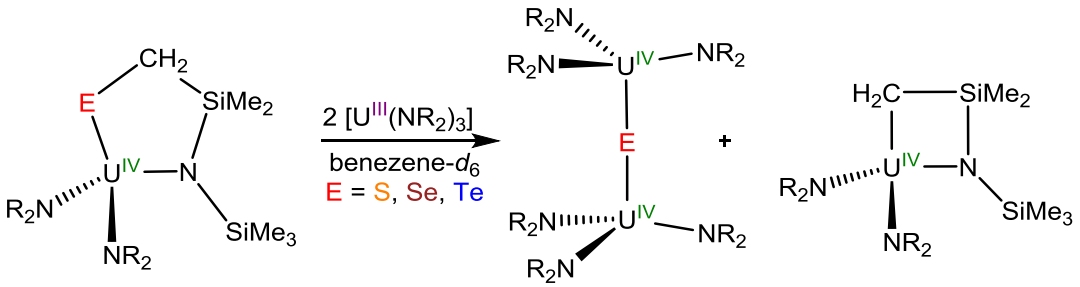

Interestingly, no evidence was seen for the formation of [U(NR$_2$)$_3$]$_2$(μ-η^2:η^2-S$_2$) at any point during the reaction of complex **7.1** with [U(NR$_2$)$_3$]. This suggests that the presence of [U(*C*H$_2$SiMe$_2$*N*SiMe$_3$)(NR$_2$)$_2$] is not responsible for the formation of this disulfide complex, and illustrates the complicated nature of chalcogen atom transfer reactions in actinide systems. Nevertheless, developing a rational method for the synthesis [U(NR$_2$)$_3$]$_2$(μ-η^2:η^2-S$_2$) could help explain the complexities of these reactions and guide future work.

7.2.5 Synthesis and Characterization of [K(Et$_2$O)$_2$][U(η^2-S$_2$)(NR$_2$)$_3$] (7.4)

An alternative route for the synthesis of [U(NR$_2$)$_3$]$_2$(μ-η^2:η^2-S$_2$) was then sought. Motivated in part by the successful synthesis of complex **2.1**, via the reaction of [U(NR$_2$)$_3$] with KSCPh$_3$, the reaction of the previously reported U(IV) chloride complex, [U(Cl)(NR$_2$)$_3$],[43] with KSCPh$_3$ was probed. The addition of 2 equiv of KSCPh$_3$ to a solution of [U(Cl)(NR$_2$)$_3$] in THF affords an orange mixture. Crystallization from diethyl ether affords the new U(IV) disulfide, [K(Et$_2$O)$_2$][U(η^2-S$_2$)(NR$_2$)$_3$] (**7.4**), as orange crystals in 44% yield (Scheme 7.7). The ^{1}H NMR spectrum of **7.4**, in benzene-d_6, features one broad resonance at -7.08 ppm, assignable to the methyl groups of the silylamide ligands. Complex **7.4** can be readily converted into is complex **6.1** via addition of 18-crown-6. This change is reflected by

the upfield shift of the resonance associated with the methyl groups of the silylamide ligands to -7.41 ppm, in benzene-d_6.

Scheme 7.7 Synthesis of $[K(Et_2O)_2][U(\eta^2\text{-}S_2)(NR_2)_3]$ (**7.4**)

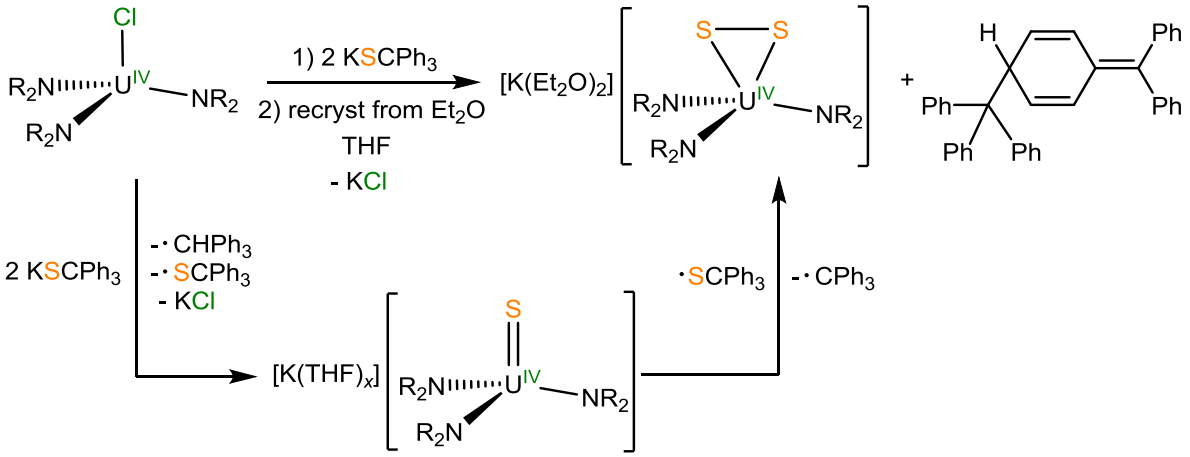

Complex **7.4** crystallizes in the monoclinic spacegroup $P2_1/c$ as a diethyl ether solvate **7.4**·$2Et_2O$, and it solid state molecular structure is shown in Figure 7.4. Complex **7.4** exists as a dimer in the solid state bridged by two $[K(Et_2O)_2]^+$ moieties. The structure sits on a crystallographically imposed center of inversion, as a result one half of the dimer is generated by symmetry. The asymmetric N-U-N angles (N1-U1-N2 = 107.99(5)°, N2-U1-N3 = 101.21(5)°, N1-U1-N3 = 123.15(5)°) of **7.4** are indicative of a distorted pseudotetrahedral geometry about uranium and are similar to those of complex **6.1**. In addition, the U-S (U1-S1 = 2.6984(5), U1-S2 = 2.7448(5) Å) and S-S (S1-S2 = 2.1031(7) Å) bond distances in **7.4** are also comparable to those of **6.1**.

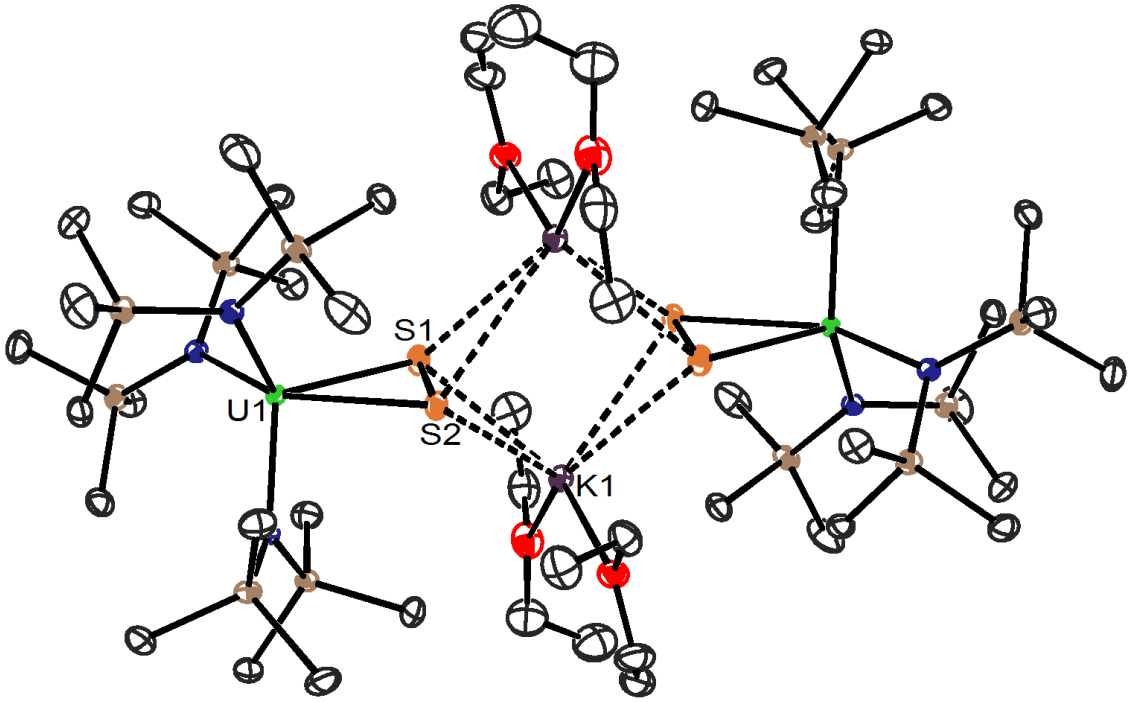

Figure 7.4. ORTEP diagram of $[K(Et_2O)_2][U(\eta^2\text{-}S_2)(NR_2)_3]$ (**7.4**·$2Et_2O$) with 50% probability ellipsoids. Hydrogen atoms are omitted for clarity. Selected bond lengths (Å) and angles (deg): U1-S1 = 2.6984(5), U1-S2 = 2.7448(5), S1-S2 = 2.1031(7), N1-U1-N2 = 107.99(5), N2-U1-N3 = 101.21(5), N1-U1-N3 = 123.15(5).

The formation of complex **7.4** is believed to proceed in a stepwise fashion. First, the reaction of $[U(Cl)(NR_2)_3]$ with 1 equiv of $KSCPh_3$ generates both a U(V) sulfide, $[U(S)(NR_2)_3]$, and the triphenylmethyl radical. The transiently formed U(V) sulfide then reacts with the second equiv of $KSCPh_3$, which reduces the metal center from U(V) to U(IV) and results in the formation of the $Ph_3CS^{\bullet}$ radical. This sulfide radical then reacts with the U(IV) sulfide, acting as a sulfur atom transfer reagent, to form the S-S bond,[17] eliminate another equiv of the triphenylmethyl radical, and generate a U(IV) disulfide (Scheme 7.7). The in situ ^{1}H NMR of the reaction of $[U(Cl)(NR_2)_3]$ with 1 equiv of $KSCPh_3$, in THF-d_8, features resonances attributable to the presence of a U(IV) disulfide, $[K(THF)_x][U(S_2)(NR_2)_3]$, in addition to Gomberg's dimer,[18,44] and unreacted $[U(Cl)(NR_2)_3]$. Furthermore, at short

reaction times a new broad resonance is observed in the in situ ^{1}H NMR spectrum, which is attributed to the presence of the U(IV) monosulfide, $[K(THF)_x][U(S)(NR_2)_3]$ (Figure 7.5).[18]

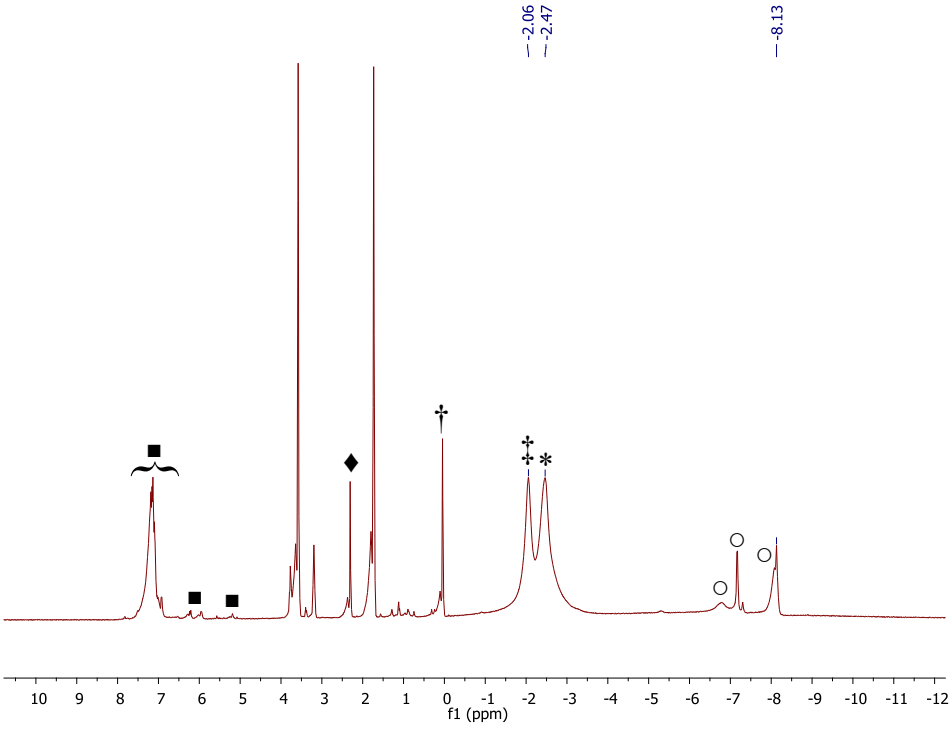

Figure 7.5. In situ ^{1}H NMR of the reaction of the reaction of $[U(Cl)(NR_2)_3]$ with 1 equiv of $KSCPh_3$ in tetrahydrofuran-d_8, after 2 h. (*) indicates the presence of unreacted $[U(Cl)(NR_2)_3]$, (■) indicates the presence of Gomberg's dimer, (†) indicates the presence of $HN(SiMe_3)_2$, (‡) indicates the presence of a complex tentatively assigned as $[K(THF)_x][U(S)(NR_2)_3]$, (♦) indicates the presence of toluene, and (○) indicates the presence of unidentified intermediates.

The reaction of complex **2.1** with $Ph_3CSSCPh_3$[45,46] was then investigated in order to further support the proposed mechanism for the formation of complex **7.4**. Accordingly, addition of 0.5 equiv of $Ph_3CSSCPh_3$ to a solution of **2.1**, in THF-d_8, results in the formation of $[K(18\text{-crown-6})][U(\eta^2\text{-}S_2)(NR_2)_3]$ (**6.1**) and Gomberg's dimer as determined by ^{1}H NMR spectroscopy (Scheme 7.8, Figure A7.2). In this example, $Ph_3CSSCPh_3$ is simply acting as a single sulfur atom transfer reagent.

Scheme 7.8 Reaction of [K(18-crown-6)][U(S)(NR$_2$)$_3$] (**2.1**) with Ph$_3$CSSCPh$_3$

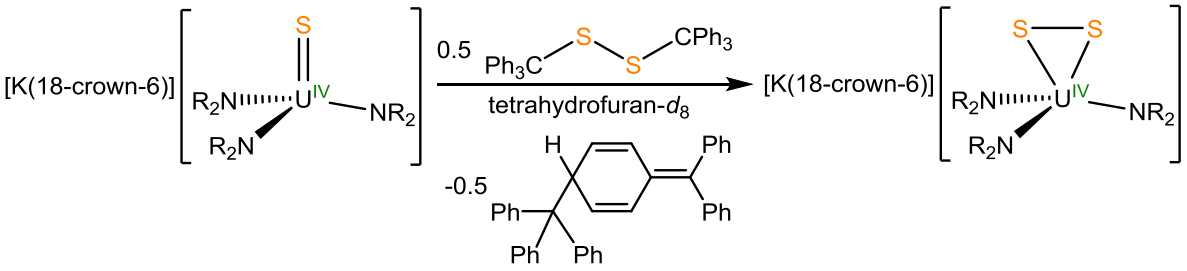

7.2.6 Reaction of [U(NR$_2$)$_3$] with Ph$_3$CSSCPh$_3$

The disulfide, Ph$_3$CSSCPh$_3$, was also investigated as a possible 'S_2' transfer reagent. Accordingly, reaction of 0.5 equiv of Ph$_3$CSSCPh$_3$ with [U(NR$_2$)$_3$], in benzene-d_6, was monitored by ^{1}H NMR spectroscopy. The in situ ^{1}H NMR spectrum, obtained after 5 min reveals formation of the bridging monosulfide, [U(NR$_2$)$_3$]$_2$(μ-S) and Gomberg's dimer, as well as the presence of unreacted Ph$_3$CSSCPh$_3$ (Scheme 7.9, Figure A7.2). This demonstrates that Ph$_3$CSSCPh$_3$ can act as a sulfur atom transfer reagent, however, no evidence for the formation of [U(NR$_2$)$_3$]$_2$(μ-η^2:η^2-S$_2$) is observed, and indicates that more work will be required to not only explain its formation, but also develop a rational route to its synthesis.

Scheme 7.9 Reaction of [U(NR$_2$)$_3$] with Ph$_3$CSSCPh$_3$

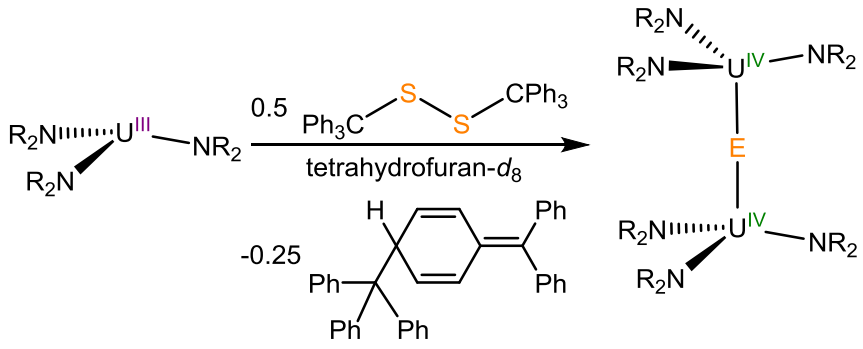

7.3 Summary

In summary, reaction of U(IV) metallacycle, [U(*C*H$_2$SiMe$_2$*N*SiMe$_3$)(NR$_2$)$_2$] with elemental chalcogens (S, Se, Te) affords [U(*E*CH$_2$SiMe$_2$*N*SiMe$_3$)(NR$_2$)$_2$] (**7.1**, E = S; **7.2**, E =

Se; **7.3**, E = Te) in good yields. Complex **7.1** can also be synthesized using ethylene sulfide as the S atom source. All three complexes can act as chalcogen atoms transfer reagents, and react with 2 equiv of $[U(NR_2)_3]$ to give the previously reported bridging monochalcogenides, $[U(NR_2)_3](\mu\text{-}E)$ (E = S, Se, Te), and regenerate the starting metallacycle.

Investigation into the formation of the bridging disulfide, $[U(NR_2)_3]_2(\mu\text{-}\eta^2\text{:}\eta^2\text{-}S_2)$, led to the discovery of the U(IV) disulfide, $[K(Et_2O)_2][U(\eta^2\text{-}S_2)(NR_2)_3]$ (**7.4**). Complex **7.4** is generated from the reaction of $[U(Cl)(NR_2)_3]$ with 2 equiv of $KSCPh_3$, and forms in a stepwise manner. Conversion of complex **7.4** into $[K(18\text{-crown-}6)][U(\eta^2\text{-}S_2)(NR_2)_3]$ (**6.1**) is accomplished via addition of 18-crown-6. In addition, the sulfur atom transfer capability of $Ph_3CSSCPh_3$ was explored. This species readily reacts with $[U(NR_2)_3]$ and $[K(18\text{-crown-}6)][U(S)(NR_2)_3]$ (**2.1**) to give the bridging monosulfide, $[U(NR_2)_3](\mu\text{-}S)$, and the U(IV) disulfide, $[K(18\text{-crown-}6)][U(\eta^2\text{-}S_2)(NR_2)_3]$ (**6.1**), respectively, and Gomberg's dimer. Notably, in both instances, $Ph_3CSSCPh_3$ acts as a single S atom transfer reagent, rather than the expected 'S_2' transfer source.

These reactions demonstrate the wide variety of reagents and routes that can be utilized for chalcogen atom transfer to the actinides. Additionally, a rational route towards the synthesis of $[U(NR_2)_3]_2(\mu\text{-}\eta^2\text{:}\eta^2\text{-}S_2)$ has been investigated, and several operative pathways have been eliminated. The mechanism of formation of this disulfide remains unknown and demonstrates the need for further investigations into chalcogen atom transfer to the actinides.

7.4 Experimental

7.4.1 General Methods

All reactions and subsequent manipulations were performed under anaerobic and anhydrous conditions under an atmosphere of nitrogen. Hexanes, Et_2O, and toluene were

dried using a Vacuum Atmospheres DRI-SOLV Solvent Purification system and stored over 3Å sieves for 24 h prior to use. Tetrahydrofuran (THF) was distilled twice, first from calcium hydride and then from sodium benzophenone ketyl, and stored over 3Å molecular sieves for 24 h prior to use. Pyridine, benzene-d_6, pyridine-d_5, and THF-d_8 were dried over 3Å molecular sieves for 24 h prior to use. [U(*C*H_2SiMe$_2$*N*SiMe$_3$)(NR_2)$_2$],[36] [U(NR_2)$_3$],[47] [U(Cl)(NR_2)$_3$],[43] and [K(18-crown-6)][U(S)(NR_2)$_3$] (**2.1**)[18] were synthesized according to the previously reported procedures. All other reagents were purchased from commercial suppliers and used as received.

NMR spectra were recorded on a Varian UNITY INOVA 400, a Varian UNITY INOVA 500 spectrometer, a Varian UNITY INOVA 600 MHz spectrometer, or an Agilent Technologies 400-MR DD2 400 MHz Spectrometer. ^{1}H NMR spectra were referenced to external SiMe$_4$ using the residual protio solvent peaks as internal standards. IR spectra were recorded on a Nicolet 6700 FT-IR spectrometer with a NXR FT Raman Module. UV-Vis / NIR experiments were performed on a UV-3600 Shimadzu spectrophotometer. Elemental analyses were performed by the Micro-Analytical Facility at the University of California, Berkeley.

7.4.2 Synthesis of [U(*S*CH$_2$SiMe$_2$*N*SiMe$_3$)(NR_2)$_2$] (7.1)

Method A. To a brown, cold (-25 °C), stirring solution of [U(*C*H_2SiMe$_2$*N*SiMe$_3$)(NR_2)$_2$] (155.5 mg, 0.22 mmol) in hexanes (4 mL) was added S_8 (11.4 mg, 0.044 mmol). This mixture was allowed to stir for 30 min, whereupon the solvent was removed in vacuo to give a yellow-brown solid. This solid was extracted with hexanes (4 mL) and filtered through a Celite column supported on glass wool (0.5 cm × 2 cm) to provide a yellow-brown filtrate. The solvent was then removed in vacuo and the resulting yellow-brown solid was extracted with

diethyl ether (4 mL) to provide a yellow-brown solution. This solution was filtered through a Celite column supported on glass wool (0.5 cm × 2 cm) to provide a yellow-brown filtrate. The volume of this filtrate was reduced in vacuo to 1 mL and the solution was transferred to a 4 mL scintillation vial that was placed inside a 20 mL scintillation vial. Toluene (6 mL) was then added to the outer vial. Storage of this two vial system at -25 °C for 72 h resulted in the deposition of yellow-brown crystals, which were isolated by decanting away the supernatant (101 mg, 62%). Anal. Calcd for $C_{18}H_{53}N_3SSi_6U$: C, 28.82; H, 7.12; N, 5.60. Found: C, 29.67; H, 7.03; N, 5.81. ^{1}H NMR (400 MHz, 25 °C, benzene-d_6): δ -11.44 (br s, 9H, Si(CH_3)$_3$), -9.97 (br s, 2H, CH_2), -4.22 (br s, 36H, N(Si(CH_3)$_3$)$_2$), 3.38 (br s, 6H, Si(CH_3)$_2$). IR (KBr Pellet, cm^{-1}): 615 (m), 662 (m), 683 (m), 757 (m), 818 (sh), 841 (s), 872 (sh), 933 (s), 1101 (w), 1182 (m), 1252 (s), 1404 (m). UV-Vis/NIR (C_4H_8O, 4.98 mM, 25 °C, L·mol^{-1}·cm^{-1}): 524 (ε = 31.0), 694 (ε = 25.5), 822 (ε = 7.1), 956 (ε = 7.9), 1069 (ε = 27.9), 1154 (sh) (ε = 17.3), 1406 (ε = 14.3), 1560 (ε = 10.9). Unit Cell: a = 16.3753(5) Å, b = 16.3753(5) Å, c = 8.3665(3) Å, α = 90°, β = 90°, γ = 120°.

Method B. To a brown, cold (-25 °C), stirring solution of [U(*C*H$_2$SiMe$_2$*N*SiMe$_3$)(NR$_2$)$_2$] (206.1 mg, 0.29 mmol) in hexanes (4 mL) was added ethylene sulfide (20 μL, 0.31 mmol). This solution was allowed to stir for 24 h, whereupon the color of the solution changed to yellow-brown. The solvent was removed in vacuo, and the resulting yellow-brown solid was extracted with hexanes (5 mL) to give a yellow-brown solution. This solution was then filtered through a Celite column supported on glass wool (0.5 cm × 2 cm) to provide a yellow-brown filtrate. The filtrate was then dried in vacuo to give a yellow-brown powder (200 mg, 93%). ^{1}H NMR (400 MHz, 25 °C, benzene-d_6): δ -11.40 (br s, 9H, Si(CH_3)$_3$), -10.06 (br s, 2H, CH_2), -4.18 (br s, 36H, N(Si(CH_3)$_3$)$_2$), 3.41 (br s, 6H, Si(CH_3)$_2$).

7.4.3 Reaction of [U(*C*H$_2$SiMe$_2$*N*SiMe$_3$)(NR$_2$)$_2$] with Ethylene Sulfide

To a brown solution of [U(*C*H$_2$SiMe$_2$*N*SiMe$_3$)(NR$_2$)$_2$] (**2**) (11.1 mg, 0.015 mmol) in benzene-d_6 (0.5 mL), in an NMR tube fitted with a J-Young valve, was added ethylene sulfide (1 μL, 0.016 mmol). This solution was allowed to stand for 24 h, whereupon a ^{1}H NMR spectrum was recorded, which revealed the complete consumption of [U(*C*H$_2$SiMe$_2$*N*SiMe$_3$)(NR$_2$)$_2$] and the formation of **7.1** and ethylene. ^{1}H NMR (400 MHz, 25 °C, benzene-d_6): δ -11.40 (br s, 9H, Si(C*H*$_3$)$_3$), -9.90 (br s, 2H, C*H*$_2$), -4.20 (br s, 36H, N(Si(C*H*$_3$)$_3$)$_2$), 3.39 (br s, 6H, Si(C*H*$_3$)$_2$), 5.26 (s, 4H, ethylene C*H*$_2$).

7.4.4 Synthesis of [U(*Se*CH$_2$SiMe$_2$*N*SiMe$_3$)(NR$_2$)$_2$] (7.2)

To a brown, cold (-25 °C), stirring solution of [U(*C*H$_2$SiMe$_2$*N*SiMe$_3$)(NR$_2$)$_2$] (149.4 mg, 0.21 mmol) in hexanes (4 mL) was added Se powder (35.9 mg, 0.45 mmol). This mixture was allowed to stir for 18 h, whereupon the color changed to yellow-brown. This mixture was filtered through a Celite column supported on glass wool (0.5 cm × 2 cm) to provide a yellow-brown filtrate. The filtrate was then dried in vacuo and extracted with diethyl ether (3 mL). The volume of this solution was reduced to 1.5 mL in vacuo and the solution was transferred to a 4 mL scintillation vial that was placed inside a 20 mL scintillation vial. Toluene (5 mL) was then added to the outer vial. Storage of this two vial system at -25 °C for 48 h resulted in the deposition of yellow crystalline needles, which were isolated by decanting off the supernatant (99.8 mg, 60%). Anal. Calcd for C$_{18}$H$_{53}$N$_3$SeSi$_6$U: C, 27.12; H, 6.70; N, 5.27. Found: C, 27.83; H, 6.48; N, 5.63. ^{1}H NMR (400 MHz, 25 °C, benzene-d_6): δ -12.24 (br s, 9H, Si(C*H*$_3$)$_3$), -7.18 (br s, 2H, C*H*$_2$), -3.69 (br s, 36H, N(Si(C*H*$_3$)$_3$)$_2$), 4.67 (br s, 6H, Si(C*H*$_3$)$_2$). IR (KBr Pellet, cm^{-1}): 602 (sh), 617 (m), 667 (m), 676 (m), 712 (m), 729 (m), 756 (m), 793 (sh), 818 (sh), 841 (s), 866 (sh), 935 (s), 1067 (w), 1182 (m), 1250 (s), 1379 (w), 1404 (m).

UV-Vis/NIR (C_4H_8O, 5.36 mM, 25 °C, $L \cdot mol^{-1} \cdot cm^{-1}$): 694 (ε = 35.2), 804 (ε = 14.9), 952 (ε = 12.4), 1056 (ε = 27.5), 1152 (sh) (ε = 17.9), 1388 (ε = 14.6), 1540 (ε = 11.7). Unit Cell: a = 16.248(1)Å, b = 16.248(1) Å, c = 8.4815(6) Å, α = 90°, β = 90°, γ = 120°.

7.4.5 Synthesis of [U(*Te*CH_2SiMe_2*N*$SiMe_3$)$(NR_2)_2$] (7.3)

To a brown, cold (-25 °C), stirring solution of [U(*C*H_2SiMe_2*N*$SiMe_3$)$(NR_2)_2$] (135.4 mg, 0.19 mmol) in hexanes (4 mL) was added Te powder (25.0 mg, 0.20 mmol). This mixture was allowed to stir for 48 h, whereupon the color changed to red. This mixture was filtered through a Celite column supported on glass wool (0.5 cm × 2 cm) to provide a dark-red filtrate. The volume of this filtrate was reduced in vacuo to 1 mL and the solution was transferred to a 4 mL scintillation vial that was placed inside a 20 mL scintillation vial. Toluene (6 mL) was then added to the outer vial. Storage of this two vial system at -25 °C for 72 h resulted in the deposition of red crystalline needles, which were isolated by decanting off the supernatant (80.6 mg, 51%). Anal. Calcd for $C_{18}H_{53}N_3TeSi_6U$: C, 25.56; H, 6.32; N, 4.97. Found: C, 25.21; H, 5.96; N, 4.80. ^{1}H NMR (400 MHz, 25 °C, benzene-d_6): δ -16.30 (br s, 9H, Si(CH_3)$_3$), -3.22 (br s, 36H, N(Si(CH_3)$_3$)$_2$), -0.32 (br s, 2H, CH_2), 7.21 (br s, 6H, Si(CH_3)$_2$). IR (KBr Pellet, cm^{-1}): 615 (m), 663 (m), 681 (m), 706 (sh), 756 (m), 784 (m), 841 (s), 874 (sh), 933 (s), 1182 (m), 1252 (s), 1404 (m). UV-Vis/NIR (C_4H_8O, 4.91 mM, 25 °C, $L \cdot mol^{-1} \cdot cm^{-1}$): 686 (ε = 20.7), 811 (ε = 5.9), 854 (ε = 8.7), 1062 (ε = 25.7), 1156 (ε = 15.3), 1348 (ε = 12.3), 1523 (ε = 11.4).

7.4.6 Reaction of [U(*C*H_2SiMe_2*N*$SiMe_3$)$(NR_2)_2$] with Ethylene sulfide

To a brown solution of [U(*C*H_2SiMe_2*N*$SiMe_3$)$(NR_2)_2$] (11.1 mg, 0.015 mmol) in benzene-d_6 (0.5 mL), in an NMR tube fitted with a J-Young valve, was added ethylene sulfide (1 μL,

0.016 mmol). This solution was allowed to stand for 24 h, whereupon a ^{1}H NMR spectrum was recorded, which revealed the complete consumption of [U(*C*H$_2$SiMe$_2$*N*SiMe$_3$)(NR$_2$)$_2$] and the formation of **7.1** and ethylene. ^{1}H NMR (400 MHz, 25 °C, benzene-d_6): δ -11.40 (br s, 9H, Si(C*H*$_3$)$_3$), -9.90 (br s, 2H, C*H*$_2$), -4.20 (br s, 36H, N(Si(C*H*$_3$)$_3$)$_2$), 3.39 (br s, 6H, Si(C*H*$_3$)$_2$), 5.26 (s, 4H, ethylene C*H*$_2$).

7.4.7 Reaction of [U(*S*CH$_2$SiMe$_2$*N*SiMe$_3$)(NR$_2$)$_2$] (7.1) with [U(NR$_2$)$_3$]

To a solution of **7.1** (23.6 mg, 0.031 mmol) in benzene-d_6 (0.75 mL), in an NMR tube fitted with a J-Young valve, was added a solution of [U(NR$_2$)$_3$] (23.2 mg, 0.032 mmol) in benzene-d_6 (0.5 mL). This solution was allowed to stand for 2 h during which time the color changed to orange. A ^{1}H NMR spectrum was then recorded, which revealed the formation of [U(*C*H$_2$SiMe$_2$*N*SiMe$_3$)(NR$_2$)$_2$] and [U(NR$_2$)$_3$](μ-S),[24] along with the presence of **7.1**. ^{1}H NMR (400 MHz, 25 °C, benzene-d_6): δ -118.8 (br s, 2H, [U(*C*H$_2$SiMe$_2$*N*SiMe$_3$)(NR$_2$)$_2$] C*H*$_2$), -13.44 (br s, 36H, [U(*C*H$_2$SiMe$_2$*N*SiMe$_3$)(NR$_2$)$_2$] N(Si(C*H*$_3$)$_3$)$_2$), -11.45 (br s, 9H, **7.1** Si(C*H*$_3$)$_3$), -10.00 (br s, 2H, **7.1** C*H*$_2$), -6.82 (br s, 108H, [U(NR$_2$)$_3$](μ-S) N(Si(C*H*$_3$)$_3$)$_2$), -4.22 (br s, 36H, **7.1** N(Si(C*H*$_3$)$_3$)$_2$), 3.38 (br s, 6H, **7.1** Si(C*H*$_3$)$_2$), 9.90 (br s, 9H, [U(*C*H$_2$SiMe$_2$*N*SiMe$_3$)(NR$_2$)$_2$] Si(C*H*$_3$)$_3$), 11.61 (br s, 6H, [U(*C*H$_2$SiMe$_2$*N*SiMe$_3$)(NR$_2$)$_2$] Si(C*H*$_3$)$_2$). Another aliquot of [U(NR$_2$)$_3$)] (26.7 mg, 0.037 mmol) in benzene-d_6 (0.5 mL) was added to the reaction mixture. This solution was allowed to stand for another 2 h, whereupon a ^{1}H NMR spectrum was recorded, which revealed the complete consumption of **7.1** and an increase in the intensities of the resonances attributable to [U(*C*H$_2$SiMe$_2$*N*SiMe$_3$)(NR$_2$)$_2$] and [U(NR$_2$)$_3$](μ-S). ^{1}H NMR (400 MHz, 25 °C, benzene-d_6): δ -119.0 (br s, 2H, [U(*C*H$_2$SiMe$_2$*N*SiMe$_3$)(NR$_2$)$_2$] C*H*$_2$), -13.38 (br s, 36H, [U(*C*H$_2$SiMe$_2$*N*SiMe$_3$)(NR$_2$)$_2$] N(Si(C*H*$_3$)$_3$)$_2$), -6.78 (br s, 108H, [U(NR$_2$)$_3$](μ-S) N(Si(C*H*$_3$)$_3$)$_2$), 9.87 (br s, 9H,

[U(*C*H$_2$SiMe$_2$*N*SiMe$_3$)(NR$_2$)$_2$] Si(C*H*$_3$)$_3$), 11.55 (br s, 6H, [U(*C*H$_2$SiMe$_2$*N*SiMe$_3$)(NR$_2$)$_2$] Si(C*H*$_3$)$_2$).

7.4.8 Reaction of [U(*Se*CH$_2$SiMe$_2$*N*SiMe$_3$)(NR$_2$)$_2$] (7.2) with [U(NR$_2$)$_3$]

To a solution of **7.2** (25.3 mg, 0.032 mmol), in benzene-d_6 (0.75 mL), in an NMR tube fitted with a J-Young valve, was added a solution of [U(NR$_2$)$_3$] (22.6 mg, 0.031 mmol) in benzene-d_6 (0.75 mL). This solution was allowed to stand for 30 min during time which the color changed to orange. A ^{1}H NMR spectrum was then recorded, which revealed the formation of [U(*C*H$_2$SiMe$_2$*N*SiMe$_3$)(NR$_2$)$_2$] and [U(NR$_2$)$_3$](μ-Se),[24] along with the presence of **7.2**. ^{1}H NMR (400 MHz, 25 °C, benzene-d_6): δ -118.8 (br s, 2H, [U(*C*H$_2$SiMe$_2$*N*SiMe$_3$)(NR$_2$)$_2$] C*H*$_2$), -13.40 (br s, 36H, [U(*C*H$_2$SiMe$_2$*N*SiMe$_3$)(NR$_2$)$_2$] N(Si(C*H*$_3$)$_3$)$_2$), -12.29 (br s, 9H, **7.2** Si(C*H*$_3$)$_3$), -7.21 (br s, 2H, **7.2** C*H*$_2$), -6.62 (br s, 108H, [U(NR$_2$)$_3$](μ-Se) N(Si(C*H*$_3$)$_3$)$_2$), -3.70 (br s, 36H, **7.2** N(Si(C*H*$_3$)$_3$)$_2$), 4.68 (br s, 6H, **7.2** Si(C*H*$_3$)$_2$), 9.87 (br s, 9H, [U(*C*H$_2$SiMe$_2$*N*SiMe$_3$)(NR$_2$)$_2$] Si(C*H*$_3$)$_3$), 11.58 (br s, 6H, [U(*C*H$_2$SiMe$_2$*N*SiMe$_3$)(NR$_2$)$_2$] Si(C*H*$_3$)$_2$). Another aliquot of [U(NR$_2$)$_3$] (23.0 mg, 0.032 mmol) in benzene-d_6 (0.5 mL) was then added to the reaction mixture. This solution was allowed to stand for 15 min whereupon a ^{1}H NMR spectrum was recorded, which revealed complete consumption of **7.2** and an increase in the intensities of the resonances attributable to [U(*C*H$_2$SiMe$_2$*N*SiMe$_3$)(NR$_2$)$_2$] and [U(NR$_2$)$_3$](μ-Se). ^{1}H NMR (400 MHz, 25 °C, benzene-d_6): δ -119.0 (br s, 2H, [U(*C*H$_2$SiMe$_2$*N*SiMe$_3$)(NR$_2$)$_2$] C*H*$_2$), -13.42 (br s, 36H, [U(*C*H$_2$SiMe$_2$*N*SiMe$_3$)(NR$_2$)$_2$] N(Si(C*H*$_3$)$_3$)$_2$), -6.62 (br s, 108H, [U(NR$_2$)$_3$](μ-Se) N(Si(C*H*$_3$)$_3$)$_2$), 9.89 (br s, 9H, [U(*C*H$_2$SiMe$_2$*N*SiMe$_3$)(NR$_2$)$_2$] Si(C*H*$_3$)$_3$), 11.59 (br s, 6H, [U(*C*H$_2$SiMe$_2$*N*SiMe$_3$)(NR$_2$)$_2$] Si(C*H*$_3$)$_2$).

7.4.9 Reaction of [U(*Te*CH_2SiMe_2*N*$SiMe_3$)$(NR_2)_2$] (7.3) with [U$(NR_2)_3$]

To a solution of **7.3** (24.3 mg, 0.029 mmol) in benzene-d_6 (0.75 mL), in an NMR tube fitted with a J-Young valve, was added a solution of [U$(NR_2)_3$] (20.7 mg, 0.029 mmol) in benzene-d_6 (0.5 mL). The solution was allowed to stand for 5 min, whereupon a ^{1}H NMR spectrum was recorded, which revealed the formation of [U(*C*H_2SiMe_2*N*$SiMe_3$)$(NR_2)_2$] and [U$(NR_2)_3$](μ-Te),[24] along with the presence of **7.3**. ^{1}H NMR (400 MHz, 25 °C, benzene-d_6): δ -118.9 (br s, 2H, [U(*C*H_2SiMe_2*N*$SiMe_3$)$(NR_2)_2$] C*H*$_2$), -16.50 (br s, 9H, **7.3** Si(C*H*$_3$)$_3$), -13.40 (br s, 36H, [U(*C*H_2SiMe_2*N*$SiMe_3$)$(NR_2)_2$] N(Si(C*H*$_3$)$_3$)$_2$), -6.13 (br s, 108H, [U$(NR_2)_3$](μ-Te) N(Si(C*H*$_3$)$_3$)$_2$), -3.25 (br s, 36H, **7.3** N(Si(C*H*$_3$)$_3$)$_2$), -0.27 (br s, 2H, **7.3** C*H*$_2$), 7.27 (br s, 6H, **7.3** Si(C*H*$_3$)$_2$), 9.88 (br s, 9H, [U(*C*H_2SiMe_2*N*$SiMe_3$)$(NR_2)_2$] Si(C*H*$_3$)$_3$), 11.59 (br s, 6H, [U(*C*H_2SiMe_2*N*$SiMe_3$)$(NR_2)_2$] Si(C*H*$_3$)$_2$). After 30 min, another aliquot of [U$(NR_2)_3$] (20.2 mg, 0.028 mmol) in benzene-d_6 (0.5 mL) was added to the reaction mixture. This solution was then allowed to stand for 15 min, whereupon a ^{1}H NMR spectrum was recorded, which revealed complete consumption of **7.3** and an increase in the intensities of the resonances attributable to [U(*C*H_2SiMe_2*N*$SiMe_3$)$(NR_2)_2$] and [U$(NR_2)_3$](μ-Te). ^{1}H NMR (400 MHz, 25 °C, benzene-d_6): δ -119.0 (br s, 2H, [U(*C*H_2SiMe_2*N*$SiMe_3$)$(NR_2)_2$] C*H*$_2$), -13.42 (br s, 36H, [U(*C*H_2SiMe_2*N*$SiMe_3$)$(NR_2)_2$] N(Si(C*H*$_3$)$_3$)$_2$), -6.13 (br s, 108H, [U$(NR_2)_3$](μ-Te) N(Si(C*H*$_3$)$_3$)$_2$), 9.91 (br s, 9H, [U(*C*H_2SiMe_2*N*$SiMe_3$)$(NR_2)_2$] Si(C*H*$_3$)$_3$), 11.61 (br s, 6H, [U(*C*H_2SiMe_2*N*$SiMe_3$)$(NR_2)_2$] Si(C*H*$_3$)$_2$).

7.4.10 Reaction of [U(Cl)$(NR_2)_3$] with $KSCPh_3$

To a solution of [U(Cl)$(NR_2)_3$] (13.6 mg, 0.018 mmol) in tetrahydrofuran-d_8 (0.5 mL), in an NMR tube fitted with a J-Young valve, was added a solution of $KSCPh_3$ (5.8 mg, 0.018 mmol) in tetrahydrofuran-d_8 (0.5 mL). The solution was allowed to stand for 2 h, whereupon

a ^{1}H NMR spectrum was recorded, which revealed the formation of complex **7.4**, Gomberg's dimer, and unreacted [U(Cl)(NR$_2$)$_3$]. A resonance tentatively assigned to a U(IV) terminal sulfide, [K(THF)$_x$][U(S)(NR$_2$)$_3$], was also observed. ^{1}H NMR (400 MHz, 25 °C, tetrahydrofuran-d_8): δ -8.13 (br s, 54H, **7.4**), -2.47 (br, s, 54H, [U(Cl)(NR$_2$)$_3$]), -2.06 (br, s, 54H, [U(S)(NR$_2$)$_3$]$^-$), 5.19 (m, 1H, allylic), 5.96 (m, 2H, vinylic), 6.22 (m, 2H, vinylic), 7.03-7.28 (m, 25H, aryl C*H*). The solution was allowed to stand for 6 d, whereupon another ^{1}H NMR spectrum was recorded, which revealed the presence of **7.4**, Gomberg's dimer, [U(Cl)(NR$_2$)$_3$], and the disappearance of the resonance assigned to [U(S)(NR$_2$)$_3$]$^-$. ^{1}H NMR (400 MHz, 25 °C, tetrahydrofuran-d_8): δ -8.14 (br s, 54H, **7.4**), -2.49 (br, s, 54H, [U(Cl)(NR$_2$)$_3$]), 5.19 (m, 1H, allylic), 5.96 (m, 2H, vinylic), 6.22 (m, 2H, vinylic), 7.03-7.28 (m, 25H, aryl C*H*).

7.4.11 Synthesis of [K(Et$_2$O)$_2$][U(η^2-S$_2$)(NR$_2$)$_3$] (7.4)

To a cold (-25 °C), stirring solution of [U(Cl)(NR$_2$)$_3$] (147.5 mg, 0.20 mmol) in THF (3 mL) was added a cold (-25 °C) solution of KSCPh$_3$ (137.1 mg, 0.44 mmol) in THF (3 mL). This mixture was allowed to stir for 24 h, whereupon the solvent was removed in vacuo and the resulting orange solid was triturated with hexanes (4 mL) and Et$_2$O (4 mL). The orange powder was then extracted with hexanes (8 mL) and filtered through a Celite column supported on glass wool (0.5 cm × 3 cm), to provide an orange solution. The filtrate was then dried in vacuo, extracted with Et$_2$O (6 mL), and filtered again through a Celite column supported on glass wool (0.5 cm × 3 cm) to afford an orange solution. The volume of the filtrate was reduced in vacuo to 2 mL. Storage of this solution at -25 °C for 24 h resulted in the deposition of orange crystals where were isolated by decanting off the supernatant (83.7

mg, 44%). ^{1}H NMR (400 MHz, 25 °C, benzene-d_6): δ -7.08 (br s, 108H, N(Si(CH_3)$_3$)$_2$), 1.08 (t, 24H, CH_2CH_3, J_{HH} = 8.0 Hz), 3.21 (q, 16H, CH_2CH_3, J_{HH} = 8.0 Hz).

7.4.12 Reaction of [K(Et$_2$O)$_2$][U(η^2-S$_2$)(NR$_2$)$_3$] (7.4) with 18-crown-6

To a solution of **7.4** (6.6 mg, 0.0034 mmol) in benzene-d_6 (0.5 mL), in an NMR tube fitted with a J-Young valve, was added a solution 18-crown-6 (1.9 mg, 0.0072 mmol). A ^{1}H NMR spectrum was then recorded, which revealed the formation of **2.1**. The identity of **2.1** was confirmed by comparison of the ^{1}H NMR spectrum with that of authentic material.[17] ^{1}H NMR (400 MHz, 25 °C, benzene-d_6): δ -7.41 (br s, 54H, N(Si(CH_3)$_3$)$_2$), 2.53 (br s, 24H, 18-crown-6).

7.4.13 Synthesis of Ph$_3$CSSCPh$_3$

To a stirring solution of Ph_3CSH (338.0 mg, 1.22 mmol) in THF (4 mL) was added $NaN(SiMe_3)_2$ (228.0 mg, 1.24 mmol). After 5 min, I_2 (156.2 mg, 0.62 mmol) in THF (3 mL) was added to this solution. This mixture was allowed to stir for a further 10 min. The solvent was then removed in vacuo and the resulting yellow solid was triturated with diethyl ether (5 mL). The resulting powder was extracted with diethyl ether (6 mL) and filtered through a Celite column supported on glass wool (0.5 cm × 3 cm) to provide a pale yellow filtrate. The volume of the filtrate was reduced in vacuo to 2 mL. Storage of this solution at -25 °C for 24 h resulted in the deposition of yellow solid which was isolated by decanting off the supernatant (124.7 mg, 18%). Melting point: 150-153 °C (lit. value = 153-155 °C).[45] ^{1}H NMR (500 MHz, 25 °C, benzene-d_6): δ 6.93-7.0 (m, 18H, *m*-, *p*-C*H*), 7.30-7.36 (m, 12H, *o*-C*H*). Pale yellow crystals suitable for X-ray crystallographic analysis were grown from a concentrated CH_2Cl_2 solution layered with hexanes (Unit Cell: a = 13.89 Å, b = 12.06 Å, c = 17.23 Å, α = 90°, β =

103.56°, γ = 90°). These unit cell parameters matched those previously reported for this material.[46]

7.4.14 Reaction of [U(NR$_2$)$_3$] with Ph$_3$CSSCCPh$_3$

To a purple solution of [U(NR$_2$)$_3$] (13.3 mg, 0.018 mmol) in benzene-d_6 (0.5 mL) was added a solution of Ph$_3$CSSCCPh$_3$ (5.2 mg, 0.009 mmol) in benzene-d_6 (0.5 mL). A color change to orange was observed immediately upon addition. After 5 min, a ^{1}H NMR spectrum was obtained, revealing the formation of [U(NR$_2$)$_3$]$_2$(μ-S) and Gomberg's dimer, along with unreacted Ph$_3$CSSCCPh$_3$. ^{1}H NMR (400 MHz, 25 °C, benzene-d_6): δ -6.83 (br s, 54H, [U(NR$_2$)$_3$]$_2$(μ-S) N(Si(C*H*$_3$)$_3$)$_2$,), 4.92 (m, 1H, allylic, Gomberg's dimer), 5.93 (m, 2H, vinylic, Gomberg's dimer), 6.44 (m, 2H, vinylic, Gomberg's dimer), 6.96-7.4 (m, aryl C*H*, overlapping signals for Gomberg's dimer and Ph$_3$CSSCCPh$_3$).

7.4.15 Reaction of [K(18-crown-6)][U(S)(NR$_2$)$_3$] (2.1) with Ph$_3$CSSCPh$_3$

To an orange solution of [K(18-crown-6)][U(S)(NR$_2$)$_3$] (10.6 mg, 0.01 mmol) in tetrahydrofuran-d_8 (0.5 mL), in an NMR tube fitted with a J-Young valve, was added a solution of Ph$_3$CSSCCPh$_3$ (3.0 mg, 0.005 mmol) in tetrahydrofuran-d_8 (0.5 mL). This solution was allowed to stand for 3 d, whereupon a ^{1}H NMR spectrum was recorded, which revealed the formation of **7.4**, Gomberg's dimer, and triphenylmethane. ^{1}H NMR (400 MHz, 25 °C, tetrahydrofuran-d_8): δ -8.56 (br s, 54H, **7.4** N(Si(C*H*$_3$)$_3$)$_2$), -2.64 (br s, 54H, [K(18-crown-6)][U(S)(NR$_2$)$_3$], N(Si(C*H*$_3$)$_3$)$_2$)), 3.15 (br s, 24H, **7.4** 18-crown-6), 5.18 (m, 1H, allylic, Gomberg's dimer), 5.57 (s, 1H, *H*CPh$_3$), 5.94 (m, 2H, vinylic, Gomberg's dimer), 6.21-6.23 (m, 2H, vinylic, Gomberg's dimer), 6.9-7.4 (m, aryl C*H*, overlapping signals for Gomberg's dimer and triphenylmethane).

7.4.16 X-ray Crystallography

Data for **7.3**, and **7.4** were collected on a Bruker KAPPA APEX II diffractometer equipped with an APEX II CCD detector using a TRIUMPH monochromator and a Mo Kα X-ray source (α = 0.71073 Å). The crystals were mounted on a cryoloop under Paratone-N oil, and all data were collected at 100(2) K using an Oxford nitrogen gas cryostream. Data were collected using ω scans with 0.5° frame widths. Frame exposures of 2 s (low angle) and 5 s (high angle) were used for **7.3**. Frame exposures of 10 s were used for **7.4**. Data collection and cell parameter determinations were conducted using the SMART program.[48] Integration of the data frames and final cell parameter refinement were performed using SAINT software.[49] Absorption correction of the data was carried out using the multi-scan method SADABS.[50] Subsequent calculations were carried out using SHELXTL.[51] Structure determinations were done using direct or Patterson methods and difference Fourier techniques. All hydrogen atom positions were idealized, and rode on the atom of attachment. Structure solution, refinement, graphics, and creation of publication materials were performed using SHELXTL.[51]

Table 7.1. X-ray Crystallographic Data for Complexes **7.3** and **7.4**

	7.3	**7.4**
empirical formula	$C_{18}H_{53}N_3TeSi_6U$	$C_{26}H_{74}KN_3O_2S_2Si_6U$
crystal habit, color	needle, orange-red	block, orange
crystal size (mm)	0.1 × 0.05 × 0.02	0.2 × 0.1 × 0.05
space group	$P\bar{1}$	$P2_1/c$
volume (Å^3)	1672.15(8)	4594.6(6)
a (Å)	8.3155(2)	15.629(1)
b (Å)	11.8276(3)	20.397(2)
c (Å)	17.5749(5)	14.649(1)
α (deg)	88.157(1)	90.00
β (deg)	89.051(1)	100.297(4)
γ (deg)	75.447(1)	90.00
Z	2	4
formula weight (g/mol)	845.78	970.67
density (calculated) (Mg/m^3)	1.680	1.403
absorption coefficient (mm^{-1})	5.935	3.895
F_{000}	820	1976
total no. reflections	38455	52766
unique reflections	16143	11508
R_{int}	0.0260	0.0298
final R indices (I >2σ(I)]	R_1 = 0.0213 wR_2 = 0.0464	R_1 = 0.0174 wR_2 = 0.0385
largest diff. peak and hole (e$^-$ A^{-3})	2.450 and -0.810	0.845 and -0.494
GOF	0.979	1.020

7.5 Appendix

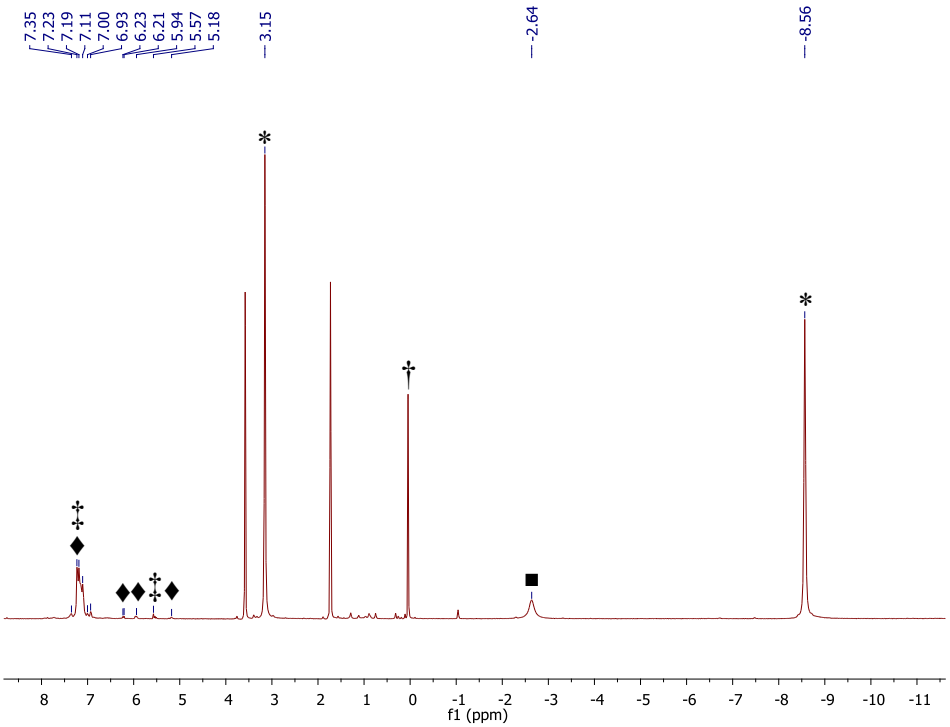

Figure A7.1. In situ ^{1}H NMR spectrum of the reaction of [K(18-crown-6)][U(S)(NR$_2$)$_3$] with 0.5 equiv of Ph$_3$CSSCPh$_3$ in tetrahydrofuran-d_8, after 3 d. (*) indicates the presence of complex **6.1**, (■) indicates the presence of unreacted [K(18-crown-6)][U(S)(NR$_2$)$_3$], (♦) indicates the presence of Gomberg's dimer, (†) indicates the presence of HN(SiMe$_3$)$_2$, (‡) indicates the presence of triphenylmethane.

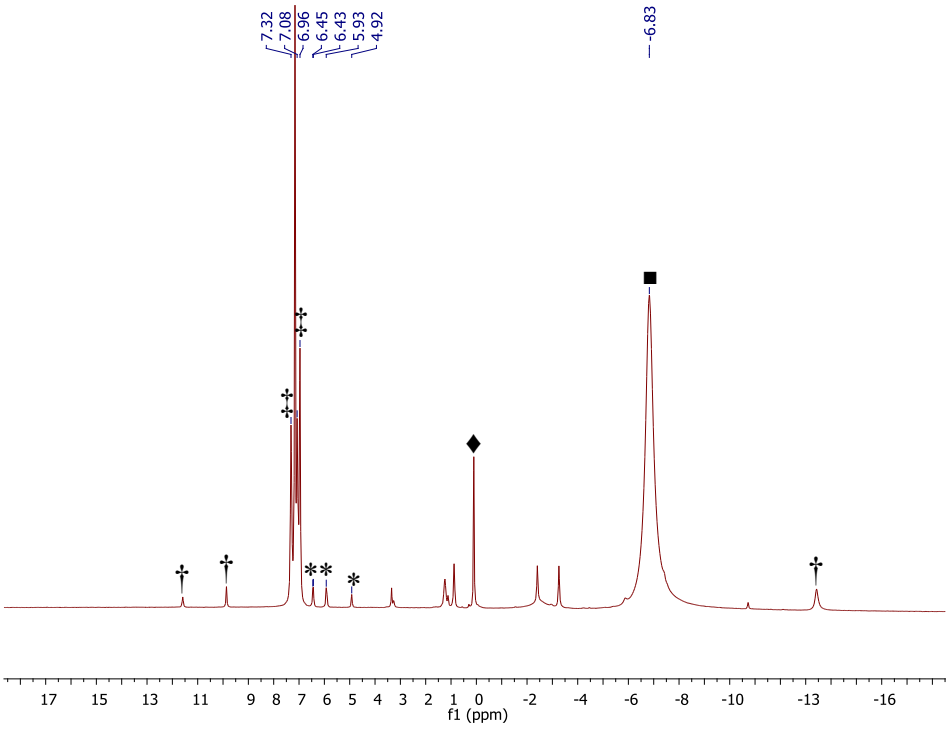

Figure A7.2. In situ ^{1}H NMR spectrum of the reaction of $[U(NR_2)_3]$ and 0.5 equiv of $Ph_3CSSCPh_3$ in benzene-d_6 after 5 min. (*) indicates the presence of Gomberg's dimer, (■) indicates the presence of $[U(NR_2)_3]_2(\mu\text{-S})$, (♦) indicates the presence of $HN(SiMe_3)_2$, (†) indicates the presence of $[U(CH_2SiMe_2NSiMe_3)(NR_2)_2]$, an impurity in the starting material, and (‡) indicates the presence of unreacted $Ph_3CSSCPh_3$.

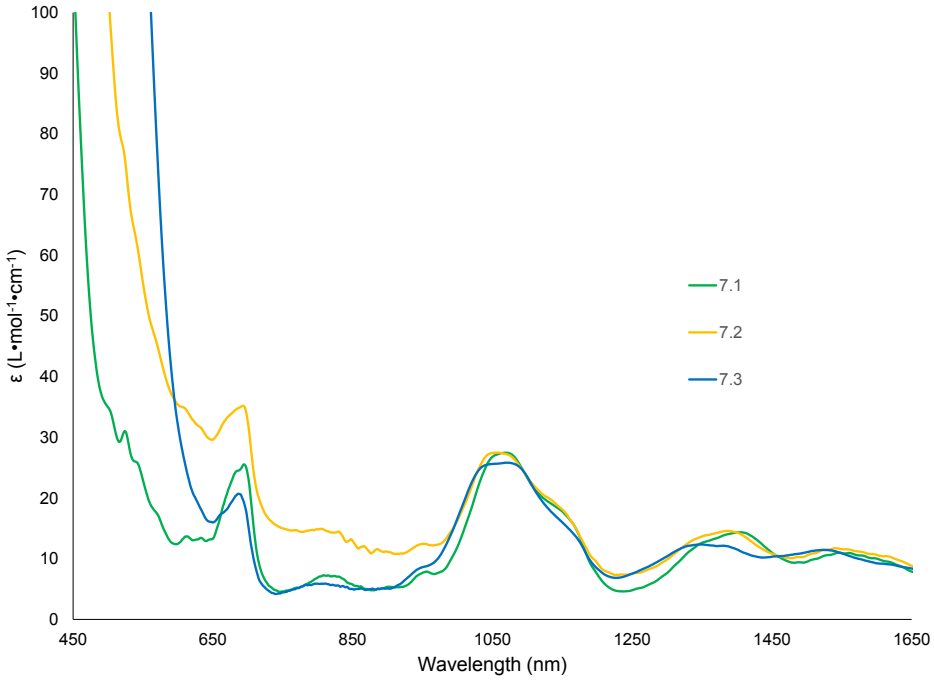

Figure A7.3. NIR Spectra of Complexes **7.1**, **7.2**, and **7.3**. Concentration (mM) in C_4H_8O: **7.1**, 4.98; **7.2**, 5.36; **7.3**, 4.91.

7.6 References

(1) Dam, H. H.; Reinhoudt, D. N.; Verboom, W. *Chem. Soc. Rev.* **2007**, *36*, 367.
(2) Nash, K. L. *Solvent Extr. Ion Exch.* **1993**, *11*, 729.
(3) Ionova, G.; Ionov, S.; Rabbe, C.; Hill, C.; Madic, C.; Guillaumont, R.; Krupa, J. C. *Solvent Extr. Ion. Exch.* **2001**, *19*, 391
(4) Lewis, F. W.; Hudson, M. J.; Harwood, L. M. *Synlett* **2011**, *2011*, 2609.
(5) Modolo, G.; Odoj, R. *J. Alloys Compounds* **1998**, *271–273*, 248.
(6) Arnold, P. L.; Turner, Z. R.; Kaltsoyannis, N.; Pelekanaki, P.; Bellabarba, R. M.; Tooze, R. P. *Chem. Eur. J.* **2010**, *16*, 9623.
(7) Neidig, M. L.; Clark, D. L.; Martin, R. L. *Coord. Chem. Rev.* **2013**, *257*, 394.
(8) Ingram, K. I. M.; Tassell, M. J.; Gaunt, A. J.; Kaltsoyannis, N. *Inorg. Chem.* **2008**, *47*, 7824.
(9) Kaltsoyannis, N. *Inorg. Chem.* **2013**, *52*, 3407.
(10) Ingram, K. I. M.; Kaltsoyannis, N.; Gaunt, A. J.; Neu, M. P. *J. Alloys Compd.* **2007**, *444–445*, 369.
(11) Jensen, M. P.; Bond, A. H. *J. Am. Chem. Soc.* **2002**, *124*, 9870.
(12) Ephritikhine, M. *Coord. Chem. Rev.* **2016**, *319*, 35.
(13) Jones, M. B.; Gaunt, A. J. *Chem. Rev.* **2013**, *113*, 1137.
(14) Hayton, T. W. *Chem. Commun.* **2013**, *49*, 2956.
(15) Smiles, D. E.; Wu, G.; Kaltsoyannis, N.; Hayton, T. W. *Chem. Sci.* **2015**, *6*, 3891.
(16) Smiles, D. E.; Wu, G.; Hayton, T. W. *Inorg. Chem.* **2014**, *53*, 10240.
(17) Smiles, D. E.; Wu, G.; Hayton, T. W. *Inorg. Chem.* **2014**, *53*, 12683.
(18) Smiles, D. E.; Wu, G.; Hayton, T. W. *J. Am. Chem. Soc.* **2014**, *136*, 96.
(19) Smiles, D. E.; Wu, G.; Hrobárik, P.; Hayton, T. W. *J. Am. Chem. Soc.* **2016**, *138*, 814.
(20) Andrez, J.; Pecaut, J.; Scopelliti, R.; Kefalidis, C. E.; Maron, L.; Rosenzweig, M. W.; Meyer, K.; Mazzanti, M. *Chem. Sci.* **2016**.
(21) Camp, C.; Antunes, M. A.; Garcia, G.; Ciofini, I.; Santos, I. C.; Pecaut, J.; Almeida, M.; Marcalo, J.; Mazzanti, M. *Chem. Sci.* **2014**, *5*, 841.
(22) Rosenzweig, M. W.; Scheurer, A.; Lamsfus, C. A.; Heinemann, F. W.; Maron, L.; Andrez, J.; Mazzanti, M.; Meyer, K. *Chem. Sci.* **2016**.
(23) Brown, J. L.; Fortier, S.; Lewis, R. A.; Wu, G.; Hayton, T. W. *J. Am. Chem. Soc.* **2012**, *134*, 15468.
(24) Brown, J. L.; Wu, G.; Hayton, T. W. *Organometallics* **2013**, *32*, 1193.
(25) Matson, E. M.; Goshert, M. D.; Kiernicki, J. J.; Newell, B. S.; Fanwick, P. E.; Shores, M. P.; Walensky, J. R.; Bart, S. C. *Chem. Eur. J.* **2013**, *19*, 16176.
(26) Franke, S. M.; Heinemann, F. W.; Meyer, K. *Chem. Sci.* **2014**, *5*, 942.
(27) Lam, O. P.; Heinemann, F. W.; Meyer, K. *Chem. Sci.* **2011**, *2*, 1538.
(28) Wrobleski, D. A.; Cromer, D. T.; Ortiz, J. V.; Rauchfuss, T. B.; Ryan, R. R.; Sattelberger, A. P. *J. Am. Chem. Soc.* **1986**, *108*, 174.
(29) Brennan, J. G.; Andersen, R. A.; Zalkin, A. *Inorg. Chem.* **1986**, *25*, 1761.
(30) Franke, S. M.; Rosenzweig, M. W.; Heinemann, F. W.; Meyer, K. *Chem. Sci.* **2015**, *6*, 275.
(31) Simpson, S. J.; Andersen, R. A. *J. Am. Chem. Soc.* **1981**, *103*, 4063.
(32) Dormond, A.; El Bouadili, A. A.; Moise, C. *J. Chem. Soc. Chem. Commun.* **1985**, 914.

(33) Dormond, A.; Aaliti, A.; Moise, C. *J. Org. Chem.* **1988**, *53*, 1034.
(34) Dormond, A.; Elbouadili, A.; Moise, C. *J. Org. Chem.* **1989**, *54*, 3747.
(35) Dormond, A.; Aaliti, A.; Elbouadili, A.; Moise, C. *J. Organomet. Chem.* **1987**, *329*, 187.
(36) Dormond, A.; El Bouadili, A.; Aaliti, A.; Moise, C. *J. Organomet. Chem.* **1985**, *288*, C1.
(37) Dormond, A.; Elbouadili, A.; Moïse, C. *J. Organomet. Chem.* **1989**, *369*, 171.
(38) Fortier, S.; Brown, J. L.; Kaltsoyannis, N.; Wu, G.; Hayton, T. W. *Inorg. Chem.* **2012**, *51*, 1625.
(39) Evans, W. J.; Miller, K. A.; Ziller, J. W.; DiPasquale, A. G.; Heroux, K. J.; Rheingold, A. L. *Organometallics* **2007**, *26*, 4287.
(40) Evans, W. J.; Miller, K. A.; Kozimor, S. A.; Ziller, J. W.; DiPasquale, A. G.; Rheingold, A. L. *Organometallics* **2007**, *26*, 3568.
(41) Lescop, C.; Arliguie, T.; Lance, M.; Nierlich, M.; Ephritikhine, M. *J. Organomet. Chem.* **1999**, *580*, 137.
(42) Evans, W. J.; Takase, M. K.; Ziller, J. W.; DiPasquale, A. G.; Rheingold, A. L. *Organometallics* **2009**, *28*, 236.
(43) Turner, H. W.; Andersen, R. A.; Zalkin, A.; Templeton, D. H. *Inorg. Chem.* **1979**, *18*, 1221.
(44) Chen, C.; Lee, H.; Jordan, R. F. *Organometallics* **2010**, *29*, 5373.
(45) Oba, M.; Tanaka, K.; Nishiyama, K.; Ando, W. *J. Org. Chem.* **2011**, *76*, 4173.
(46) Ostrowski, M.; Jeske, J.; Jones, P. G.; Mont, W.-W. D. *Chem. Ber.* **1993**, *126*, 1355.
(47) Avens, L. R.; Bott, S. G.; Clark, D. L.; Sattelberger, A. P.; Watkin, J. G.; Zwick, B. D. *Inorg. Chem.* **1994**, *33*, 2248.
(48) *SMART Apex II*, Version 2.1. 2005
(49) *SAINT Software User's Guide*, Version 7.34a. 2005
(50) *SADABS*, 2005
(51) *SHELXTL PC*, Version 6.12. 2005

Chapter 8 Synthesis, Electrochemistry, and Reactivity of Actinide Trisulfides

Table of Contents

8.1 Introduction

The great diversity exhibited by chalcogenide ligands is not only limited to transition metal complexes,[1-5] but seen in actinide chalcogenide complexes as well.[6] These include an array of multimetallic complexes with bridging chalcogenides such as, $[(({}^{Ad}ArO)_3N)U]_2(\mu\text{-}E)_2$ (E = S, Se, Te), reported by Meyer and co-workers in 2011,[7] and $[U(NR_2)_3]_2(\mu\text{-}S)$ and $[U(NR_2)_3]_2(\mu\text{-}\eta^2\text{:}\eta^2\text{-}S_2)$, reported by Hayton and co-workers in 2013,[8] among many others.[7,9-13] In addition, various types of actinide terminal chalcogenides have also been reported.[9,14-19] For example, Bart and co-workers reported the synthesis and characterization of the U(IV) dichalcogenides, $[Tp^*_2U(\eta^2\text{-}E_2)]$ (Tp^* = hydrotris(3,5-dimethylpyrazolyl)borate); E = S, Se),[17] and Hayton and co-workers reported the isolation of a series of U(IV) monochalcogenides, $[Ph_3PCH][U(E)(NR_2)_3]$ (E = S, Se, Te).[18] Additionally, Mazzanti and co-workers reported the synthesis of a U(V) persulfide complex, $[U(\eta^2\text{-}S_2)((SiMe_2NPh)_3\text{-tacn})]$.[9]

Interestingly, one ligand has not yet been isolated is the trisulfur radical anion, $[S_3]^{\bullet-}$.[20,21] While this species is best known for being responsible for the blue color of the mineral *lapis lazuli*,[22-24] this fragment has actually been observed on various other occasions.[20,25] For example, evidence for the formation of $[S_3]^{\bullet-}$ is observed during the discharge of Li-S batteries.[26-30] In addition, $[S_3]^{\bullet-}$ has also been hypothesized to be the active S-atom source in a number of reactions that incorporate sulfur into organic substrates.[31-33] Nevertheless, the closely related $[S_3]^{2-}$ ligand has been isolated in a number of transition metal complexes.[34-40] This ligand has been observed bridging multiple metal centers like in $[(Cp^*Rh)_4(\mu_3\text{-}S_2)_2(\mu_4\text{-}S_3)][CuCl_2]_2$,[34] and as a terminal ligand in $[Cp^*_2M(\kappa^2\text{-}S_3)]$ (M = Ti, Zr, Hf).[36-38] Actinide

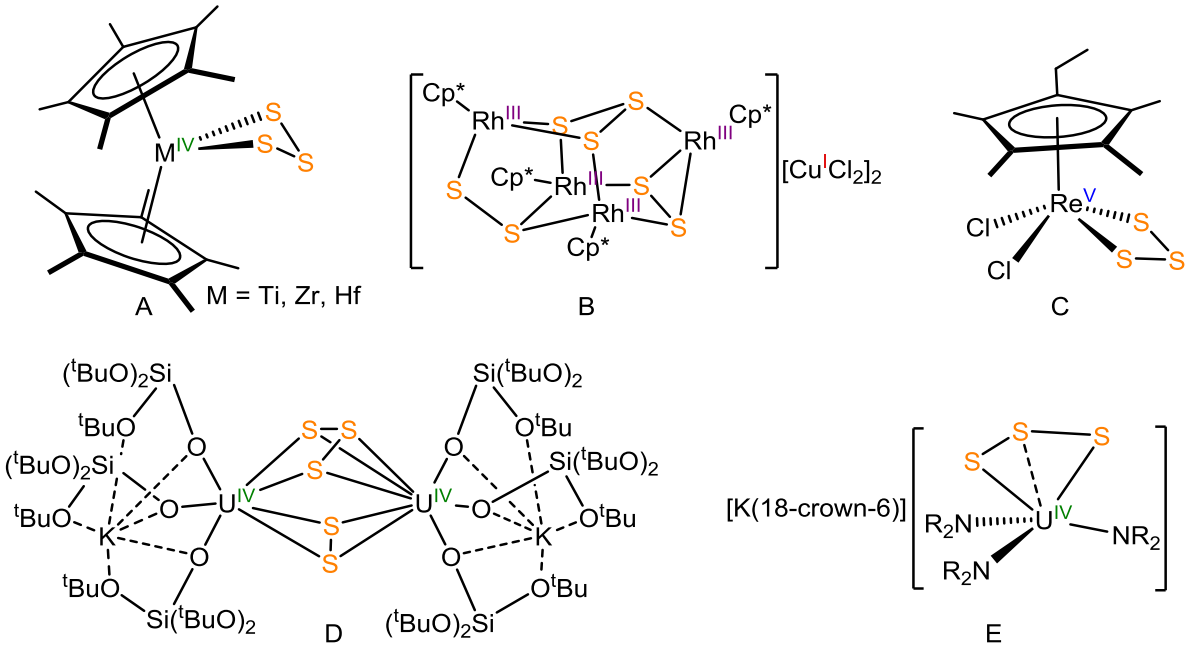

Figure 8.1. Complexes with an $[S_3]^{2-}$ ligand. A, Refs. 36-38; B, Ref. 34; C, Ref. 35; D, Ref. 15; E, Ref. 41.

examples are extremely uncommon. The only two that have been reported are $[K(U(OSi(O^tBu)_3)_3)]_2(\mu\text{-}S_2)(\mu\text{-}S_3)$,[15] featuring a bridging $[S_3]^{2-}$ ligand, that could only be isolated as a crude mixture of products, and $[K(18\text{-crown-6})][U(\eta^3\text{-}S_3)(NR_2)_3]$ (**6.3**),[41] featuring a terminal $[\eta^3\text{-}S_3]^{2-}$ ligand, which was discussed in Chapter 6.

This chapter describes the synthesis of the first thorium complex with an $[S_3]^{2-}$ ligand. Furthermore, the electrochemistry of this complex along with its uranium analogue, complex **6.3**, are investigated as a way to access the elusive $[S_3]^{\bullet-}$ ligand. These results along with those of chemical oxidation experiments are detailed. Additionally, the results are discussed with respect the stability and coordinative ability of this species and compared to what has been previously reported for the $[S_3]^{\bullet-}$ ligand.

8.2 Results and Discussion

8.2.1 Synthesis and Characterization of [K(18-crown-6)][Th(η^3-S_3)(NR_2)$_3$] (8.1)

The synthesis of [K(18-crown-6)][U(η^3-S_3)(NR_2)$_3$] (**6.2**), via the reaction of [U(I)(NR_2)$_3$][42] and [K(18-crown-6)]$_2$[S_4] (**6.4**), and the availability of the [Th(I)(NR_2)$_3$] (**3.3**) suggested that the analogous thorium complex could also be accessed. This was then pursued in order to study the reactivity of both complexes in conjunction. Thus, reaction of [Th(I)(NR_2)$_3$] (**3.3**) with 1 equiv of [K(18-crown-6)]$_2$[S_4] (**6.4**) in THF affords a pale green-yellow solution. From this, the thorium trisulfide, [K(18-crown-6)][Th(η^3-S_3)(NR_2)$_3$] (**8.1**), can be isolated as a green-yellow crystalline solid in 53% yield, after crystallization from diethyl ether (Scheme 8.1). Similar to what was observed in the synthesis of the analogous uranium trisulfide, **6.2**, only the observed [η^3-S_3]$^-$ moiety only accounts for three of the sulfur atoms from [K(18-crown-6)]$_2$[S_4] (**6.4**). The fourth atom is likely ejected as 0.125 equiv of S_8, and is likely a result of presence of the sterically bulky silylamide ligands. The ^{1}H NMR spectrum of complex **8.1** features two resonances at 0.73 and 3.16 ppm, assignable to the methyl groups of the silylamide ligands and the methylene groups of the 18-crown-6 moiety respectively.

Scheme 8.1 Synthesis of [K(18-crown-6)][Th(η^3-S_3)(NR_2)$_3$] (**8.1**)

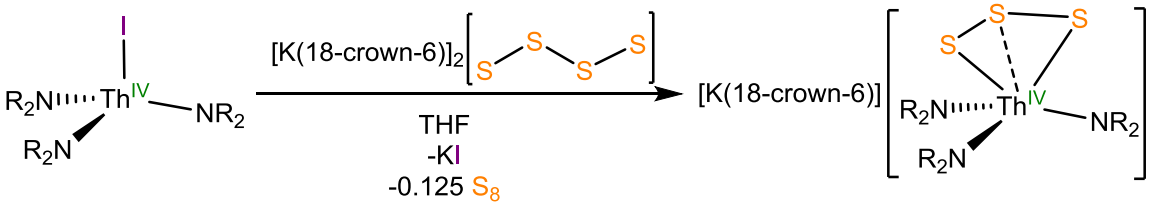

Complex **8.1** crystallizes in the triclinic spacegroup $P\bar{1}$ as a diethyl ether solvate, **8.1**·Et_2O, and its solid state molecular structure is shown in Figure 8.2. **8.1** is isostructural to its uranium

analogue, **6.2**. It features a distorted pseudotetrahedral geometry about thorium, with asymmetric Th-S bond distances (Th1-S1 = 2.9224(9), Th1-S2 = 2.8679(9), Th1-S3 = 2.811(1) Å) and N-Th-N angles (N1-Th1-N2 = 96.2(1)°, N2-Th1-N3 = 107.4(1)°, N1-Th1-N3 = 122.0(1)°). These are attributed to the steric clash between the large $[\eta^3\text{-}S_3]^-$ and $[NR_2]^-$ ligands. Lastly, the S-S bond distances of **8.1** () are comparable to those of complex **6.2**, other actinide polysulfide complexes,[8,9,17,41,43-47] and $Cp^*_2M(\kappa^2\text{-}S_3)$ (M = Ti, Zr, Hf).[36-38]

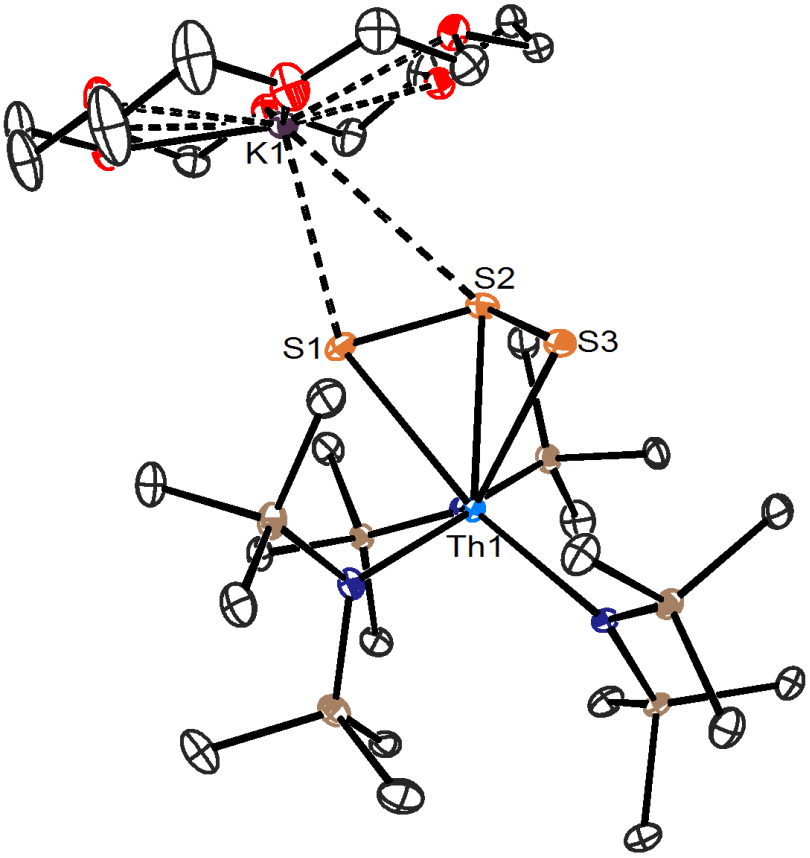

Figure 8.2. ORTEP diagram of $[K(18\text{-crown-6})][Th(\eta^3\text{-}S_3)(NR_2)_3]$ (**8.1**·Et_2O) with 50% probability ellipsoids. Diethyl ether solvate and hydrogen atoms are omitted for clarity. Selected bond lengths (Å) and angles (deg): Th1-S1 = 2.9224(9), Th1-S2 = 2.8679(9), Th1-S3 = 2.811(1), S1-K1 = 3.172(1), S2-K1 = 3.760(1), S1-S2 = 2.062(1), S2-S3 = 2.072(1), N1-Th1-N2 = 96.2(1), N2-Th1-N3 = 107.4(1), N1-Th1-N3 = 122.0(1).

8.2.2 Cyclic Voltammetry of [K(18-crown-6)][M(η^3-S_3)(NR_2)$_3$] (M = U, 6.2; Th, 8.1)

The ability of complexes **6.2** and **8.1** to stabilize the $[S_3]^{2-}$ moiety as a ligand spurred investigation into the possibility of also stabilizing the $[S_3]^{\bullet-}$ radical anion, which could be readily accessed via a $1e^-$ oxidation of either of these complexes. Investigation of the electrochemistry of complexes **6.2** and **8.1** was done using cyclic voltammetry. The cyclic voltammogram of **6.2** in THF features a quasi-reversible oxidation feature at -0.61 V (vs. Fc/Fc^+), while complex **8.1** features an irreversible oxidation feature at -0.52 V (vs. Fc/Fc^+ at 200 mV/s) (Figure 8.3). This feature remains irreversible at all scan rates (Figure A8.4). This

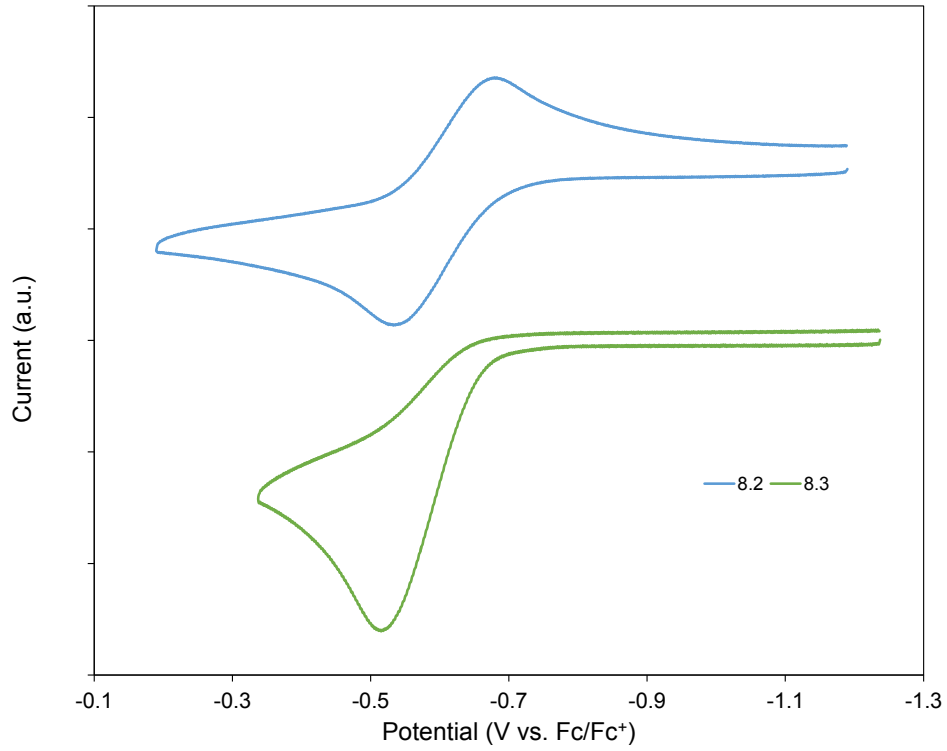

Figure 8.3. Partial cyclic voltammograms of complexes **8.2** and **8.3** in THF vs. Fc/Fc^+. Scan rate 200 mV/s, 0.1 M $[NBu_4][BPh_4]$ as supporting electrolyte.

irreversible feature is attributable to the $[S_3]^{2-}/[S_3]^{\bullet-}$ oxidation, due to the inability of complex **8.1** to experience metal based redox chemistry. Consequently, the quasi-reversible feature

observed for **6.2** can be attributed to a U(IV)/U(V) oxidation. Furthermore, an irreversible reduction feature at -2.99 V (vs. Fc/Fc^+ at 200 mV/s) is seen in the cyclic voltammogram of complex **6.2**, which is designated to be a U(IV)/U(III) reduction (Figure A8.1). The absence of a similar feature in the cyclic voltammogram of complex **8.1** supports this assignment (Figure A8.4). Taken together these data imply that the $[S_3]^{\bullet-}$ moiety is produced, but it is likely unstable under the experimental conditions. For comparison, the $[S_3]^{2-}/[S_3]^{\bullet-}$ couple was previously reported at -1.77 V (vs. Fc/Fc^+),[48] and the difference observed is likely due to coordination to the Th(IV) metal center. Thus, the stabilization of this species as evidenced by the shift in redox potential suggests that, with the right ligand scaffold, the $[S_3]^{\bullet-}$ species could indeed be isolated. This promising observation suggests that more work should be done in this area.

8.2.3 Chemical Oxidation of [K(18-crown-6)][M(η^3-S_3)(NR_2)$_3$] (M = U, 6.2; Th, 8.1)

Chemical oxidation of complexes **6.2** and **8.1** was then explored as a means to generate and isolate a complex with an $[S_3]^{\bullet-}$ ligand. Accordingly, oxidation of complex **6.2** with 1 equiv of AgOTf in THF affords an orange solution concomitant with the formation of a black precipitate. The U(IV) triflate, [K(18-crown-6)][U($OTf)_2$(NR_2)$_3$] (**8.2**), was isolated from this mixture as the only identifiable product. Crystallization from diethyl ether affords complex **8.2** as colorless crystals in 16% yield (Scheme 8.2). Likewise, oxidation of complex **8.1** with 1 equiv of AgOTf, in THF, affords the Th(IV) triflate, [K(18-crown-6)][Th($OTf)_2$(NR_2)$_3$] (**8.3**), as the only identifiable product. Crystallization from diethyl ether affords 8.3 as a colorless crystalline solid in 21% yield (Scheme 8.2). Both **8.2** and **8.3** are likely formed via

exchange of the $[S_3]^{\bullet-}$ moiety with $[OTf]^-$, and subsequent incorporation of 1 equiv of KOTf into the final product. Because of this the maximum yield that can be obtained is only 50%.

Scheme 8.2 Oxidation of $[K(18\text{-crown-}6)][M(\eta^3\text{-}S_3)(NR_2)_3]$ (M = U, **6.2**; Th, **8.1**) with AgOTf

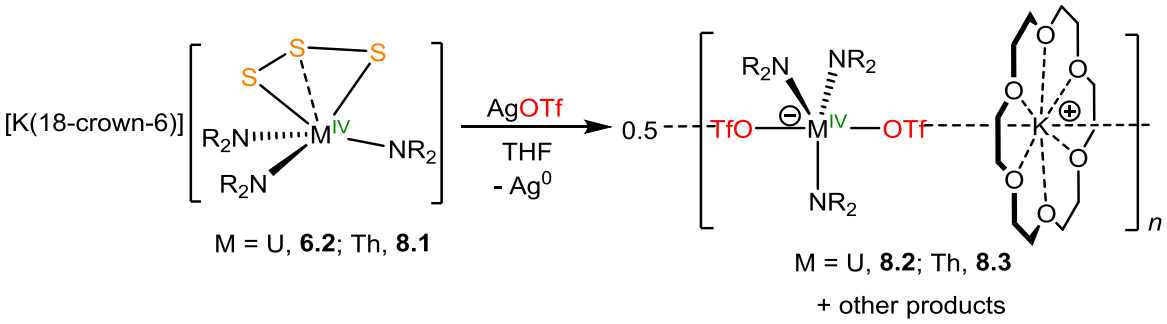

The fate of the $[S_3]^{\bullet-}$ species is currently unknown. At no point during the reaction is the distinctive blue color of the $[S_3]^{\bullet-}$ anion observed. Furthermore, other oxidants, including $[Fc][PF_6]$ and $[Fc][BPh_4]$, were also unsuccessful at generating a complex with an $[S_3]^{\bullet-}$ ligand from either complexes **6.2** or **8.1**.

8.2.4 Structural and Spectroscopic Characterization of $[K(18\text{-crown-}6)][M(OTf)_2(NR_2)_3]$ (M = U, 8.2; Th, 8.3)

Complexes **8.2** and **8.3** crystallize in the monoclinic spacegroup $P2_1/n$ and the triclinic spacegroup $P\bar{1}$, respectively, and their solid state molecular structures are shown in Figure 8.4. Both complexes crystallizes as diethyl ether solvates, **8.2**·Et_2O and **8.3**·Et_2O, and are 1-dimensional coordination polymers, with $[K(18\text{-crown-}6)]^+$ cations bridging two $[OTf]^-$ moieties, in the solid state. Both complexes feature trigonal bipyramidal geometries about the metal center (**8.2**: O1-U1-O4 = 174.0(3)°, av. N-U-N = 120.0°, av. N-U-O = 90.2°; **8.3**: O1-Th1-O4 = 171.7(4)°, av. N-Th-N = 120.0°, av. N-Th-O = 90.2°). The M-N bond distances of **8.2** (av. 2.25 Å) and **8.3** (av. 2.34 Å) are comparable to those of other U(IV) and Th(IV)

complexes with a similar geometry and ligand framework.[49-52] Additionally, the U-O bond lengths of **8.2** (U1-O1 = 2.402(7), U1-O4 = 2.374(7) Å) are shorter than the analogous Th-O bond lengths of **8.3** (Th1-O1 = 2.43(1), Th1-O4 = 2.44(1) Å), consistent with the difference in ionic radii between U^{4+} and Th^{4+}.[53]

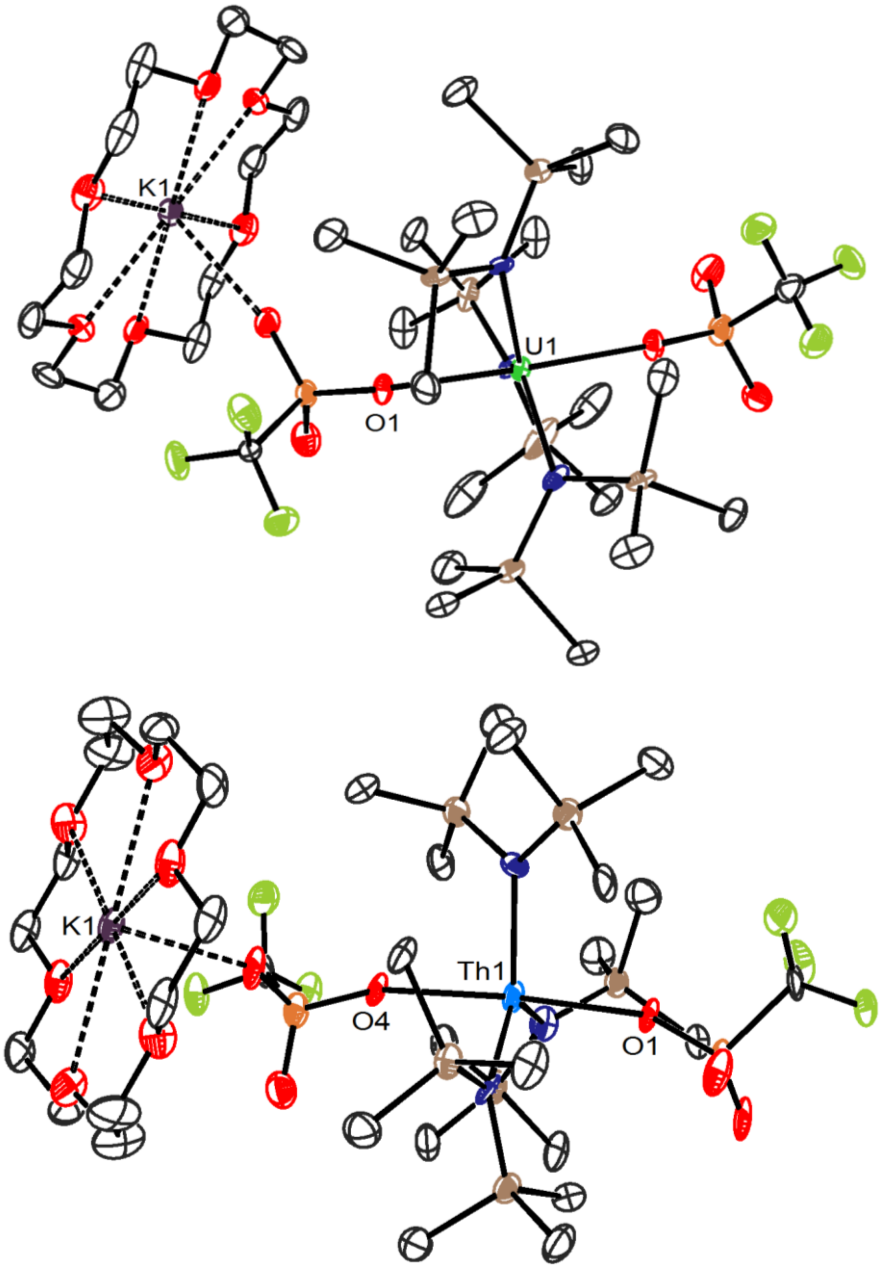

Figure 8.4. ORTEP diagram of [K(18-crown-6)][$U(OTf)_2(NR_2)_3$] (**8.2**·Et_2O) and [K(18-crown-6)][$Th(OTf)_2(NR_2)_3$] (**8.3**·Et_2O) with 50% probability ellipsoids. Diethyl ether solvate

and hydrogen atoms are omitted for clarity. Selected bond lengths (Å) and angles (deg): **8.2**, U1-O1 = 2.402(7), U1-O4 = 2.374(7), U-N (av.) = 2.25, N-U-N (av.) = 120, N-U-O (av.) = 90.2, O1-U1-O4 = 174.0(3); **8.3**, Th1-O1 = 2.43(1), Th1-O4 = 2.44(1), Th-N (av.) = 2.34, N-Th-N (av.) = 120.0, N-Th-O (av.) = 90.2, O1-Th1-O4 = 171.7(4).

In benzene-d_6, the ^{1}H NMR spectrum of complex **8.2** exhibits two resonances, one broad and one sharp, at -1.68 and 3.47 ppm, respectively, assignable to the methyl groups of the silylamide ligands and the methylene groups of the 18-crown-6 moiety. **8.2** also features one broad resonance at -91.50 ppm in its ^{19}F{^{1}H} NMR spectrum, attributable to the fluorines of the [OTf]$^-$ moieties. Similarly, the ^{1}H NMR spectrum of complex **8.3**, in benzene-d_6, features two sharp resonances, at 0.65 and 3.12 ppm, again assignable to the methyl groups of the silylamide ligands and the methylene groups of the 18-crown-6 moiety, respectively. The ^{19}F{^{1}H} NMR spectrum of complex **8.3** features a single sharp resonance at -75.43 ppm assignable to the [OTf]$^-$ moieties.

8.2.5 Reaction of [K(18-crown-6)][Th(η^3-S_3)(NR_2)$_3$] (8.1) with Et_3P

The reactivity of complex **8.1** with phosphines was also explored, in an identical manner to what was done for complex **6.2**. Addition of 2 equiv of Et_3P to a benzene-d_6 solution of **8.1** results in a color change from green-yellow to colorless within 5 min (Scheme 8.3). The in situ ^{1}H and ^{13}C{^{1}H} NMR spectra taken after 15 min reveal the clean formation of the thorium monosulfide, [K(18-crown-6)][Th(S)(NR_2)$_3$] (**3.8**) (Figure A8.5, Figure A8.6). Et_3P=S is also formed in this reaction as evidenced by the growth of a new resonance in the in situ ^{31}P{^{1}H} NMR spectrum (Figure A8.7).[54]

Scheme 8.3 Reaction of [K(18-crown-6)][Th(η^3-S_3)(NR_2)$_3$] (**8.1**) with Et_3P

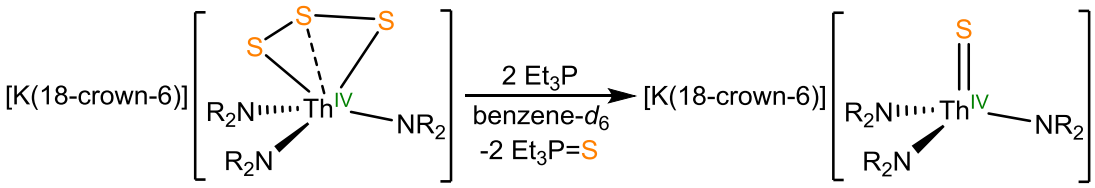

8.3 Summary

In summary, reaction of [Th(I)(NR_2)$_3$] with 1 equiv of [K(18-crown-6)]$_2$[S_4] yields the thorium trisulfide, [K(18-crown-6)][Th(η^3-S_3)(NR_2)$_3$] (**8.1**). Complex **8.1** is isostructural to its uranium analogue, **6.3**, and again features a notable distortion in its geometry attributed to the presence of the large $[\eta^3\text{-}S_3]^{2-}$ ligand in addition to the sterically demanding silylamide ligands. The electrochemistry of complex **8.1** and its uranium analogue, **6.3**, were investigated using cyclic voltammetry, which suggested that stabilization of the $[S_3]^{\bullet-}$ radical anion is possible. Oxidation of complexes **6.3** and **8.1** with AgOTf affords [K(18-crown-6)][M(OTf)$_2$(NR_2)$_3$] (**8.2**, M = U; **8.3**, M = Th), as the only identifiable products.

The results from the chemical oxidation experiments taken in conjunction with the cyclic voltammetry data suggest that if the $[S_3]^{\bullet-}$ ligand is generated, it is readily replaced, even by weak nucleophiles like $[OTf]^-$. This is consistent with previous theoretical studies of the $[S_3]^{\bullet-}$ moiety. The steric clash experienced by the $[S_3]^{2-}$ ligand, most likely felt by the $[S_3]^{\bullet-}$ ligand, together with the lower charge of the latter species, make coordination of this species even more difficult. This could explain a coordination complex with the $[S_3]^{\bullet-}$ ligand is still unknown, and demonstrates the need for alteration of the co-ligands to better stabilize this moiety.

8.4 Experimental

8.4.1 General Methods

All reactions and subsequent manipulations were performed under anaerobic and anhydrous conditions under an atmosphere of nitrogen. Hexanes, Et_2O, toluene, and tetrahydrofuran (THF) were dried using a Vacuum Atmospheres DRI-SOLV Solvent Purification system and stored over 3Å sieves for 24 h prior to use. Benzene-d_6 was dried over 3Å molecular sieves for 24 h prior to use. $[Th(I)(NR_2)_3]$ (**3.3**) ,[49] $[U(I)(NR_2)_3]$,[42] [K(18-crown-6)][$U(\eta^3\text{-}S_3)(NR_2)_3$] (**6.2**),[41] and $[K(18\text{-crown-6})]_2[S_4]$[41] (**6.4**) were synthesized according to the previously reported procedures. $[NBu_4][BPh_4]$ was recrystallized from dichloromethane prior to use. All other reagents were purchased from commercial suppliers and used as received.

NMR spectra were recorded on a Varian UNITY INOVA 400 spectrometer, a Varian UNITY INOVA 500 spectrometer, a Varian UNITY INOVA 600 MHz spectrometer, or an Agilent Technologies 400-MR DD2 400 MHz Spectrometer. ^1H and $^{13}C\{^1H\}$ NMR spectra were referenced to external $SiMe_4$ using the residual protio solvent peaks as internal standards. $^{19}F\{^1H\}$ and $^{31}P\{^1H\}$ NMR spectra were referenced indirectly with the ^1H resonance of $SiMe_4$ at 0 ppm, according to IUPAC standard,[55,56] using the residual solvent peaks as internal standards. IR spectra were recorded on a Nicolet 6700 FT-IR spectrometer with a NXR FT Raman Module. Elemental analyses were performed by the Micro-Analytical Facility at the University of California, Berkeley.

8.4.2 Synthesis of [K(18-crown-6)][Th(η^3-S_3)(NR_2)$_3$] (8.1)

To a colorless, cold (-25 °C), stirring solution of [Th(I)(NR_2)$_3$] (187.8 mg, 0.22 mmol) in THF (4 mL) was added [K(18-crown-6)]$_2$[S_4] (171.5 mg, 0.23 mmol). The color of the solution became pale green-yellow upon addition. This mixture was allowed to stir for 1 h, whereupon the deposition of a white powder was observed. The volatiles were removed in vacuo to afford a green-yellow solid. The resulting solid was then triturated with diethyl ether (3 mL) to give a green-yellow powder. This powder was then extracted with diethyl ether (5 mL) and filtered through a Celite column supported on glass wool (0.5 cm × 3 cm) to afford a very pale green-yellow solution. The volume of the filtrate was reduced to 2 mL in vacuo. Subsequent storage of this solution at -25 °C for 48 h resulted in the deposition of pale green-yellow crystals, which were isolated by decanting the supernatant (124.8 mg, 47%). The volume of the supernatant was then reduced in vacuo to ca. 0.75 mL. This solution was transferred to a 4 mL scintillation vial that was placed inside a 20 mL scintillation vial. Toluene (5 mL) was then added to the outer vial. Storage of this two vial system for 48 h resulted in the deposition of more green-yellow crystals, which were isolated by decanting off the supernatant. Total yield 140.7 mg, 53%. Anal. Calcd for $C_{30}H_{78}KN_3O_6S_3Si_6Th$: C, 32.38; H, 7.07; N, 3.78. Found: C, 32.51; H, 7.20; N, 3.75. ^{1}H NMR (400 MHz, 25 °C, benzene-d_6): δ 0.73 (s, 54H, N(Si(CH_3)$_3$)$_2$), 3.16 (s, 24H, 18-crown-6). ^{13}C{^{1}H} NMR (100 MHz, 25 °C, benzene-d_6): δ 6.80 (N(Si(*C*H$_3$)$_3$)$_2$), 70.15 (18-crown-6). IR (KBr pellet, cm^{-1}): 493 (w), 529 (w), 608 (m), 666 (m), 687 (m), 774 (m), 845 (s), 885 (m), 928 (s), 964 (s), 1058 (w), 1112 (s), 1182 (w), 1249 (s), 1284 (w), 1352 (m), 1401 (w), 1454 (w), 1473 (w).

8.4.3 Reaction of [K(18-crown-6)][U(η^3-S_3)(NR_2)$_3$] (6.2) with AgOTf and isolation of [K(18-crown-6)][U(OTf)$_2$(NR_2)$_3$] (8.2)

To an orange, cold (-25 °C), stirring solution of **6.2** (65.4 mg, 0.058 mmol) in THF (3 mL) was added AgOTf (15.2 mg, 0.059 mmol). The color of the solution immediately darkened, concomitant with the deposition of a black precipitate. After 10 min, the volatiles were removed in vacuo to give a dark brown solid. This material was then triturated with diethyl ether (3 mL). The resulting solids were then extracted with diethyl ether (4 mL) and filtered through a Celite column supported on glass wool (0.5 cm × 3 cm) to afford an orange solution. The volume of the filtrate was reduced to 2 mL in vacuo. Subsequent storage of this solution at -25 °C for 48 h resulted in the deposition of colorless crystals, which were isolated by decanting the supernatant (12.6 mg, 16%). Anal. Calcd for $C_{32}H_{78}F_6KN_3O_{12}S_2Si_6U$: C, 29.10; H, 5.95; N, 3.18. Found: C, 28.99; H, 6.19; N, 3.38. ^{1}H NMR (400 MHz, 25 °C, benzene-d_6): δ -1.68 (s, 54H, N(Si(CH_3)$_3$)$_2$), 3.47 (s, 24H, 18-crown-6). ^{19}F{^{1}H} NMR (376.38 MHz, 25 °C, benzene-d_6): δ -95.10 (br s). IR (KBr pellet, cm^{-1}): 616 (m), 632 (m), 655 (m), 683 (w), 774 (m), 845 (s), 964 (w), 993 (m), 1032 (m), 1111 (m), 1163 (w), 1196 (m), 1254 (s), 1335 (m), 1353 (m), 2901(m), 2958 (m).

8.4.4 Reaction of [K(18-crown-6)][Th(η^3-S_3)(NR_2)$_3$] (8.1) with AgOTf and isolation of [K(18-crown-6)][Th(OTf)$_2$(NR_2)$_3$] (8.3)

To a pale green-yellow, cold (-25 °C), stirring solution of **8.1** (32.8 mg, 0.029 mmol) in THF (3 mL) was added AgOTf (7.5 mg, 0.029 mmol). The color of the solution immediately darkened, concomitant with the deposition of a black precipitate. After 10 min, the volatiles were removed in vacuo to give a dark black solid. This solid was extracted with diethyl ether (3 mL) and filtered through a Celite column supported on glass wool (0.5 cm × 3 cm) to afford

a colorless solution. The volume of the filtrate was reduced to 1.5 mL in vacuo. Subsequent storage of this solution at -25 °C for 48 h resulted in the deposition of colorless crystals, which were isolated by decanting the supernatant (8.3 mg, 21%). Anal. Calcd for $C_{32}H_{78}F_6KN_3O_{12}S_2Si_6Th$: C, 29.23; H, 5.98; N, 3.20. Found C, 29.56; H, 6.25; N, 3.13. ^{1}H NMR (400 MHz, 25 °C, benzene-d_6): δ 0.65 (s, 54H, N(Si(CH_3)$_3$)$_2$), 3.12 (s, 24H, 18-crown-6). ^{19}F{^{1}H} NMR (376.38 MHz, 25 °C, benzene-d_6): δ -75.43 (s). ^{13}C{^{1}H} NMR (100 MHz, 25 °C, benzene-d_6): δ 5.56 (N(Si(*C*H$_3$)$_3$)$_2$), 69.90 (18-crown-6). IR (KBr pellet, cm^{-1}): 511 (w), 519, (w), 617 (m), 633 (s), 667 (m), 777 (m), 851 (s), 894 (s), 964 (m), 990 (s), 1000 (s), 1021 (m), 1033 (m), 1110 (s), 1201 (s), 1253 (s), 1340 (m), 1354 (m), 1456 (w), 1474 (w), 2904 (m), 2956 (m).

8.4.5 Reaction of [K(18-crown-6)][Th(η^3-S$_3$)(NR$_2$)$_3$] (8.1) with Et$_3$P

To a pale green-yellow solution of **8.1** (27.0 mg, 0.024 mmol) in benzene-d_6 (0.75 mL), in an NMR tube fitted with a J-Young valve, was added Et$_3$P (8 μL, 0.054 mmol). A bleaching of the color from green-yellow to colorless was observed within 5 min of addition. After 15 min, ^{1}H, ^{13}C{^{1}H}, and ^{31}P{^{1}H} NMR spectra were recorded, which revealed the clean formation of [K(18-crown-6)][Th(S)(NR$_2$)$_3$] (**2.1**)[49] and Et$_3$P=S.[54] These assignments were confirmed by comparison with the spectra of authentic material. ^{1}H NMR (400 MHz, 25 °C, benzene-d_6): δ 0.72 (s, 54H, N(Si(CH_3)$_3$)$_2$), 0.84-1.01 (m, 9H, overlapping CH_3 of Et$_3$P and Et$_3$P=S), 1.19-1.28 (m, 6H, overlapping CH_2 of Et$_3$P and Et$_3$P=S), 3.18 (s, 24H, 18-crown-6). ^{13}C{^{1}H} (100 MHz, 25 °C, benzene-d_6): δ 5.47 (N(Si(*C*H$_3$)$_3$)$_2$), 6.53 (d, $J_{C\text{-}P}$ = 4.3 Hz, *C*H$_3$ of Et$_3$P=S), 9.88 (d, $J_{C\text{-}P}$ = 13.1 Hz, *C*H$_3$ of Et$_3$P), 19.04 (d, $J_{C\text{-}P}$ = 13.4 Hz, *C*H$_2$ of Et$_3$P), 23.3 (d, $J_{C\text{-}P}$ = 51.5 Hz, *C*H$_2$ of Et$_3$P=S), 70.09 (18-crown-6). ^{31}P{^{1}H} NMR (161.92 MHz, 25 °C, benzene-d_6): δ -19.88 (s, Et$_3$P), 52.85 (s, Et$_3$P=S).

8.4.6 X-ray Crystallography

Data for **8.1**, **8.2**, and **8.3** were collected on a Bruker KAPPA APEX II diffractometer equipped with an APEX II CCD detector using a TRIUMPH monochromator with a Mo Kα X-ray source (α = 0.71073 Å). The crystals were mounted on a cryoloop under Paratone-N oil, and all data were collected at 100(2) K using an Oxford nitrogen gas cryostream. Data were collected using ω scans with 0.5° frame widths. Frame exposures of 10 s were used for **8.1** and **8.3**. Frame exposures of 10 s (low angle) and 15 s (high angle) were used for **8.2**. Data collection and cell parameter determinations were conducted using the SMART program.[57] Integration of the data frames and final cell parameter refinements were performed using SAINT software.[58] Absorption corrections of the data were carried out using the multi-scan method SADABS.[59] Subsequent calculations were carried out using SHELXTL.[60] Structure determination was done using direct or Patterson methods and difference Fourier techniques. All hydrogen atom positions were idealized, and rode on the atom of attachment. Structure solution, refinement, graphics, and creation of publication materials were performed using SHELXTL.[60] The diethyl ether solvate of complex **8.3** exhibited positional disorder and was modeled over two positions in a 50:50 ratio. Hydrogen atoms were not added to disordered carbon atoms.

Table 8.1. X-ray crystallographic data for Complex **8.1**

	8.1·$C_4H_{10}O$
empirical formula	$C_{34}H_{88}KN_3O_6S_3Si_6Th$
crystal habit, color	block, green-yellow
crystal size (mm)	0.2 × 0.1 × 0.1
space group	$P\bar{1}$
volume (Å^3)	2804.7(7)
a (Å)	11.299(2)
b (Å)	12.953(2)
c (Å)	20.985(3)
α (deg)	98.696(2)
β (deg)	97.064(2)
γ (deg)	109.856(2)
Z	2
formula weight (g/mol)	1186.93
density (calculated) (Mg/m^3)	1.405
absorption coefficient (mm^{-1})	3.012
F_{000}	1220
total no. reflections	22547
unique reflections	13635
R_{int}	0.0207
final R indices (I >2σ(I)]	R_1 = 0.0338 wR_2 = 0.0787
largest diff. peak and hole (e$^-$ A^{-3})	8.255 and -1.187
GOF	1.048

Table 8.2. X-ray crystallographic data for complexes **8.2** and **8.3**

	8.2·$C_4H_{10}O$	**8.3**·$C_4H_{10}O$
empirical formula	$C_{36}H_{88}F_6KN_3O_{13}S_2Si_6U$	$C_{36}H_{88}F_6KN_3O_{13}S_2Si_6Th$
crystal habit, color	plate, colorless	plate, colorless
crystal size (mm)	0.2 × 0.1 × 0.1	0.2 × 0.1 × 0.05
space group	$P2_1/n$	$P\bar{1}$
volume (Å^3)	6178(2)	3257(2)
a (Å)	14.095(3)	13.365(5)
b (Å)	23.499(4)	14.225(5)
c (Å)	19.344(4)	18.497(6)
α (deg)	90	102.032(5)
β (deg)	105.370(4)	109.232(5)
γ (deg)	90	96.868(52)
Z	4	2
formula weight (g/mol)	1394.88	1388.89
density (calculated) (Mg/m^3)	1.500	1.416
absorption coefficient (mm^{-1})	2.948	2.594
F_{000}	2840	1416
total no. reflections	40590	28627
unique reflections	13643	14089
R_{int}	0.0679	0.0608
final R indices (I >2σ(I)]	R_1 = 0.0920 wR_2 = 0.1950	R_1 = 0.1166 wR_2 = 0.3035
largest diff. peak and hole (e$^-$ A^{-3})	8.790 and -2.385	12.366 and -4.581
GOF	1.198	1.086

8.4.7 Cyclic Voltammetry

CV experiments were performed with a CH Instruments 600c Potentiostat, and the data were processed using CHI software (version 6.29). All experiments were performed in a glove box using a 20 mL glass vial as the cell. The working electrode consisted of a platinum disk embedded in glass (2 mm diameter), the counter electrode and the reference electrode were a platinum wire. Solutions employed for CV studies were typically 1 mM in analyte, and 0.1 M in $[NBu_4][BPh_4]$. All potentials are reported versus the $[Cp_2Fe]^{0/+}$ couple.

8.5 Appendix

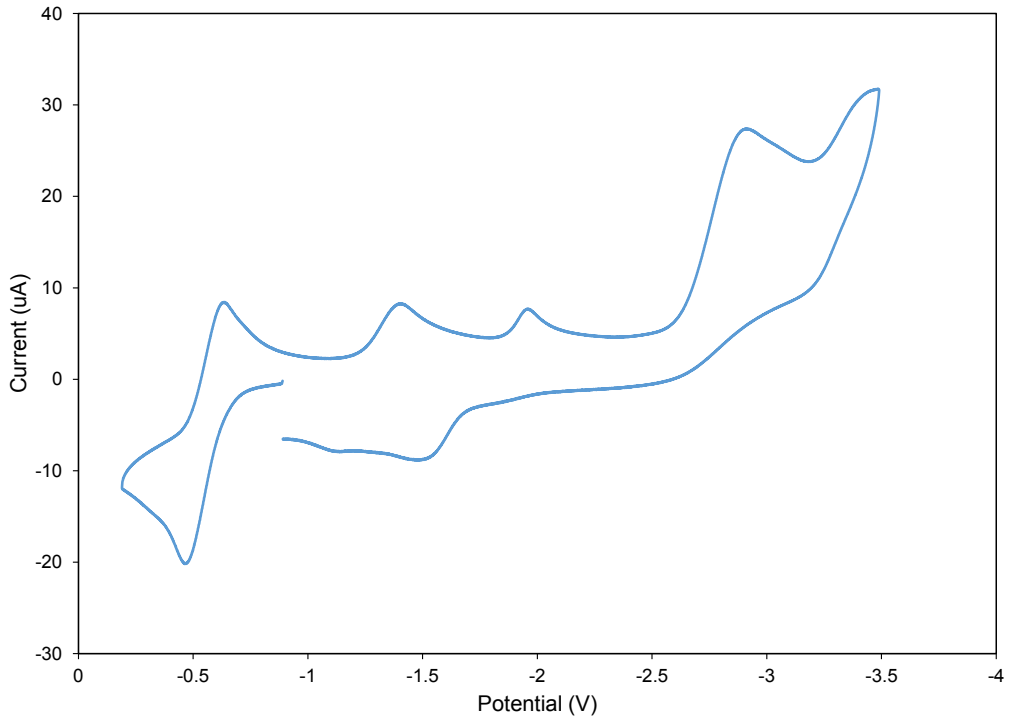

Figure A8.1. Complete cyclic voltammogram of complex **6.2** in THF vs. Fc/Fc^+. Scan rate 200 mV/s, 0.1 M $[NBu_4][BPh_4]$ as supporting electrolyte.

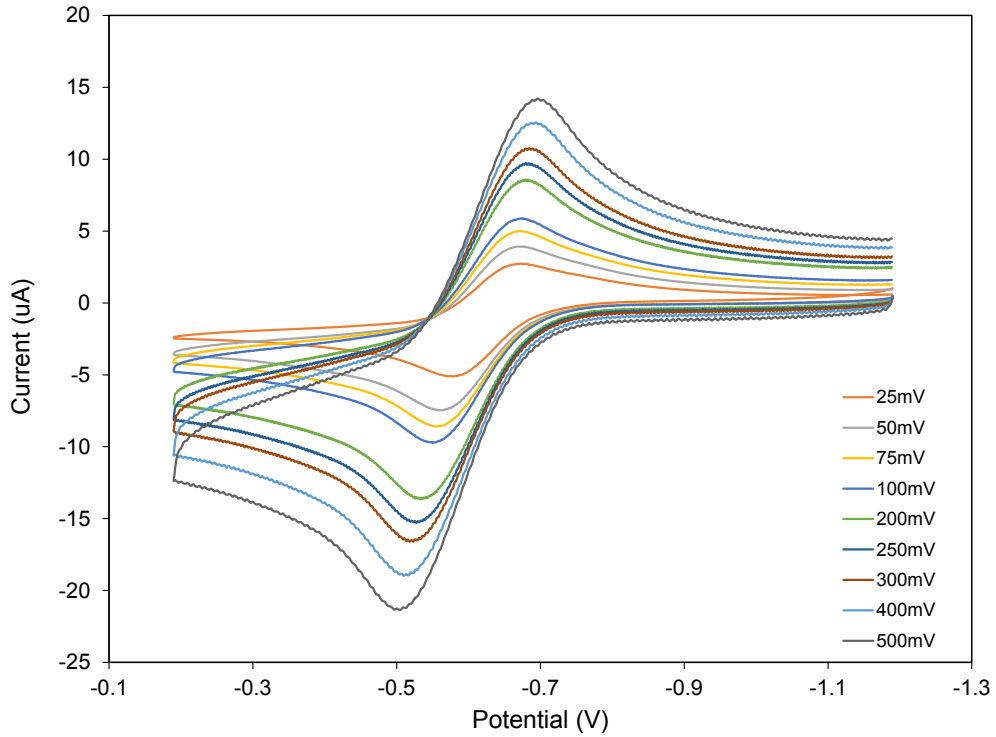

Figure A8.2. Partial cyclic voltammogram of complex **6.2** in THF vs Fc/Fc^{+}. 0.1 M $[NBu_4][BPh_4]$ as supporting electrolyte.

Table A8.1. Electrochemical parameters for $[K(18\text{-crown-6})][U(\eta^3\text{-}S_3)(NR_2)_3]$ (**6.2**) in THF (vs. Fc/Fc^{+}, $[NBu_4][BPh_4]$ as the supporting electrolyte)

Oxidation Feature	Scan rate, V/s	$E_{p,c}$, V	$E_{p,a}$, V	ΔE_p[a]	$i_{p,a}/i_{p,c}$
	0.025	-0.670	-0.579	0.093	1.28
	0.050	-0.669	-0.564	0.105	1.39
	0.075	-0.672	-0.555	0.117	1.33
	0.100	-0.677	-0.551	0.126	1.33
	0.200	-0.679	-0.533	0.146	1.34
	0.250	-0.680	-0.528	0.152	1.34
	0.300	-0.684	-0.524	0.160	1.35
	0.400	-0.694	-0.510	0.184	1.36
	0.500	-0.697	-0.505	0.192	1.38

[a] ΔE_p is defined as the potential difference between the anodic wave and the cathodic wave generated after the change in sweep direction.

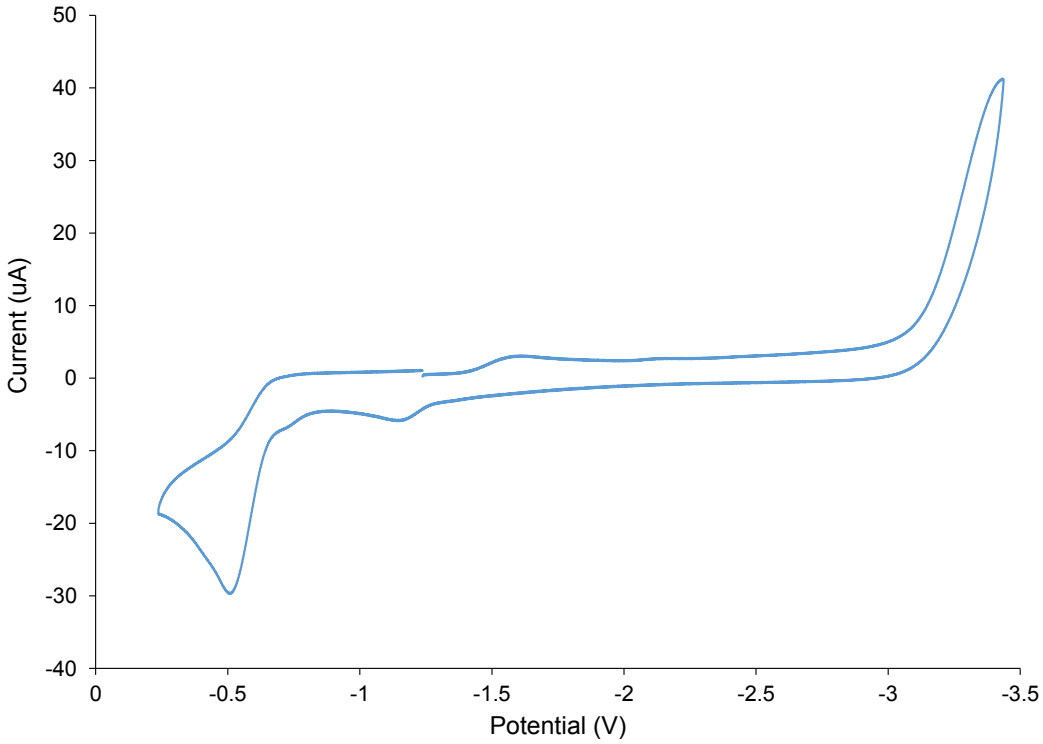

Figure A8.3. Complete cyclic voltammogram of complex **8.1** in THF vs. Fc/Fc^{+}. Scan rate 200 mV/s, 0.1 M $[NBu_4][BPh_4]$ as supporting electrolyte.

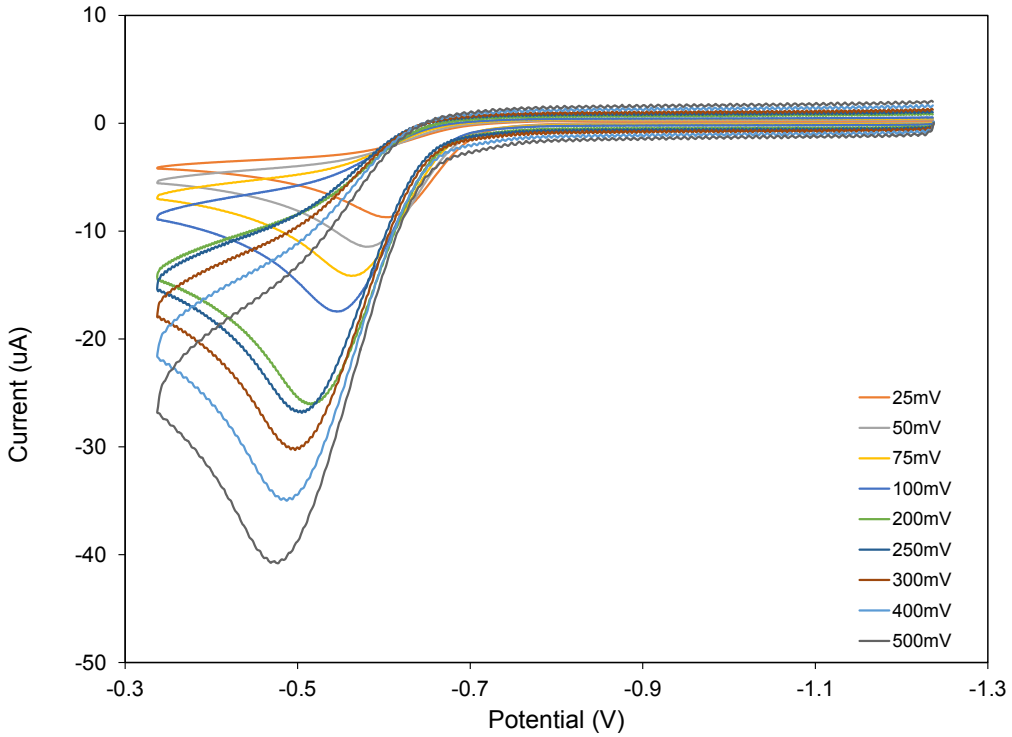

Figure A8.4. Partial cyclic voltammogram of complex **8.1** in THF vs Fc/Fc^{+}. 0.1 M $[NBu_4][BPh_4]$ as supporting electrolyte

Table A8.2. Electrochemical parameters for $[K(18\text{-crown-6})][Th(\eta^3\text{-}S_3)(NR_2)_3]$ (**8.1**) in THF (vs. Fc/Fc^{+}, $[NBu_4][BPh_4]$ as the supporting electrolyte)

Oxidation feature	Scan rate, V/s	$E_{p,a}$, V
	0.025	-0.602
	0.050	-0.579
	0.075	-0.562
	0.100	-0.545
	0.200	-0.515
	0.250	-0.505
	0.300	-0.497
	0.400	-0.487
	0.500	-0.477

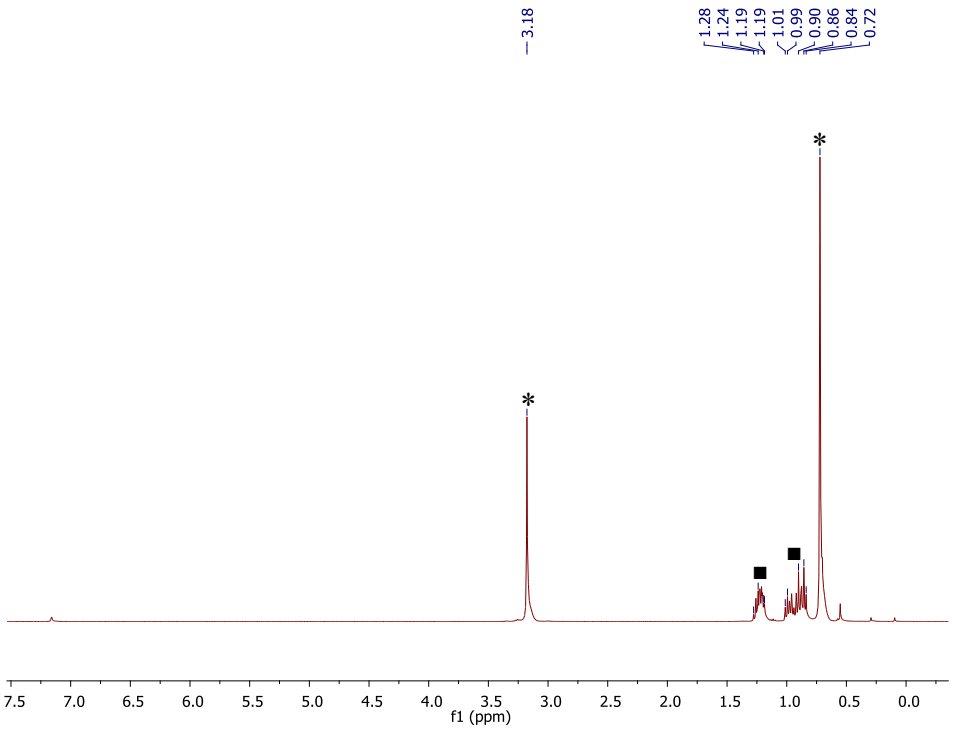

Figure A8.5. In situ ^{1}H NMR spectrum of the reaction of [K(18-crown-6)][Th(η^3-S_3)(NR_2)$_3$] (**8.1**) with Et_3P after 15 min in benzene-d_6. (*) indicates the presence of [K(18-crown-6)][Th(S)(NR_2)$_3$] (**3.8**) and (■) indicates the overlapping resonances for Et_3P and Et_3P=S.

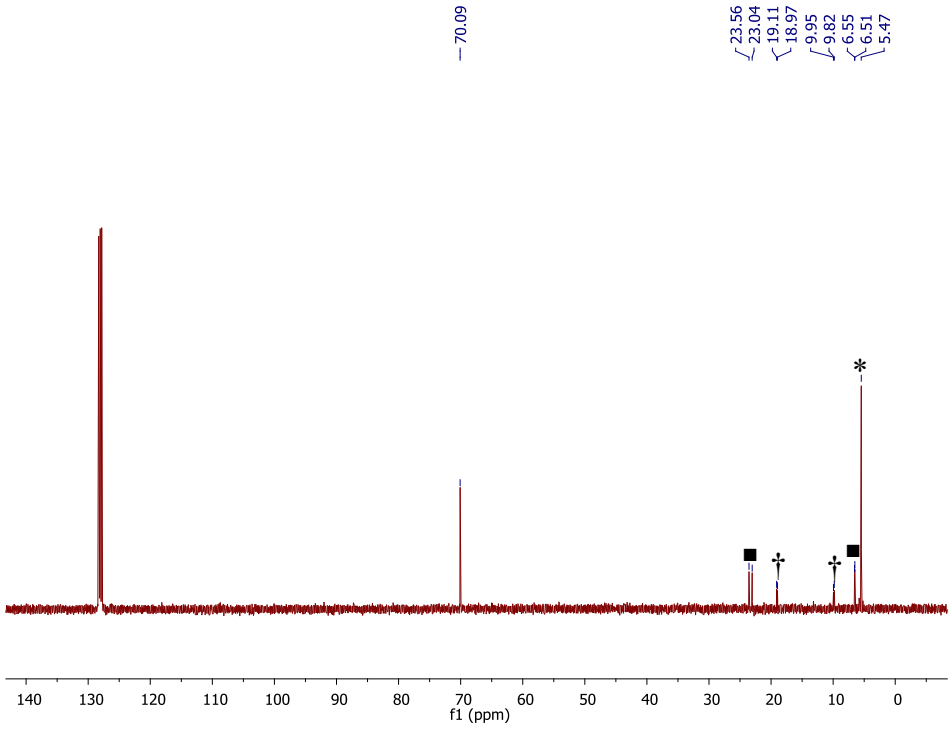

Figure A8.6. In situ $^{13}C\{^{1}H\}$ NMR spectrum of the reaction of [K(18-crown-6)][Th(η^3-S_3)$(NR_2)_3$] (**8.1**) with Et_3P after 15 min in benzene-d_6. (*) indicates the presence of [K(18-crown-6)][Th(S)$(NR_2)_3$] (**3.8**) and (■) indicates the presence of Et_3P=S and (†) indicates the presence of Et_3P.

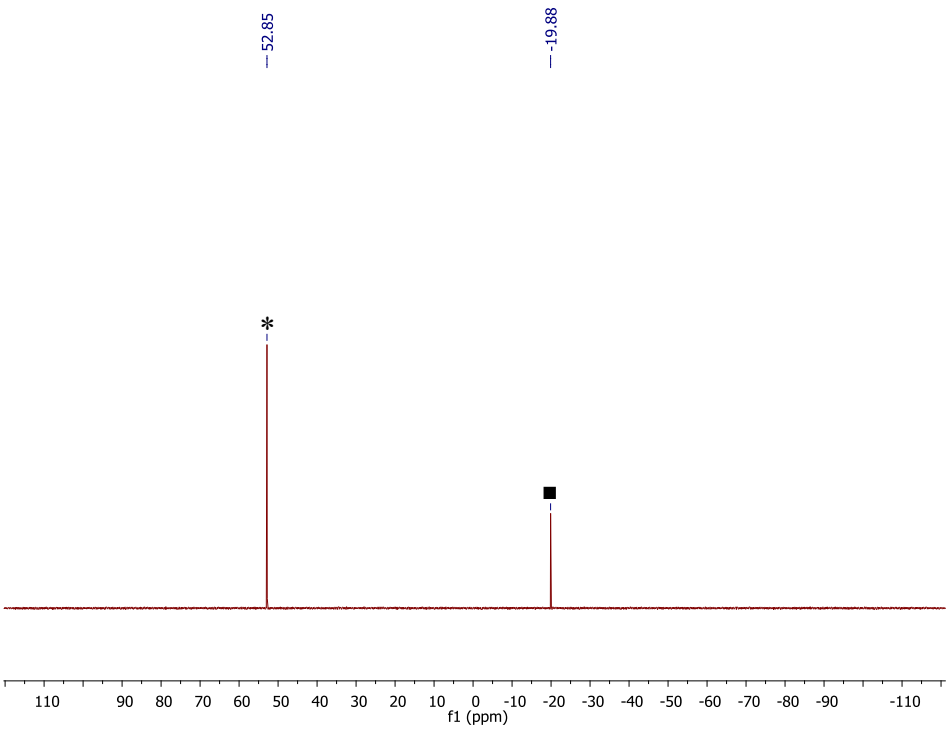

Figure A8.7. In situ $^{31}P\{^{1}H\}$ NMR spectrum of the reaction of [K(18-crown-6)][Th(η^3-S_3)$(NR_2)_3$] (**8.1**) with Et_3P in benzene-d_6. (*) indicates the presence of Et_3P=S and (■) indicates the presence of Et_3P.

8.5.1 Isolation of [U(η^2-S_3NR_2)$(NR_2)_3$] (8.4)

Interestingly, one oxidation attempt of complex **6.2** with AgOTf afforded a few colorless crystals which were identified as [U(η^2-S_3NR_2)$(NR_2)_3$] by X-ray crystallography. This complex could not be made reproducibly and as such further characterization was not possible. It features the rare [η^2-S_3NR_2]$^-$ ligand, which has been observed once before in [Y(η^2-S_3NR_2)$(NR_2)_2$].[61] This complex was isolated from the reaction of [Y$(NR_2)_2]_2$(μ-η^2:η^2-N_2) with S_8. Similarly, this complex was not reproducibly made and only characterized by X-ray crystallography. The presence of an [S_3NR_2]$^-$ ligand suggests that [NR_2]$^\bullet$ radicals could be forming during this reaction, however no evidence to support this hypothesis was found.

These results further illustrate the complicated nature of this reaction (Scheme 8.2) and demonstrate the need for further studies.

Complex **8.4** crystallizes in the triclinic spacegroup $P\bar{1}$, and its solid state molecular structure is shown in Figure A8.8. **8.4** features asymmetrical U-S bond distances (U1-S1 = 2.721(2), U1-S2 = 2.955(2) Å), as well as N-U-N angles (N1-U1-N2 = 101.1(2)°, N2-U1-N3 = 110.4(2)°, N1-U1-N3 = 128.6(2)°) that are severely distorted from idealized tetrahedral, all similar to what is observed for the structurally similar U(IV) disulfide, [K(18-crown-6)][U(η^2-S_2)(NR_2)$_3$] (**6.1**). In addition, the S-S bond distances of **8.4** (S1-S2 = 2.066(3), S2-S3 = 2.077(3) Å) are comparable to the S-S bond distances of complex **6.1**. Furthermore, the metrical parameters of the [S_3NR_2]$^-$ ligand are similar to those seen in [Y(η^2-S_3NR_2)(NR_2)$_2$].[61]

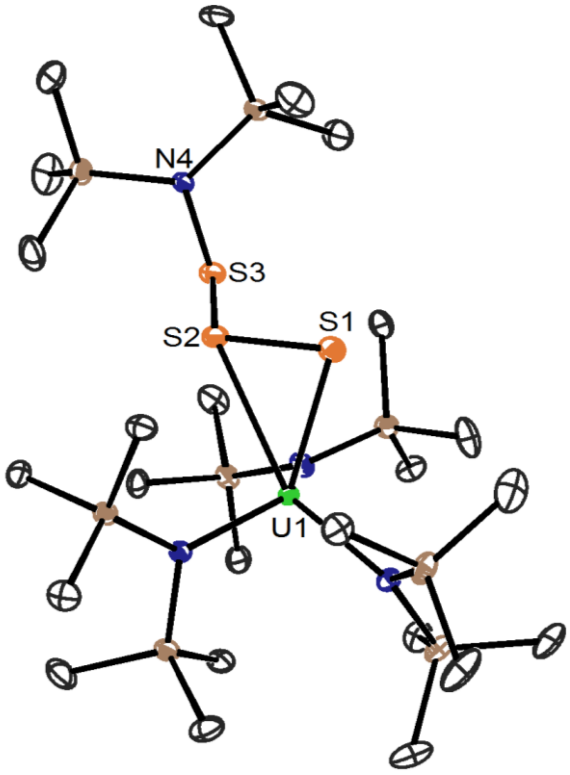

Figure A8.8. ORTEP diagram of [U(η^2-S_3NR_2)(NR_2)$_3$] (**8.4**) with 50% probability ellipsoids. Hydrogen atoms are omitted for clarity. Selected bond lengths (Å) and angles (deg): U1-S1 = 2.721(2), U1-S2 = 2.955(2), S1-S2 = 2.066(3), S2-S3 = 2.077(3), S3-N4 = 1.681(6), N1-

U1-N2 = 101.1(2), N2-U1-N3 = 110.4(2), N1-U1-N3 = 128.6(2), S1-S2-S3 = 111.8(1), S2-S3-N4 = 106.7(2).

8.6 References

(1) Sokolov, M. N. In *Handbook of Chalcogen Chemistry: New Perspectives in Sulfur, Selenium and Tellurium*; The Royal Society of Chemistry: 2007, p 503.
(2) Sheldrick, W. S.; Wachhold, M. *Angew. Chem. Int. Ed.* **1997**, *36*, 206.
(3) Mitchell, K.; Ibers, J. A. *Chem. Rev.* **2002**, *102*, 1929.
(4) Sokolov, M. N.; Abramov, P. A. *Coord. Chem. Rev.* **2012**, *256*, 1972.
(5) Kanatzidis, M. G.; Huang, S.-P. *Coord. Chem. Rev.* **1994**, *130*, 509.
(6) Ephritikhine, M. *Coord. Chem. Rev.* **2016**, *319*, 35.
(7) Lam, O. P.; Heinemann, F. W.; Meyer, K. *Chem. Sci.* **2011**, *2*, 1538.
(8) Brown, J. L.; Wu, G.; Hayton, T. W. *Organometallics* **2013**, *32*, 1193.
(9) Camp, C.; Antunes, M. A.; Garcia, G.; Ciofini, I.; Santos, I. C.; Pecaut, J.; Almeida, M.; Marcalo, J.; Mazzanti, M. *Chem. Sci.* **2014**, *5*, 841.
(10) Franke, S. M.; Heinemann, F. W.; Meyer, K. *Chem. Sci.* **2014**, *5*, 942.
(11) Brennan, J. G.; Andersen, R. A.; Zalkin, A. *Inorg. Chem.* **1986**, *25*, 1761.
(12) Avens, L. R.; Barnhart, D. M.; Burns, C. J.; McKee, S. D.; Smith, W. H. *Inorg. Chem.* **1994**, *33*, 4245.
(13) Evans, W. J.; Montalvo, E.; Ziller, J. W.; DiPasquale, A. G.; Rheingold, A. L. *Inorg. Chem.* **2010**, *49*, 222.
(14) Ventelon, L.; Lescop, C.; Arliguie, T.; Leverd, P. C.; Lance, M.; Nierlich, M.; Ephritikhine, M. *Chem. Commun.* **1999**, 659.
(15) Andrez, J.; Pecaut, J.; Scopelliti, R.; Kefalidis, C. E.; Maron, L.; Rosenzweig, M. W.; Meyer, K.; Mazzanti, M. *Chem. Sci.* **2016**.
(16) Rosenzweig, M. W.; Scheurer, A.; Lamsfus, C. A.; Heinemann, F. W.; Maron, L.; Andrez, J.; Mazzanti, M.; Meyer, K. *Chem. Sci.* **2016**.
(17) Matson, E. M.; Goshert, M. D.; Kiernicki, J. J.; Newell, B. S.; Fanwick, P. E.; Shores, M. P.; Walensky, J. R.; Bart, S. C. *Chem. Eur. J.* **2013**, *19*, 16176.
(18) Brown, J. L.; Fortier, S.; Lewis, R. A.; Wu, G.; Hayton, T. W. *J. Am. Chem. Soc.* **2012**, *134*, 15468.
(19) Brown, J. L.; Fortier, S.; Wu, G.; Kaltsoyannis, N.; Hayton, T. W. *J. Am. Chem. Soc.* **2013**, *135*, 5352.
(20) Chivers, T.; Elder, P. J. W. *Chem. Soc. Rev.* **2013**, *42*, 5996.
(21) *Cambridge Structural Database*, version 1.18. 2015
(22) Nguyen, S. T.; Grubbs, R. H.; Ziller, J. W. *J. Am. Chem. Soc.* **1993**, *115*, 9858.
(23) Doyle, M. P. *Chem. Rev.* **1986**, *86*, 919.
(24) Wanzlick, H. W.; Schönherr, H. J. *Angew. Chem. Int. Ed.* **1968**, *7*, 141.
(25) In *The Organometallic Chemistry of the Transition Metals*; John Wiley & Sons, Inc.: 2014, p 290.
(26) Yandulov, D. V.; Schrock, R. R. *J. Am. Chem. Soc.* **2002**, *124*, 6252.
(27) Yandulov, D. V.; Schrock, R. R.; Rheingold, A. L.; Ceccarelli, C.; Davis, W. M. *Inorg. Chem.* **2003**, *42*, 796.
(28) Rittle, J.; Peters, J. C. *J. Am. Chem. Soc.* **2016**, *138*, 4243.
(29) Yandulov, D. V.; Schrock, R. R. *Inorg. Chem.* **2005**, *44*, 1103.
(30) Chauvin, Y. *Angew. Chem. Int. Ed.* **2006**, *45*, 3740.
(31) Schrock, R. R. *Angew. Chem. Int. Ed.* **2006**, *45*, 3748.

(32) Grubbs, R. H. *Angew. Chem. Int. Ed.* **2006**, *45*, 3760.
(33) Öfele, K. *J. Organomet. Chem.* **1968**, *12*, P42.
(34) Kochi, T.; Tanabe, Y.; Tang, Z.; Ishii, Y.; Hidai, M. *Chem. Lett.* **1999**, *28*, 1279.
(35) Leblanc, J.-C.; Moise, C.; Volpato, F.; Brunner, H.; Gehart, G.; Wachter, J.; Nuber, B. *J. Organomet. Chem.* **1995**, *485*, 237.
(36) Shaver, A.; McCall, J. M.; Bird, P. H.; Siriwardane, U. *Acta Crystallogr. Sect. C* **1991**, *47*, 659.
(37) Shaver, A.; Lopez, O.; N. Harpp, D. *Inorg. Chim. Acta* **1986**, *119*, 13.
(38) Shaver, A.; McCall, J. M. *Organometallics* **1984**, *3*, 1823.
(39) Hobert, S. E.; Noll, B. C.; Rakowski DuBois, M. *Organometallics* **2001**, *20*, 1370.
(40) Herberhold, M.; Jin, G.-X.; Milius, W. *Angew. Chem. Int. Ed.* **1993**, *32*, 85.
(41) Smiles, D. E.; Wu, G.; Hayton, T. W. *Inorg. Chem.* **2014**, *53*, 12683.
(42) Fortier, S.; Brown, J. L.; Kaltsoyannis, N.; Wu, G.; Hayton, T. W. *Inorg. Chem.* **2012**, *51*, 1625.
(43) Sutorik, A. C.; Kanatzidis, M. G. *Polyhedron* **1997**, *16*, 3921.
(44) Kwak, J.-e.; Gray, D. L.; Yun, H.; Ibers, J. A. *Acta Crystallogr. Sect. E* **2006**, *62*, i86.
(45) Grant, D. J.; Weng, Z.; Jouffret, L. J.; Burns, P. C.; Gagliardi, L. *Inorg. Chem.* **2012**, *51*, 7801.
(46) Wrobleski, D. A.; Cromer, D. T.; Ortiz, J. V.; Rauchfuss, T. B.; Ryan, R. R.; Sattelberger, A. P. *J. Am. Chem. Soc.* **1986**, *108*, 174.
(47) Smiles, D. E.; Wu, G.; Hayton, T. W. *New J. Chem.* **2015**, *39*, 7563.
(48) Paris, J.; Plichon, V. *Electrochim. Acta* **1982**, *27*, 1501.
(49) Smiles, D. E.; Wu, G.; Kaltsoyannis, N.; Hayton, T. W. *Chem. Sci.* **2015**, *6*, 3891.
(50) Fortier, S.; Wu, G.; Hayton, T. W. *Dalton Trans.* **2010**, *39*, 352.
(51) Hervé, A.; Bouzidi, Y.; Berthet, J.-C.; Belkhiri, L.; Thuéry, P.; Boucekkine, A.; Ephritikhine, M. *Inorg. Chem.* **2015**, *54*, 2474.
(52) Camp, C.; Chatelain, L.; Kefalidis, C. E.; Pecaut, J.; Maron, L.; Mazzanti, M. *Chem. Commun.* **2015**, *51*, 15454.
(53) Shannon, R. D. *Acta Crystallogr. Sect. A* **1976**, *A32*, 751.
(54) Baccolini, G.; Boga, C.; Mazzacurati, M. *J. Org. Chem.* **2005**, *70*, 4774.
(55) Harris, R. K.; Becker, E. D.; Cabral De Menezes, S. M.; Goodfellow, R.; Granger, P. *Pure Appl. Chem.* **2001**, *73*, 1795.
(56) Harris, R. K.; Becker, E. D.; Cabral De Menezes, S. M.; Granger, P.; Hoffman, R. E.; Zilm, K. W. *Pure Appl. Chem.* **2008**, *80*, 59.
(57) *SMART Apex II*, Version 2.1. 2005
(58) *SAINT Software User's Guide*, Version 7.34a. 2005
(59) *SADABS*, 2005
(60) *SHELXTL PC*, Version 6.12. 2005
(61) Corbey, J. F.; Fang, M.; Ziller, J. W.; Evans, W. J. *Inorg. Chem.* **2015**, *54*, 801.

Chapter 9 Synthesis of a Thorium Carbene Complex

Table of Contents

9.1 Introduction

Transition metal carbenes have been known for over 50 years.[1-4] These complexes have been shown to display a wide range of reactivity, and have been used for a variety of organic transformations including olefin metathesis.[5-11] In contrast to the abundance of transition metal carbenes, f-element carbenes are much less common.[12-27] The first example of an actinide carbene, [Cp$_3$U(CHPMe$_2$Ph)], was reported by Gilje and co-workers.[20-22] Since then, slow but steady progress has been made in the synthesis of uranium carbenes, however carbene complexes of other actinides, including thorium, remain relatively rare.[24-26] Andrews

and co-workers first reported evidence of the formation of [Th(H)(X)(CH_2)] (X = F, Cl, Br) in the gas phase, in 2005.[28] The first structurally characterized thorium carbene complex was not reported until 2011, when Cavell and co-workers reported the synthesis of [Cp^*_2Th(κ^3-C(Ph_2P=N$SiMe_3$)$_2$)].[24] A few other examples have been reported (Figure 9.1), however, nearly all of these utilize chelating pincer ligands that feature either NCN or SCS binding

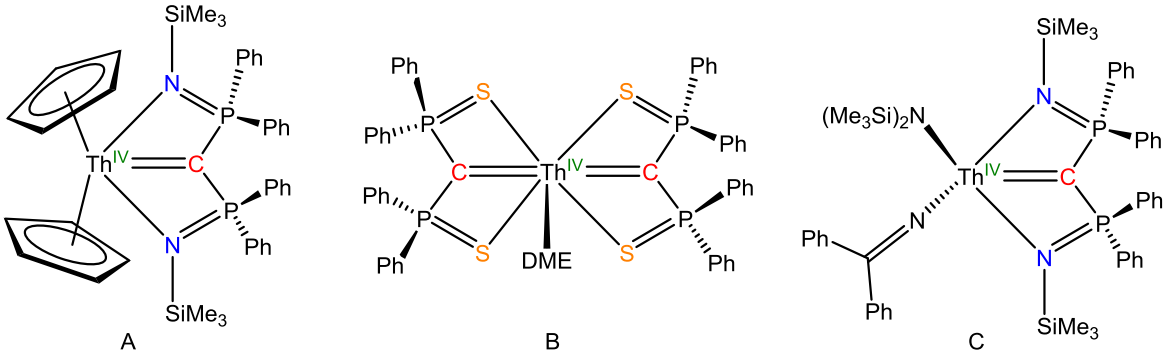

Figure 9.1. Previously reported thorium carbene complexes. A, Ref. [24]; B, Ref. [25]; C, Ref. [26].

motifs, in addition to diphosphorus stabilized carbene moieties. Interestingly, all reported examples of f-element carbenes feature this type of stabilization. The need for a heteroatom, such as phosphorus, to stabilize the carbene moiety is a necessity exclusive to the f-elements, as examples of transition metal carbenes without these features are well known.[4,11,29-31]

Recently, Hayton and co-workers reported the synthesis of a U(IV) carbene, [U(CHPPh_3)(NR_2)$_3$], via the 1e^- oxidation of the U(III) ylide adduct, [U(CH_2PPh_3)(NR_2)$_3$].[23] This complex could also be accessed via the reaction of the U(IV) metallacycle, [U(*C*$H_2$$SiMe_2$*N*$SiMe_3$)($NR_2$)$_2$], and the Wittig reagent, Ph_3P=CH_2. It was discovered that [U(CHPPh_3)(NR_2)$_3$] exhibited some interesting solution state behavior, and was found to form an equilibrium between the U(IV) metallacycle, [U(*C*$H_2$$SiMe_2$*N*$SiMe_3$)($NR_2$)$_2$], and the

Wittig reagent Ph_3PCH_2. The equilibrium established between these species afforded the opportunity to quantify the thermodynamics of the reaction and study the U-C bond.

The availability of the Th(IV) metallacycle, [Th(CH$_2$SiMe$_2$$N$SiMe$_3$)(NR$_2$)$_2$], in addition to recent reports that protonation of this complex afforded several thorium imido complexes,[32] suggested that a new Th(IV) carbene, analogous to [U(CHPPh$_3$)(NR$_2$)$_3$] could be accessed. Furthermore, the inherent similarities between these two species would allow for complementary studies that could provide insight into actinide bonding. This chapter details the synthesis and characterization of a rare Th(IV) carbene complex. The solution state behavior of this species is investigated, as, like its uranium analogue, it forms an equilibrium with the Th(IV) metallacycle. This equilibrium is probed using variable temperature NMR studies, and the thermodynamic parameters are extracted from these experiments. A comparison of the thermodynamic data obtained for the Th(IV) complex and its U(IV) analogue is made, and how this relates to the differences in bonding is discussed.

9.2 Results and Discussion

9.2.1 Synthesis and Characterization of [Th(CHPPh$_3$)(NR$_2$)$_3$] (9.1)

Following the procedure described for the synthesis of [U(CHPPh$_3$)(NR$_2$)$_3$][23] and using the corresponding thorium starting material, the analogous thorium complex could be accessed. Thus, addition of 1 equiv of $Ph_3{=}CH_2$ to a cold (-25 °C) solution of [Th(CH$_2$SiMe$_2$$N$SiMe$_3$)(NR$_2$)$_2$] in diethyl ether affords a light yellow solution, from which the Th(IV) carbene complex, [Th(CHPPh$_3$)(NR$_2$)$_3$] (**9.1**), can be isolated as a yellow crystalline solid, in 70% yield, after crystallization from pentane (Scheme 9.1).

Scheme 9.1 Synthesis of [Th(CHPPh$_3$)(NR$_2$)$_3$] (**9.1**)

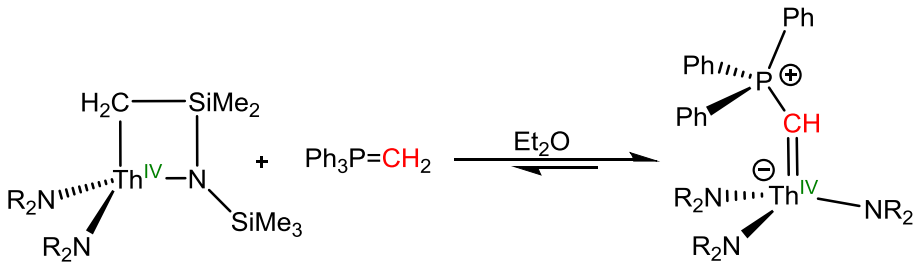

Complex **9.1** crystallizes in the triclinic spacegroup $P\bar{1}$, and it solid state molecular structure is shown in Figure 9.2. Complex **9.1** is isostructural to its uranium analogue and features a pseudotetrahedral geometry about the Th center (av. N-Th-N = 113.0°, av. N-Th-C = 105.8°). The Th-C bond distance of **9.1** (2.362(2) Å) is markedly shorter than those of all other structurally characterized thorium carbene complexes (av. = 2.49 Å / range 2.436-2.552 Å).[12,24-26] The series of thorium carbenes [Th(H)(X)(CH$_2$)] (X = F, Cl, Br) exhibited shorter Th-C bond distances (av. = 2.127 Å), but were only characterized in the gas phase.[28] Furthermore, the Th-C of **9.1** bond distance is in between the sums of the single bond (2.5 Å) and double bond (2.1 Å) covalent radii for Th and C, suggestive of some multiple bond character.[33] Complex **9.1** also features a bent Th-C-P angle (148.2(1)°), similar to the U-C-P angle (151.7(4)°) of [U(CHPPh$_3$)(NR$_2$)$_3$].[23]

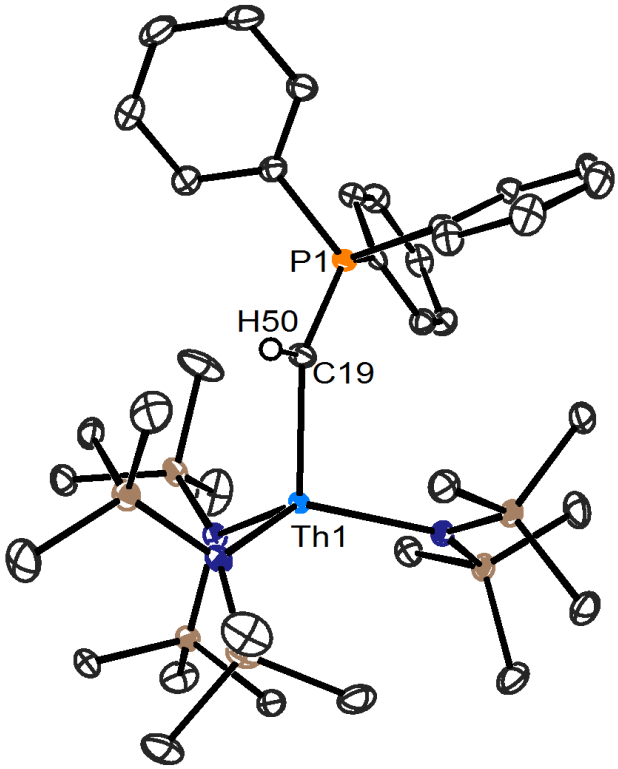

Figure 9.2. ORTEP diagram of [Th(CHPPh$_3$)(NR$_2$)$_3$] (**9.1**) with 50% probability ellipsoids. Hydrogen atoms, except for the C-H proton, are omitted for clarity. Selected bond lengths (Å) and angles (deg): Th1-C19 = 2.362(2), C19-P1 = 1.680(2), Th1-C19-P1 = 148.2(1).

The room temperature ^{1}H NMR spectrum of complex **9.1**, in benzene-d_6, exhibits a sharp singlet at 0.49 ppm, assignable to the methyl groups of the silylamide ligands, in addition to three distinct multiplets between 7.00 and 7.74 ppm, assignable to the three distinct aryl proton environments of the PPh$_3$ moiety (Figure 9.3, Figure A9.1, Figure A9.2). The methine proton

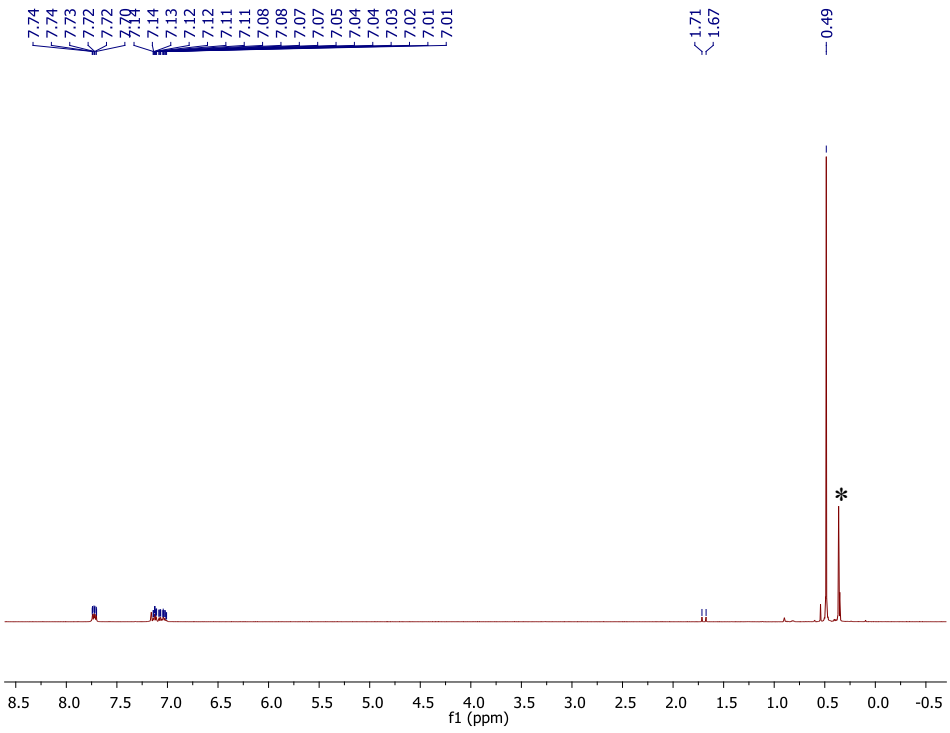

Figure 9.3. ^{1}H NMR spectrum of [Th(CHPPh$_3$)(NR$_2$)$_3$] (**9.1**) in benzene-d_6. (*) indicates the presence [Th(*C*H$_2$SiMe$_2$*N*SiMe$_3$)(NR$_2$)$_2$], present due to the solution state equilibrium.

is assignable to a doublet at 1.69 ppm with a $J_{H\text{-}P}$ = 20 Hz. This is slightly shifted from the doublet assignable to the methylene resonance of free Ph$_3$P=CH$_2$, which appears at 0.81 ppm ($J_{H\text{-}P}$ = 7.6 Hz). The methine resonance of **9.1** collapses to a singlet at 1.70 ppm in the ^{1}H{^{31}P} spectrum (Figure A9.6 and Figure A9.7). The ^{13}C{^{1}H} NMR spectrum of **9.1** features a singlet at 5.58 ppm assignable to the methyl groups of the silylamide ligands (Figure A9.3). Also seen are four doublets at 128.52 ($J_{C\text{-}P}$ = 10.5 Hz), 130.80 ($J_{C\text{-}P}$ = 1.5 Hz), 132.97 ($J_{C\text{-}P}$ = 10.5 Hz), and 136.02 ($J_{C\text{-}P}$ = 81 Hz) ppm, assignable to the *m*-, *p*-, *o*-, and ipso aryl carbons, respectively (Figure 9.4). These are nearly identical both in chemical shift values and coupling constants, to the four aryl resonances of Ph$_3$P=CH$_2$ (128.42, $J_{C\text{-}P}$ = 11 Hz, *m*-*C*; 130.60, $J_{C\text{-}P}$ = 2 Hz, *p*-*C*; 132.63, $J_{C\text{-}P}$ = 10 Hz, *o*-*C*; 135.17, $J_{C\text{-}P}$ = 83 Hz, ipso-*C*), indicative that there is little change in the electronics of the phenyl rings upon coordination. This is in

stark contrast to the carbene carbon, whose resonance, also a doublet, shifts from -4.18 ppm, for the free Wittig, to 116.54 ppm upon formation of complex **9.1** (Figure 9.4). Furthermore, the coupling constant for the carbene resonance of **9.1** ($J_{C\text{-}P}$ = 22.5 Hz) is dramatically smaller than that of $Ph_3P{=}CH_2$ ($J_{C\text{-}P}$ = 98.6 Hz), suggestive of a weaker C-P interaction upon coordination to the metal center. The downfield shift of this ^{13}C resonance is likely due in part to the spin-orbits effects that results from coordination of the Ph_3PCH fragment to the actinide center, similar to what has been seen for other actinide complexes, including $[Li(DME)_3]_2[Th(C_6H_5)_6]$.[34,35] Lastly, the $^{31}P\{^1H\}$ NMR spectrum of complex **9.1** features a sharp singlet at -17.55 ppm, assignable to the phosphorus of the PPh_3 moiety (Figure A9.4), which transforms into a broad multiplet without ^1H decoupling (Figure A9.5).

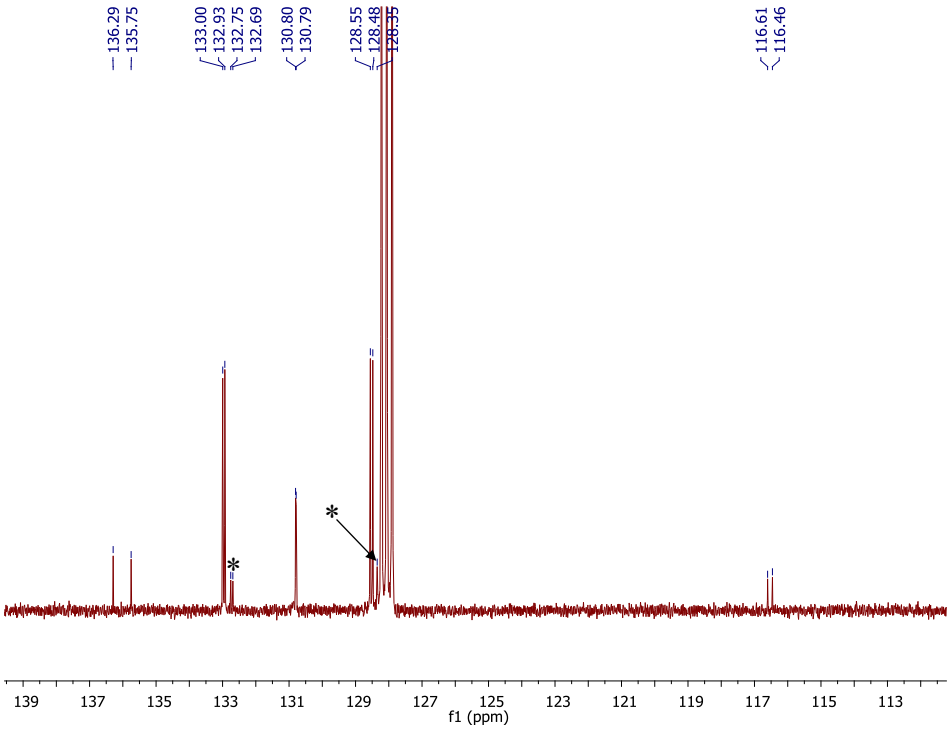

Figure 9.4. Partial $^{13}C\{^1H\}$ NMR spectrum of $[Th(CHPPh_3)(NR_2)_3]$ (**9.1**) in benzene-d_6. (*) indicates the presence of $Ph_3P{=}CH_2$, present due to the solution state equilibrium.

Notably, both the Th(IV) metallacycle, [Th(*C*H_2SiMe$_2$*N*SiMe$_3$)(NR_2)$_2$], and free Wittig, $Ph_3P{=}CH_2$, are also observed in these NMR spectra. This is a result of the solution state equilibrium that exists between complex **9.1** and these species, and is identical to what has been observed for the analogous uranium complex.[23] Similarly, this equilibrium is also solvent and temperature dependent. Dissolution in non-polar solvents such as pentane, combined with lower temperatures, favor the formation of **9.1**, and allow for its isolation (Scheme 9.1). In polar solvents, like THF, this equilibrium shifts dramatically in the other direction, and the metallacycle [Th(*C*H_2SiMe$_2$*N*SiMe$_3$)(NR_2)$_2$] is favored 2:1 over complex **9.1** when dissolved in this solvent, similar to what was seen for [U(CHPPh_3)(NR_2)$_3$].[23]

9.2.2 Van't Hoff Analysis of Solution of [Th(CHPPh_3)(NR_2)$_3$] (9.1)

The solution phase behavior of complex **9.1** afforded the opportunity not only to investigate the thermodynamics of its formation, but also to compare thermodynamic parameters to those of the isostructural uranium analogue, for which a similar analysis has already been done.[23] Thus, the equilibrium between complex **9.1** and the Th(IV) metallacycle was probed using variable temperature NMR spectroscopy. ^{1}H NMR spectra were recorded for a solution of **9.1** in toluene-d_8 at five temperatures between 263 and 308 K (Figure 9.5). Thermodynamic parameters were calculated using the equilibrium concentrations of [Th(CHPPh_3)(NR_2)$_3$] (**9.1**), [Th(*C*H_2SiMe$_2$*N*SiMe$_3$)(NR_2)$_2$], and $Ph_3P{=}CH_2$, and the van't Hoff plot is linear (Figure 9.6). This data reveals that dissociation of the carbene to form the metallacycle is endothermic

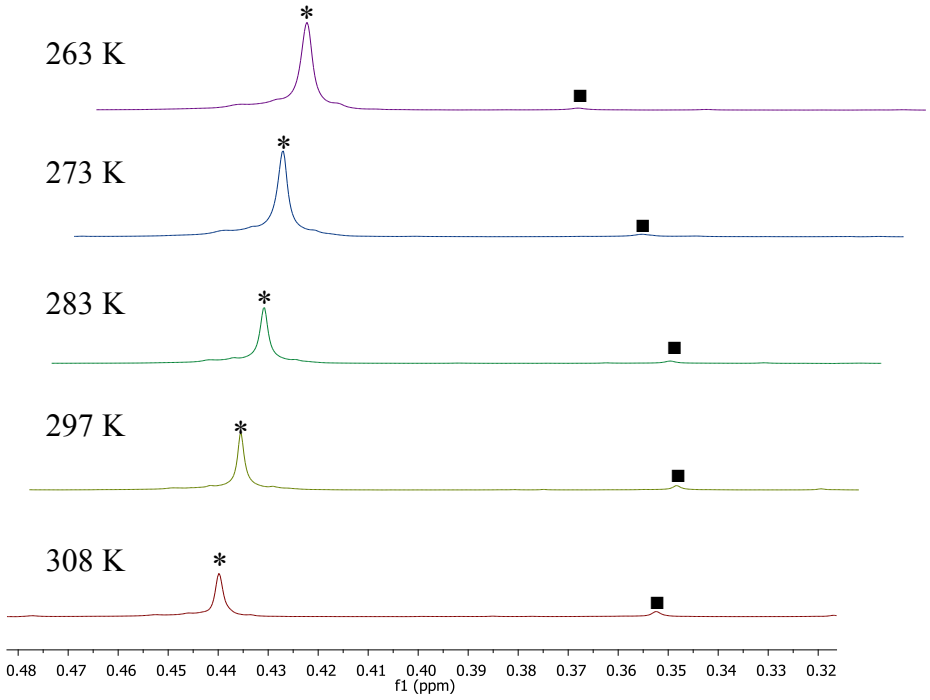

Figure 9.5. Variable temperature ^{1}H NMR spectrum of [Th(CHPPh$_3$)(NR$_2$)$_3$] (**9.1**) in toluene-d_8 (27.9 mM) showing the N(SiMe$_3$)$_2$ resonances. (*) denotes the N(SiMe$_3$)$_2$ resonance of [Th(CHPPh$_3$)(NR$_2$)$_3$] (**9.1**), and (■) denotes the N(SiMe$_3$)$_2$ resonance of [Th(*C*H$_2$SiMe$_2$*N*SiMe$_3$)(NR$_2$)$_2$].

(ΔH = 9.4 kcal/mol) and entropically favored (ΔS = 16.5 eu). As expected, the enthalpic component in this system is similar to that of the analogous uranium system (ΔH = 11 kcal/mol), consistent with the fact that very similar bonds are being formed and broken in both cases. There is, however, a rather large difference in the entropic factors. The ΔS of formation of the U(IV) metallacycle in this reaction is nearly twice that of the analogous thorium species (U, ΔS = 31 eu; Th, ΔS = 16 eu). The cause of this difference is currently not understood. However, the entropic difference is likely responsible for the observed differences in equilibria between the thorium and uranium systems. For example, the metallacycle is favored in the uranium system 5:1 over the carbene in a solution of toluene-d_8 at room temperature, while in the thorium system, the carbene, complex **9.1**, is favored ~20:1 over the

metallacycle under similar conditions. Further investigation is likely required to discover the origin of this difference, and in this regard, computational analysis is being performed by Dr. Peter Hrobárik, at the Technical University of Berlin, to probe this system.

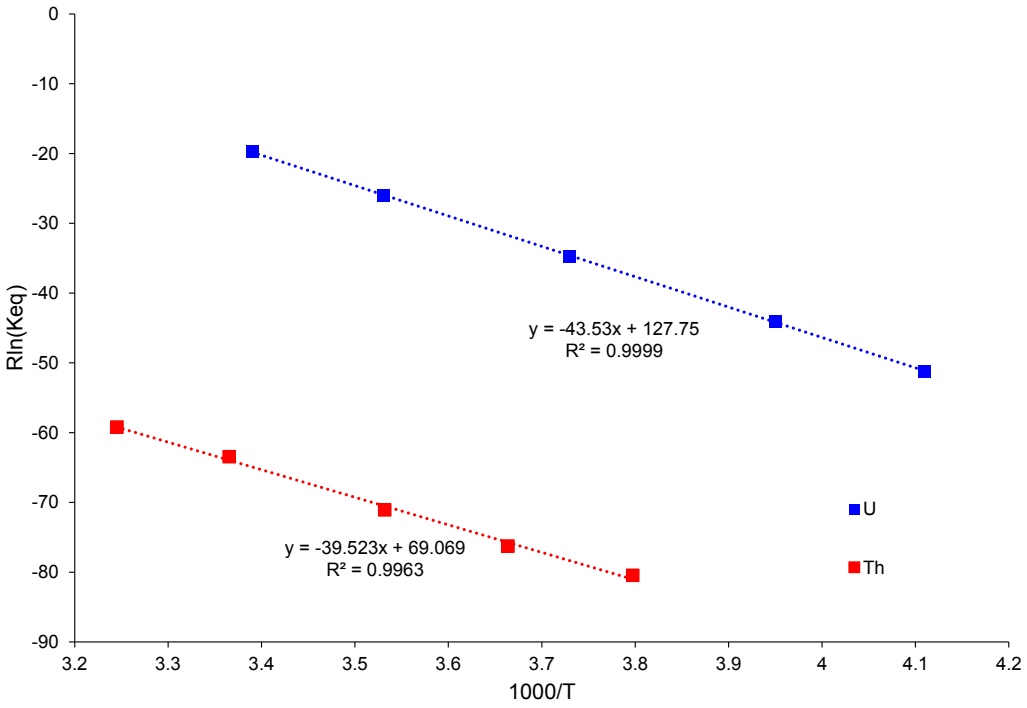

Figure 9.6. van't Hoff plot for [Th(CHPPh$_3$)(NR$_2$)$_3$] (**9.1**) and [U(CHPPh$_3$)(NR$_2$)$_3$] in toluene-d_8. Th, 27.9 mM, U, 25.3 mM. Data for [U(CHPPh$_3$)(NR$_2$)$_3$] taken from Ref. [23].

9.3 Summary

In summary, reaction of the Th(IV) metallacycle, [Th(*C*H$_2$SiMe$_2$*N*SiMe$_3$)(NR$_2$)$_2$], and Ph$_3$P=CH$_2$ affords the new Th(IV) carbene complex, [Th(CHPPh$_3$)(NR$_2$)$_3$] (**9.1**). This complex is characterizes both structurally and spectroscopically. Similar to all other actinide carbene complexes, **9.1** features a heteroatom stabilized carbene moiety, in this case phosphorus, however unlike all other examples the carbene moiety is only stabilized by one heteroatom. In addition, the Th-C bond of **9.1** is the shortest yet reported, possibly due to less

heteroatom derived stabilization. This suggests that heteroatom stabilization may not be required, and a true alkylidene could one day be synthesized. Complex **9.1** forms an equilibrium in solution with the Th(IV) metallacycle, and the thermodynamics of this conversion were probe using variable temperature ^{1}H NMR spectroscopy. Van't Hoff analysis reveals that dissociation of the carbene complex is an endothermic process that is entropically favored. These results are similar to those determined for the analogous uranium system, but are much less entropically driven. The differences between these systems are currently under investigation and hopefully will lend insight into the differences between uranium and thorium bonding.

9.4 Experimental

9.4.1 General Methods

All reactions and subsequent manipulations were performed under anaerobic and anhydrous conditions under an atmosphere of nitrogen. Hexanes, Et_2O, toluene, and THF were dried using a Vacuum Atmospheres DRI-SOLV Solvent Purification system and stored over 3Å sieves for 24 h prior to use. Benzene-d_6, and toluene-d_8, were dried over 3Å molecular sieves for 24 h prior to use. [Th(*C*H_2SiMe_2*N*SiMe_3)(NR_2)$_2$][36] and $Ph_3P{=}CH_2$[37] were synthesized according to the previously reported procedures. All other reagents were purchased from commercial suppliers and used as received.

NMR spectra were recorded on a Varian UNITY INOVA 400, a Varian UNITY INOVA 500 spectrometer, a Varian UNITY INOVA 600 MHz spectrometer, or an Agilent Technologies 400-MR DD2 400 MHz Spectrometer. ^{1}H NMR spectra were referenced to external $SiMe_4$ using the residual protio solvent peaks as internal standards. $^{13}C\{^{1}H\}$ and $^{31}P\{^{1}H\}$, NMR spectra were referenced indirectly with the ^{1}H resonance of $SiMe_4$ at 0 ppm,

according to IUPAC standard,[38,39] using the residual solvent peaks as internal standards. IR spectra were recorded on a Nicolet 6700 FT-IR spectrometer with a NXR FT Raman Module. Elemental analyses were performed by the Micro-Analytical Facility at the University of California, Berkeley.

9.4.2 Synthesis of [Th(CHPPh$_3$)(NR$_2$)$_3$] (9.1)

To a colorless, cold (-25 °C), stirring solution of [Th(*C*H$_2$SiMe$_2$*N*SiMe$_3$)(NR$_2$)$_2$] (384.9 mg, 0.54 mmol) in diethyl ether (4 mL) was added a solution of Ph$_3$P=CH$_2$ (150.8 mg, 0.55 mmol) in diethyl ether (3 mL). The color of the solution became yellow upon addition and was allowed to stir for 1 h. The solvent was then removed in vacuo to afford a yellow solid. This was then extracted with pentane (7 mL) and filtered a Celite column supported on glass wool (0.5 cm × 3 cm) to afford a yellow solution. The volume of the filtrate was reduced to 4 mL in vacuo. Storage of this solution at -25 °C for 4 h resulted in the deposition of yellow crystals, which were isolated by decanting the supernatant (252.1 mg, 47%). The volume of the supernatant was then reduced in vacuo to 2 mL and storage of this solution at -25 °C for 24 h resulted in the deposition of more yellow crystals, which were isolated by decanting off the supernatant. Total yield 375.5 mg, 70%. Anal. Calcd for C$_{37}$H$_{70}$N$_3$PSi$_6$Th: C, 44.96; H, 7.14; N, 4.25. Found: C, 45.23; H, 7.29; N, 4.21. ^{1}H NMR (500 MHz, 25 °C, benzene-d_6): δ 0.49 (s, 54H, N(Si(C*H*$_3$)$_3$)$_2$), 1.69 (d, 1H, $J_{H\text{-}P}$ = 20 Hz, C*H*PPh$_3$), 7.00-7.09 (m, 6H, *m*-C*H*), 7.11-7.14 (m, 3H, *p*-C*H*), 7.70-7.74 (m, 6H, *o*-C*H*). ^{13}C{^{1}H} NMR (150 MHz, 25 °C, benzene-d_6): δ 5.58 (N(Si(*C*H$_3$)$_3$)$_2$), 116.54 (d, $J_{C\text{-}P}$ = 22.5 Hz, *C*HPPh$_3$), 128.52 (d, $J_{C\text{-}P}$ = 10.5 Hz, *m*-*C*), 130.80 (d, $J_{C\text{-}P}$ = 1.5 Hz, *p*-*C*), 132.97 (d, $J_{C\text{-}P}$ = 10.5 Hz, *o*-*C*), 136.02 (d, $J_{C\text{-}P}$ = 81 Hz, ipso-*C*). ^{31}P{^{1}H} (161.92 MHz, 25 °C, benzene-d_6): δ 17.55. ^{1}H NMR (500 MHz, 35 °C, toluene-d_8, 27.9 mM): δ 0.35 (s, 36H, N(Si(C*H*$_3$)$_3$)$_2$, [Th(*C*H$_2$SiMe$_2$*N*SiMe$_3$)(NR$_2$)$_2$]), 0.44 (s,

54H, N(Si(CH_3)$_3$)$_2$, **9.1**), 1.62 (d, 1H, $J_{H\text{-}P}$ = 21 Hz, CHPPh$_3$, **9.1**), 6.98-7.15 (m, 9H, *m*-CH and *p*-CH, **9.1**), 7.66-7.70 (m, 3H, *o*-CH, **9.1**). ^{1}H NMR (500 MHz, 24 °C, toluene-d_8, 27.9 mM): δ 0.35 (s, 36H, N(Si(CH_3)$_3$)$_2$, [Th(*C*H$_2$SiMe$_2$*N*SiMe$_3$)(NR$_2$)$_2$]), 0.44 (s, 54H, N(Si(CH_3)$_3$)$_2$, **9.1**), 1.63 (d, 1H, $J_{H\text{-}P}$ = 20.5 Hz, CHPPh$_3$, **9.1**), 7.01-7.14 (m, 9H, *m*-CH and *p*-CH, **9.1**), 7.66-7.70 (m, 3H, *o*-CH, **9.1**). ^{1}H NMR (500 MHz, 10 °C, toluene-d_8, 27.9 mM): δ 0.36 (s, 36H, N(Si(CH_3)$_3$)$_2$, [Th(*C*H$_2$SiMe$_2$*N*SiMe$_3$)(NR$_2$)$_2$]), 0.44 (s, 54H, N(Si(CH_3)$_3$)$_2$, **9.1**), 1.65 (d, 1H, $J_{H\text{-}P}$ = 20 Hz, CHPPh$_3$, **9.1**), 7.01-7.12 (m, 9H, *m*-CH and *p*-CH, **9.1**), 7.65-7.69 (m, 3H, *o*-CH, **9.1**). ^{1}H NMR (500 MHz, 0 °C, toluene-d_8, 27.9 mM): δ 0.37 (s, 36H, N(Si(CH_3)$_3$)$_2$, [Th(*C*H$_2$SiMe$_2$*N*SiMe$_3$)(NR$_2$)$_2$]), 0.44 (s, 54H, N(Si(CH_3)$_3$)$_2$, **9.1**), 1.66 (d, 1H, $J_{H\text{-}P}$ = 20 Hz, CHPPh$_3$, **9.1**), 7.01-7.11 (m, 9H, *m*-CH and *p*-CH, **9.1**), 7.65-7.69 (m, 3H, *o*-CH, **9.1**). ^{1}H NMR (500 MHz, -10 °C, toluene-d_8, 27.9 mM): δ 0.39 (s, 36H, N(Si(CH_3)$_3$)$_2$, [Th(*C*H$_2$SiMe$_2$*N*SiMe$_3$)(NR$_2$)$_2$]), 0.44 (s, 54H, N(Si(CH_3)$_3$)$_2$, **9.1**), 1.67 (d, 1H, $J_{H\text{-}P}$ = 20 Hz, CHPPh$_3$, **9.1**), 6.99-7.10 (m, 9H, *m*-CH and *p*-CH, **9.1**), 7.65-7.69 (m, 3H, *o*-CH, **9.1**).

NMR Data for Ph$_3$P=CH$_2$. ^{1}H NMR (400 MHz, 25 °C, benzene-d_6): δ 0.81 (d, 2H, $J_{H\text{-}P}$ = 7.6 Hz, CH_2PPh$_3$), 7.00-7.08 (m, 9H, *m*-CH and *p*-CH), 7.71-7.77 (m, 3H, *o*-CH). ^{13}C{^{1}H} NMR (100 Hz, 25 °C, benzene-d_6): δ -4.18 (d, $J_{C\text{-}P}$ = 98.6 Hz, *C*HPPh$_3$), 128.42 (d, $J_{C\text{-}P}$ = 11 Hz, *m*-*C*), 130.60 (d, $J_{C\text{-}P}$ = 2 Hz, *p*-*C*), 132.63 (d, $J_{C\text{-}P}$ = 10 Hz, *o*-*C*), 135.17 (d, $J_{C\text{-}P}$ = 83 Hz, ipso-*C*).

9.4.3 Van't Hoff Analysis for solution of (9.1)

A solution of **9.1** was prepared in C$_7$D$_8$ (27.9 mM) and transferred to an NMR tube fitted with a J-Young valve. The experiments were conducted at 263, 273, 283, 297, and 308 K, and the solution was given 10 min to equilibrate within the NMR probe upon establishment

of each temperature. The K_{eq} was determined by integration of the methyl protons of the N(Si(CH_3)$_3$)$_2$ ligands of complex **9.1** and [Th(*C*H$_2$SiMe$_2$*N*SiMe$_3$)(NR$_2$)$_2$].

Table 9.1. Data for van't Hoff Analysis for **9.1** in C_7D_8 (27.9 mM)

Temp (K)	K_{eq}	Rln(K_{eq})	1000/T
263.4	6.28E-05	-80.4	3.80
273.0	1.04E-04	-76.3	3.66
283.2	1.94E-04	-71.0	3.53
297.2	4.86E-04	-63.4	3.37
308.2	8.08E-04	-59.2	3.25

9.4.4 X-ray Crystallography

Data for **9.1** was collected on a Bruker KAPPA APEX II diffractometer equipped with an APEX II CCD detector using a TRIUMPH monochromator with a Mo Kα X-ray source (α = 0.71073 Å). The crystals were mounted on a cryoloop under Paratone-N oil, and all data were collected at 100(2) K using an Oxford nitrogen gas cryostream. Data were collected using ω scans with 0.5° frame widths. Frame exposures of 2 s were used for **9.1**. Data collection and cell parameter determinations were conducted using the SMART program.[40] Integration of the data frames and final cell parameter refinements were performed using SAINT software.[41] Absorption corrections of the data were carried out using the multi-scan method SADABS.[42] Subsequent calculations were carried out using SHELXTL.[43] Structure determination was done using direct or Patterson methods and difference Fourier techniques. All hydrogen atom positions were idealized, and rode on the atom of attachment. Structure solution, refinement, graphics, and creation of publication materials were performed using SHELXTL.[43]

Table 9.2. X-ray crystallographic data for complex **9.1**

	9.1
empirical formula	$C_{37}H_{70}N_3PSi_6Th$
crystal habit, color	plate, yellow
crystal size (mm)	0.5 × 0.5 × 0.1
space group	$P\bar{1}$
volume (Å^3)	2804.7(7)
a (Å)	11.299(2)
b (Å)	12.953(2)
c (Å)	20.985(3)
α (deg)	98.696(2)
β (deg)	97.064(2)
γ (deg)	109.856(2)
Z	2
formula weight (g/mol)	1186.93
density (calculated) (Mg/m^3)	1.405
absorption coefficient (mm^{-1})	3.012
F_{000}	1220
total no. reflections	22547
unique reflections	13635
R_{int}	0.0207
final R indices (I >2σ(I)]	R_1 = 0.0338 wR_2 = 0.0787
largest diff. peak and hole (e$^-$ A^{-3})	8.255 and -1.187
GOF	1.048

9.5 Appendix

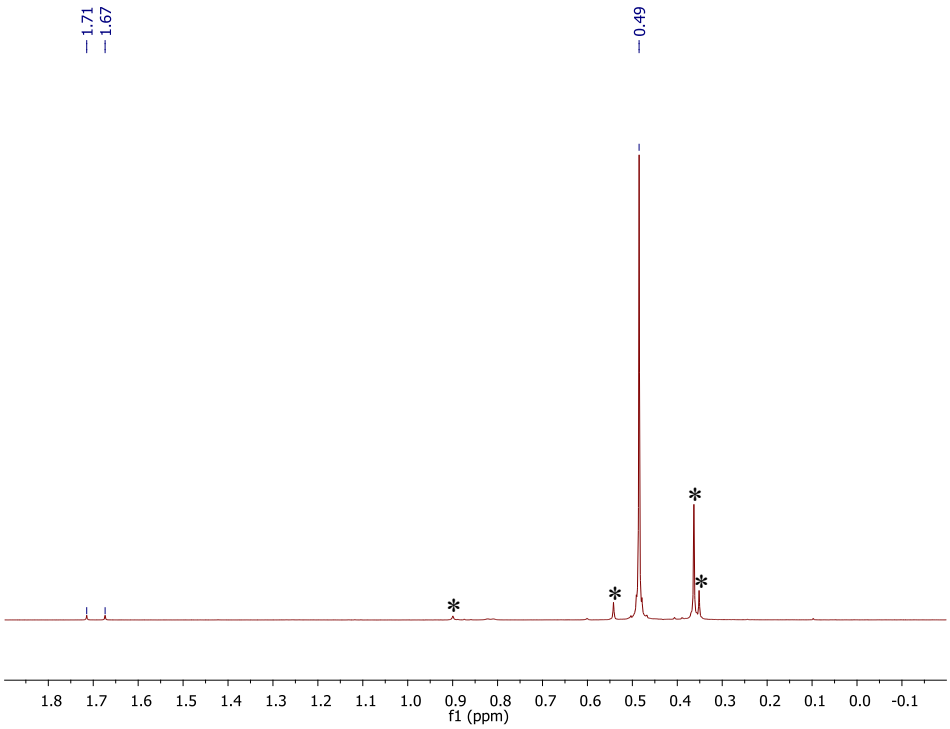

Figure A9.1. Partial ^{1}H NMR spectrum of [Th(CHPPh$_3$)(NR$_2$)$_3$] (**9.1**) in benzene-d_6. (*) indicates the presence [Th(*C*H$_2$SiMe$_2$*N*SiMe$_3$)(NR$_2$)$_2$], present due to the solution state equilibrium.

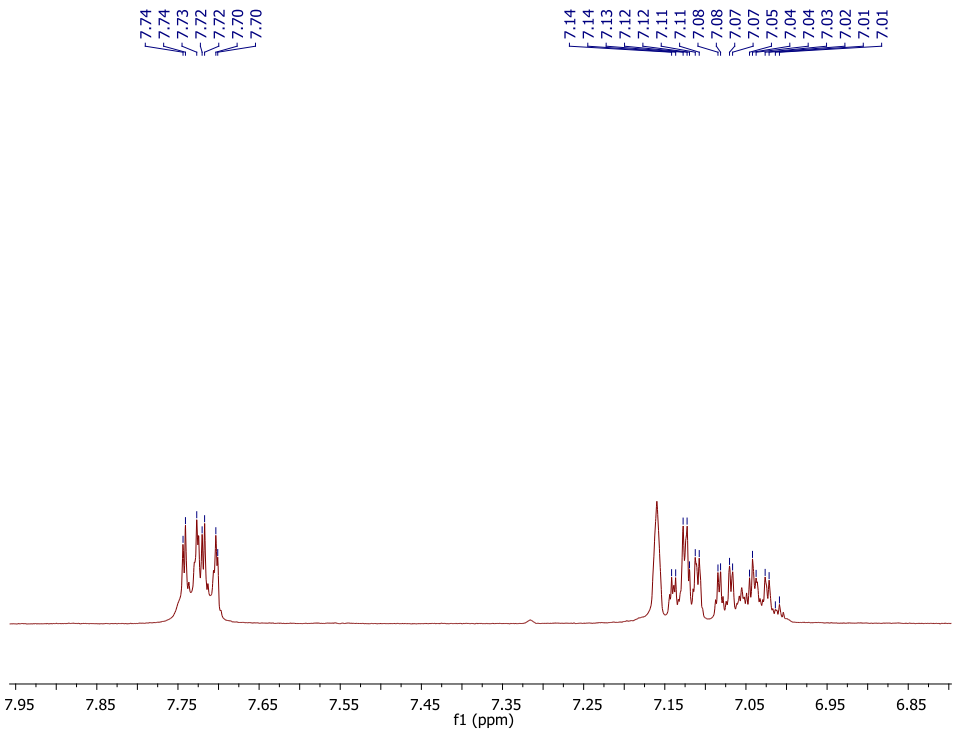

Figure A9.2. Partial ^{1}H NMR spectrum of [Th(CHPPh$_3$)(NR$_2$)$_3$] (**9.1**) in benzene-d_6.

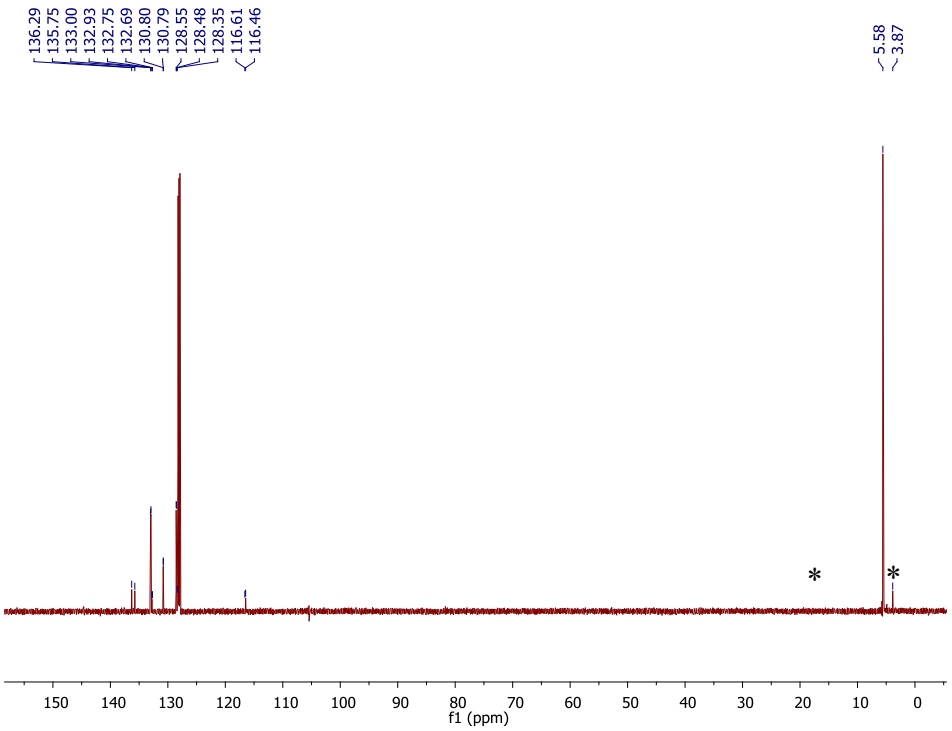

Figure A9.3. $^{13}C\{^{1}H\}$ NMR spectrum of [Th(CHPPh$_3$)(NR$_2$)$_3$] (**9.1**) in benzene-d_6. (*) indicates the presence of [Th(CH$_2$SiMe$_2$$N$SiMe$_3$)(NR$_2$)$_2$], present due to the solution state equilibrium.

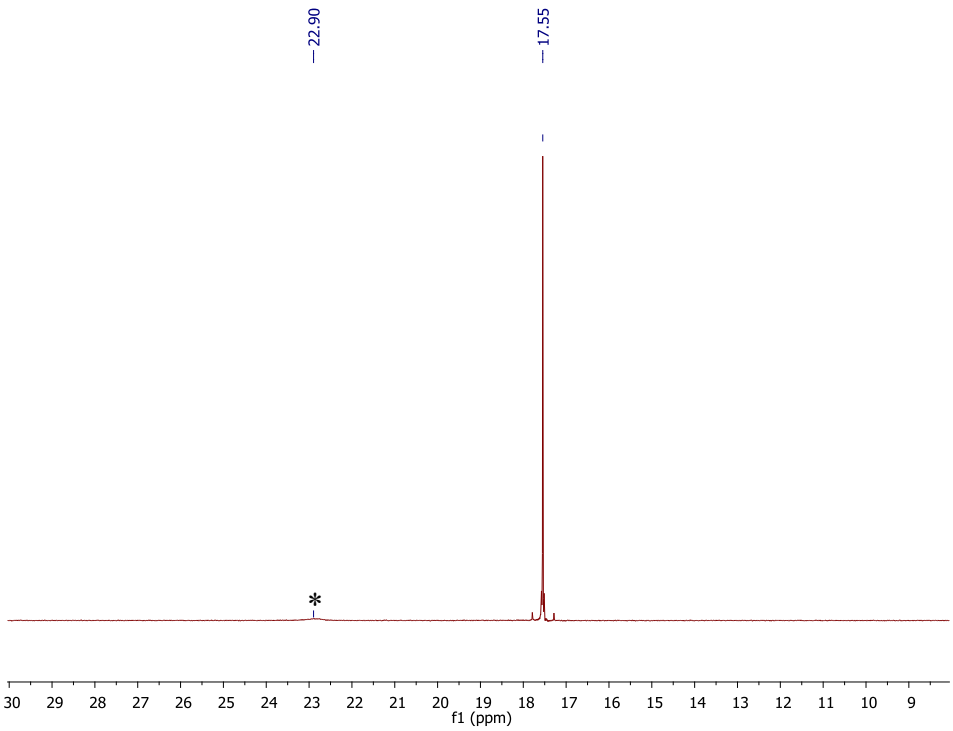

Figure A9.4. $^{31}P\{^{1}H\}$ NMR spectrum of [Th(CHPPh$_3$)(NR$_2$)$_3$] (**9.1**) in benzene-d_6. (*) indicates the presence of Ph$_3$P=CH$_2$, present due to the solution state equilibrium.

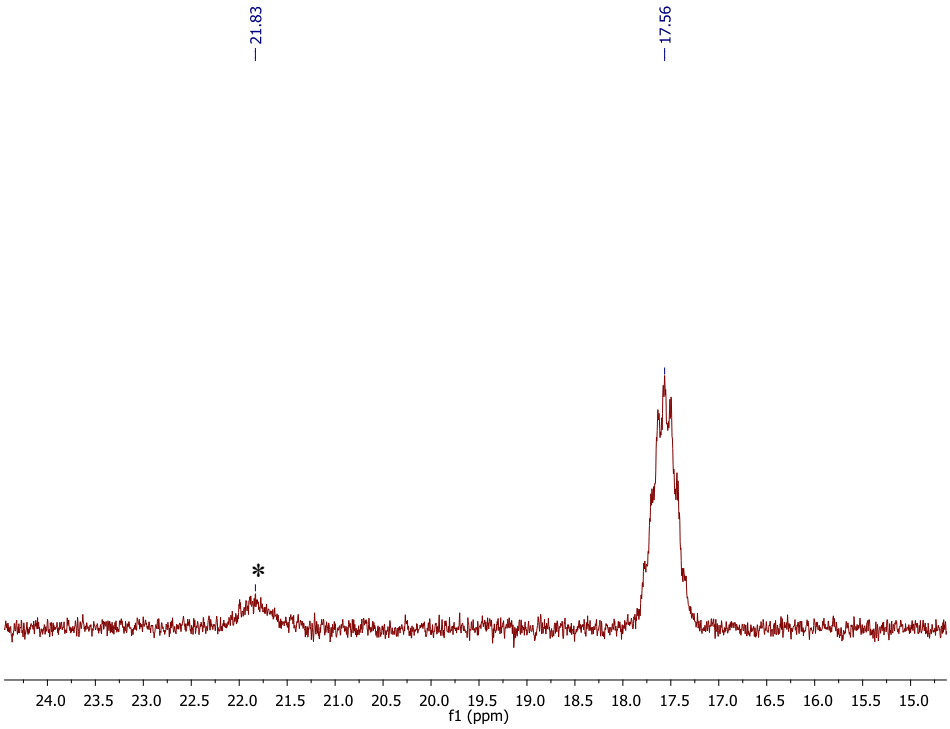

Figure A9.5. ^{31}P NMR spectrum of [Th(CHPPh$_3$)(NR$_2$)$_3$] (**9.1**) in benzene-d_6. (*****) indicates the presence of Ph$_3$P=CH$_2$, present due to the solution state equilibrium.

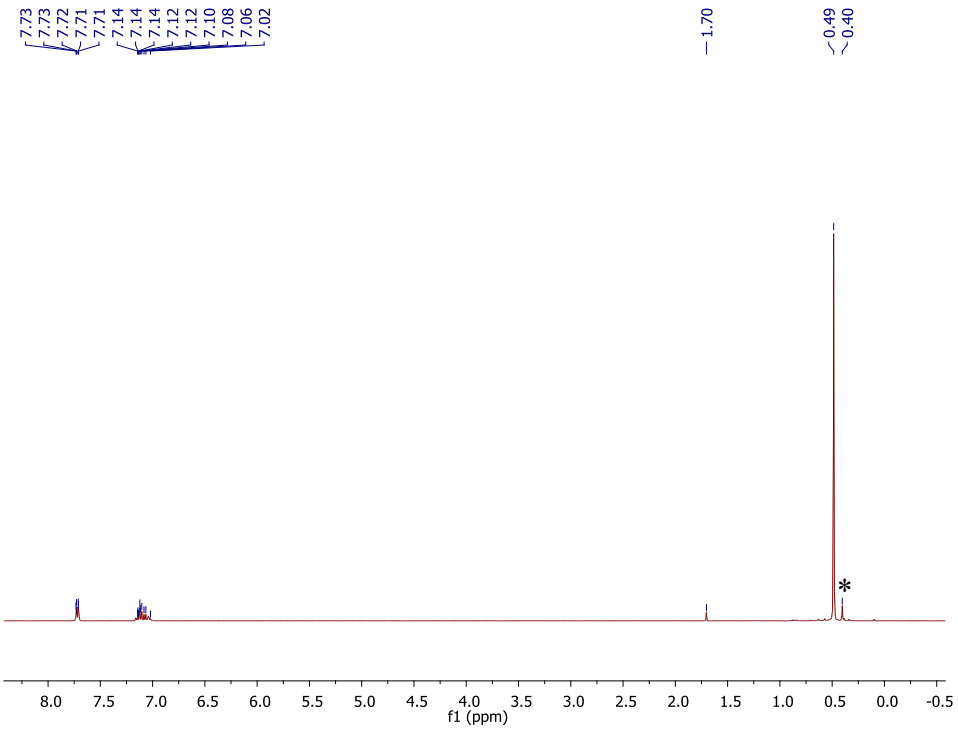

Figure A9.6. $^{1}H\{^{31}P\}$ NMR spectrum of $[Th(CHPPh_3)(NR_2)_3]$ (**9.1**) in benzene-d_6. (*) indicates the presence of $[Th(CH_2SiMe_2NSiMe_3)(NR_2)_2]$, present due to the solution state equilibrium.

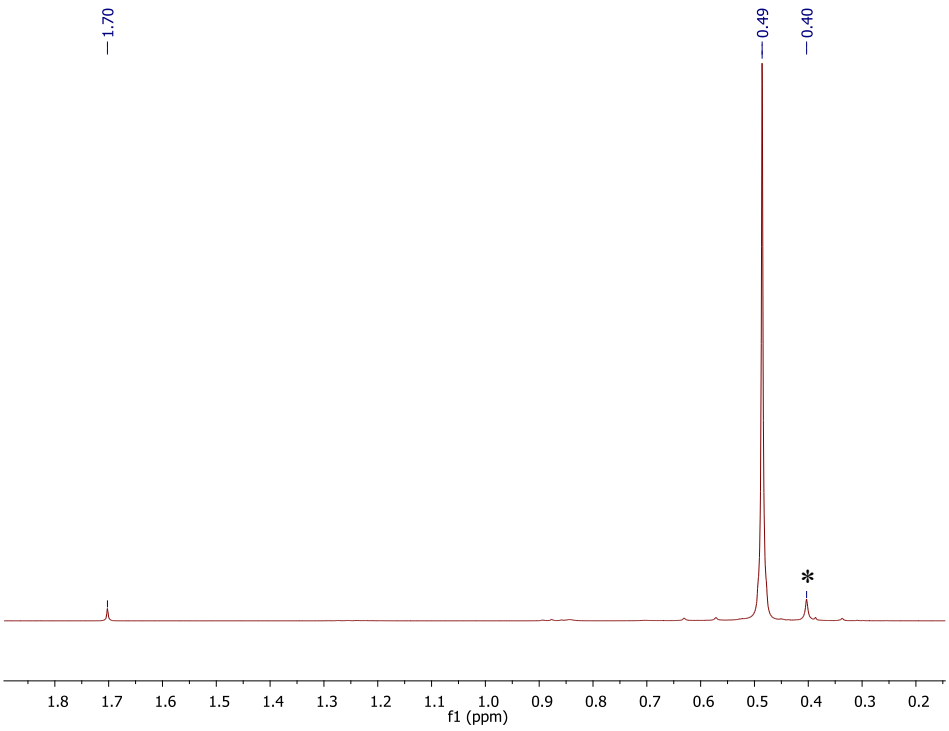

Figure A9.7. Partial $^{1}H\{^{31}P\}$ NMR spectrum of $[Th(CHPPh_3)(NR_2)_3]$ (**9.1**) in benzene-d_6. (*) indicates the presence of $[Th(CH_2SiMe_2NSiMe_3)(NR_2)_2]$, present due to the solution state equilibrium.

9.6 References

(1) Fischer, E. O. In *Pure Appl. Chem.* 1970; Vol. 24, p 407.
(2) Mills, O. S.; Redhouse, A. D. *Angew. Chem. Int. Ed.* **1965**, *4*, 1082.
(3) Fischer, E. O.; Maasböl, A. *Angew. Chem. Int. Ed.* **1964**, *3*, 580.
(4) Schrock, R. R. *J. Am. Chem. Soc.* **1974**, *96*, 6796.
(5) In *The Organometallic Chemistry of the Transition Metals*; John Wiley & Sons, Inc.: 2014, p 290.
(6) Cardin, D. J.; Cetinkaya, B.; Lappert, M. F. *Chem. Rev.* **1972**, *72*, 545.
(7) Kaufhold, S.; Petermann, L.; Staehle, R.; Rau, S. *Coord. Chem. Rev.* **2015**, *304–305*, 73.
(8) Dötz, K. H.; Stendel, J. *Chem. Rev.* **2009**, *109*, 3227.
(9) Vougioukalakis, G. C.; Grubbs, R. H. *Chem. Rev.* **2010**, *110*, 1746.
(10) Dötz, K. H. *Metal Carbenes in Organic Synthesis*; Springer Berlin Heidelberg: Berlin, Heidelberg, 2004.
(11) Tebbe, F. N.; Parshall, G. W.; Reddy, G. S. *J. Am. Chem. Soc.* **1978**, *100*, 3611.
(12) Gregson, M.; Lu, E.; Tuna, F.; McInnes, E. J. L.; Hennig, C.; Scheinost, A. C.; McMaster, J.; Lewis, W.; Blake, A. J.; Kerridge, A.; Liddle, S. T. *Chem. Sci.* **2016**, *7*, 3286.
(13) Lu, E.; Cooper, O. J.; McMaster, J.; Tuna, F.; McInnes, E. J. L.; Lewis, W.; Blake, A. J.; Liddle, S. T. *Angew. Chem. Int. Ed.* **2014**, *53*, 6696.
(14) Cantat, T.; Arliguie, T.; Noel, A.; Thuery, P.; Ephritikhine, M.; Le Floch, P.; Mezailles, N. *J. Am. Chem. Soc.* **2009**, *131*, 963.
(15) Cooper, O. J.; McMaster, J.; Lewis, W.; Blake, A. J.; Liddle, S. T. *Dalton Trans.* **2010**, *39*, 5074.
(16) Tourneux, J.-C.; Berthet, J.-C.; Cantat, T.; Thuery, P.; Mezailles, N.; Le Floch, P.; Ephritikhine, M. *Organometallics* **2011**, *30*, 2957.
(17) Tourneux, J.-C.; Berthet, J.-C.; Thuery, P.; Mezailles, N.; Le Floch, P.; Ephritikhine, M. *Dalton Trans.* **2010**, *39*, 2494.
(18) Arnold, P. L.; Turner, Z. R.; Kaltsoyannis, N.; Pelekanaki, P.; Bellabarba, R. M.; Tooze, R. P. *Chem. Eur. J.* **2010**, *16*, 9623.
(19) Nakai, H.; Hu, X.; Zakharov, L. N.; Rheingold, A. L.; Meyer, K. *Inorg. Chem.* **2004**, *43*, 855.
(20) Cramer, R. E.; Maynard, R. B.; Paw, J. C.; Gilje, J. W. *Organometallics* **1983**, *2*, 1336.
(21) Cramer, R. E.; Maynard, R. B.; Paw, J. C.; Gilje, J. W. *J. Am. Chem. Soc.* **1981**, *103*, 3589.
(22) Cramer, R. E.; Bruck, M. A.; Edelmann, F.; Afzal, D.; Gilje, J. W.; Schmidbaur, H. *Chem. Ber.* **1988**, *121*, 417.
(23) Fortier, S.; Walensky, J. R.; Wu, G.; Hayton, T. W. *J. Am. Chem. Soc.* **2011**, *133*, 6894.
(24) Ma, G.; Ferguson, M. J.; McDonald, R.; Cavell, R. G. *Inorg. Chem.* **2011**, *50*, 6500.
(25) Ren, W.; Deng, X.; Zi, G.; Fang, D.-C. *Dalton Trans.* **2011**, *40*, 9662.
(26) Lu, E.; Lewis, W.; Blake, A. J.; Liddle, S. T. *Angew. Chem. Int. Ed.* **2014**, *53*, 9356.
(27) Arnold, P. L.; Casely, I. J. *Chem. Rev.* **2009**, *109*, 3599.
(28) Lyon, J. T.; Andrews, L. *Inorg. Chem.* **2005**, *44*, 8610.
(29) Schrock, R. R. *Chem. Rev.* **2009**, *109*, 3211.

(30) Schrock, R. R. *Acc. Chem. Res.* **1986**, *19*, 342.
(31) Schrock, R. R. *Acc. Chem. Res.* **1979**, *12*, 98.
(32) Bell, N. L.; Maron, L.; Arnold, P. L. *J. Am. Chem. Soc.* **2015**, *137*, 10492.
(33) Pyykkö, P. *J. Phys. Chem. A* **2015**, *119*, 2326.
(34) Seaman, L. A.; Hrobárik, P.; Schettini, M. F.; Fortier, S.; Kaupp, M.; Hayton, T. W. *Angew. Chem. Int. Ed.* **2013**, *52*, 3259.
(35) Pedrick, E. A.; Hrobarik, P.; Seaman, L. A.; Wu, G.; Hayton, T. W. *Chem. Commun.* **2016**, *52*, 689.
(36) Cantat, T.; Scott, B. L.; Kiplinger, J. L. *Chem. Commun.* **2010**, *46*, 919.
(37) Bestmann, H. J.; Stransky, W.; Vostrowsky, O. *Chem. Ber.* **1976**, *109*, 1694.
(38) Harris, R. K.; Becker, E. D.; Cabral De Menezes, S. M.; Goodfellow, R.; Granger, P. *Pure Appl. Chem.* **2001**, *73*, 1795.
(39) Harris, R. K.; Becker, E. D.; Cabral De Menezes, S. M.; Granger, P.; Hoffman, R. E.; Zilm, K. W. *Pure Appl. Chem.* **2008**, *80*, 59.
(40) *SMART Apex II*, Version 2.1. 2005
(41) *SAINT Software User's Guide*, Version 7.34a. 2005
(42) *SADABS*, 2005
(43) *SHELXTL PC*, Version 6.12. 2005